

The effects of neuroinflammation on the Subventricular Zone neurogenic compartment following Theiler's Murine Encephalomyelitis Virus infection and its regulation by Galectin-3.

A thesis submitted to the Department of Physiology, Anatomy and Genetics

in partial fulfilment of the requirements for the degree of

Doctor of Philosophy

by

Rachel Elizabeth James

St Cross College, University of Oxford, United Kingdom

Trinity Term, 2012

For Nana

ABSTRACT

James RE. The effects of neuroinflammation on the Subventricular Zone neurogenic compartment following Theiler's Murine Encephalomyelitis Virus infection and it's regulation by Galectin-3. St Cross College.

Submitted in partial fulfilment for the degree of Doctor of Philosophy, Trinity Term, 2012

The subventricular zone (SVZ) is an adult neurogenic niche that contains multipotent stem/progenitor cells that may be a viable target for remyelination in Multiple Sclerosis. In response to demyelination, SVZ progenitors are recruited into myelin lesions. Currently, the effect of inflammation on the endogenous brain stem cell compartment remains poorly characterised. Theiler's murine encephalomyelitis virus (TMEV) induces a demyelinating disease in susceptible SJL/J mice, due to persistence of the virus, which models the chronic progressive form of multiple sclerosis. In contrast, virus is rapidly cleared in TMEV resistant C57BL/6 mice. This viral clearance is critically dependent on infiltration of $CD4^+$ and $CD8^+$ T cells during the first 3-14 days after infection, through the blood vessels and meninges. This project aimed to characterise the impact of TMEV induced inflammation on SVZ homeostasis.

In both strains of mice the most pronounced and consistent inflammation in the CNS was observed in periventricular regions and in particular, the SVZ, which showed targeted infection by the TMEV virus. However, the time course and kinetics for infiltration at 3,7 and 14 days post infection have very different profiles between resistant C57BL/6 and susceptible SJL mice. Using RT-PCR arrays and ELISA I have shown that these differences in T cell infiltration to the SVZ may be due to much higher chemokine and cytokine expression levels in B6 mice. TMEV infection decreases SVZ cell proliferation and results in a loss of neuroblast numbers.

Galectin-3 (Gal-3) is a β-galactoside binding protein that is constitutively expressed specifically in the SVZ. Following TMEV infection Gal-3 levels are significantly up-regulated in the SVZ, with higher expression in B6 mice compared to SJL mice. Primary SVZ astrocytes secrete extracellular Galectin-3 at much higher levels than cortical astrocytes. Galectin-3 is a pro-inflammatory mediator which upon secretion is able to activate immune and inflammatory signaling events and amplify pro-inflammatory cytokine production. Both SJL and B6 Gal-$3^{-/-}$ KO mice have decreased expression of CCL2, CCL5 CXCL10 and CCL8 chemokines in the SVZ after TMEV infection. Deletion of Gal-3 prevents the loss of SVZ proliferation and in B6 mice decreases hematopoietic cell infiltration and enhances ectopic neuroblast emigration. These data implicate Galectin-3 as a novel regulator of the SVZ inflammatory response and may provide a new target for regulating T cell CNS immigration in autoimmune disease.

ACKNOWLEDGEMENTS

I would like to express my gratitude to all of the people who have supported me throughout my graduate career. First, I would like to thank my supervisor, Dr Francis Szele, who has been an incredible mentor throughout the last four years I have spent in his lab. I would like to thank him for accepting me into his lab as a student and creating an environment where I could learn and develop my skills as a scientist. I would also like to thank all the other supervisors and Heads of Lab who have dedicated their time to my education. Professor Phil Hockberger for teaching me how to use the 2-photon microscope and his incredible patience with all the issues, Professor Stephen Miller for allowing me the opportunity to come and learn techniques vital to my thesis in his lab at Northwestern University and Dr David Greaves for his invaluable advice on chemokines. I would also like to thank Professor Zoltan Molnar and Dr Shankar Srinivas for their help and advice and for making our department an excellent place to come to work. Dr Maureen Richards who taught me all I needed to know about working with the TMEV virus and being an excellent friend across the water.

During my time at Oxford University I have been lucky to work with many talented individuals. Every current and former member of the Szele lab has impacted this work in some way or another. I would like to thank Dr Isabelle Comte and Dr Yongsoo Kim for teaching me many of the techniques used in this thesis and being ever patient with my questions. In particular, I would like to thank Dr Chris Young, Eunhyuk Chang, Dr Preshanti Kotagiri and Hugo Fernandes for making my time in the lab as enjoyable as it has been and being incredible co-workers and friends over the years. Betty Gration, Moon-Moon Majumbar, Adam Kelly and Leah Nennot are all dedicated young scientists who have been a pleasure to train and I thank them for their help in counting thousands and

thousands of T-cells. I am grateful for the incredible support of Mrs Denise Jelfs, Mrs Caroline Barnwell and Mr James Ward whose endless patience and creativity with my mice have made this work possible.

I am hugely grateful to the Wellcome Trust for providing the funds that has made this PhD possible and for my Wellcome Committee members Dr Deborah Clarke and Dr Jeremy Taylor for their guidance and support right through my masters and PhD.

I am lucky to come from a supportive family who have shown infinite patience with my many years of studenthood, despite subtle hints to ‘get a job’. I owe every accomplishment in my life to my parents and grandparents constant love and support and to my sister Katie, who I am lucky to have in my life. I have many incredible friends who have provided support and encouragement throughout my time in Oxford, in particular Dr Michael Hart and Dr Michael Baker who have been invaluable friends (and occasional mathematicians) and kept me afloat in rough seas.

Finally, I think my incredible fiancé Daniel Bates to who I owe a tremendous amount. Dan has been a true supporter and has unconditionally loved me during my good and bad times.

AUTHORSHIP STATEMENT

I conceptualised and designed the experiments in this thesis with input from my supervisor, Dr Francis Szele.

The SJL/J mice used for the chronic TMEV studies were injected and perfused by Ms Gwen Goings at Northwestern University. Ms Goings performed immunohistochemistry on these mice. Ms Goings also performed immunohistochemistry for the CD11C and schematics of CD45 in chronic stages of TMEV.

For quantification of T-cell immigration into different CNS regions and Ph3 proliferation in chapter 1 Ms Moon-moon Majumdar and Ms Betty Gration assisted in parts with tissue dissection, immunohistochemistry and quantification under my supervision.

For the Galectin-3 study I trained Mr Adam Kelly to help with the running of the Gal-3 ELISAs on tissue and supernatant samples as well as quantification of Dcx emigration numbers in C57BL/6 mice.

Parts of chapter 1 have been published in Goings et al (2008).

All other experimental procedures, quantifications and analysis were performed by myself with generous guidance from members of our laboratory, the University and the greater scientific community.

© Copyright by Rachel Elizabeth James 2012. All rights reserved.

TABLE OF CONTENTS

Abstract **3**

Acknowledgements **4**

Authorship statement **6**

Table of contents **7**

List of figures **15**

List of tables **19**

Abbreviations **20**

Chapter 1:

Introduction…….. 24

1.1 Multiple sclerosis 25

1.2 Genetics of multiple sclerosis 26

1.3 A viral etiology for multiple sclerosis 27

1.4 Theiler's murine encephalomyelitis model of MS 28

1.5 Structure of TMEV BeAN virus 30

1.6 Early pathology of TMEV infection 30

1.6.1 Role of T-cells

1.6.2 Mechanisms of axonal damage

1.6.3 Viral persistence

1.6.4 Demyelination and remyelination

1.7 Similarities between human MS and TMEV 37

1.8 Experimental autoimmune encephalomyelitis 38

1.9 Relevance of animals for drug development 38

1.10 Stem cells for treatment of multiple sclerosis 39

1.11 Adult neurogenesis 41

1.12 The SVZ neuronal stem cell niche 42

1.13 Oligodendrocyte production in the SVZ 43

1.14 The role of remyelination and the SVZ in human multiple sclerosis 44

1.15 Mechanisms of remyelination 46

1.15.1 Changes in cell fate

1.15.2 Enhancing proliferation

1.15.3 Mobilisation of cells

1.16 Effects of inflammation on the SVZ niche 48

1.17 Effect of T-cell on neural progenitor cells 51

1.18 Role of microglia in influencing neurogenesis 51

1.19 The role of neuroprotection in multiple sclerosis 53

1.20 The Galectin family 55

1.21 Glycosylation and galectin-lattices 56

1.22 The importance of glycosylation in multiple sclerosis 56

1.23 Effect of glycosylation on T-cell function in MS 58

1.24 Galectin-3 as a potential novel therapeutic target 61

1.25 Investigating the adult neural stem cell niche in TMEV 64

Chapter 2

Materials and methods……. 66

2.1 Animals 67

2.2 Galectin-3 null mice 67

2.3 Genotyping 69

2.4 TMEV viral production 70

2.5 TMEV infection of mice 70

2.6 Immunohistochemistry 72

2.7 Cell counting 77

2.8 RT-PCR arrays 79

2.9 Neurosphere experiments 82

2.10 Measuring cytokine levels 84

2.11 Astrocyte culture 86

2.12 Statistics 88

Chapter 3:

TMEV induced inflammation in the SVZ and its impact on niche homeostasis

3.1 Introduction…….. 90

3.1.1 Research question 94

3.2 Results…… 95

3.2.1 Patterns of CD45 infiltration in the CNS after TMEV 95

3.2.2 The identities of haematopoietic cells 97

3.2.3 Infiltrating $CD3^+$ cells target the SVZ 100

3.2.4 Different patterns of T-cell immigration into the SVZ between mouse strains 104

3.2.5 Preferential viral infection of the SVZ 105

3.2.6 Disruption of neuroblast chain integrity and changes in migration 107

3.2.7 TMEV infection decreases neural-lineage cell proliferation 109

3.2.8 TMEV leads to cell death in vitro 112

3.2.9 Profiles of SVZ inflammatory mediators varies between strains 112

3.2.10 Chemokine protein levels in SVZ differ between strains 116

3.2.11 Cytokine profiles from primary astrocyte cultures 117

3.3 Discussion…… 121

3.3.1 The BeAn virus directly infects cells of the SVZ niche 121

3.3.2 T-cell infiltration targets the SVZ 124

3.3.3 SVZ cytokine profiles are different between SJL and B6 mice 125

3.3.4 The use of SVZ primary astrocyte cultures 127

3.3.5 SVZ astrocytes express TLR2 after TMEV infection 128

3.3.6 Complement system activation in TMEV 129

3.3.7 TMEV infection decreases SVZ proliferation 131

3.3.8 Loss of neuroblast chain integrity and neuroblast numbers 132

3.3.9 Conclusion 134

Chapter 4:

Characterisation of Galectin-3 in the SVZ

4.1 Introduction…… 137

4.1.1 Research questions 140

4.2 Results …… 141

4.2.1 Genotyping of Gal-3 deficient mice 141

4.2.2 SVZ expression of Galectin-3 differs between B6 and SJL mice 143

4.2.3 Gal-3 was expressed in postnatal mouse SVZ and cortex 147

4.2.4 Deletion of Gal-3 does not affect proliferation 148

4.2.5 Emigration of neuroblasts into the parenchyma is altered in SJL 148

4.2.6 Gal-3 deletion increases astrocyte process width in SJL mice 152

4.2.7 Gal-3 is expressed in glial tubes in the RMS of SJL mice 152

4.2.8 Gal-3 is expressed by a subset of cells within neurospheres 152

4.2.9 RGal-3 decreases the proliferation of SJL/J neurospheres 155

4.2.10 rGal3 has less of an effect on B6 neurosphere proliferation 156

4.2.11 Gal-3 blocking antibodies stimulate proliferation of neurospheres 159

4.2.12 Gal-3 is express by all cell types in differentiating neurospheres 161

4.3 Discussion……..... 166

4.3.1 Only subset of galectins are expressed in the CNS 166

4.3.2 Expressions of Gal-3 in the SVZ differs with genetic background 166

4.3.3 Gal-3 expression in the neurogenic niche 168

4.3.4 Decreased neuroblast number and migration in SJL Gal3 null mice 170

4.3.5 Gal-3 deletion does not alter proliferation in vivo 171

4.3.6 Gal-3 influences proliferation in neurosphere cells 172

4.3.7 Galectin and neuronal growth 174

4.3.8 Galectin and oligodendrocytes 174

4.3.9 Conclusions 176

Chapter 5:

Role of Galectin-3 in regulation of neuroinflammation

5.1 Introduction…….... 178

5.1.2 Research questions 179

5.2 Results……. 180

5.2.1 Galectin-3 is upregulated after TMEV infection 180

5.2.2 TMEV infection stimulated Gal-3 expression CNS astrocytes 180

5.2.3 SVZ primary astrocyte cultures make more Gal-3 than cortical Cultures 183

5.2.4 Phagocytosing microglia in the hippocampus express Gal-3 186

5.2.5 Galectin-3 expression by $CD3^+$ cells 187

5.2.6 Deletion of Galectin-3 reduced haematopoietic cell infiltration after TMEV 190

5.2.7 Loss of Gal-3 increases ectopic neuroblast emigration 194

5.2.8 $Ph3^+$ proliferation after Gal-3 KO 194

5.2.9 TMEV infection of neurospheres stimulates secretion of Gal-3 197

5.2.10 Gal-3 deletion protects from TMEV cytotoxicity in neurospheres 198

5.2.11 Role IFNγ on regulation of Galectin-3 secretion 199

5.2.12 Loss of Gal-3 in B6 mice alters chemokines mRNA levels in the SVZ 203

5.2.13 Chemokine ELISAs on SVZ tissue (D3 and D7) 203

5.3 Discussion……..... 207

5.3.1 Galectin-3 and its involvement with multiple sclerosis 207

5.3.3 Galectin-3 levels are different between resistant and susceptible strains 208

5.3.3 Galectin-3 up-regulation in the SVZ 209

5.3.4 Gal-3 is expressed by astrocytes 210

5.3.5 Regulation of inflammatory molecule expression by Galectin-3 211

5.3.6 Gal-3 may mediate differences in cytokine levels between strains 213

5.3.7 Galectin-3 expression by phagocytosing microglia 214

5.3.8 Gal-3 expressed by subpopulation immigrating T-cells 215

5.3.9 Reduced haematopoietic cell l infiltration after Gal-3 deletion in B6 mice 216

5.3.10 The role of other Galectins 217

5.3.12 Gal-3 effects on proliferation and cell death in neurospheres cultures. 218

5.3.12 SVZ proliferation preserved in Gal-3 null mice 219

5.3.13 Increased neuroblast migration in Gal-3 KO mice 220

5.3.14 Conclusions 221

Chapter 6:

Discussion …….. 224

6.1 Overall 225

6.1.1 Persistent viral infections in the SVZ

6.1.2 Regulation of inflammation in TMEV

6.1.3 Susceptibility in TMEV

6.2 Limitation 230

6.3 Future work 233

References 236

Appendices 269

1. Recipes of solutions
2. Fold gene changes with RT-PCR array

LIST OF FIGURES

Chapter 1:

Introduction

Figure 1.1	The geography of multiple sclerosis	26
Figure 1.2	Comparison of the immune response to TMEV in resistant and susceptible strains	31
Figure 1.3	The adult SVZ niche in mice	41
Figure 1.4	Th1 and Th2 differentiation produces different cytokine profiles	53
Figure 1.5	Glycosylation pathways and their role in galectin-3 binding	57

Chapter 2:

Materials and methods

Figure 2.1	Time course of TMEV pathology	72

Chapter 3:

TMEV induced inflammation in the SVZ and its impact on niche homeostasis

Figure 3.1	Periventricular lesions in MS	91
Figure 3.2	Schematic of brain regions showing typical areas of $CD45^+$ activation	96
Figure 3.3	Regions of high CD45 activation in periventricular regions, RMS and hippocampus	98
Figure 3.4	Widespread microglia activation through forebrain and hippocampus	99
Figure 3.5	Comparison of dendritic cell CD11c immunolabelling with CD45	100
Figure 3.6	$CD3^+$ infiltration targets the SVZ of SJL/J mice	102

Figure 3.7	$CD3^+$ cells accumulate in the dorsal SVZ of SJL mice	103
Figure 3.8	$CD3^+$ cells are more evenly spread in SVZ of B6 mice	104
Figure 3.9	BeAn infection of cells of the CNS	107
Figure 3.10	Loss of PSA-NCAM and disruption of chains over time	109
Figure 3.11	TMEV causes a transient increase in ectopic neuroblast emigration in SJL mice	111
Figure 3.12	TMEV causes an increase in neuroblast emigration into the striatum of B6 mice	112
Figure 3.13	Decrease in SVZ proliferation after TMEV infection in SJL/J	114
Figure 3.14	Proliferation in C57BL/6 mice shows signs of recovery at later time points	115
Figure 3.15	Infection of SVZ derived neurospheres inhibits cell growth	116
Figure 3.16	Levels of cytokine mRNA in SVZ tissue from B6 and SJL mice at 7 dpi	119
Figure 3.17	Protein levels of chemokines in SVZ tissue from B6 and SJL mice at 7 dpi	120
Figure 3.18	Levels of cytokine mRNA in primary SVZ astrocytes cultures infected with TMEV at MOI 10	121

Chapter 4:

Galectin-3 and the SVZ after TMEV

Figure 4.1	Expression of different galectins in Allen brain atlas	138
Figure 4.2	Galectin-3 homozygous null mutant mice	142
Figure 4.3	Gal-3 expression levels differ between strains of mice	144
Figure 4.4	Gal-3 expression in SVZ cell types	145
Figure 4.5	Expression of Gal-3 in postnatal mice	146

Figure 4.6	Proliferation does not change in SVZ of Gal-3$^{-/-}$ mice	149
Figure 4.7	Gal-3 loss causes loss of neuroblast number and chain integrity	150
Figure 4.8	Gal-3 deletion increase GFAP process width in SJL astrocytes	151
Figure 4.9	Loss of Gal-3 does not alter TMEV surface area	153
Figure 4.10	Galectin-3 is produced by a subset of cells within neurospheres	154
Figure 4.11	Exogenous rGal-3 alters SJL/J neurosphere growth	157
Figure 4.12	Effects of exogenous rGal-3 on C57BL/6 neurosphere growth	158
Figure 4.13	Functional blocking antibody and IgG stimulate proliferation	160
Figure 4.14	Gal-3 is expressed by all cell types in differentiated neurosphere Cultures and does not change cell fate	162

Chapter 5:

Galectin-3 and regulation of neuroinflammation

Figure 5.1	Galectin-3 is upregulated after TMEV infection	181
Figure 5.2	Gal-3 is expressed by SVZ and periventricular astrocytes	182
Figure 5.3	Gal-3 is upregulated in TMEV infected astrocytes	184
Figure 5.4	Phagocytosing microglia in the hippocampus express Gal-3	185
Figure 5.5	A subset of T-cells co-label for Gal-3	188
Figure 5.6	A subset of T-cells are Gal-3^{+}	189
Figure 5.7	Decreases in amoeboid CD45^{+} infiltration in SJL mice	191
Figure 5.8	Fewer amoeboid CD45^{+} cells in B6 Gal-3$^{-/-}$	192
Figure 5.9	Loss of Gal-3 increases ectopic neuroblast migration	193
Figure 5.10	Gal-3 deletion restores proliferation in SJL/J mice	195
Figure 5.11	Gal-3 deletion restores proliferation in B6 mice	196
Figure 5.12	TMEV infection of neurospheres stimulates secretion of Gal-3	198
Figure 5.13	Loss of Gal-3 decreases TMEV induced cell lysis in SJL	200

	Neurospheres	
Figure 5.14	Loss of Gal-3 decreases TMEV induced cell lysis in SJL neurospheres	201
Figure 5.15	IFNg does not stimulate the secretion of Gal-3 from neurospheres	202
Figure 5.16	Loss of Gal-3 in B6 mice alters chemokine mRNA levels in the SVZ	205
Figure 5.17	Protein levels of chemokines in SVZ and cortical tissue	206

LIST OF TABLES

2.1	Antibodies for immunohistochemistry and immunoblotting	76
7.2	Fold changes in gene expression in SVZ tissue and astrocytes cultures after TMEV infection by RT-PCR array	272

ABBREVIATIONS

APC	Antigen presenting cell
B6	C57BL/6 mouse strain
BBB	Blood brain barrier
CRD	Carbohydrate recognition domain
CSF	Cerebral spinal fluid
CNS	Central nervous system
CP-MS	chronic progressive multiple sclerosis
CRD	Carbohydrate recognition domain
CTL	Cytotoxic T Lymphocyte
CVB3	Coxsackievirus B3
DAPI	4’,6-diamidino-2-phenylindole
Dcx	Doublecortin
DIV	Days *in vitro*
DMEM	Dulbecco’s modified Eagle media
DMSO	Dimethyl sulfoxide
DPI	Days post infection
EAE	Experimental allergic encephalomyelitis
EGF	Epidermal growth factor

ELISA	Enzyme-linked immunosorbent assay
FGF	Fibroblast growth factor
Gal-3	Galectin-3
GFAP	Glial fibrillary acidic protein
GI	Gastrointestinal tract
IFN	Interferon
IDD	Inflammatory demyelinating disease
IL	Interleukin
JCV	John Cunningham virus
JEV	Japanese encephalomyelitis virus
KO	Knock-out
LDH	Lactate dehydrogenase
MBP	Myelin basic peptide
MHC	Major histocompatibility complex
MMP	Matrix metalloproteinases
MOG	Myelin oligodendrocyte protein
MOI	Moiety of infection
MS	Multiple sclerosis
MTS	(3-(4,5-dimethylthiazol-2-yl)-5-(3-carboxymethoxyphenyl)-2-(4-sulfophenyl)-2H-tetrazolium)

OD	Optical density
NSC	Neural stem cells
OB	Olfactory bulb
OPC	Oligodendrocyte progenitor cells
PB	Phosphate buffer
PBS	Phosphate buffered saline
PECAM	platelet endothelial cell adhesion molecule-1
PH3	Phosphorylated histone H3
PFA	Paraformaldehyde
PFU	plaque forming units
PLP	Proteolipid peptide
PML	progressive multifocal leukoencephalopathy
PSA-NCAM	Polysialylated neural cell adhesion molecule
RMS	Rostral migratory stream
RR-MS	Relapsing remitting multiple sclerosis
SAFV	Saffold virus
SVZ	Subventricular zone
TAP	Transit amplifying cells
TGFβ	Transforming growth factor beta
TMEV	Theiler’s murine encephalomyelitis virus

TMEV-IDD	Theiler’s murine encephalomyelitis virus induced demyelinating disease
TPM	2-photon microscopy
ICAM-1	cell adhesion molecule-1
MS	Multiple sclerosis
TIMPs	Tissue inhibitors of matrix metalloproteinases
TMEV	Theiler’s murine encephalomyelitis virus
VCAM-1	Vascular cell adhesion molecule-1
WT	Wildtype

Chapter 1

Introduction

1.1	**Multiple sclerosis**	**25**
1.2	**Genetics of multiple sclerosis**	**26**
1.3	**A viral etiology for multiple sclerosis**	**27**
1.4	**Theiler's murine encephalomyelitis model of MS**	**28**
1.5	**Structure of TMEV BeAN virus**	**30**
1.6	**Early pathology of TMEV infection**	**30**
1.7	**Similarities between human MS and TMEV**	**37**
1.8	**Experimental autoimmune encephalomyelitis**	**38**
1.9	**Relevance of animals for drug development**	**38**
1.10	**Stem cells for treatment of multiple sclerosis**	**39**
1.11	**Adult neurogenesis**	**41**
1.12	**The SVZ neuronal stem cell niche**	**42**
1.13	**Oligodendrocyte production in the SVZ**	**43**
1.14	**The role of remyelination and the SVZ in human multiple sclerosis**	**44**
1.15	**Mechanisms of remyelination**	**45**
1.16	**Effects of inflammation on the SVZ niche**	**48**
1.17	**Effect of T-cell on neural progenitor cells**	**50**
1.18	**Role of microglia in influencing neurogenesis**	**51**
1.19	**The role of neuroprotection in multiple sclerosis**	**53**
1.20	**The Galectin family**	**55**
1.21	**Glycosylation and galectin-lattices**	**56**
1.22	**The importance of glycosylation in multiple sclerosis**	**56**
1.23	**Effect of glycosylation on T-cell function in MS**	**58**
1.24	**Galectin-3 as a potential novel therapeutic target**	**61**
1.25	**Investigating the adult neural stem cell niche in TMEV**	**64**

1.1 Multiple sclerosis

Multiple sclerosis (MS) is an inflammatory disease of the central nervous system white and grey matter, characterised by demyelination of axons, focal T-cell and macrophage infiltrates and a loss of neurological function. Symptoms include, but are not limited to, cognitive impairments, musculoskeletal weakness, spasms, ataxia and pain (Paty et al., 1994). Approximately 2.5 million people worldwide are afflicted with MS. Diagnosis is based on symptomatic episodes and MRI evidence of demyelinated lesions within the central nervous system (CNS) (Polman et al., 2011). MS lesions are heterogeneous in nature and defined by inflammation, demyelination and variable degrees of axonal damage. Patients with MS typically develop symptoms between the ages of 20 and 40; and women are two times as likely to develop MS compared to men (Alonso and Hernan, 2008). As these patients are affected in their most productive years the resulting impact on their health, employment and social status means that there is likely to be a large socioeconomic cost to the individual, their families, and those countries with a high prevalence of multiple sclerosis (Kobelt et al., 2006; McCrone et al., 2008).

MS can be characterised by three main types of disease (Lublin and Reingold, 1996). The most common form is Relapsing-Remitting MS (RR-MS) affecting over 80% of patients. These patients experience symptoms with short periods of remission, but not a full recovery. Around 65% of patients with RR-MS go on to develop the second kind of MS, secondary chronic progressive (CP-MS), in which they no longer have periods of remission, but symptoms continually get worse. This usually occurs within 15 years from the date of diagnosis. The final 10-20% of MS patients display Primary Progressive MS. In this case, patients do not experience any relief from symptoms but will continually get worse from the point of diagnosis. These patients often become severely handicapped

within 5 years of disease onset. Within these subtypes there is still much heterogeneity as to how the disease will present clinically and which areas are primarily affected, identified by examination of MRI scans and histopathological sections. The etiology that underlies this heterogeneity remains unclear but most likely a complex genetic trait in susceptible individuals translates into different immune abnormalities that can increase their vulnerability to environmental triggers.

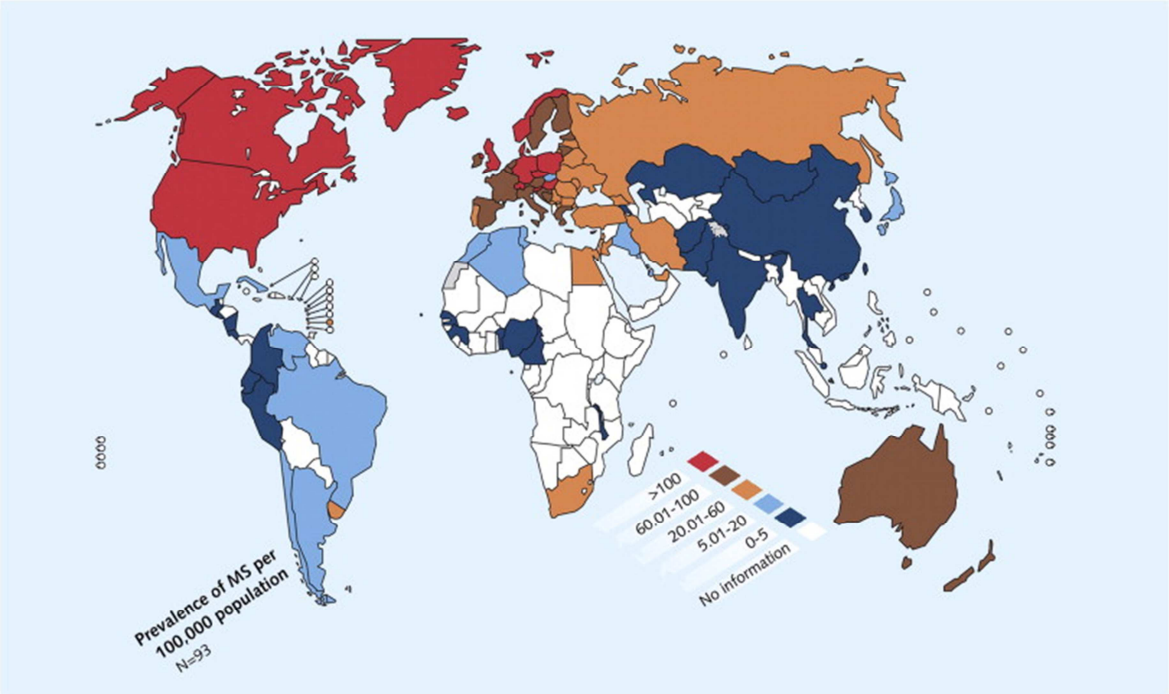


Figure 1.1 The geography of multiple sclerosis: prevalence per 100,00 population (Milo and Kahana, 2010).

1.2 Genetics of multiple sclerosis

MS is a polygenic controlled disease and several candidate susceptibility genes have been identified. Susceptibility appears to be linked to several haplotypes of the MHC locus, specifically, the class II MHC alleles HLA-DR2, DR15 and DQ6 (DRB1*1501 and DQB2*0602 and DQA1*0102) (Gourraud et al., 2012). The HLA*DRB1*1501 haplotype

is carried by 28-33% of Northern Caucasian MS patients compared to 9-15% of healthy controls. Different disease forms of MS are associated with different HLA haplotypes (Lincoln et al., 2005). An Australian study showed that HLA-A3, B7 and DR2 are associated with RR-MS and HLA-A1, B8 and DR3 are more strongly associated with CP-MS (Hammond et al., 1988). Larger genome-wide association studies have identified loci outside the HLA region such as interkeukin-2 receptor α, interleukin-7 receptor α, CD58, IL12A, PTGER4 and TNFRSF1A genes (International Multiple Sclerosis Genetics et al., 2011). Of particular interest to this thesis, a genome wide analysis of 1040 MS patients found mutations in a gene coding for a glycosylation enzyme called MGAT5 were linked to disease progression and severity (Brynedal et al., 2010). The role of glycosylation in MS will be discussed in detail later in the introduction. However, no loci with an effect significantly larger than MHC have been detected, indicating that there is no single major susceptibility gene for MS.

1.3 A viral etiology for multiple sclerosis

Whilst the development of MS can be linked to genetic factors, twin studies show a concordance rate of 25-40% for monozygotic twins, but only 4% for dizygotic twins (Sadovnick et al., 1993). This indicates that genetics are not the sole risk factor for MS but rather they act in concert with environmental factors. Interestingly, there is some evidence that suggests that disease development could be triggered by a viral pathogen. What is unknown is which viral pathogen it may be and when in relation to disease symptom onset this trigger would occur. As disease onset can occur over such a wide age range it is possible that environmental exposure may occur long before the disease becomes clinically evident.

Epidemiological studies of the geographical spread of MS, suggesting a relationship between latitude and disease prevalence, provide supporting evidence for a viral trigger of MS (figure 1.1). Areas with heightened risk of MS include North and Central Europe, the northern USA and Canada as well as Southeastern Australia and New Zealand (Alonso and Hernan, 2008). Strong evidence for a causative infectious agent comes from the Faroe Islands, where before 1940 there were no documented cases of MS. Due to the similarities in gene pool and climate to high risk areas this was considered unusual. In 1940 British Troops occupied the Island and shortly after in 1943 the first cases of MS appeared, suggesting transmission of an unknown infectious agent (Kurtze, 1993). Similar phenomenon have been reported for immigrants from the UK to the northern territories of Australia (Hammond, 2000).

Association studies have named several potential viral candidates. Epstein Barr Virus (EBV, aka Human Herpes Virus 4) has been the most heavily studied and EBV patients appear to have an increased susceptibility to MS (Ascherio et al., 2001). More than 95% of the adult population contain antibodies directed against EBV, suggesting infection may be a prerequisite for development of MS. A study of blood samples collected before the onset of MS, showed that high titres of antibodies to the EBV nuclear antigen complex increases the risk 36-fold for MS (Levin et al., 2005). The risk of MS doubles in individuals who develop EBV induced infectious mononucleosis especially after the age of 15 (Thacker et al., 2006). A substantial proportion of the B cells and plasma cells in the brains of MS patients are infected with EBV (Serafini et al., 2010). Several other candidates have been proposed, including herpes simplex virus 6, measles virus and Torque Teno Virus.

So far all attempts at isolating and proving a causal role for a viral pathogen have failed but several reasons may account for this difficulty including inaccessibility of target

tissue, limited expression of viral antigens and the possibility that the virus cannot be grown in culture. Treatments in current use for MS also provide support for a viral etiology. Polyoma virus reactivation resulting in progressive multifocal leukoencephalopathy (PML) has been observed during immunosuppressive treatment of MS with the humanised monoclonal antibody natalizumub (Tan et al., 2010; Tan et al., 2011). Recombinant IFNβ and natural IFNβ, presently used to treat MS, were originally discovered as broad-spectrum antiviral agents (Billiau, 1977; Weinstock-Guttman et al., 2008). However, it is still unknown if any of the beneficial clinical effect is through an antiviral mechanism of action.

As there is evidence for a viral pathogen component to MS disease development, understanding how chronic viral infections impact upon the CNS may be of great importance in understanding its ability for repair . The work in this dissertation looks at a viral infection model of MS, Theiler's Murine Encephalomyelitis Virus (TMEV).

1.4 Theiler's murine encephalomyelitis model of MS

TMEV was first identified in 1933 by Max Theiler's laboratory (Monteyne et al., 1997). This initial strain only produced a persistent infection in the anterior horn of the spinal cord leading to destruction of neurons. It wasn't until 1950 that Damels identified the DA strain, which caused a chronic white matter disease characterised by focal demyelination. There are now several reported strains that are distinguished from each other by their neurovirulence, as well as other characteristics. TMEV strains are divided into two subgroups. The first group contains strains GDVII and FA that are extremely virulent and induce only acute encephalomyelitis. Whilst almost always fatal, in the few animals that do survive the virus does not persist.

The second group, known as Theiler's Original (TO), include the DA and BeAn strains, and lead to a biphasic disease with early poliomyelitis and later demyelinating disease. Through careful sequencing we know that the capsid proteins of these two viruses have 93% amino acid homology, but that in susceptible SJL mice they produce very different disease phenotypes. Whilst both of these strains lead to demyelinating disease, clinical signs develop early at 30-40 days post infection (dpi) in BeAn infected mice but much later at 140-180 dpi in DA infected mice. Typical symptoms of TMEV include disruption in motor coordination, hind limb paralysis, spasticity, ataxia and incontinence. For this dissertation the BeAn strain of virus was chosen, so it is this strain that I will now focus on for the introduction. This strain was chosen as it has a low neurovirulence that doesn't result in fatalities and clinical signs develop earlier than for some other strains.

1.5 Structure of TMEV BeAN virus

The TMEV virus is a single stranded positive-polarity RNA cardiovirus, a genus of picornavirus. The virus comprises around 8,100 nucleotides organised in the usual picornavirus genomic format (L4-3-4) encoding 12 proteins. The capsid contains 60 copies of each of four polypepetide species, VP1 (37 kDa), VP2 (34 kDa), VP3 (27 kDa), and VP4 (6 kDa) (Luo et al., 1992). The virus enters the host cells after binding to an as yet unidentified receptor. Following entry, the viral RNA is translated into a single polyprotein and is cleaved through the actions of the viral protease protein 3C to give the final product.

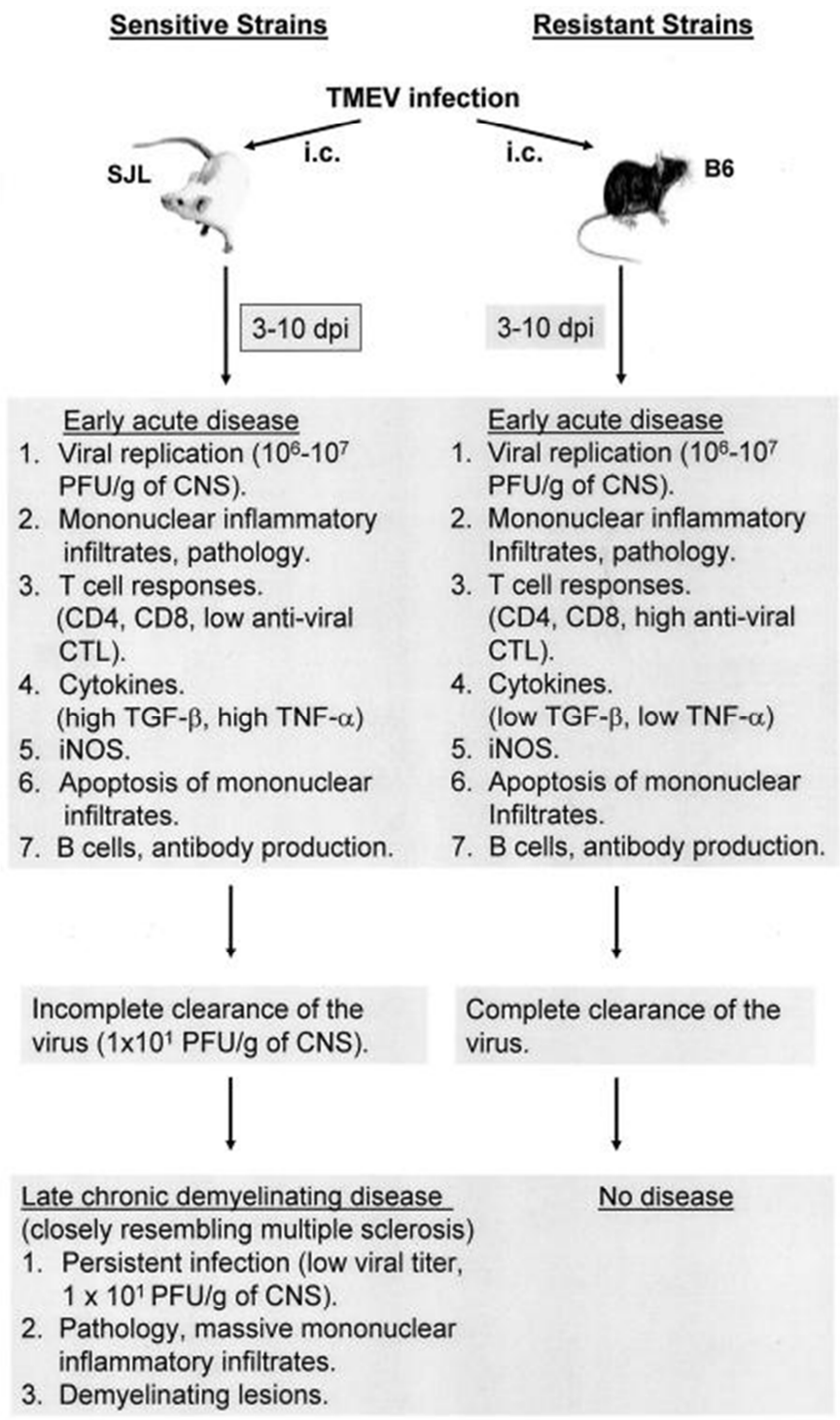


Figure 1.2 Comparison of the immune response to TMEV in resistant and susceptible strains of mice.

In the early stages of the disease there are differences in the immune response between resistant (B6) and susceptible (SJL) strains. Resistant strains are able to completely clear the virus and do not go on to develop demyelination. A failure to clear the virus in susceptible strains develops to a persistent viral infection and a late chronic demyelinating disease. (Oleszak et al., 2004)

1.6 Early pathology of TMEV infection

Different strains of mice have different susceptibilities to TMEV infection. In both susceptible (SJL/J) and resistant (C57BL/6) strains there is acute encephalomyelitis for the first 3-14 days, characterised by variably intense and multifocal inflammation that involves the cerebral and spinal cord grey matter. The inflammatory infiltrate is composed of mononuclear cells including peripheral T cells (CD4 and CD8), macrophages and a few B lymphocytes. Infiltration has a distinct meningeal and perivascular pathology. These early stages tend to be asymptomatic and not clinically apparent. Resistant strains of mice are able to efficiently clear the virus and do not go on to develop demyelinating disease. In contrast, susceptible mice are unable to completely clear the virus and the resulting persistent infection leads to an autoimmune demyelinating disease (figure 1.2). The differences in susceptibility between strains of mice are related to genetic differences and the responses of the immune system (Brahic et al., 2005; Pavelko et al., 2000).

1.6.1 T-cells

Both $CD4^+$ and $CD8^+$ T-cells have important roles in the pathogenesis of TMEV. $CD4^+$ cells can be divided into T helper (Th) 1 and Th2 subtypes. Studies in susceptible SJL mice, show that a Th1 response to viral capsid proteins is involved in the pathogenesis of demyelination. The $CD4^+$ T-cell response assists in the clearance of virus through induction and maintenance of $CD8^+$ cytotoxic lymphocytes (CTL), activation of microglia and production of anti-virus antibodies. $CD4^+$ cells recognise three predominant viral epitopes ($VP1_{233-250}$, $VP2_{74-86}$, and $VP3_{24-37}$) (Gerety et al., 1994; Yauch and Kim, 1994). Whilst numbers of $CD4^+$ cells are higher in SJL than B6 mice less than 4% are reactive to these epitopes compared to over 40% in B6 mice. Nevertheless, the overall level of $CD4^+$

T-cells in SJL mice is significantly higher in susceptible SJL mice, suggesting that either the majority of $CD4^+$ T-cells in SJL mice are non-functional or reactive to epitopes derived from non-capsid viral proteins (Jin et al., 2009).

C57BL/6 mice may be more disease resistant due to their ability to mount a strong and effective $CD8^+$ T-cell response that rapidly clears the viral infection. $CD8^+$ T cells from TMEV-IDD resistant C57BL/6 mice respond to three CD8 epitopes ($VP2_{121–131,}$ $VP2_{165–173,}$ $VP2_{110–120}$) and T-cells specific for all three epitopes, produce IFNγ and efficiently lyse virus-infected target cells (Borson et al., 1997; Dethlefs et al., 1997). $CD8^+$ T-cells from susceptible SJL/J mice can also response to capsid protein epitopes ($VP3_{159–166}$, $VP3_{173–181}$ and $VP1_{11–20)}$ but IFNγ levels are lower and the $VP1_{11–20}$ specific T cells are non-lytic (Kang et al., 2002). As well as having less efficient CTL responses compared to resistant mice, $CD8^+$ T-cells occur at 3-fold lower frequencies in SJL/J mice (Lyman et al., 2004). It is possible that SJL mice are unable to generate a proper CD8 CTL response due to high levels of TGFβ, which has a strong immunosuppressive effect, as transcripts are expressed in SJL mice 9 to 10 times higher than in B6 mice (Chang et al., 2000).

1.6.2 Mechanisms of axonal damage

TMEV predominantly infects neurons in the acute stages of infection (Tsunoda et al., 2003). Infected neurons are found in the grey matter, including the cerebral cortex, hippocampus and anterior horns of the spinal cord. TMEV infection of neurons can lead to apoptosis, shown by chromatin condensation and apoptotic (fragmented) nuclei (karyorrhexis) (Tsunoda et al., 1997). Wallerian degeneration of axons due to this apoptosis is still detected in the late chronic phases, 6 to 9 months after infection. Since TMEV is able to use axons to disseminate through the CNS, axonal degeneration may be a

beneficial self-destructive mechanism to attempt to limit spread of the virus. Indeed, elimination of virus infected host cells by apoptosis, prior to the assembly of infectious virion, can inhibit viral replication in the CNS and contribute to the induction of virus specific CTLs (Tsunoda, 2008).

These regions of damaged axons correspond to areas of subsequent demyelination during the chronic phase. Damaged axons are not associated with T-cell infiltration until the chronic phase (1 month post-infection) suggesting that degeneration itself, as well as virus-infected glial cells, can contribute to recruitment of T-cells into the CNS leading to demyelination. This is consistent with an accumulating body of evidence for an inside-out model of demyelination where axonal degeneration precedes the loss of oligodendrocytes. In MS, axonal injury does not always correlate with the number of $CD3^+$ T cells (Bitsch et al., 2000) or with plaque load (DeLuca et al., 2006). Axonal damage occurs early on in the course of MS and is not only present in active lesions, but also in normal appearing peri-plaque white matter, displaying no overt signs of demyelination (Bjartmar et al., 2001; Kuhlmann et al., 2002). This may be indicative of a viral trigger for MS. Axonal damage has been reported after several viral infections, including human immunodeficiency virus (Zhang et al., 2011), human T-lymphotropic virus 1 (Endo and Tsukamoto, 1997), herpes simplex virus (Zambrano et al., 2008) and mouse hepatitis virus (Das Sarma et al., 2009), which also cause demyelination.

What is most likely is that inside-out demyelination, potentially virally triggered, can develop into outside-in demyelination (myelin loss precedes axonal loss). Activated microglia act as APCs and present myelin debris to $CD4^+$ T-cells, this leads to production of inflammatory cytokines and recruitment of $CD8^+$ T cells, that attack oligodendrocyte myelin sheaths from the outside, leading to secondary axonal degeneration. In this scenario the two models act in synergy and further drive the deleterious immune cascades

promoting even further disease progression. This concept has great importance when considering therapeutic strategies aimed at remyelination discussed in detail later in this introduction. If axonal death occurs independently of oligodendrocyte death then remyelination may not be enough to preserve axon integrity and prevent degeneration.

1.6.3 Viral persistence

Viral persistence is a prerequisite for developing late chronic demyelinating disease following TMEV infection and only occurs in susceptible strains. In the chronic stages viral replication of the TMEV virus persists within the CNS at levels of 10^3 to 10^6 plaque forming units/g CNS tissue in macrophages, oligodendrocytes and astrocytes (Lipton et al., 2005; Trottier et al., 2001). Direct infection of neurons is much less apparent at later stages. Virus persistence during the chronic stages is partially explained by a limited viral protein synthesis which induces only a mild cytopathic effect, and therefore allows the virus to bypass immunological clearance in susceptible mice (Obuchi and Ohara, 1999).

Along with viral persistence, autoimmune responses to myelin antigens generated through epitope spreading, may also play a role in propagating the disease (Miller and Eagar, 2001; Miller et al., 2001). Epitope spreading is an acquisition of reactivity resulting from endogenous *de novo* priming to self-antigens generated from the destruction of myelin, such as myelin basic protein (MBP), proteolipid protein (PLP) and myelin oligodendrocyte glycoprotein (MOG). Epitope spreading is believed to be a good candidate for the development of demyelinating disease as new myelin reactive $CD4^+$ T-cells only appear after myelin damage has occurred. The first clinical symptoms appear at 30 to 40 days post infection (dpi) due to axonal death but it isn't until around 50 to 60 days post infection (dpi) that specific T-cell responses against PLP begin to appear (Miller et

al., 1997). It is also possible that T-cells specific for viral antigens are able to cross-react with myelin antigens thereby attacking the myelin sheath in a process known as molecular mimicry (Olson et al., 2001; Olson et al., 2005).

1.6.4 Demyelination and remyelination

There is so far no consensus about the exact mechanisms that cause demyelination in the TMEV model. It may be a secondary consequence due to the axonal damage discussed above or due to attack from autoimmune T-cells. Alternatively, TMEV may have a direct lytic effect on oligodendrocytes in the absence of immune cells, as direct infection has been demonstrated both *in vivo* and *in vitro* (O'Shea et al., 1997). Another possibility is oligodendrocyte damage through cytokines and immune mediators secreted from virally infected microglia or excitotoxicity mediated by glutamate from infected astrocytes (Carlson et al., 2010).

A key feature of TMEV is that there is very limited remyelination, although increases in $NG2^+$ oligodendrocyte precursor cells have been reported after TMEV (Ulrich et al., 2008). Direct viral infection of oligodendrocyte precursor cells can cause a dysregulation and block of oligodendrocyte maturation (Pringproa et al., 2010; Ulrich et al., 2008). Whilst it is unclear whether T-cell responses directly induce demyelination, it does appear that they can prevent remyelination. Depletion of $CD4^+$ and $CD8^+$ T cells with monoclonal antibodies enhanced remyelination in the spinal cord (Miller et al., 1994). C57BL/6 mice show signs of remyelination once T-cell responses have decreased whilst SJL mice show minimal, if any, myelin repair whilst $CD8^+$ T-cells are present (Njenga et al., 1999). This strongly indicates that T-cell mediated inflammation may be detrimental to the ability of endogenous stem cells to mediate repair. To date we still have little

understanding of how the presence of T-cells may impact upon neural stem cells. In this thesis I hope to address how infiltrating T-cells can impact upon one particular population of stem cells in the subventricular zone.

1.7 Similarities between human MS and TMEV

Several features of MS have been successfully captured by the TMEV model, as the virus-induced pathology has clear similarities to human MS. Inflammatory infiltrates in both TMEV and MS consist of predominantly lymphocytes and macrophages, with similar patterns of perivascular infiltration through small and medium sized blood vessels. In both TMEV infection and MS disease demyelinating lesions have similar morphological patterns of oligodendrocyte damage and cell death accompanied by axonal damage. T1 hypointensities, commonly called 'black holes' are correlated to disability in human MS patients and, through studies in TMEV mice, $CD8^+$ T-cells have been shown to be responsible for their formation (Pirko et al., 2008).

In recent years, several human cardioviruses have been identified although whether they are related to autoimmune disease remains very controversial (Liang et al., 2008). Cardioviruses in humans are most frequently found in the gastrointestinal tract (GI). This is very similar to murine TMEV, where naturally acquired TMEV infections affect the GI tract, with only a very small percentage of mice developing a demyelinating disease (Brahic et al., 2005). Recently, a new virus was isolated from the stool of an infant with a high fever, named Saffold virus (SAFV) (Jones et al., 2007) and its sequence was found to be similar to TMEV (Liang et al., 2008). There are now 8 identified strains of SAFV, of which the most interesting so far is SAFV-3. SAFV-3 infection occurs early in life and shows a seroprevalence of over 90% in older children and adults (Zoll et al., 2009). A high

prevalence is considered a prerequisite for a potential candidate virus to cause MS. Despite unsuccessful attempts to look for cardiovirus' in MS patients (Chiu et al., 2008) the isolation of SAFV-3 from the CSF of a 9-year old boy with aseptic meningitis suggests that SAFV may have CNS tropism and pathogenicity (Himeda and Ohara, 2012).

B cells have been shown to play an important role in human MS as well as in animals models of MS. It has long been known that there is an increase in antibodies in the CSF of patients with MS as well as an increase in memory B cells (Johnson and Nelson, 1977; Perez et al., 1995). The prognosis of patients with an increase in oligoclonal bands in the CSF is worse than those with evidence of fewer oligoclonal bands and presence of memory B cells in the CSF has often correlated with a more rapid progression of disability (Lucchinetti et al., 2000). It has been observed that an antibody response is also required for protection from TMEV in B6 mice, although these studies were done in the absence of $CD8^+$ T cells as well (Kang et al., 2005).

1.8 Experimental autoimmune encephalomyelitis

Whilst the focus of this thesis is the TMEV model, the vast majority of what we know about the subventricular zone discussed in the rest of this introduction has come from the more extensively studied experimental autoimmune encephalomyelitis (EAE) model. EAE is induced by subcutaneous injection of an emulsion that contains an adjuvant and synthetic peptides derived from myelin proteins: myelin oligodendrocyte glycoprotein (MOG), myelin basic protein (MBP) or proteolipid protein (PLP). Immunisation leads to activation and expansion of peripheral antigen-specific T-cells. These enter the CNS, encounter the specific myelin antigen and subsequently induce disease. $CD4^+$ Th1 cells are generally considered the primary mediators in EAE development, unlike TMEV that has a

large $CD8^+$ component. In contrast to TMEV, which has a chronic progressive pathology, the resultant autoimmune disease in EAE can be progressive or relapsing-remitting.

1.9 Relevance of animal models for drug development

A number of partially effective treatments for MS are now available (Denic et al., 2011). Three of these treatments, glatiramer acetate, mitoxantron and natalizumub, came directly from the EAE model. However, many more therapeutic approaches that looked promising in EAE ultimately turned out to be either inefficient or, in rare cases, harmful to humans (Rossi et al., 2012). Natalizumab is associated with patients developing progressive multifocal leukoencephalopathy (PML) due to reactivation of latent JC virus in the brain (Bellizzi et al., 2012). Fingolimod can increase the risk of herpes infections and paradoxical activation of MS (Cohen and Chun, 2011). A recent assessment of MS related clinical trials proposed that treatments effective in TMEV appear more likely to predict a positive impact on MS than effective EAE treatments (Nelson et al., 2004). As several side effects are related directly to reactivation of latent viruses, or vulnerability to viral infection, TMEV may prove a strong model to test future drugs. Encouragingly, every currently available treatment for MS is effective in TMEV and the potential role of anti-glatiramer acetate antibodies in remyelination was first described in TMEV (Ure and Rodriguez, 2002).

1.10 Stem cells for treatment of multiple sclerosis

For many years there has been a great motivation to further our understanding of whether stem cells, from a variety of sources, could be utilised for remyelination and replacement of neurons in MS. The term ‘stem-cell’ can be used to define populations of cells characterised by an ability to self-renew and display multipotency. Clinical approaches to

multiple sclerosis can generally be grouped into 3 categories: (1) the transplantation of diverse populations of exogenous stem cells derived from embryonic tissues, foetal and adult brains and immortalised cell lines, (2) the transplantation of autologous stem cells such as mesenchymal stem cells or fibroblast derived iPS cell lines and (3) the stimulation of endogenous multipotent stem cells such as adult neural stem cells. Several proof-of-concept studies have shown that injection of autologous stem cells into MS patients may provide some degree of neuroprotection (Connick et al., 2012; Odinak et al., 2011; Xu et al., 2011; Yamout et al., 2010).

This thesis will concentrate of a population of neural stem cells that are found endogenously in the adult subventricular zone (SVZ). There will be a particular focus on how inflammation in MS can impact upon the homeostasis of the stem cell niche and affect parameters such as proliferation, the migration of progenitor cells and their ability to divert from normal migratory pathways to relocate to areas of tissue damage. The following sections review our current understanding of the endogenous neural stem cell population in both human and animal models of MS, as well as its therapeutic potential.

The SVZ is of particular interest as a source of endogenous stem cells that can circumvent problems with immune rejection associated with cell transplantation (Ashton-Chess et al., 2006; Barker and Widner, 2004; D'Intino et al., 2006). Recent studies have shown that neurogenesis increases in response to brain injuries such as stroke (Katakowski et al., 2007) and in neurodegenerative conditions such as Alzheimer's disease (Sotthibundhu et al., 2009) and Huntington's disease (Jin et al., 2005). These newly generated cells have the capacity to migrate long distances into damaged regions and differentiate into functional neural stem cells (Zhang et al., 2007). Following ischemia SVZ derived cells were able to migrate into the cortex and differentiate into mature neurons (Kreuzberg et al., 2010). As well as being able to migrate substantial distances

neural progenitor cells are multipotent and can differentiate into neurons, astrocytes and oligodendrocytes. High migration potential and the ability to differentiate into myelin-forming cells have been described as crucial properties in cell repair therapies for demyelinating diseases (Blakemore and Franklin, 2000). Therefore, recruitment of oligodendrocytes by stimulation of endogenous neural stem cells (NSCs) derived from the SVZ may be a feasible method for remyelination. The study of NSCs for repair is still in its infancy and a greater understanding of how pathology in diseases like MS affects proliferation, migration, differentiation and survival of NSCs and their progeny is critical for the development of cell replacement therapies.

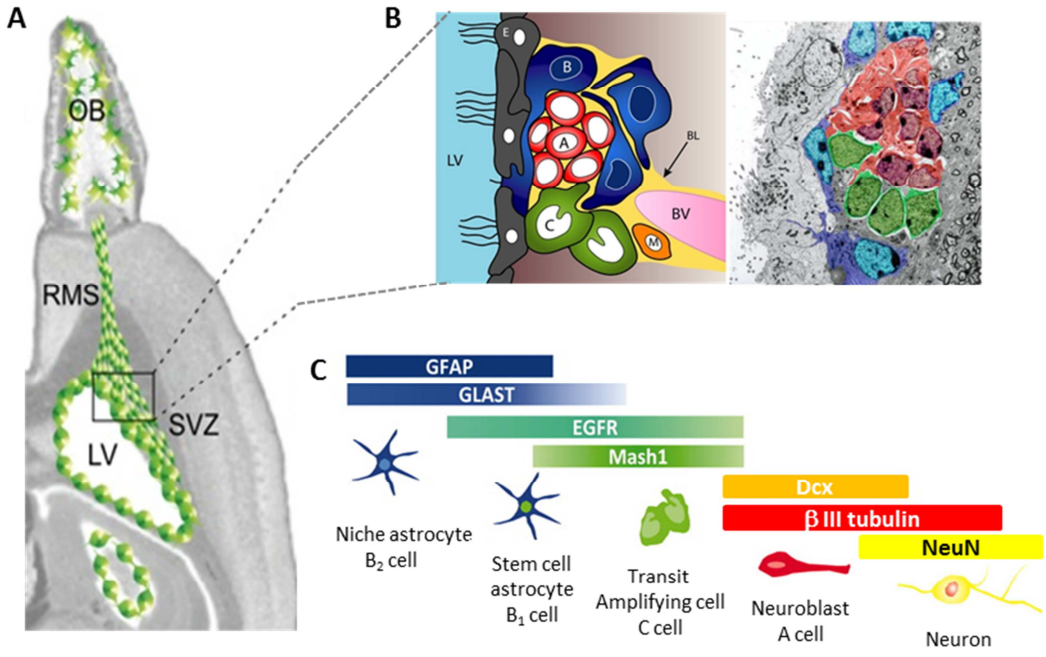


Figure 1.3 The adult SVZ niche in mice

(A) The SVZ lines the lateral ventricles where migrating cells form the rostral migratory stream (RMS) that extends to the olfactory bulb (OB).

(B) Schematic and electron-micrograph of the SVZ showing the different cell types and their anatomical relationship. The SVZ niche is also made up of other non-cellular components including cerebrospinal fluid (LV), blood vessels (BV) and microglia (M).

(C) Common molecular markers used to label SVZ cell types. Note the overlapping expression of several markers such as EGFR, Mash-1, βIII-tubulin and NeuN in different cell types.

(Modified from Doetsch et al, 1997 and Pastrana et al, 2009)

1.11 Adult neurogenesis

In the mammalian brain endogenous neural stem cells reside in two distinct populations and continue to generate neurons throughout adult life in a process called neurogenesis. This process occurs in the SVZ which lines the lateral ventricles and the subgranular zone (SGZ) of the hippocampal dentate gyrus. Adult neurogenesis has been reported in many mammalian species examined including mice, rats, cats, dogs, as well as non-human primates and humans. The SVZ is a specialised stem cell niche where astrocyte-like stem cells (type B cells) and progenitor cells (type C cells) reside and give rise to neuroblasts (type A cells) that migrate long distances through the rostral migratory stream (RMS) to the olfactory bulb (OB). In the OB the majority become GABAergic interneurons (Lois and Alvarez-Buylla, 1994) and fewer glutamatergic interneurons (Brill et al., 2009). Deficient adult neurogenesis has been implicated with a broad range of neurodevelopmental and neurodegenerative disease but the mechanisms that result in this are still poorly understood.

1.12 The SVZ neural stem cell niche

The adult neural stem cell niche is defined by a unique region of tissue which contains stem cells and regulates their self-renewal and production of progeny *in vivo* (Conover and Notti, 2008). The SVZ is an adult neural stem cell niche and is composed of several distinct cell types involved in the generation of new neurons and the regulation of the niche (Doetsch et al., 1997). Radial glia are derived from astrocyte-like stem cells, which express glial fibrillary acidic protein (GFAP), slowly divide to give rise to transit amplifying progenitors (TAGs) (Doetsch et al., 1999). These Mash-1^{+} progenitors rapidly divide to generate doublecortin- (Dcx) and PSA-NCAM expressing neural precursors (neuroblasts). These young neurons migrate tangentially in long chains through the RMS to the OB and differentiate into interneurons. A variety of different cellular and molecular

signalling pathways regulate the processes of quiescence, proliferation, migration and differentiation. Involved in this regulation are several other cell types present in the SVZ including $GFAP^+$ niche astrocytes, microglia, vimentin/s100β expressing ependymal cells and the vasculature (Conover and Notti, 2008). The niche is also regulated by molecules from the cerebral spinal fluid and blood (Ihrie and Alvarez-Buylla, 2011) and through interactions with the extracellular matrix (ECM).

1.13 Oligodendrocyte production in the SVZ

In the adult brain, mature myelinating oligodendrocytes come from oligodendrocyte precursors cells (OPCs) that are either locally resident in the brain parenchyma (Fancy et al., 2004) or migrate from the SVZ (Menn et al., 2006; Nait-Oumesmar et al., 1999; Picard-Riera et al., 2002). Local precursors in the parenchyma express the chrondroitin sulphate proteoglycan NG2, the ganglioside GD3 and the platelet-derived growth factor-alpha receptor (PDGFRα). These $NG2^+/GD3^+/PDGFR\alpha^+$ precursors can actively respond to demyelination through proliferation and differentiation into mature oligodendrocytes, but show little ability to migrate extensively (Fancy et al., 2004).

In the SVZ, the type-B cells are able to produce OPCs that migrate radially to populate the white matter tracts of the corpus callosum, fimbria fornix and striatum and differentiate into myelinating oligodendrocytes (Gonzalez-Perez et al., 2009). This occurs in parallel to the normal tangential migration to the RMS. SVZ type B cells produce a small population of intermediate transit amplifying cells that express the transcription factor Olig2 (Hack et al., 2004; Menn et al., 2006) which encodes basic helix-loop-helix transcription factor proteins that are crucial in generation of OPCs (Rowitch, 2004). These Olig2 cells do not participate in cell genesis in the olfactory bulb but leave the SVZ or RMS to migrate toward the corpus callosum, striatum, and fimbria fornix where they

differentiate into either $NG2^+$/PSA-$NCAM^+$ glia or mature myelinating oligodendrocytes. These $NG2^+$ cells express an identical pattern of marker proteins, including Dlx, Mash1 and LeX, as Type C progenitor cells *in vitro* (Aguirre et al., 2005). However, C cells in the SVZ do not express NG2 and the exact lineage relationship is not yet clear. Under normal conditions, production of oligodendrocytes from SVZ type B cells in the SVZ is scarce when compared to the numbers of neurons produced (Menn et al., 2006).

1.14 The role of remyelination and the SVZ in human multiple sclerosis

To achieve consistent increased remyelination the rescuing cells have to be attracted to the lesion, protected from damage and induced to proliferate and remyelinate over prolonged periods of time, which becomes even more difficult with continued progression of the underlying disease. Shadow plaques represent fully remyelinated lesions demonstrating that complete repair may be possible, but it is more common to find oligodendrocyte precursors near the edges of plaques in MS (Lucchinetti et al., 1999; Wilson et al., 2006; Wolswijk, 1998). One particularly interesting study examining brain tissue from 51 MS patients found that the extent of remyelination differed markedly between patients. Some patients primarily had fully remyelinated lesions whereas others mainly had sparse remyelination that was restricted to small zones at the edges of lesions (Patrikios et al., 2006). Further study will clarify why remyelination is widespread in some patients but sparse in others. This heterogeneity is most likely related to inflammatory mechanisms and greater understanding of how inflammatory molecules influence endogenous stem cells will be beneficial.

The high migration potential and the ability for SVZ derived OPCs to differentiate into mature myelinating oligodendrocytes means they are strong candidates as the source of these remyelinating cells (Blakemore et al., 2000). Indeed, the generation of OPCs and

neuronal precursors from SVZ progenitors increases significantly in the presence of demyelinating lesions (Nait-Oumesmar et al., 1999; Picard-Riera et al., 2002; Wu et al., 2009). However, a large problem with studying the function of SVZ derived precursors in human MS, is our inability to use cell tracers or transgenic markers making it very difficult to confirm the origin of these cells and distinguish SVZ progenitors from local parenchymal progenitors.

In mammals, the main function of the SVZ in adulthood is to provide new neurons to the olfactory bulb, important in olfactory function. Common olfactory deficits in MS patients, such as reduced odour thresholds, identification and discrimination may represent abnormal functioning of the SVZ (Demarquay et al., 2007). Impairment in olfactory dysfunction is more common in patients with secondary progressive than relapsing-remitting or primary progressive MS (Silva et al., 2012). Although, in another study the threshold for odour perception was impaired most in patients with clinically active lesions (Lutterotti et al., 2011). Goektas and colleagues showed in mice there was a strong correlation between decreased olfactory function and a decrease in olfactory bulb volume (Goektas et al., 2011). However, caution should be used when assuming that olfactory deficits may indicate changes in the subventricular zone as recent evidence suggests that neuroblast migration through the RMS is nearly extinct by adulthood in humans and its role in human olfaction is questionable (Sanai et al., 2011). Despite these limitations there is strong evidence to suppose that therapeutic stimulation of endogenous stem cells may have great potential for promoting oligodendrocyte production and remyelination in individuals with MS.

1.15 Mechanisms of remyelination

The use of animal models of demyelination has greatly expanded our understanding of changes that occur in the SVZ during demyelination and helped elucidate some of the mechanisms that may regulate these changes. As is seen in human MS, animal models of demyelination show similar increases in proliferation of neural progenitor cells as well as enhanced production and mobilisation of OPCs (Gensert and Goldman, 1997; Picard-Riera et al., 2002). One study of EAE in rats suggests that this increase in actively dividing cells may occur through a shortening of the cell cycle length in G1 phase as a means to regenerate a depleted progenitor pool caused by increased migration (Sajad et al., 2011a).

1.15.1 Change in cell fate

The increase in the endogenous stem cell pool after demyelination suggests that external signals may promote the gain-of-function of Olig2 in SVZ progenitor cells which stimulates myelination (Jablonska et al., 2010; Maire et al., 2010). Lysolecithin induced demyelination increases the number of $GAD65^{+}Olig2^{+}$ cells (Jablonska et al., 2010) and after cuprizone induced demyelination there is an increase in $BrdU^{+}GFAP^{+}Olig2^{+}$ cells (Chen et al., 2012). Studies suggest a mechanism where BMPs regulate the directional differentiation of OPCs, and Olig2 inhibition of BMP2/4-mediated astroglial differentiation may act as a molecular switch during the glial subtype specification of progenitor cells in demyelinating diseases. This is supported as the infusion of noggin, a BMP inhibitor, into the lateral ventricles of cuprizone-treated mice increases the number of $GFAP^{+}$ cells and decreases the number of $Olig2^{+}$ oligodendrocytes in the SVZ (Cate et al., 2010).

1.15.2 Enhancing proliferation

Increasing evidence suggests that EGF may be a key regulator of oligodendrocyte production and a potential means to increase oligodendrocyte production (Aguirre and Gallo, 2007). Epidermal growth factor is a small protein (6045 Da) that acts by binding to EGFR on the cell membrane and triggering intrinsic protein-tyrosine kinase activity (Povlsen et al., 2008). EGFR overexpression in the SVZ during early postnatal development expands the population of $NG2^{+}Mash1^{+}Olig2^{+}$ progenitors and enhances oligodendrocyte generation (Aguirre et al., 2005). Intracerebral infusion of EGF is able to increase the number of myelinating oligodendrocytes derived from SVZ astrocytes by as much as 300-400%. This ability to produce oligodendrocytes is specific to SVZ astrocytes (Gonzalez-Perez and Alvarez-Buylla, 2011; Gonzalez-Perez et al., 2009). Several other studies have shown EGF induced increases in highly migratory cells that express NG2, PDGFRα, Olig2 and nestin, a phenotype consistent with OPCs, but that this increase comes at the expense of neuroblast production (Doetsch et al., 2002; Gonzalez-Perez and Quinones-Hinojosa, 2010; Gonzalez-Perez et al., 2009). These OPCs are able to migrate extensively along white matter tracts and blood vessels close to the SVZ, until the EGF is withdrawn, when migration halts and they differentiate into myelinating oligodendrocytes. Experimental models have suggested the use of EGF as a treatment option for demyelination but there is evidence that long lasting constitutive EGF stimulation of OPCs can have undesirable side effects including diffuse hyperplasia in post natal white matter (Ivkovic et al., 2008) and formation of polyp-like structures (Kuhn et al., 1997).

Other growth factors may have similar effects. Nerve growth factor (NGF) improves the clinical signs and recovery of EAE in rodents (Flugel, 2001) and reduces neuropathological deficits in EAE in nonhuman primates (Villosalada, 2000). In NGF-

deprived rats both clinical signs and neuroinflammation are exacerbated (Micera, 2000). This neuroprotective NGF mechanism acts through prevention of immune cell infiltration in rodents (Flugel, 2001) and through enhanced proliferation in the SVZ (Triaca, 2003). One study showed that single injections of the growth factors FGF-2 or TGF-α were sufficient to enhance cell proliferation but were not able to improve cell recruitment to lesions sites in older animals (Decker et al., 2002).

1.15.3 Mobilisation of cells

Recent studies from several laboratories have demonstrated that chemokines play a key role in regulating the migration of stem cells. Oligodendrocyte progenitor cells express numerous types of chemokine receptors (Banisadr et al., 2011). One chemokine shown to be able to regulate OPC migration is SDF-1 secreted by cells in the corpus callosum that attracts cells through its receptor CXCR4 expressed on OPCs in the SVZ. Other reports have indicated that signalling via the CCR2 chemokine receptor may also be important. Indeed, in TMEV MCP-1/CCL2, the ligand for this receptor is highly up-regulated by microglia and astrocytes and CCR2 receptors are expressed by migrating neural progenitors and OPCs (Banisadr et al., 2011; Belmadani et al., 2006; Tran et al., 2007).

1.16 Effects of inflammation on SVZ niche

In MS periventricular white matter is a site of intense inflammation and it can be speculated that involvement of the SVZ in myelin repair would be seriously compromised by these events. Analyses of human SVZ that in proximity to these inflammatory lesions have suggested that increased early oligodendrogenesis and emigration of PSA-NCAM^{+} precursors into the parenchyma occurs irrespective of disease length thus indicating that

prolonged exposure of SVZ cells to repetitive inflammatory insults may not exhaust their proliferative effect (Nait-Oumesmar et al., 2007). However, in this study only a few of these cells were $Olig2^{+}$ and it is not clear to what extent these cells contributed to remyelination. Long term neurogenesis in the SVZ has also been reported for stroke, even with the accumulation of activated microglia (Thored et al., 2009; Thored et al., 2007). In stroke few T-cells are detected and microglial versus T-cell derived immune mediators may influence the SVZ differently.

Whilst models such as lysolecithin injection and cuprizone can provide excellent tools for studying mechanisms of demyelination and remyelination they have strong limitations for studying multiple sclerosis pathology as they provide no understanding on the role inflammation has upon SVZ niche cells. To be able to combine our understanding of inflammation and its effects upon SVZ regulation we need to use inflammation based models like TMEV and EAE.

Using a chronic-progressive whole myelin–induced EAE model Picard-Riera and colleagues (Picard-Riera et al., 2002) showed that at 20 and 30 days post immunisation (DPI) there was an increase in the number of proliferating cells in the SVZ. In contrast to this, using a MOG-peptide induced EAE model Pluchino (Pluchino et al., 2008) found that proliferation decreased at 20, 30 and 60 dpi but it was returning to baseline levels by 90 dpi. Both the type B astrocytes and type C cells showed decreases in numbers with as much as a 39-46% decrease in the type C cells. Other studies have confirmed this decrease in the MOG 35-55 model and found similar decreases in the dentate gyrus (Guo et al., 2010), whereas, in proteolipid protein (PLP)–induced relapsing-remitting EAE in SJL mice SVZ proliferation increased in the acute but not chronic phases (Rasmussen et al., 2011). In spite of studies suggesting that increased SVZ cell proliferation is a prevalent response to demyelination (Magalon et al., 2007; Picard-Riera et al., 2002), refined

analyses reveal there is a more complicated dynamic in SVZ reactivity and mitotic activity depending on mouse strain and the model used and consequently such generalisations may be too simplistic.

One caveat to the models used above is that there are minimal pathological alterations in the forebrain and lesions are disseminated and their location hard to predict. By injecting TNFα/IFNγ stereotactically into the CC it is possible to target EAE induced inflammation to the SVZ (Magalon et al., 2007; Merkler et al., 2006; Pluchino et al., 2008; Tepavcevic et al., 2011). Targeted EAE produced amplification of $Olig2^{+}$ Dlx^{+} pro-oligodendrogenic type C cells accompanied by a 3.3-fold reduction in neuroblast generation, probably through apoptosis of cells. Whilst cytokine injection produced a short term decrease in proliferation (Pluchino et al., 2008; Tepavcevic et al., 2011) changes in neuroblast numbers only occurred after immunisation with MOG. This altered SVZ neurogenesis caused an impairment in long-term olfactory memory which possibly mimics the olfactory dysfunction in MS patients that I have discussed above.

This indicates that the inflammatory environment may be able to influence the temporal and spatial relationship in the neural stem cell niche and thus alter self-renewal, survival, migration and neuronal differentiation (Martino and Pluchino, 2006). However, we know very little about the mechanism and function of the modulation of neurogenesis during inflammatory processes and there still remains a lot to be elucidated. Neuroinflammation during human MS and the mouse models of TMEV and EAE is due to activation of resident microglia and astrocytes and infiltrating immune cells, such as T cells and macrophages (D'Aversa et al., 2012; Tepavcevic et al., 2011).

1.17 Effect of T-cells on neural progenitor cells

There is surprisingly little data about how T-cells can impact upon neural progenitor cells, as most studies have focused on immunomodulation of lymphocytes by exogenously injected NPCs. It remains unclear whether the microenvironment of T-cell infiltration is conducive or hostile to NPCs although given the above studies it is most likely inhibitory. When NPCs are cultured in media from activated cytotoxic $CD8^+$ cells, those most commonly found following TMEV infection, a serine protease called Granzyme B (GrB) released by the T cell impaired both the ability of these cells to proliferate and to differentiate into neurons (Wang et al., 2010b). GrB mediated its effects by the activation of a Gi-protein-coupled receptor leading to decreased intracellular levels of cAMP and subsequent expression of the voltage-dependent potassium channel, Kv1.3, a channel known to be involved in oligodendrocyte differentiation (Chittajallu et al., 2002). T-cells are most likely to influence SVZ cells through the prolife of cytokines that they secrete leading to activation of resident microglia and astrocytes (see figure 1.3).

1.18 Role of microglia in influencing neurogenesis

Microglia are the resident macrophages of the brain parenchyma and play a central role in the inflammatory response. In the healthy brain they are present in a resting state, although previous data from our lab has shown that SVZ microglia may be constitutively in a 'semi-activated' state (Goings et al., 2006). In response to inflammatory signals microglia can rapidly react by changing morphology and acquiring an array of functions including phagocytosis and secretion of inflammatory mediators such as IFNγ, TNFα and IL-1β (Russo et al., 2011).

Several studies have demonstrated that one of these mediators, IFNγ, can inhibit proliferation and oligodendrogenesis both *in vivo* and *in vitro* (Butovsky et al., 2006b; Turbic et al., 2011). Stimulation of microglia by high levels of IFNγ, such as Th1 T-cells would secrete, imposed on them a phenotype that impeded oligodendrogenesis from adult NPCs most likely through up-regulation of TNFα. However, when microglia were stimulated with IL-4, as would be secreted by Th2 T-cells, the impediment on oligodendrogenesis was reversed, an effect mediated at least in part by insulin-like growth factor-1 (Butovsky et al., 2006b). This was confirmed as injection of IL-4 activated microglia into the spinal cord of rodents with acute or chronic EAE resulted in increased oligodendrogenesis and improved clinical symptoms (Butovsky et al., 2006a). Similarly, stimulation of SVZ-derived neurospheres from EAE mice with pro- (Th1) but not anti- (Th2) inflammatory cytokines increased the number of quiescent NPCs by up to 70%. This suggests that these cytokines may also be able to regulate cell cycle by up-regulation of cell cycle inhibitors (Pluchino et al., 2008).

Some models of EAE such as the SJL relapsing-remitting model show persistent activation of microglia in forebrain regions. This was accompanied by an initial increase in proliferation in the acute phase but in subsequent relapses proliferation remained unchanged (Rasmussen et al., 2011). This raises an interesting question of whether recurrent bouts of inflammation can induce permanent changes in the SVZ niche that leads to irreversible failure of homeostatic and repair capabilities. There is strong evidence that chronic activation of microglia produces an environment that is non-permissive for repair as specific inactivation of microglia with minocycline ameliorates the loss of reparative potential of endogenous stem cells in the chronic stages with increased $NG2^{+}$ OPC precursor production (Rasmussen et al., 2011). This makes it a strong possibility that the phenotype of infiltrating T cells and hence the secreted cytokine milieu can have a long

term impact on neurogenesis. It does raise the hope though that the ability to regulate T-cell phenotypes in autoimmune disease may allow us to modulate neurogenesis.

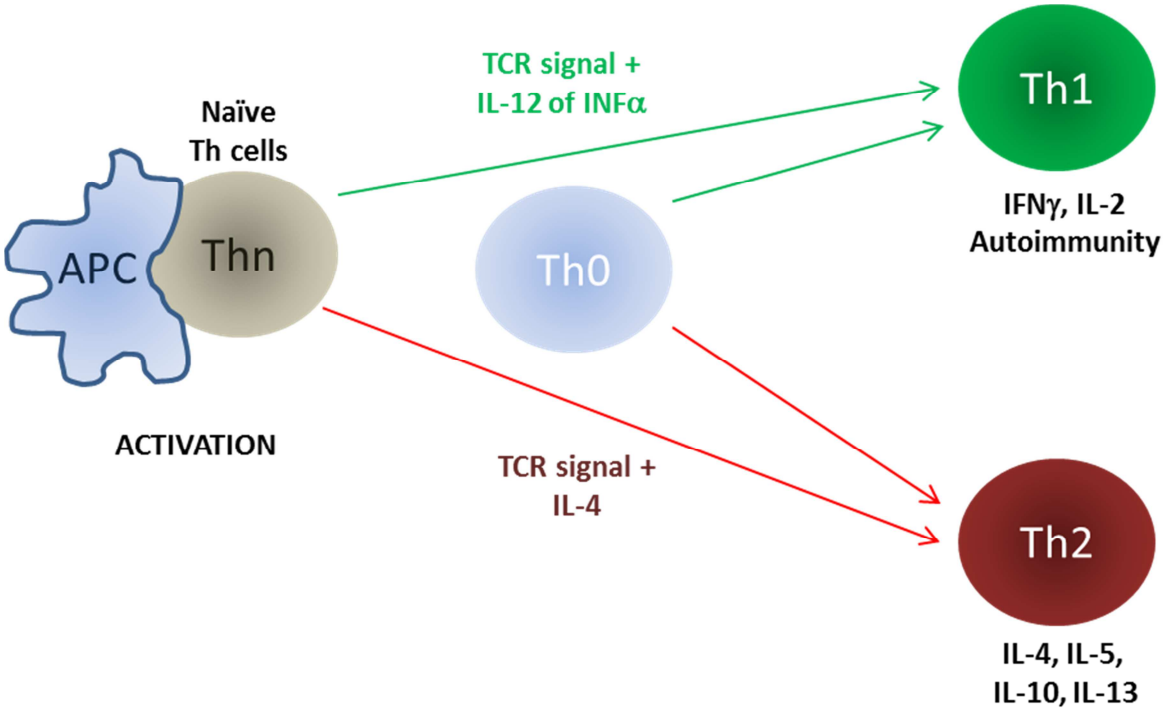


Figure 1.4 Th1 and Th2 differentiation produces different cytokine profiles.

Naïve TH cells are activated by antigen presenting cells (APC), presenting an appropriate peptide via MHC class II molecules. When they are activated in the presence of co-stimulatory signals can produce different arrays of cytokines. Th0 cells stimulated with IL-12 or IFNα become TH1 cells which produce IL-1 and IFNγ. These Th1 cells are largely responsible for autoimmune diseases. When stimulated to proliferate in the presence of IL-1 they become polarised Th2 cells which produce IL-4, IL-5, IL-10 and IL-13 but no IFNγ.

Adapted from (Biederman, Rocken et al. 2004)

1.19 The role of neuroprotection in multiple sclerosis

Whilst the vast majority of MS research has focused on the loss of myelin and oligodendrogenesis it has become increasingly apparent that substantial axonal and neuronal loss are equally important features. During inflammatory demyelination white

matter subcortical neurons are destroyed and the permanent disability in MS can be attributed to the impact that inflammation has on the viability of axons and neurons (Bjartmar and Trapp, 2003; Bjartmar et al., 2003). The majority of chronic lesions have marked neuronal loss but a small subset display an increase in mature interneuron density and cells with phenotypic characteristic of immature neurons (Chang et al., 2008). The discovery of increased PSA-NCAM$^+$ and NeuN$^+$ cells in human subventricular zone suggest some immature white matter interneurons may originate in part from the SVZ (Chang et al., 2008; Nait-Oumesmar et al., 2007).

The importance of neuroprotection and neurogenesis has been very clearly highlighted in recent years with the use of Glatiramer acetate (GA Copaxone, Copolymer 1), an approved drug for the treatment of MS. GA exerts its therapeutic activity by immunomodulating various levels of the immune response, which differ in their degree of specificity (Arnon and Aharoni, 2004). GA treatment applied at various disease phases of EAE augmented neuronal proliferation in both SVZ and dentate gyrus and this effect persisted for a prolonged duration (Aharoni et al., 2005a; Aharoni et al., 2005b). GA treatment also stimulated ectopic migration of Dcx$^+$ neural progenitors into the striatum, nucleus accumbens and cortex where they displayed a mature morphology and the neuronal marker NeuN. The group reported that these cells were not found in non-GA treated EAE mice. Findings from human studies support the notion that GA confers neuroprotection in MS patients as GA reduced the formation of permanent T1 hypo-intense lesions that evolve into ‘‘black holes’’ and have been associated with irreversible neurological disability (Filippi et al., 2001).

Whilst there have been numerous studies examining how EAE induced inflammation affects the neural stem cell niche, to date, the Szele laboratory have conducted the only investigation into how TMEV induced inflammation can affect the

neuroblast population in the chronic stages of the disease (Goings et al., 2008). For my thesis I have examined how high levels of inflammation in the acute stages of TMEV infection alters SVZ niche homeostasis. As the ability to replace damaged neurons has implications in preventing neurological deficits in MS patients I will pay particular attention to how inflammation affects the neural progenitor population. In this thesis I have also addressed the question of whether prolonged inflammation in the TMEV model can have long-term effects on the SVZ niche.

1.20 The Galectin family

As inflammation may have a significant impact on endogenous stem cells finding novel therapeutic targets that can be used for immunomodulation is of great importance. One such potential candidate is the beta-galactoside binding lectin Galectin-3 which has been implicated as a specific regulator of inflammation in many disorders, including multiple sclerosis. The rest of this introduction will focus on the links between Galectin-3 and its related pathways and multiple sclerosis.

So far, 15 mammalian galectins have been identified through evolutionarily conserved amino acid sequences and by recognition of β-galactoside structures by a conserved carbohydrate-recognition-binding domain (CRD). Galectins can be classified into three subtypes based on the number and organisation of their CRD domains. These are the prototype group, the chimera group and the tandem repeat group. The members of the prototype group (galectin-1, -2, -5, -7, -10, -11, -13, -14 and -15) contain only one CRD. Galectin-4, -6, -8, -9 and -12 make up the tandem repeat group that are built of a single polypeptide chains that forms two distinct but homologous CRDs, separated by a linker sequence of up to 70 amino acids.

Galectin-3 is a 29- to 35-kDa protein that has been called many things over the years, Mac-2, CBP-35, εBP, RL-29, HL-29, L-34 and LBP, but in 1994 the protein was finally designated as Galectin-3 (Barondes et al., 1994). As the only member of the chimaera group, Galectin-3 seems to be unique within the galectin family as its single polypeptide chain forms two structurally distinct domains: an unusual long N-terminal domain and a single CRD domain. The N-terminal domain is composed of 110-130 amino acids depending on the species. This relatively flexible structure contains multiple homologue repeats (7-14) which each include a consensus sequence Pro-GLy-Ala-Tyr-Pro-Gly, followed by three additional amino acids. Whilst the N-domain does not have any carbohydrate binding activity it is essential for the full biological activity of galectin-3. As this region is sensitive to proteases, such as collagenase and matrix metalloproteinases (MMPs), the *in vivo* biological activities of galectin-3 are likely to be modulated by these enzymes (Ochieng et al., 1998). The C-terminal domain composed of 130 amino acids forms a globular structure which accommodates the whole carbohydrate binding site and is thus responsible for the lectin activity of gal-3. Binding of the CRD with carbohydrate ligands is accompanied by a conformational change in the protein.

1.21 Glycosylation and galectin-lattices

Glycosylation is a common posttranslational modification made to secretory and membrane-anchored proteins, such as cell-surface receptors, in eukaryotic cells. Within the endoplasmic reticulum (ER) initiating asparagine (N)-linked glycans are added before transportation to the golgi complex for further modifications (Schachter, 1991). N-glycan branching produced in the golgi is generated by the sequential action of the golgi α-mannisidases and n-acetylglucosaminyltransferases I, II, IV and V (encoded by Mgat1,2,4

and 5) and the hexosamine pathway production of the substrate uridine disphophate N-acetyleglucosamine (UDP-GlcNAc). Galectins preferentially bind to β-galactoside containing glycans comprised of repeating units of N-acetyllactosamine (Galb1, 4GlcNAc). Glycoproteins display affinities for galectins in proportion to the number of N-glycans (gene-encoded) and their structural modifications (i.e. N-glycan branching) as a result of passage through the Golgi (Boscher et al., 2011) (figure 1.5).

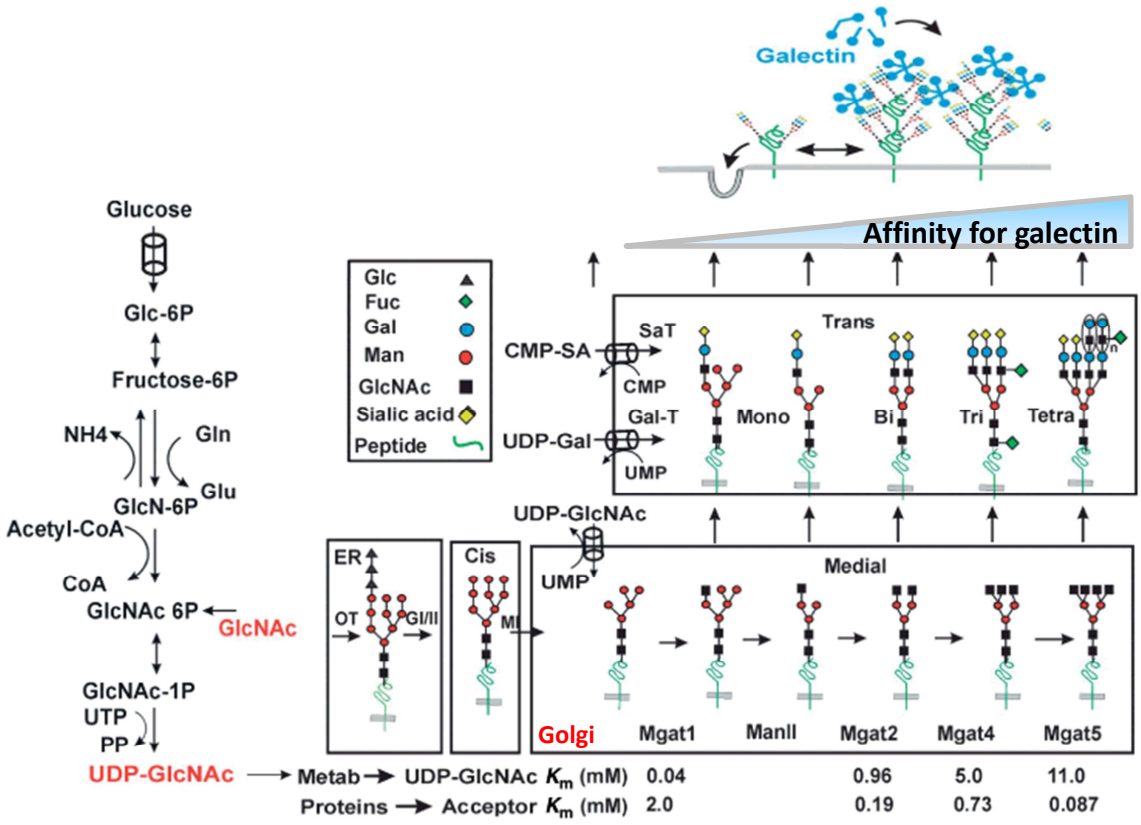


Figure 1.5 Glycosylation pathways and their role in galectin-3 binding.

In glycoproteins sugars are attached to an amide nitrogen atom in the side chain of asparagine (N-linkage). N-linked glycoproteins acquire their initial sugars from Dolichol donors in the endoplasmic reticulum in a reaction called core glycosylation. Glycoproteins transit from the ER to the Golgi en route to the cell surface. The *N*-acetylglucosaminyltransferases, designated by their gene names (Mgat1, Mgat2, Mgat4 and Mgat5), generate branched *N*-glycans that display a range of affinities for galectins. The higher the N-glycan branching the higher the affinity for Galectin.

Adapted from Dennis et al (2009)

Glycoprotein concentrations at the cell surface can be differentially regulated according to their affinities for the galectin family of endogenous lectins. Galectin-3 binds as a monomer to glycosylated proteins through carbohydrate ligand binding and undergoes a conformational change. This enables its oligomerisation (up to pentamers) and the formation of a complex galectin-lattice (Ahmed et al., 2004). The lattice can be regulated through proteolysis by metalloproteinases of the N-terminal domain (Ochieng et al., 1994). The best studied example of the function of this lattice is the regulation of growth factor receptors such as EGFR and TGFR. Growth promoting receptors like EGFR frequently have high numbers of N-glycans (n>5) while growth inhibitory receptors such as TGFR have fewer (N-<5). This allows differential association with the galectin-lattice that is dependent on golgi branching activity thereby regulating cellular transitions from growth to arrest (Lau et al., 2007).

1.22 The importance of glycosylation in multiple sclerosis

Evidence has been building in recent years that multiple sclerosis may be related to dysfunctions in glycosylation. A paper by Mkhikian and colleagues (Mkhikian et al., 2011) recently suggested that multiple environmental factors related to MS susceptibility converge with multiple genetic risk factors (IL7Rα, IL2Rα, MGAT1 and CTLA4) to dysregulate golgi N-glycosylation in MS. Although each seemingly unrelated allele and environmental factor may only have a minor role or biological effect on risk and *N*-glycosylation, when in specific combinations together they can converge to dysregulate a final common pathway and produce a complex trait disease like MS (Grigorian and Demetriou, 2011).

There is also good evidence from genome wide association studies that genes that directly regulate the final stages of glycosylation may also be important. One study on 1913 European patients found 2 single nucleotide polymorphisms (SNPs), that were present in MGAT5 (rs3814022 and rs49539211), which showed persistent correlation with severity scores using the multiple sclerosis severity scale (MSSS) in relapsing remitting patients homozygous for these mutations (Brynedal et al., 2010). A follow up study on a further cohort of 194 Italian MS patients found that these 2 SNPs were not correlated with primary progressive MS (Esposito et al., 2011). However, they did find that 2 different SNPS (rs1257169 and rs539588) showed an association to disease severity in progressive disease. The occurrence of disease bouts and the presence of active lesions also correlates to decreases in GCNT1 activity, a gene important in formation of GlcNAc structures (Orlacchio et al., 1997). This could suggest that mutations at different regions of various glycosylation related genes may be related to different forms of MS.

1.23 Effect of glycosylation on T cell function in MS

These links between defective glycosylation and multiple sclerosis have been most studied as regards the function of T cells. Indeed the main reported effect of reduced GCNT1 activity was deficient glycosylation in lymphocytes taken from MS patients (Orlacchio et al., 1997). Galectin crosslinking to N-glycans on the T-cell receptor (TCR), expressed on the surface of lymphocytes, can modulate the threshold of TCR signalling in response to antigen. T-cell receptors are found on the surface of T lymphocytes and are responsible for recognising antigens bound to major histocompatibility complex (MHC) residues. When the TCR engages with antigen and MHC, the T-lymphocytes is activated through a series of biochemical events that are mediated by associated enzymes, co-receptors, and activated

or released transcription factors. Galectin-3-TCR complex lattices prevent the TCR from clustering at the immune synapse by restricting TCR movement within the plane of the membrane, thus increasing the agonist threshold for TCR signalling (Demetriou et al., 2001). This is a system whereby the cytokines IL-1 and IL-17, secreted upon antigen detection, regulate mRNA expression of golgi glycosylation genes to suppress N-glycan branching and enhance TCR clustering and signalling (Mkhikian et al., 2011). Later on, they promote self-tolerance by enhancing branching so that CTLA-4 is retained at the surface and transmits an inhibitory signal to promote growth arrest (Lau et al., 2007).

Removal of the Mgat5 enzyme from 129sv mice leads to defective N-glycosylation of the T cell receptor. A reduction in Galectin binding due to fewer N-glycans enables TCR clustering with peptide-MHC complexes and induces T cells hyperactivity and proliferation. This can occur even in the absence of the co-stimulatory signal CD28, normally required for T-cell activation. The result of this is a loss of self-tolerance and a heightened sensitivity to EAE (Demetriou et al., 2001). Myelin-reactive $Mgat5^{-/-}$ T-cells were transferred into either $Mgat5^{+/+}$ or $Magt5^{-/-}$ recipients. Transfer into the latter revealed a more severe EAE suggesting that a Mgat5 branching deficiency in recipient naïve T cells and/or non T-cells may contribute to the disease pathogenesis (Grigorian and Demetriou, 2011).

Examination of N-glycan branching differences and golgi enzyme activity reveals differences between resistant and susceptible strains to EAE. Susceptible strains such SJL/J, PL/J and NOD, display defective N-glycan branching in T-cells when compared to resistant strains like 129/sv, BABLc and B10.S (Lee et al., 2007). Targeted deletion of Mgat5 from PL/J mice, who have the lowest levels of N-glycan branching, leads to the development of a spontaneous late-onset clinical MS-like disease manifested by inflammatory demyelination and neurodegeneration. This phenotype was markedly

enhanced in Mgat5$^{+/-}$ and Mgat5$^{-/-}$ genotypes in a dose-dependent manner. Spontaneous disease development was also characterised by neuronal loss and axonal damage, a phenotype also seen in MS even in the absence of inflammation.

It is likely that N-glycosylation is also required for normal function and viability of cell of the CNS such as oligodendrocytes and neurons. Indeed, dysfunction in a different golgi enzyme, Mgat1, results in a unique pattern of glycoprotein deficiency that induces neuronal apoptosis (Ye and Marth, 2004). Mgat1 dysfunction may also expose cryptic mannose linkages on the cell surface of oligodendrocytes that mimics microbial and pathogen glycans, therefore chronically activating the innate immune responses (Ilarregui et al., 2009; Ishii et al., 2007).

It should be noted that whilst Gal-3 has been shown to be a key galectin that binds to Mgat5 end products and is vital in the regulation of TCR expression the exact role of Gal-3 in the Mgat5$^{-/-}$ TCR studies has not been convincingly demonstrated using reagents or tools that were specific to Gal-3. Therefore, the possibility that other galectins, such as Gal-1 function in this capacity cannot be excluded.

Overall, these studies show that deficient glycosylation can act as a positive regulator of T cell growth and activation through up-regulation of inflammatory cytokines and either induce or enhance sensitivity to demyelination. It has been suggested that vitamin D3 deficiency can increase susceptibility to MS. Interestingly when vitamin D_3 ($1,25(OH)_2D_3$) is given orally to mice with EAE it can prevent or markedly reduce symptoms (Lemire and Archer, 1991). The proposed mechanism for this is through increased β1,6GlcNAc-branched N-glycans on T-cells that suppresses T-cell receptor signalling (Grigorian et al., 2007). This raises some very interesting questions about whether supplementation to N-glycan biosynthesis through oral GlcNAc may be a

therapeutic option to suppress the phenotypic expression of MS risk factors (Mkhikian et al., 2011).

1.24 Galectin-3 as a potential novel therapeutic target

Galectins have a key role in the initiation and resolution of many chronic and acute inflammatory processes (Rabinovich et al., 2007). It is currently unknown what role Gal-3 may play in MS pathology. An examination of human post mortem tissue from MS patients showed high levels of galectin-1, -8 and -9 in both active and inactive lesions (Stancic et al., 2011). In contrast, Galectin-3 was only found in chronically active lesions suggesting that enhanced Gal-3 levels are associated with increased inflammatory activity. Interestingly, mRNA levels did not parallel those of the protein implying the presence of post-translational regulation mechanisms. They found that Gal-3 in the lesions was not susceptible to proteolytic cleavage by MMPs suggesting there is a possible additional regulatory mechanism at the translational levels that is unknown as yet. In the human lesions Gal-3 and -1 were localised to astrocytes and microglia, whereas Gal-8 and -9 were only present in microglia.

Jiang and colleagues immunised Gal-3 deficient mice with MOG 35-55 peptide and found they developed a markedly attenuated EAE compared to similarly immunised WT mice (Jiang et al., 2009). This attenuation was accompanied by reduced cellular infiltration of monocytes and macrophages in the CNS and increased apoptosis of CNS infiltrates. The lymph nodes produced less IL-17 and IFNγ, but serum levels of IL-10, IL-5 and IL-13 were increased. They also found a higher frequency of $Foxp3^{+}$ Treg cells. This study did not include any characterisation of Gal-3 expression through immunohistochemistry so it is not known which cell types were responsible for mediating these changes.

The data between the Mgat5 studies and Gal-3 knock-out are in apparent contrast to each other, as Gal-3 deletion attenuates EAE but Mgat5 deletion enhances susceptibility to EAE. This may be connected to the fact that other related galectins (gal-1 and gal-9) which may be upregulated after Gal-3 deletion are able to suppress EAE and are generally considered anti-inflammatory (Offner et al., 1990; Wang et al., 2009; Zhu et al., 2005). Indeed, Gal-1 KO animals show enhanced susceptibility to EAE (Toscano et al., 2007) and suppression of Gal-9 increased clinical severity of symptoms (Zhu et al., 2005).

The data suggests an interesting model where careful adjustment of the levels of select galectins can regulate inflammation: Gal-3 drives proinflammatory mechanisms whilst Gal-1 and Gal-9 work in contrast to control anti-inflammatory mediators. Galectins have been known to target the same cellular counter receptor but elicit different responses through functional divergence (Sanchez-Ruderisch et al., 2010) or the cellular reactivity can be markedly different (Kaltner et al., 2011). Mgat5 deletion reduces N-glycan branches on target proteins that all galectins need to be able to bind and so will have a global effect on galectin function.

One final link between MS and Galectin-3 came from studies showing that Glatiramer Acetate was able to enhance SVZ repair and remyelination. Glatiramer acetate promotes oligodendrogenesis and remyelination after lysolecithin-induced demyelination of the spinal cord and EAE (Aharoni et al., 2005a; Aharoni et al., 2008). When given during chronic disease phases, when substantial demyelination was already manifest, it resulted in a significant decrease in pathological damage (Reichert and Rotshenker, 1999). The Rotshenker et al (1999) study showed GA worked by generating Th2 cells that produced the anti-inflammatory cytokine IL-10 and inhibited the activation and expression of Gal-3 by microglia. This is the only study to date looking at how current treatment

methods for MS may affect galectins but it certainly suggests that this warrants more investigation in the future.

Current treatment strategies are predominated by high cost and modest efficacy with significant side effects that affect tolerability and compliance. An improved understanding of the pathogenesis of MS might identify novel cellular and molecular targets that will allow the development of more effective and specific therapies that can enhance the mobilisation and differentiation of endogenous neural progenitor cells whilst also inhibiting the detrimental aspects of the inflammatory reaction. In this thesis I hope to further understand of the exact role and mechanisms of Galectin-3 in TMEV pathology and its potential to be exploited as a novel target for MS treatment.

1.26 Investigating the adult neural stem cell niche in TMEV

From the review of the literature, it was apparent that despite significant advances in recent years in understanding the role of the SVZ in remyelination, there was insufficient information on how inflammation in models of MS can impact on the SVZ. The overwhelming focus of such studies has been the EAE model. The central theme of this thesis is to examine the changes to the SVZ niche in response to the TMEV viral model of multiple sclerosis. This thesis proposes that TMEV induced inflammation will impact on SVZ homeostasis and cytoarchitecture. Are SVZ components such as cell proliferation, astrocytic ‘glial tubes’, neuroblast chains and emigration altered after TMEV? What inflammatory cells and mediators are present in the SVZ? Can differences between resistant and susceptible strains of mice be used to reveal long-term alterations in niche repair capabilities? In addition, given the unique expression of Gal-3 in the normal SVZ

and its up-regulation in models of inflammation, this thesis proposes the hypothesis that Gal-3 regulates TMEV induced inflammation in the SVZ.

The work in this thesis shows TMEV directly infected SVZ cells accompanied by targeted infiltration of $CD3^+$ cells into the SVZ and surrounding parenchyma. This caused decreased proliferation of SVZ cells and a disruption in neuroblast chain integrity. Decreases in T-cell presence in resistant mice allowed recovery of SVZ proliferation. Resistant and susceptible strains of mice show different constitutive cellular expression of Gal-3 in the SVZ. Gal-3 null mice were used to investigate the role of this carbohydrate binding lectin that was up-regulated at higher levels in resistant B6 mice after TMEV infection. Deletion of Gal-3 prevented the loss of proliferating cells and neuroblasts and in B6 mice enhanced neuroblast emigration and decreased T-cell infiltration. Examination of SVZ cytokine profiles revealed significant differences between SJL and B6 mice after TMEV that may be regulated by Gal-3. These data have far reaching concerns in areas of autoimmunity, chronic viral infection, maintenance of SVZ homeostasis and use of endogenous stem cells for repair. The work in this dissertation outlines several necessary pieces of knowledge about the response of the SVZ to direct viral infection and identifies a novel regulator of SVZ inflammation.

Chapter 2

Materials and Methods

2.1	**Animals**	**67**
2.2	**Galectin-3 null mice**	**67**
2.3	**Genotyping**	**69**
2.4	**TMEV viral production**	**70**
2.5	**TMEV infection of mice**	**70**
2.6	**Immunohistochemistry**	**72**
2.7	**Cell counting**	**77**
2.8	**RT-PCR arrays**	**79**
2.9	**Neurospheres experiments**	**80**
2.10	**Measuring cytokine levels**	**82**
2.11	**Astrocyte culture**	**84**
2.12	**Statistics**	**88**

2.1 Animals

C57BL/6 and SJL/J WT breeding pairs were purchased from Jackson Laboratories (Bar Harbor, ME) and were maintained as in-house breeding colonies. All mice were housed in IVC units at the University of Oxford animal housing facility and were provided with unlimited access to standard laboratory chow and water. Procedures were carried out with the University of Oxford Research Ethics Committee approval, in accordance with the Animals (Scientific Procedures) Act of 1986 (UK). All efforts were made to minimise animal suffering and distress for all experiments.

2.2 Galectin-3 null mice

Galectin-3 null mice on a 129sv background had been previously generated by targeted mutation and homologous recombination by the Poirier Laboratory (Colnot et al., 1998). Briefly, a targeting vector (*tm1Poi*) containing neomycin resistance and herpes simplex virus thymidine kinase gene was used to disrupt a 3.7kb sequence that includes exons 2, 3 and 4 including the initiation codon in exon II. The construct was electroporated into WW6 embryonic stem cells (derived from 129sv, C57BL/6, SJL mixed background mice) and enriched with G418 and gancyclovir. Correctly targeted ES cells were injected into outbred MF1 blastocytes and implanted into pseudo-pregnant dames. The resultant germ-line chimeric male offspring were crossed with female 129sv mice to produce heterozygotes for the recombined allele. These heterozygotes were further crossed to generated homozygotes.

For TMEV experiments $Gal3^{-/-}$ mice on a C57BL/6 background were purchased from Jackson Laboratories (Bar Harbor, ME). These had been previously generated by Richard Cumming's Laboratory (University of Oklahoma) by backcrossing the double

mutant Gal-3/Gal-1 strain to C57BL/6 for 5 generations. After donation to Jackson Laboratories the Lgal1s mutation was removed by selective breeding. Ten pregnant C57BL/6 Lgals3^{tm1Poi} Gal-3$^{+/-}$ breeding pairs were purchased and maintained to generate female Gal-3$^{+/+}$ and Gal-3$^{-/-}$ littermate mice used for *in vivo* experiments. For *in vitro* experiments homozygous x homozygous breeding pairs were set up. These mice exhibit a transient period of hair loss between 2-6 weeks of age with most hair returning by 6 weeks age. It is possible that the movement of the alleles has exacerbated a common phenotype of C57BL/6 alopecia.

In order to examine the effects of Gal-3 deletion in SJL/J susceptible mice the 129sv Gal3$^{-/-}$ mice were backcrossed in-house to SJL/J mice (Jackson Laboratories) for seven generations. Female 129sv Gal-3 heterozygote mice were crossed with male SJL/J WT ($^{+/+}$) and after genotyping of the offspring female heterozygote mice were chosen for the next generation with a new male SJL/J WT breeding partner. We were unable to take the backcross any further than seven generations due to a very high mortality rate amongst litters and very poor breeding due to aversion to other mouse strain pheromones. SJL/J males also exhibited significant aggression often resulting in amyloidosis (sequel of social submissiveness and consequent wounds) in female breeding partners which were often very severe and required culling. The frequency of mutant homozygotes obtained in heterozygote intercrosses was close to the expected 25%. Immunohistochemistry of SVZ tissue was used to ensure no galectin-3 was present in the backcrossed SJL mutants.

2.3 Genotyping

2.3.1 DNA Extraction

The genotype of Gal-3 wildtype, heterozygote and null offspring from both C57BL/6 and SJL/J breeding pairs was determined by analysis of DNA from earclips. DNA was extracted for genotyping polymerase chain reaction (PCR) using the E.Z.N.A Tissue DNA Isolation Kit (Omega Biotek), a Proteinase K-based spin column system. Quality and integrity of DNA was determined using a NanoDrop reader, using a 260/280 ratio of -1.8 for "pure" DNA.

2.3.2 Polymerase chain reaction and gel electrophoresis

Ten microliters of the extracted DNA was added to a master mix for a reaction solution (50 µl final volume) consisting of 1X PCR buffer (10 mM Tris-HCl), pH 8.3, 50 mM KCL; Sigma-Aldrich, Dorset, UK); 0.2 mM dNTP; 0.6 µM neo, Gal-$3^{+/+}$ and Gal-$3^{-/-}$ primers, 2.5 mM MgCl2, 2.5 µl dimethyl sulfoxide (DMSO); 2.5 µL Red Taq Polymerase (1 unit/µL; #D4309, Sigma-Aldrich). The PCR programme consisted of 94°C for 3 min, then 34 cycles with denaturation at 94°C for 45 sec, annealing at 55°C for 30 sec, and elongation at 72°C for 2 min, followed by a final elongation at 72°C for 5 min. The customised primers for both C57BL/6 and SJL/J (Eurofins) were as follows: *neo* 5'-CAC GAA CGT CTT TTG CTC TCT GG-3', *Gal-*$3^{+/+}$ 5'-TGA AAT TAC CGA AAA GCT GTC TGC-3' (single band of -300bp) and Gal-$3^{-/-}$ 5'-GCT TTT CTG GAT TCA TCG ACT GTG G-3' (single band of -500bp).

PCR products were separated by agarose gel electrophoresis (1X TAE buffer, 3% agarose, 5 µg ethidium bromide/100mL agarose) at 100V for 60 minutes. DNA bands were visualised under ultraviolet light and captured by a charge-coupled device digital

camera. Backcrossing onto the SJL/J did not result in any changes in expected genotyping band sizes.

2.4 TMEV viral production

Baby hamster kidney (BHK)-21 cells were propagated in DMEM supplemented with 10% fetal bovine serum, 2 mM L-Glutamine, 100 IU penicillin G/ml and 100 μg of streptomycin/ml. These cells were routinely sub-cultured every 3-4 days. TMEV stock virus was propagated by adding 9 mL of stock to a confluent T75 flask for 24 hours at 37°C. Lysed cells were collected, centrifuged and the stock supernatant kept on ice. The cell pellet was further lysed by sonication for three 30 second bursts, centrifuged and the resulting supernatant added to stock supernatant. This was then made up to 18 mL in volume and added to 2 T75 flasks. This process was repeated 3 more times with the final 2 times in T125 flasks, allowing expansion and concentration of the viral stock with each passage.

Viral titers were determined by plating 500 μl of serial dilutions of viral lysate starting at 1:2 on BHK-21 monolayers in 60 mm dishes. Following absorption by rocking at room temperature for 1 hour the plates were overlaid with 1% noble agar in DMEM with 20% serum. After 5 days incubation at 37°C the agar was removed and the cells stained with 1% crystal violet in ethanol. The plaques were counted and the titre reported as pfu/ml.

2.5 TMEV infection of mice

For *in vivo* experiments three groups of mice were used: TMEV, sham, and naïve. Together, sham and naïve mice constituted "controls". Both TMEV and Sham mice were

anaesthetised with 4% isofluroane. 3×10^6 PFU BeAN 8386 virus, suspended in sterile 0.03 ml HBSS, was injected into the right posterior cortex through a 27 gauge needle. This was fitted with a needle guard to prevent penetration beyond 3.5 mm ventral to skull. Injections were localised to a point half-way to midline at ear level, into the right posterior cortex (figure 2.2). Sham mice received injections of 0.03 ml HBSS. Naïve mice were not anesthetized or injected. All mice were monitored daily for changes in neurological status. Easier access to food and water was provided for TMEV injected animals exhibiting neurological impairment. Home office approval was given for all procedures.

All *in vivo* experiments used 6-8 week old female mice. Female mice were chosen in order to be able to have 'resistant' and 'susceptible' strain differences. C57BL/J male mice are susceptible to TMEV-induced demyelinating disease (IDD), whereas females of this strain are completely resistant (Alley et al., 2003; Kappel et al., 1990). The factors that contribute to increased viral replication and hence more severe disease in male mice are not understood but are most likely related to oestrogen induction of immune responses (Fuller et al., 2007). SJL/J mice show an opposite phenomena with female mice being more susceptible than males (Hill et al., 1998).

For experiments comparing between WT C57Bl/6 and WT SJL strains n=7 for TMEV groups at all time points (3,7, 14, 21, 45 and 90 days post infection) with matched numbers of sham controls. Groups were classified as preclinical (21 dpi), early onset (45 dpi) and chronic (90 dpi). For experiments examining changes after deletion of Galectin-3; C57Bl6 Gal-$3^{+/+}$, C57Bl6 Gal-$3^{-/-}$, SJL Gal3 $^{+/+}$ and SJL Gal-3 $^{-/-}$ all had five groups: naive (n=3), sham (n=4), TMEV 3 dpi (n=6), 7 dpi (n=6) and 14 dpi (n=6).

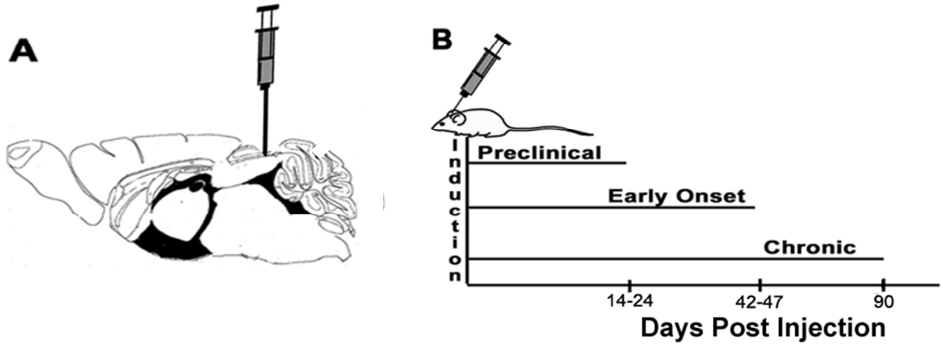


Figure 2.2 Time course of TMEV pathology

(A) Injection site for BeAn virus in mouse brain. Modified from Goings et al, 2008.
(B) Division of stages of TMEV disease progression based on days post infection.

2.6 Immunohistochemistry

2.6.1 Bromodeoxyuridine Labelling

Bromodeoxyuridine (5-bromo-2'-deoxyuridine, BrdU) is a thymidine analogue that is incorporated into the newly synthesised DNA of actively replicating cells during S phase of the cell cycle. BrdU was reconstituted in normal saline to a concentration of 10 mg/mL. Animals received a single intraperitoneal injection of BrdU (50 mg/kg body weight) 2 hours before sacrifice.

2.6.2 Perfusion and tissue preparation

Mice were anaesthetised with a lethal 0.1 ml dose of sodium pentobarbital and transcardially perfused with 50 mL of ice cold 0.9% normal saline via a 27g needle to flush out blood, followed by 50 mL of 4% paraformaldehyde (PFA). Following decapitation the brains were carefully dissected out of the skull to maintain attachment of the olfactory bulbs and post-fixed for a further 24 hours in 4% PFA at 4°C, before being

cryoprotected for 48 hours in 30% sucrose in 0.1M phosphate buffer (PB) at 4°C. The sucrose acts as a partial dehydrant that prevents the formation of ice crystal artefacts in frozen tissue sections. Brains were frozen on dry ice before storage at -80°C until needed for sectioning.

2.6.3 Microtome sectioning

The frozen brains were sectioned on a Leica microtome (Leica SM200R, Leica, Milton Keynes, UK) by mounting onto a frozen stage with PBS. Serial 30 μm coronal sections were cut from the olfactory bulbs to the caudal hippocampus. Brain sections were stored in 48-well plates as free-floating sections in cryoprotectant at -18°c.

2.6.4 Fluorescent immunohistochemistry on free-floating sections

Free-floating fluorescent immunohistochemistry was always performed at room temperature over the course of 2 days unless otherwise stated. For each individual animal a maximum of 6 free-floating brain sections was placed within porous well inserts (CLS3477, Sigma-Aldrich) in 12-well plates. These allowed the easy transfer of sections between wells for washes and incubations. A complete list of primary antibodies used is shown in table 2.1.

Sections were washed in 0.1 M phosphate buffered saline (PBS) 3 times for 10 minutes and then blocked with 50 mM glycine in PBS to reduce autofluorescence of paraformaldehyde-fixed tissue. Sections were washed in PBS a further 3 times, before blocking for 1 hour in PBS containing 0.1% Triton X-100 and 10% Donkey Serum, DS (Sigma), (PBS^{+}). Donkey serum is used to block non-specific binding sites before incubation with primary antibody. Double and triple immune-staining were carried out

using primaries produced in different host species in which sections were co-incubated overnight at 4°C. After overnight incubation they were washed in PBS 3 times for 10 min before incubation with the appropriate conjugated secondary antibodies for one hour at RT. The secondary was always matched to the primary antibody host animal conjugated to fluorophores: Alexa-488, 568 and 647 (Invitrogen Paisley, Renfrewshire, UK; 1:500) and Cy3 and Cy5 (JacksonImmunoResearch, West Grove, PA, USA; 1:500) conjugated anti-primary secondaries. After washing in PBS 3 times 10 mins sections were incubated for 10-min in 4',6-diamidino-2-phenylindole (DAPI, 10ug/mL, Sigma-Aldrich) to counterstain the cell nuclei and rinsed 3 times 10 min in 0.1M phosphate buffer (PB). This is to prevent any salt residues being produced in sections after drying. Sections were mounted and slides were coverslipped with FluorSave mounting medium (Chemicon). Omission of primary antibody was used as negative controls in all immunohistochemistry experiments. For BrdU, sections were incubated in 2mg/mL DNAse (Sigma-Aldrich) in DNAse buffer (see appendix 1) for 30 minutes prior to primary antibody addition, washed, incubated 1 hr in biotinylated anti-sheep (1:400) and 1 hr streptavidin alexa-546 (1:500). For PBS^{+} a higher Triton-X concentration of 0.5% was used.

2.6.5 Fluorescent staining of free-floating neurospheres

A neurosphere is method of growing neural stem/progenitor cells in free-floating clusters of cells. Putative neural stem cells are suspended in a medium that lacks adherent substrates but contains necessary growth factors for survival, such as epidermal growth factor and fibroblast growth factor. The neurosphere assay can be used to assay fundamental characteristics of neural stem cells: proliferation, self-renewal and multipotency.

For immunohistochemistry of free-floating neurospheres over 100 μm in size immunos were performed in porous well inserts with pore size of 30 μm (CLS3477, Sigma-Aldrich) in 12-well plates. Neurospheres were washed in ice cold 0.1M PBS 3 times 10 mins before fixation in 4% PFA for 1 hour. They were then washed in PBS 3 times 10 mins before blocking in PBS^{+} (0.5% triton-X 100, 10% Donkey serum) before overnight incubation in primary antibody at $4^{\circ}C$ in PBS^{+}. On day 2 spheres were washed in PBS 3 times 10 min before incubation in secondary antibody for 1 hour at RT, washed in PBS 3 times 10 min, incubated in DAPI for 15 minutes before final washes in PB 3 times 10 min. Spheres were mounted on coverslips using a pipette and leaving to adhere to slide for 15 minutes before removal of liquid and coverslipping with Fluorsave (Chemicon).

Table 2.1 Antibodies for immunohistochemistry and immunoblotting

Antigen	Dilution	Host	Maunfacturer Cat. #
BeAn	1:600	Rabbit	Gift from Miller Lab
BIII-tubulin	1:1000	Rabbit	Covance
BrdU	1:400	Sheep	Abcam Ab1893
CD11c	1:200	Rabbit	Ab52632
CD3	1:200	Rat	Santa-Cruz sc-18843
CD8	1:200	Rat	Santa-Cruz sc-18860
CD45	1:400	Rat	Millipore 05-1416
Doublecortin (Dcx)	1:200	Goat	Santa-Cruz sc-8066
Iba1	1:200	Goat	Abcam
Galectin-3	1:200	Rabbit	Santa-Cruz sc-20157
GFAP	1:500	Rabbit	Sigma-Aldrich G69269
GFAP	1:1000	Mouse	Millipore 557355
GFAP	1:400	Rat	Invitrogen 13-0300
GFAP	1:500	Chicken	Abcam ab4674
Mash1	1:100	Mouse	BD 556604
PECAM (CD31)	1:200	Rat	BD 557355
Phi3	1:400	Rabbit	Millipore 06-570
PSA-NCAM	1:400	Mouse	Chemicon
Vimentin	1:200	Goat	Santa Cruz SC7558

2.6.6 Fluorescent staining of differentiated neurospheres

Immunohistochemistry was performed on differentiated neurospheres within the 8-well chamber slide after 7 DIV. Differentiated cells were washed 3 times 5 min PBS and fixed in 4% PFA for 30 min, washed in PBS three times with 5 minutes each wash, blocked for an hour in PBS^{+} (no triton-X, 10% Donkey serum) before overnight incubation in mouse anti-04 antibody at 4°c, washed 3 x PBS 5 min and incubated for 1 hour in anti-mouse A488 (Invitrogen). Cells were then washed 3 times 5 min in PBS before a second hour blocking in PBS^{+} containing 0.5% Triton-X100, 10% donkey serum and incubated overnight at 4°C with rat or chicken anti-GFAP and rabbit anti-BIII-tubulin. On the 3^{rd} day cells were washed 3 x 5 min PBS, incubated at RT for 1 hour in anti-rat or anti-chicken cy3 and anti-rabbit A647, washed 3 x 5 min in PBS, incubated in DAPI (10mg/ml) for 15 minutes before a final wash in PB. The 8-well chambers were removed from the slide before mounting and coverslipping with Fluorsave (Chemicon).

2.7 Cell counting

2.7.1 Microscope analysis

For immunohistochemistry a set of brain sections from anatomical coordinates Bregma 1.7 to -0.5 mm were examined to include SVZ, striatum and cortex. Immunohistochemistry was examined and recorded on a Leica DMIRB microscope using Openlab software and on a Zeiss Meta confocal microscope, and analysed in 3-D with Zeiss and Volocity Software. Images were composed in Microsoft powerpoint.

2.7.2 $CD3^+$ quantification

For quantification of $CD3^+$ cells in SJL/J and C57BL/6 WT mice (chapter 3) images of CD3 and DAPI labelled sections were taken at 40x magnification on a Leica DMIRB microscope using Openlab software at 5 viewpoints for SVZ; dorsal-striatal, dorsal-septal, medial-septal, medial-striatal and ventral. Different areas of the SVZ were analysed in order to allow for the noted heterogeneity of adult SVZ cells (Alvarez-Buylla et al, 2008). For striatum quantification images were taken at 20x magnification with the SVZ in the left margin of the field of view, and with the SVZ in the right field of view for the septum. Pictures were taken at 20X for the septum as well as the entire length of corpus callosum and azygos pericallosal artery Images were saved as tiffs and exported into Volocity software for analysis. The number of $CD3^+$ cells was counted and the corresponding area measured to give a value of number of $CD3^+$ cells/mm^2. For SVZ regions DAPI was used to distinguish the SVZ and only cells within the DAPI dense area were included, this means that the ependymal cell layer is included in the 'SVZ region'. For Gal-3/CD3 co-localisation images were taken for both CD3 and Gal-3 and merged together in Volocity.

For chapter 5 the CD3 antibody used for analysis in chapter 3 was no longer commercially available so quantification was performed by counting the number of $CD45^+$ cells that were amoeboid in morphology. Labelling with other markers for amoeboid macrophages, dendritic cells and B-cells identified few cells, so the vast majority of quantified cells are most likely CD3 T-cells.

2.7.3 Quantification of neuroblast features

Doublecortin cell numbers.

For double cortin counts both left and right dlSVZ were counted for a minimum of 6 sections per animal. Counting was performed blind. Images of doublecortin and DAPI labelled sections of the dl SVZ were taken with a 63X objective on a Zeiss Meta confocal microscope with a single scan of both channels. The images were saved and exported as tiff images into Image J software. Using the cell counting tool all DAPI+ cells in the SVZ were labelled followed by counting the number of Dcx+ cells that were DAPI+. The percentage of DAPI+ cells that were Dcx^+ were then calculated in Excel.

Emigrated Dcx^+ cell quantification.

Emigrated Dcx^+ cells were counted unilaterally by eye. Cells were identified by having a DAPI+ nuclei. Doublecortin labelled striatal sections were viewed with a 63X objective lens on a Zeiss confocal microscope. With the SVZ to the left margin of the field of view at 63×, Dcx^+ cells in the striatum were counted, with the SVZ to the right margin of the field of view, septal Dcx^+ cells were counted, with the SVZ in the middle of the field showing the full extent of the CC thickness, Dcx^+ cells in the CC were counted, with the ventral 3rd of the SVZ in the middle of the field, emigrated Dcx^+ cells in the ventral 3rd septum, striatum and surrounding ventral SVZ were counted (previously described Going et al, (2008)). Sections were matched by Bregma between animals to ensure that areas counted were as similar as possible. Cells were only counted if they could be shown to have a $DAPI^+$ nuclei, processes that could not be traced to a cell body were not included. Where cells were present in a dense clump, images were taken and the nuclei counted by magnifying the image and using the LSM confocal imaging software. Only cells that had a

cell body more than 50 μm from the SVZ were counted as having 'emigrated'. This was determined by taking an image on both the DAPI and Dcx channel, using the measurements tool available in LSM confocal software measurements were made from the boundary of the SVZ (determined by the DAPI dense region) to the centre of the DAPI+Dcx+ nuclei.

For all Dcx quantifications a minimum of 6 sections were counted per mouse including both left and right dlSVZ. For chapter 3 n=7 for all groups, in chapter 3 n=3 for all groups and in chapter 6 n=5 for all groups.

2.7.4 Proliferating cells

Phosphohistone3 and BrdU cell counts.

Images of Phosphohistone3 or BrdU and CD45 labelled sections of 4 viewpoints; dorsal-striatal, dorsal-septal, medial-striatal and ventral were taken at 40× on a Zeiss Confocal microscope with a 30 μm stack taken of each channel that allowed co-localisation to be studied in 3-dimensions. Together these regions covered the entirety of the SVZ. The images were saved and exported as tiff images into Volocity (Improvision). The number of phosphohistone $H3^+$ or $BrdU^+$ cells that were $CD45^+$ or CD45- were counted and averaged for 4 consecutive sections per animal ranging from ~bregma 0.9 to 0.0. The volumes of the stacks was measured to give values of $PH3^+$cells/mm^3 and $PH3^+CD45^+$ cells/mm^3. The number $PH3^+$cells/mm^3 were then subtracted from $PH3^+CD45^+$ cells/mm^3 to give the number of proliferating neural cells. Only cells that had bright, complete labelling in the nuclei were included, cells that showed fragmented staining were excluded. All measurements were taken blind to avoid quantification bias. Sections were labelled with a coding system by another lab member and the code was only revealed once all

quantifications had been performed. Statistics were performed in Microsoft Excel; Student's T-tests (two tailed, equal variance) with p values < 0.05 were considered to be significant. The PH3/CD45/DAPI stained sections included a cohort of 6 naive mice in order to account for any changes in proliferation induced by the needle injury.

2.8 RT-PCR arrays

SVZ tissue was microdissected from coronal sections of brain from C57BL/6 WT, C57BL/6 Gal3$^{-/-}$ and SJL mice with a control group and TMEV 7 dpi group. For each group n=6 animals. Total RNA from virus-infected or naive SVZ tissue was extracted using the RNAeasy minikit (Qiagen, Carlsbad, CA), and Qiashredder column according to the manufacturer's instructions. 0.7 μg RNA was reverse transcribed for each sample using RT^2 First Strand Kit and applied to Inflammation Response and Autoimmunity RT-PCR array plates (PAM-077A, SABiosciences). Each sample was run in triplicate on three separate plates. Plates were processed in an Applied Biosystems 7500 Real-Time PCR System, using the software's automated baseline and threshold cycle detection as per the manufacturer's instructions. The expression data was interpreted for the 84 key genes by using a combination of SABiosciences' web-based PCR array data analysis tool and analysis in Excel. Relative fold changes in differential expression were calculated by subtracting the mean value of the cycle threshold from three plates from that of the housekeeping genes (ΔCr), subtracting the TMEV ΔCr values from those of the control values (ΔΔCr) and expressing the final quantification value as 2-ΔΔCT. Standard errors were calculated from the relative fold changes.

2.9 Neurosphere experiments

2.9.1 Neurosphere production

Neonatal mice 4 days old were used for the production of SVZ neurospheres. Brains were dissected by removing the head from the body, the skin was moved with fine scissors before the skull is peeled back using fine-pointed forceps. Intact brains were removed from 4-day-old neonatal mice, and sectioned into 400 μm slices on a McIlwan tissue chopper and suspended in ice-cold Neurobasal+. Under a 1x plan dissecting microscope the meninges were carefully removed with a sharp needle. The dorsal lateral wall of the lateral ventricle was microdissected using small cuts with a 4G needle, distinguished by eye as an area lighter in colour than the surrounding striatum. Cells were dissociated by 10 minutes incubation in Accutase at 37°C (Sigma) before centrifugation, washed and plated in Neurobasal plus [Neurobasal (Gibco 21103), B-27 (2%; Invitrogen 17504-044), N-2 supplement (1%; Invitrogen 17502-048), L-glutamine (2 mM; Invitrogen 25030), heparin (20 mg/ml; J.T. Baker M916-00), penicillin/streptomycin (1X; Gibco 15070) with 20 ng/ml EGF (Sigma E9644) and 20 ng/ml FGF2 (R&D Systems 233-FB)]. Cells were grown in non-adherent 6-well plates at $1x10^5$ cells/mL. Plates were incubated at 37°C and 7.5% CO_2. For passaging, neurospheres were dissociated with Accutase into single cells suspension and replated at $1x10^5$ cells/mL. For MTS assays and ELISA experiments secondary spheres were used.

2.9.1 Cell proliferation assay.

Cell proliferation was evaluated by using the CellTiter 96 Aqueous One Solution Cell Proliferation Assay (Promega) according to the manufacturer's protocol. The assay is based on reduction of MTS (3-(4,5-dimethylthiazol-2-yl)-5-(3-carboxymethoxyphenyl)-2-(4-

sulfophenyl)-2H-tetrazolium) to a colored formazan product, which is measured spectrophotometrically. Calibration curves were produced for B6 and SJL cell lines to determine the optimum cell number for initial plating. This was determined to be 50,000 cells/well for both strains. Following dissociation single cells were plated in 96-well plates in quadruplicate at $5x10^4$ cells/well. They were treated with rGalectin-3 at 0.1, 0.5 or 1 µg/mL or TMEV at MOI 1, MOI 10 and MOI 100 for 24, 48 and 72 hours at 37°C in a 5% CO_2 incubator. Metabolically active cells were detected by adding 20 µl of MTS to each well. After 2 hours of incubation, the OD was read on a Multilabel Counter. All data shown is representative of three independent experiments.

2.9.2 Lactate dehydrogenase cytotoxicity assay

Cell death after TMEV infection was evaluated using the CytoTox 96 Non-radioactive Cytotoxicity assay (Promega, G1780) according to the manufacturer's protocol. The assay measures lactate dehydrogenase (LDH), a stable cytosolic enzyme that is released upon cell lysis. This released LDH in culture supernatants is measured with a 3-minute coupled enzymatic assay, which results in the conversion of a tetrazolium salt (INT) into a red formazan product. The amount of colour formed is proportional to the number of lysed cells. The percentage cell death is calculated against a maximum LDH release control in which a 0.8% Triton-X solution is used to completely lyse all cells prior to harvesting supernatants. Cells were plated at 50,000 per 96 well plate in quadruplicate with TMEV at MOI 01, MOI 10 and MOI 100. All data shown is representative of three independent experiments.

2.9.3 Neurosphere differentiation.

8 well chamber slides were coated overnight with 10 μg/ml poly-D-lysine (PDL;Sigma) and rinsed with phosphate buffered saline (PBS) four times before 2 hours incubation with 0.01 mg/ml laminin in PBS. Cells were plated in $E^{+}F$ free neurobasal plus for 7 DIV. The media was changed after 4 DIV. For some experiments rGal-3 (R&D systems) was added at 0.1, 0.25 or 0.5 μg/mL immediately after plating down. Fresh rGal-3 was added after media change.

Cells were quantified from images taken at 40X magnification on a Leica confocal and analysed using Cellcounter software in ImageJ. A minimum of 4 spheres was counted for each condition and each condition was repeated in three separate experiments.

2.10 Measuring cytokine levels

2.10.1 ELISA

For analysis of tissue protein levels mice were perfused with ice cold PBS before microdissection of the SVZ. SVZ cells were lysed on ice with lysis buffer (25mM Tris-HCl pH 7.4, 150mM NaCl, 1mM EDTA, 1% NP-40 and 5% glycerol, 1mM PMSF) for 30 minutes, centrifuged and supernatant stored at -80°C until use. Protein levels were measured using standard Bradford assay protocol (Bio-Rad). For all protein experiments 0.1 mg of tissue was used per sample and run in triplicate. For each experiment tissue from n=6 animals per group was pooled and replicated in three independent experiments. For analysis of supernatant 100 μl of appropriate fluid dilutions were used: Galectin-3 1:100, CXCL10, CC2, CCL5 and IL-10 at 1:10. Cytokine levels for galectin-3 (mouse Galectin-3; R&D Duo Sets; Catalogue Number: DY1197), CXCL10 (mouse CXCL10; R&D Duo Sets, Catalogue Number DY466), CCL2 (mouse CCL2; R&D Duo Sets, Catalogue

Number DY479), CCL5 (mouse CCL5; R&D Duo Sets, Catalogue Number DY478) were assayed from samples using the respective ELISA kit according to the manufacturer's instructions.

For ELISA experiments dissociated secondary neurospheres were plated at $1x10^6$ cells in non-tissue culture treated 6 well plates. Cells were then treated with media alone, stimulated with IFNγ and TNFα or TMEV at a multiplicity of infection of 0.1 or 10 (MOI; 0.1 or 10 plaque forming units/cell). Each well was harvested after 4 or 24 hours, centrifuged and the supernatant and cell lysate aliquoted and immediately frozen on dry ice, before storage at -80°C. Recombinant murine IFNγ was purchased from Pharmingen (San Diego, CA) and used at 100 U/ml. Recombinant murine TNFα was purchased from R&D Systems (Minneapolis, MN) and used at 500 U/ml. These doses selected had been experimentally determined to elicit optimal responses in primary cultures in previous experiments by our collaborators (Carpentier et al., 2008).

2.10.2 IFNγ induced Gal-3 secretion.

For IFNγ stimulation experiments dissociated secondary neurospheres were plated in triplicate at $5x10^4$ cells/well in a 96 well plate in 100 µl of NB^+ with separate wells for each time point. Recombinant murine IFNγ diluted in NB^+ (Pharmingen) was added at 10, 100 or 1000 U/mL to make volume to 150 µl per well or plain NB^+ as a control. Each well was harvested after 3, 6 or 24 hours, centrifuged and the supernatant immediately frozen on dry ice, before storage at -80°C. The cell pellet was washed in ice cold PBS^+, centrifuged and incubated for 30 minutes in lysis buffer (1X Cell Lysis Buffer**:** 20 mM Tris-HCl (pH 7.5), 150 mM NaCl, 1 mM Na_2EDTA, 1 mM EGTA, 1% Triton, 2.5 mM sodium pyrophosphate, 1 mM beta-glycerophosphate, 1 mM Na_3VO_4, 1 µg/ml leupeptin,

1mM PMSF), centrifuged again and supernatant stored at -80°C.

2.11 Astrocyte cultures

2.11.1 Astrocyte culture production

T25 tissue culture flasks were coated overnight with 10 µg/ml poly-D-lysine (Sigma) in PBS and incubated at 37°C. The flasks and plates were then rinsed 4 times with PBS, incubated for 3 hours with 0.01 mg/ml laminin in PBS and finally rinsed with PBS.

Neonatal SJL/J mice 6 days old were used for the isolation of cortical and SVZ astrocytes. Intact brains were removed and the hindbrain dissected away. The cerebral hemispheres were sliced into 500 µm sections on a tissue chopper and suspended in ice-cold Hank's buffered salt solution (HBSS; Gibco, Invitrogen). Under a 1x plan dissecting microscope, after careful removal of meninges with a sharp needle, the cortex and lateral SVZ was micro-dissected out of each free-floating section and stored on ice in HBSS. Cortex was taken by making horizontal cuts at the insular cortex bilaterally and cutting along the edge of the corpus callosum. For the SVZ the dorsal lateral wall of the lateral ventricle was microdissected, although a small amount of striatum is usually dissected as well. The tissue was incubated in 0.25% trypsin- ethylenediamine-tetracetic acid (EDTA; 0.05g/l trypsin, 0.02g/l EDTA; Sigma) for 30 minutes to allow dissociation then centrifuged, trituated in 1mg/ml DNase and centrifuged again. Before plating, the pellet of cells was resuspended in plain Dulbecco's modified Eagle media (DMEM; Sigma) and the live cells were counted using the trypan blue exclusion method. Cells were seeded at 2-3 brains per pre-coated T75 flask for cortex and 2 x 10^6 cells per T25 flask for SVZ.

2.11.2 Passaging and purification of cultures

Mixed glial cultures were maintained at 37°C and 5% CO_2 in DMEM-F12 (Sigma) supplemented with 10% fetal calf serum (Sigma), 6 g/l glucose (Sigma), 2.4 g/l sodium bicarbonate (Sigma), 0.37 g/l L-glutamine (Life Technologies), 100 U/ml penicillin (Life Technologies) and 100 µg/ml streptomycin (Life Technologies). Media was part changed 1 day after dissection then every second subsequent day. At confluency, generally 14-21 days post-dissection, microglia and oligodendrocytes were removed by orbital shaking for 24 hours at 300 rpm. After washing off the floating glia, the remaining astroglial bed layer was removed with 1x trypsin-EDTA, centrifuged, counted and re-plated until experimental use. Astrocytes are passage twice before being used in experiments.

2.11.3 TMEV infection of astrocyte cultures

Astrocytes at P2 were plated in triplicate for each group at 50,000 cells in 6 cm Petri dishes and left to adhere for 24 hours. Cultures were treated with 0.5 mL of either plain media (controls) or TMEV at a multiplicity of infection (MOI) of either 0.1, 1, 10 or 100 (0.1, 1, 10 or 100 plaque forming units/cell). Cells were left with the virus at room temperature for 1 hour before being brought up to normal volume with complete media and returned to the 37°C incubator for a further 24 hours. Cells were counted using trypan blue, which also verified that TMEV did not cause cell death or induce morphological change. Supernatant was harvested and used at 1:100 dilutions for analysis of Galectin-3 levels (mouse Galectin-3; R&D Duo Sets; Catalog Number: DY1197). For RT-PCR arrays cells were infected at MOI 10 for 24 hours before harvesting and extraction of RNA as described above.

2.12 Statistics

Continuous numerical data were presented as mean ± standard error of the mean. Differences between two groups were assessed using the Student's t-test and for groups of three or more with analysis of variance (ANOVA) with Bonferroni post-hoc test. Groups were considered statistically difference when at least a 95% confidence level was achieved ($P<0.05$). For all graphs statistical significance is indicated by * for $P<0.05$, ** for $P<0.01$ and *** for $P<0.001$.

Chapter 3

TMEV induced inflammation in the SVZ and its impact on niche homeostasis

3.1 Introduction 90

3.2 Results 95

3.3 Discussion 121

3.1 Introduction

For many years research has focused on whether endogenous neural stem cells from the SVZ could be utilised for remyelination in multiple sclerosis. In early MS remyelination has been described as a frequent phenomenon (Goldschmidt et al., 2009; Prineas et al., 1993; Prineas et al., 1984; Raine and Wu, 1993) and imaging studies show it is most prominent in the first 7 months after gadolinium enhancement (Chen et al., 2008). Whilst remyelinated lesion areas are also present in chronic MS lesions completely remyelinated lesions, called 'shadow plaques', are less frequently observed (Goldschmidt et al., 2009; Patani et al., 2007; Patrikios et al., 2006). Remyelination of MS lesions in chronic disease stages shows heterogeneity between lesions in the same patient (Patani et al., 2007). A higher extent of remyelination is found in subcortical lesions compared with periventricular and cerebellar lesions, indicating that the localisation of a lesion influences the extent of remyelination (Goldschmidt et al., 2009). Oligodendroglial precursor cells in different CNS regions may have a different capability for remyelination or the proliferation and differentiation of progenitor cells may be influenced by the surrounding environment. In MS, the periventricular white matter is a site of intense inflammation and it has been speculated that involvement of the SVZ in repair would be seriously compromised by these events (see figure 3.1). Over 90% of MS patients have periventricular lesions (Pichiecchio et al., 2009) that radiate from the ventricular surface and in advanced stages of the disease, extensive periventricular lesions may completely cover the surface of the lateral ventricles (Gean-Marton et al., 1991; Nakashima et al., 2006) (see figure 3.1). A more thorough understanding of how inflammation impacts upon

endogenous stem cells in these regions, in particular those found in the SVZ, may help to understand why remyelination of these lesions begins to fail in chronic disease stages.

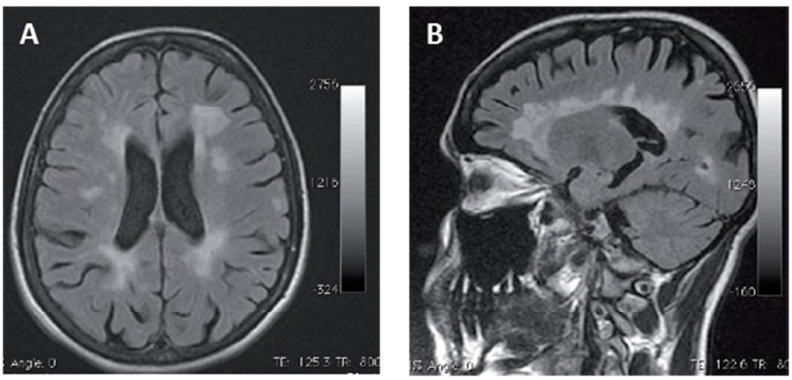


Figure 3.1 Periventricular lesions in MS

(A) T2-weighted MRI image taken at the level of the lateral ventricle showing multiple hyperintense periventricular white lesion.

(B) Sagittal view shows lesions perpendicular to lateral ventricles, also known as Dawson's fingers.

The effects of MS like inflammation on the SVZ has been largely studied using animal models. Examination of proliferation and migration after EAE provides conflicting findings (Guo et al., 2010; Picard-Riera et al., 2002; Pluchino et al., 2008; Rasmussen et al., 2011). Refined analyses reveal a complicated dynamic of SVZ self-renewal, survival and migration depending on the mouse strains and the model used. The Szele lab have conducted the only published paper to date examining inflammation in the SVZ after TMEV infection (Goings et al., 2008). This thesis will further expand upon this data and be the first to address the impact of acute TMEV induced inflammation on the SVZ niche.

Early stages of TMEV are characterised by variably intense and multifocal inflammation that involves the cerebral and spinal cord grey matter. Previous studies have described minimal inflammation in the cerebral cortex and found that the bulk is concentrated in subcortical grey matter, especially in the regions of the diencephalon

(thalamus, hypothalamus and subthalamus), the hippocampus and the basal ganglia (Oleszak et al., 2004). To date there has been no careful quantification or characterisation of haematopoietic cell infiltration into forebrain regions although the Szele lab have previously published that in the later stages of the disease in SJL mice $CD45^+$ cells accumulate in the SVZ (Goings et al., 2008). In this chapter, I hope to answer the question of whether TMEV induces inflammation in the SVZ and when and for how long this inflammation occurs.

There is evidence for a viral etiology to MS and several viral candidates have been proposed, including EBV, herpes simplex virus 6 and the measles virus. The SVZ is vulnerable to viral attacks and the characteristic periventricular lesion development may relate to subependymal viral spread (Das and Basu, 2008; Feuer et al., 2005; Krathwohl and Kaiser, 2004; Liu et al., 2005). Interestingly, the co-receptor used by the BeAn strain of virus, sialic acid, is expressed at high levels in the SVZ (Goings et al., 2008). In fact, polysialic residues are attached to the neural cell adhesion molecule (PSA-NCAM) expressed by neuroblast cells. As these cell may be vulnerable to viral attack, I will also investigate whether the BeAn virus is able to infect cells of the SVZ niche and what impact this has upon their proliferation and survival.

In TMEV, no reported alterations in myelin integrity in the forebrain grey and white matter, including the corpus callosum have been detected in either SJL or C57BL/6 mice (Kummerfeld et al., 2012) and demyelination largely occurs in the spinal cord in the chronic stages of the disease (Drescher and Tracy, 2007). Accordingly, most work on TMEV has focused on the role of T-cells in mediating demyelination in the later disease stages. However, besides myelin loss, axonal damage has attracted attention in demyelinating diseases as it has become increasingly apparent that substantial axonal and neuronal loss are equally important features (Bo et al., 2006; Bruck, 2005; DeLuca et al.,

2004). During inflammatory demyelination white matter subcortical neurons are destroyed and the permanent disability in MS can be attributed to the impact that inflammation has on the viability of axons and neurons (Bjartmar and Trapp, 2003; Bjartmar et al., 2003). TMEV is an appealing model to study this process as neuronal loss precedes demyelination and can be detected as early as one week after infection with a gradual increase in numbers of damaged axons over time (Tsunoda et al., 2003). SVZ cells are able to generate thousands of new interneurons everyday that migrate long distances through the RMS to the OB. The cells can self-renew and are multipotential when exposed to appropriate growth factors *in vitro*. As such, they may provide a possible source for cell replacement. In this thesis I have examined how TMEV induced inflammation affects the neural progenitor population and its potential for endogenous replacement of neurons.

Different strains of mice have different susceptibilities to TMEV infection. Resistant strains of mice such as C57BL/6 completely clear the virus and do not develop demyelinating disease. In contrast, sensitive strains of mice like SJL/J, fail to completely clear the virus and develop a persistent viral infection associated with low virus titres and late chronic demyelinating disease, characterized by massive mononuclear cell inflammatory infiltrates and demyelinating lesions. B6 astrocytes produce significantly higher levels of cytokines, chemokines and adhesion molecules in response to TMEV infection and this may be a potential determinant of viral persistence and disease susceptibility (Carpentier et al., 2008). It is not known how these differences in cytokine patterns may differentially effect SVZ cells. Discovering key differences between resistant and susceptible mice may help to elucidate the mechanisms through which changes in neurogenesis are mediated. In this study I shall examine the impact on inflammation in the SVZ for both resistant and susceptible mice and study differences in levels of inflammatory mediators.

3.1.1 Research questions

In Goings et al (Goings et al., 2008) high levels of $CD45^+$ staining was found in the SVZ of susceptible SJL/J mice at 21 dpi that persisted through to chronic stages at 90 dpi. This caused changes in neuroblast morphology and ectopic emigration. This raised the question of what was the phenotype of the $CD45^+$ cells and how the SVZ might be affected during acute encephalomyelitis (3-14 dpi) compared to chronic stages? As both resistant and susceptible strains of mice develop acute encephalomyelitis, do differences in their immune responses have differential impacts on the SVZ? I hypothesised that during acute TMEV infection the SVZ would have high levels of BeAn antigen due to the expression of co-receptors for the BeAn virus and this would induce high levels of inflammation within the SVZ. In addition it is postulated that this would impact upon the homeostasis of the SVZ niche. The aims of this chapter are therefore to: (1) quantify and characterise haematopoietic infiltration in forebrain regions, (3) determine if acute inflammation impacts upon features of the SVZ niche including proliferation and emigration, (3) study the effects of viral infection on SVZ cells and (4) look for differences in SVZ cytokines between resistant and susceptible mice.

3.2 Results

3.2.1 Patterns of CD45 infiltration in the CNS after TMEV

The first aim of my DPhil was to elucidate the location and identities of haematopoietic cells infiltrating the brain following TMEV infection. Initially, CD45 immunohistochemistry was used to study patterns of inflammation during the progression of TMEV infection in susceptible SJL/J mice through preclinical stages (21 dpi), to early onset (45 dpi) and finally chronic stages (90 dpi) (figure 3.2). Sham mice show an even spread of $CD45^{low}$ cells throughout the central nervous system, consistent with resident resting microglia. The forebrain of TMEV mice showed the greatest amount of cell activation at 14 dpi, that preceded cerebellum and spinal activation and this continued through to chronic stages at 90 dpi (Goings et al., 2008).

The specific location of $CD45^{+}$ cell activation was stochastic from mouse to mouse and from section to section. In contrast, $CD45^{+}$ activation was very consistent in the SVZ and immediately surrounding periventricular areas of the dorsal septum and striatum (figure 3.3B). The corpus callosum, immediately dorsal to the SVZ also contained activated CD45 cells, although to a lesser extent than the grey matter. $CD45^{+}$ cell activation was also consistently high in the RMS as it courses through anterior cerebral cortex into the olfactory bulb (figure 3.3C-D).

This preclinical to chronic gradation was reversed in the hippocampus where the greatest $CD45^{+}$ cell activation was seen in chronic sections (figure 3.2). In the hippocampus the majority of activity was in the dorsal hippocampus subjacent to the lateral ventricle, sandwiched between it and the corpus callosum. CD45 activation was

evident in the CA1, CA2, pyramidal and oriens layers of the hippocampus (figure 3.3E). However, it was noticeably absent from the dentate gyrus (figure 3.3F). Nearby activation was observed in the dorsal fimbria and consistently in the 3rd ventricle. Foci of ischaemic type coagulative necrosis can be seen particularly near dense perivascular inflammation that may be suggestive of vasculitis (arrow, figure 3.3F).

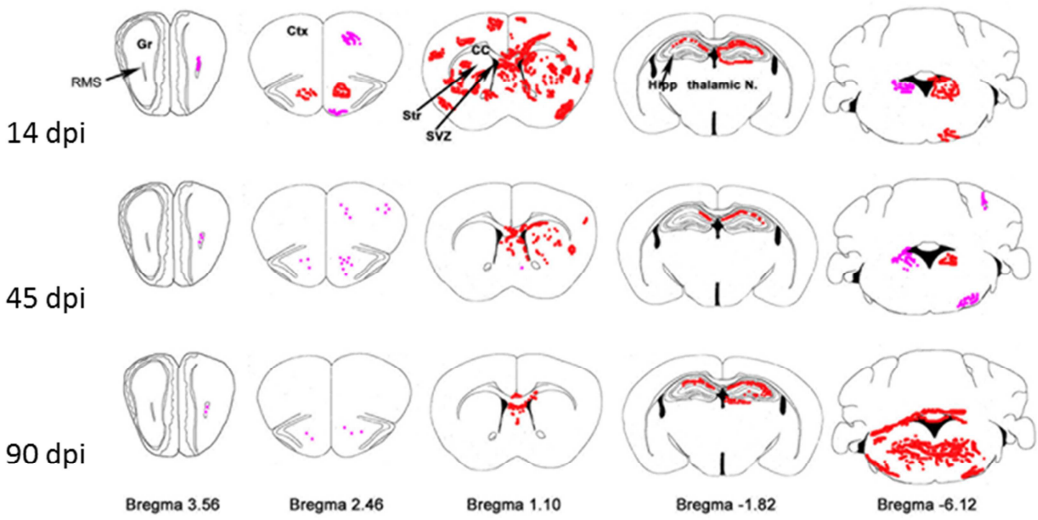


Figure 3.2 Schematic of brain regions showing typical areas of CD45+ cell activation

Shown are qualitative averages of intensity and location of CD45+ cell activation. Pink represents low levels and red areas of high activation. Anterior – posterior distances are given as distances from bregma.

Dpi = days post infection, Gr = granular layer of olfactory bulb, RMS = rostral migratory stream. Ctx – cerebral cortex, Str = striatum, SVZ = subventricular zone, CC = corpus callosum, Hipp = hippocampus. Modified from Paxinos and Franklin. Derived from Goings et al (2006)

3.2.2 The identities of haematopoietic cells

CD45 inflammatory cells were labelled with various immunohistochemistry markers to identify the cell type: Iba1 for microglia/macrophages, CD11c for dendritic cells and CD3 for T-cells.

Previously published data has shown that microglia within the SVZ seem to be constitutively 'semi-activated' with ramified processes and higher levels of CD45 (Goings et al., 2008; Goings et al., 2006). Similarly, constitutive SVZ activation was seen in SJL and B6 sham mice with Iba1 immunohistochemistry (arrow, figure 3.4A) but not in other regions (figure 3.4B-C). After TMEV infection reactive microglia are seen throughout the SVZ (figure 3.4D) and periventricular regions including the striatum, septum and corpus callosum (figure 3.4E-F) and in the hippocampus (figure 3.4I). Activated microglia were characterised by an increase in Iba1 fluorescence and a change from highly ramified morphology (figure 3.4G) to cells with larger soma and shorter, thicker processes (figure 3.4H). Amoeboid 'macrophage-like' cells were not detected in forebrain regions but were present in the hippocampus.

Myeloid dendritic cells have been implicated in antigen presentation in EAE model of MS. To see if they were present after TMEV infection an antibody against CD11c was used. $CD11c^{+}$ dendritic cells were present in areas of $CD45^{high}$ activation at preclinical stages (figure 3.5A-C). In chronic disease stages $CD11c^{+}$ comprised the majority of $CD45^{+}$ cells in hippocampal and spinal regions (figure 3.5B-C). Few $CD11c^{+}$ cells were evident in the pre-clinical spinal cord with CD45 activation in the grey matter (figure 3.5D), however, many $CD11c^{+}$ cells were seen in the white matter of the chronic spinal cord, paralleling $CD45^{high}$ activation (figure 3.5E) (Goings et al., 2008).

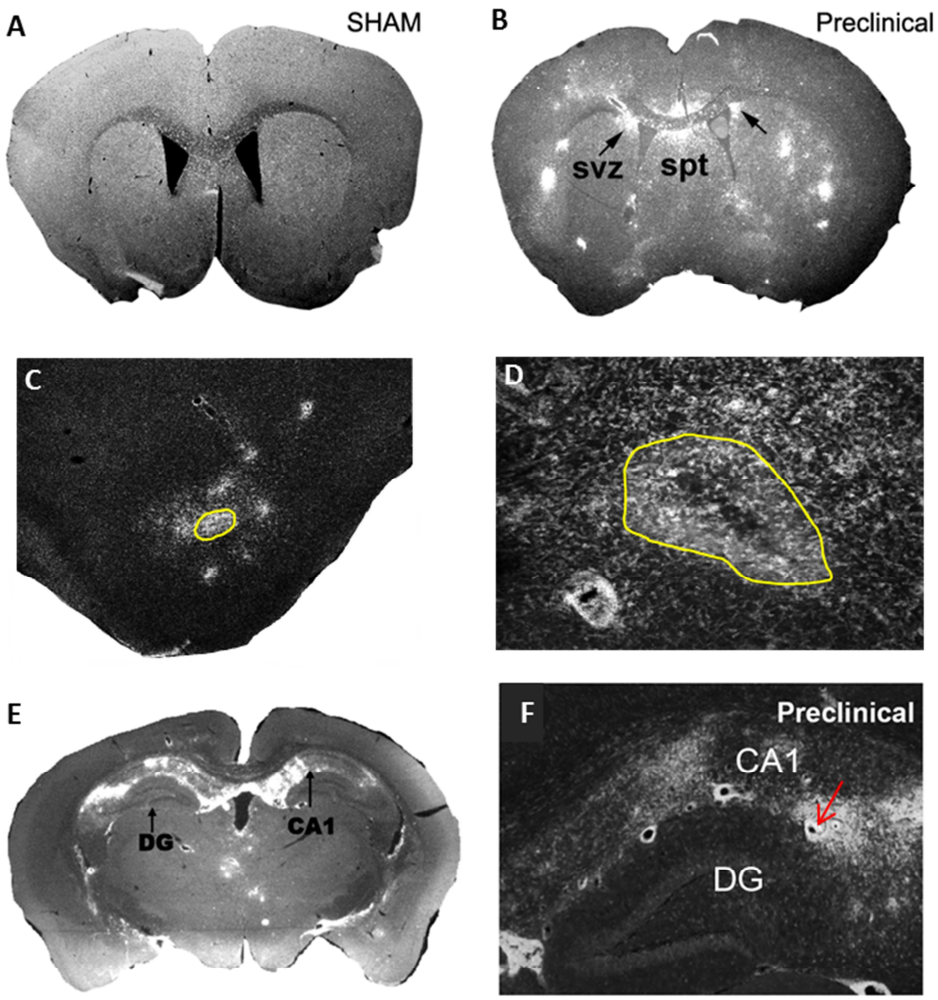


Figure 3.3 Regions of high CD45 activation in periventricular regions, RMS and hippocampus

(A) CD45 on sham sections shows little staining

(B) Preclinical mice have heterogeneous staining throughout forebrain regions that is most consistent in periventricular regions

(C) The RMS and surrounding parenchyma have high levels of CD45+ staining

(D) Higher magnification image shows significant CD45 activation within the RMS with lower levels in surrounding parenchyma

(E) In the hippocampus CD45 activation is seen in CA1, CA2, pyramidal and oriens layers.

(F) CD45 activation is noticeably absent from the dentate gyrus in preclinical mice. Arrow indicates area of dense perivascular inflammation.

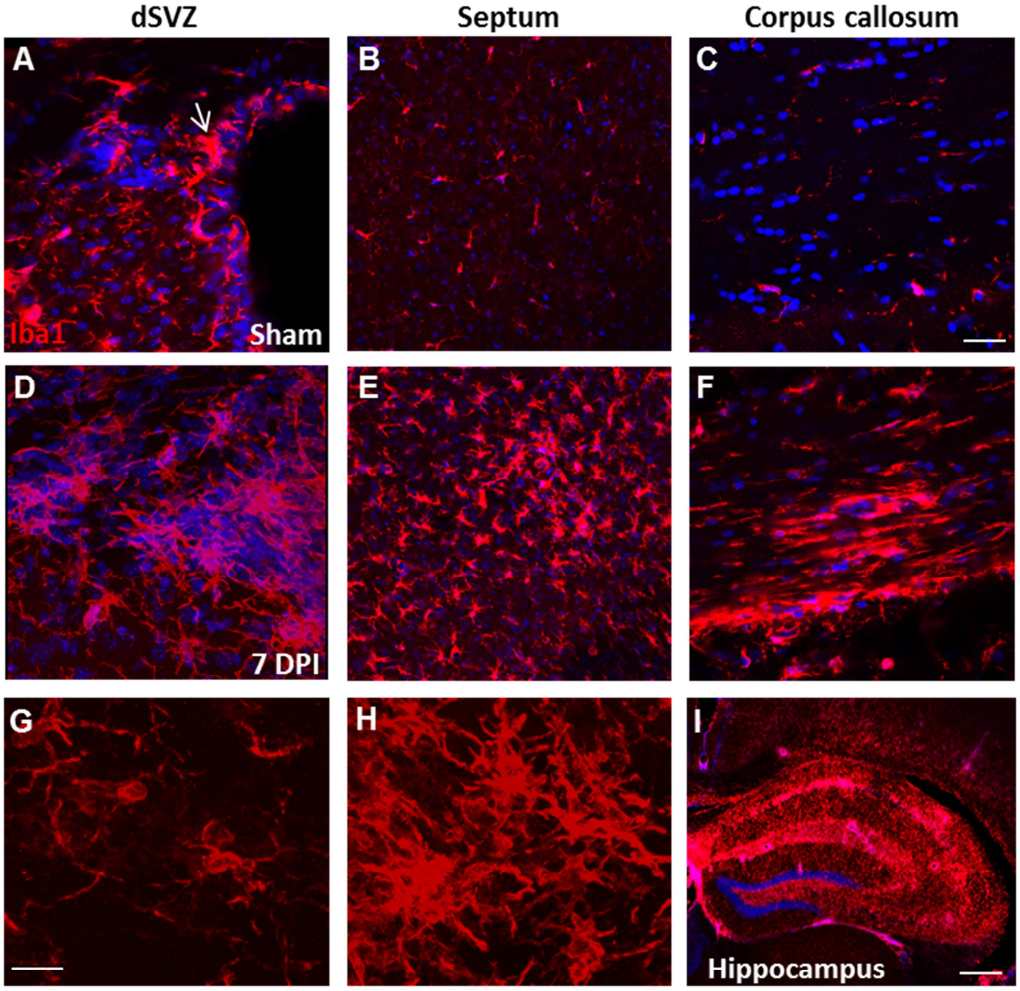


Figure 3.4 Widespread microglia activation throughout forebrain and hippocampus

(A-C) Iba+ immunohistochemistry in sham SJL/J mice. Scale bar = 15 μm

(D-F) Microglial activation 7 dpi TMEV as shown by increased iba1 fluorescence in SJL/J mice

(G) Typical morphology of resting microglia. Scale bar = 20 μm

(H) Change in morphology of activated microglia.

(I) Iba1 staining in hippocampus. Scale bar = 200 μm

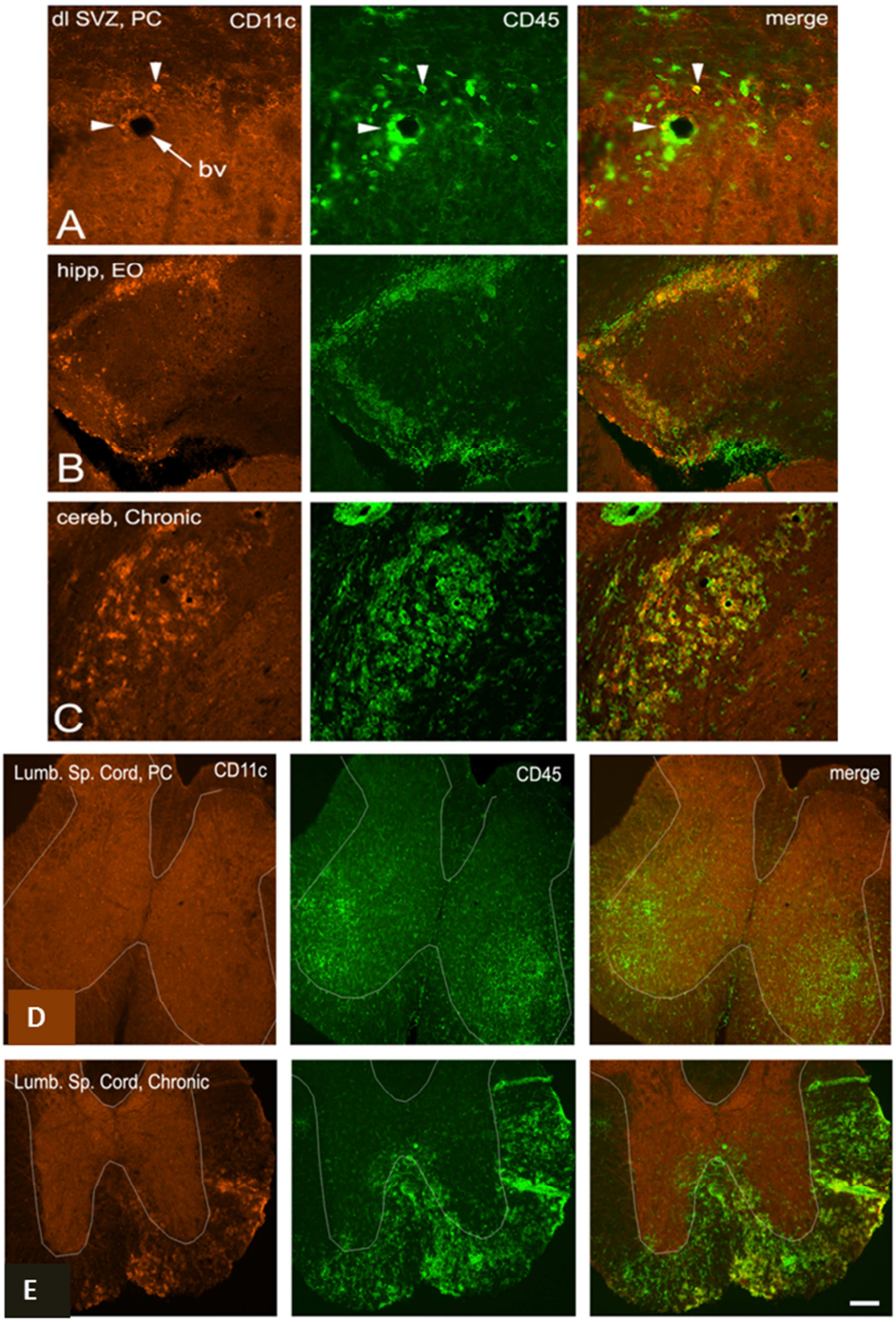


Figure 3.5 Comparison of dendritic cell CD11c immunolabelling with CD45 expression

(A) Relatively few CD45+ cells are CD11c+ (arrowheads) in the SVZ of preclinical mice. Bv = blood vessels.

(B-C) CD11c+ cells are more frequent in the hippocampus and cerebellum during early onset and chronic stages

(D) In preclinical stages lumbar spinal cord has no CD11c+ cells.

(E) Subset of CD45+ cells CD11c+ in lumbar spinal cord white matter in chromic mice. White line outline approximate border between grey and white matter. Scale bar = 100 μm

3.2.3 Infiltrating $CD3^+$ cells target the SVZ

Immunostaining revealed that the vast majority of cell infiltrate was composed of $CD3^+$ T-cells. As infiltration was highest in preclinical periods I included two earlier time points, 3 and 7 dpi, for the rest of the experiments. At the earliest time point examined of 3 dpi T-cell infiltration was already evident in the subventricular zone and statistically higher than in the striatum ($n=7$, $p<0.05$) and septum ($n=7$, $p<0.05$) (figure 3.6A). Infiltrating $CD3^+$ cells display a peak of infiltration at 7 dpi and gradual decline in numbers until the chronic stages (D42) (fig 3.6A). At 7 dpi T-cell infiltration was significantly higher in the SVZ compared to striatum ($n=7$, $p<0.001$) and septum ($n=7$, $p<0.001$) (figure 3.6C-E). At all other time points infiltration was highest in the SVZ compared to the striatum and the septum with the exception of the striatum at d14, which was not statistically different from the SVZ. No $CD3^+$ cells were present in sham mice.

$CD3^+$ cells showed high numbers in the meninges and around major blood vessels throughout the brain suggesting these are their main points of entry. As the meninges does not reliably stay attached to brain sections the azygos pericallosal artery (AZPG) was chosen in order to examine a major blood vessel and section of meningeal layer. Quantification of $CD3^+$ cell numbers in the azygos pericallosal artery showed high T-cell numbers by day 3 that continue to increase until day 14, longer than the peak period of infiltration into the CNS (figure 3.6F). Infiltration at 14 dpi was significantly higher than 3 dpi ($n=7$, $t=6.3$, $p<0.01$), 24 dpi ($n=7$, $t=7.4$, $p<0.001$) and 42 dpi ($n=7$, $t=6.78$, $p<0.001$). This suggests whilst T-cells are still present in the meninges, infiltration into the CNS decreases. CD3 staining revealed that the high $CD45^+$ within the RMS and immediately surrounding parenchyma was composed of largely $CD3^+$ T-cells. This might imply that the $CD3^+$ cells are using the RMS as a means of migration through the brain all the way to the olfactory bulb (data not shown).

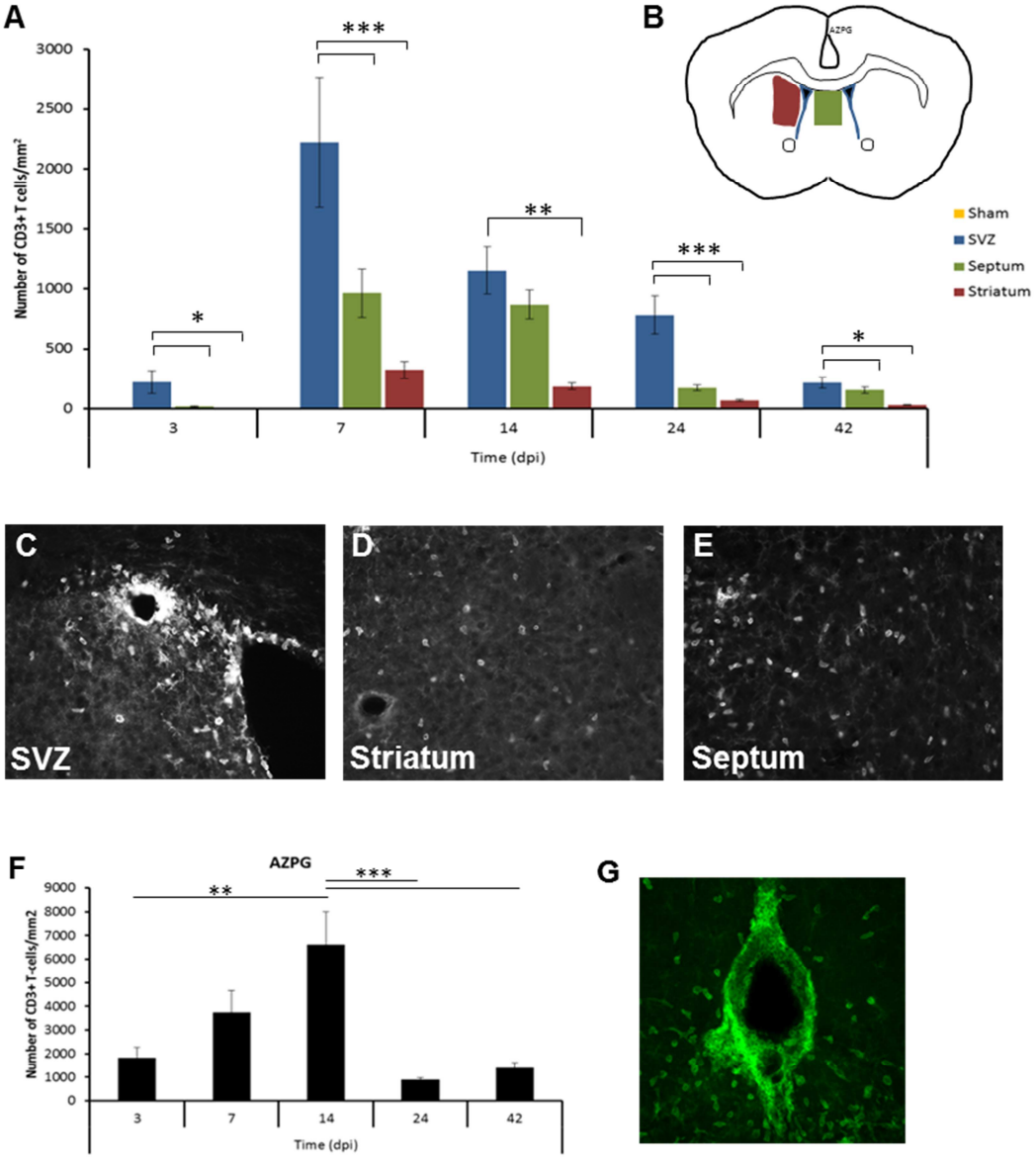


Figure 3.6 CD3+ infiltration targets the SVZ of SJL/J mice

(A) Quantification of CD3+ cells numbers in forebrain regions in SJL mice.

(B) Schematic of division of forebrain regions for quantification

(C-E) CD3+ T-cell infiltrate in SVZ (C), septum (D) and striatum (E) at 7 dpi.

(F) Number of CD3+ cells in azygos pericallosal artery (AZPG).

(G) Image of accumulation of CD3+ cells within vessel wall of AZPG.

*= p<0.05, ** = p<0.01, *** = p<0.001. n=7 all groups. ANOVA

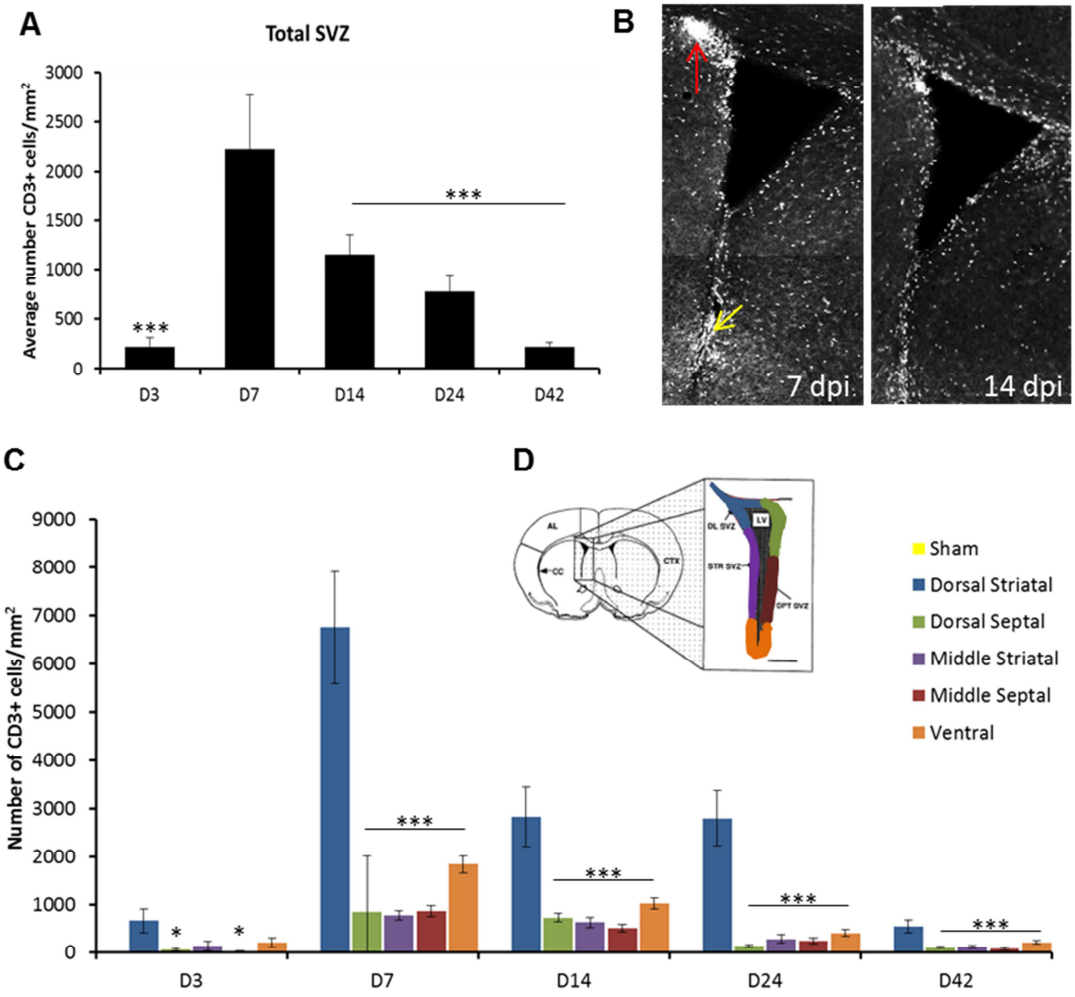


Figure 3.7 Immigrating CD3+ cell accumulate in the dorsal SVZ of SJL mice

(A) Quantification of CD3+ cells numbers in total SVZ in SJL/J mice. Statistics represent ANOVA between 7 dpi and other groups.

(B) Representative images of CD3+ infiltrating into SVZ at 7 and 14 dpi. Red arrow indicates dorsal SVZ, yellow arrow indicates ventral SVZ.

(C) Number of CD3+ cells in different SVZ subregions.

(D) Schematic of division of SVZ subregions for quantification

* = $p<0.05$, *** = $p<0.001$, n=7, ANOVA

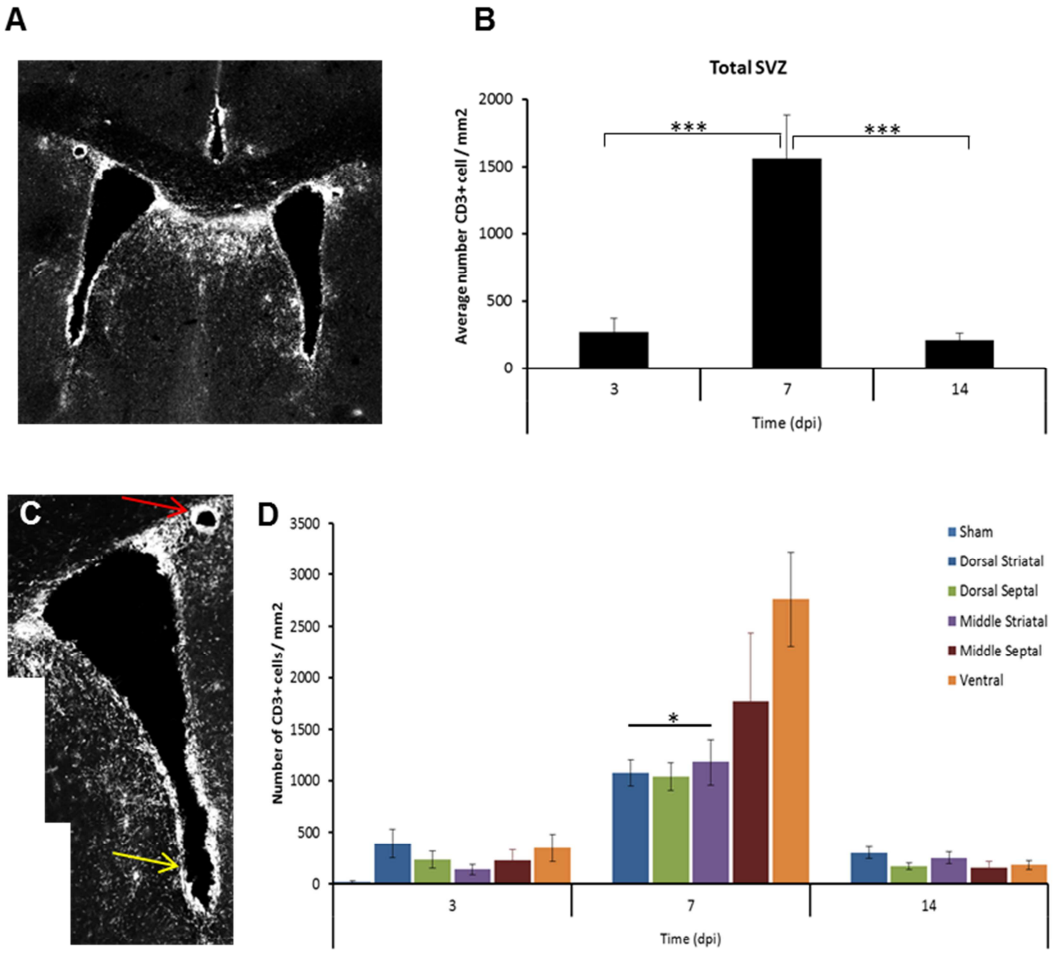


Figure 3.8 Immigrating CD3+ cell are more evenly spread in SVZ of B6 mice

(A) CD3+ infiltration in periventricularregions of B6 mice at 7 dpi.

(B) Quantification of CD3+ cells numbers in total SVZ in B6 mice. Statistics represent ANOVA between 7 dpi and other groups.

(C) Representative images of CD3+ infiltrating into SVZ at 7 dpi. Red arrow indicates blood vessel by dorsal SVZ, yellow arrow indicates ventral SVZ.

(D) Number of CD3+ cells in different SVZ subregions.

* = $p<0.05$, *** = $p<0.001$, n=7, ANOVA

3.2.4 Different patterns of T-cell immigration into the SVZ between mouse strains

Examining the average number of T cells in the SVZ showed the peak of infiltration in SJL/J mice was significantly higher at 7 dpi compared to all other time points (n=7, $p<0.001$, figure 3.7A). Within the SVZ $CD3^+$ cells were seen the length of the lateral ventricles but were most prominent in the dorsal and ventral SVZ regions (figure 3.7B). It is important to distinguish between different SVZ subregions as each is a unique stem cell niche that produces distinct cell types during neurogenesis (Alvarez-Buylla et al., 2008; Merkle et al., 2007). To examine whether T-cell infiltration affects different regions the SVZ was split into 5 subregions for quantification (figure 3.7D). In SJL/J mice at every time-point the number of $CD3^+/mm^2$ was statistically higher in the dorsal striatal region of the SVZ relative to the other measured regions (n=7, $p<0.001$, figure 3.7C).

TMEV infection of resistant B6 mice causes a similar periventricular inflammatory response (figure 3.8A). Quantification of T-cell infiltration in C57B/6 mice showed the same significantly high levels of infiltration at 7 dpi compared to other time points (ANOVA, $p<0.001$, figure 3.8B). B6 mice show a much sharper decline in numbers by 14 dpi (figure 3.8B). When the same subregional analysis was performed it showed a different pattern of infiltration within the SVZ than SJL mice. In the C57BL/6 mice T-cell immigration was highest in ventral regions at 7 dpi compared to other subregions (figure 3.8D). At other time points $CD3^+$ cells are spread more evenly throughout the entire SVZ. For both SJL/J and C57BL/6 T-cell entry appears to be a combination of migration through the choroid plexus and large blood vessels that run alongside the dorsal and ventral SVZ (figure 3.8C, red arrow). Between the two strains of mice the greatest differences were seen between the dorsal and ventral SVZ, in particular the dorsal striatal SVZ showed 7x fold higher $CD3^+$ numbers in the SJLs than B6s. Overall, the average CD3 density in total SVZ was comparable between the two strains (figure 3.7A and 3.8B).

3.2.5 Preferential viral infection of the SVZ

TMEV infects macrophages but has been recently proposed to target polysialic acids. The SVZ has the highest concentration of sialic acid in the forebrain in the form of polysialylated neural cell adhesion molecule (PSA-NCAM) which is specifically expressed by SVZ neuroblasts. I queried whether TMEV infects SVZ neuroblasts, and thereby concentrates the viral load in the periventricular zone. Immunohistochemistry against the BeAn strain of virus which recognises the VP1, VP2 and VP3 proteins of the TMEV virus, revealed that the virus was found in and around the SVZ in regions of high CD45 activation at 14 dpi (n=7, figure 3.9A) (Goings et al., 2008). Immunostaining for BeAn and doublecortin (Dcx) a marker of SVZ neuroblasts, showed the virus was associated with Dcx^+ neuroblasts at 14 dpi (figure 3.9B). Co-labelling between BeAn and CD45 showed virally infected haematopoietic cells in the SVZ at 7 dpi (n=3) (figure 3.9C). BeAn staining was also closely associated with Dcx and CD45 cells in the RMS (data not shown). In other brain regions at 7 dpi BeAn was often associated with $GFAP^+$ cells especially in the striatum and septum (n=3) (figure 3.9D-E). In the corpus callosum BeAn staining was seen in cells that were negative for both CD45 and GFAP and may be oligodendrocyte cells (figure 3.9F). BeAn virus has previously been detected in the cerebrospinal fluid and leakage into the ventricular system has been proposed as a mechanism of viral spread throughout the CNS (Trottier et al., 2001). BeAn positive cells were frequently seen in $CD45^+$ cells in the choroid plexus suggesting the presence of BeAn virus in CSF fluid in these mice.

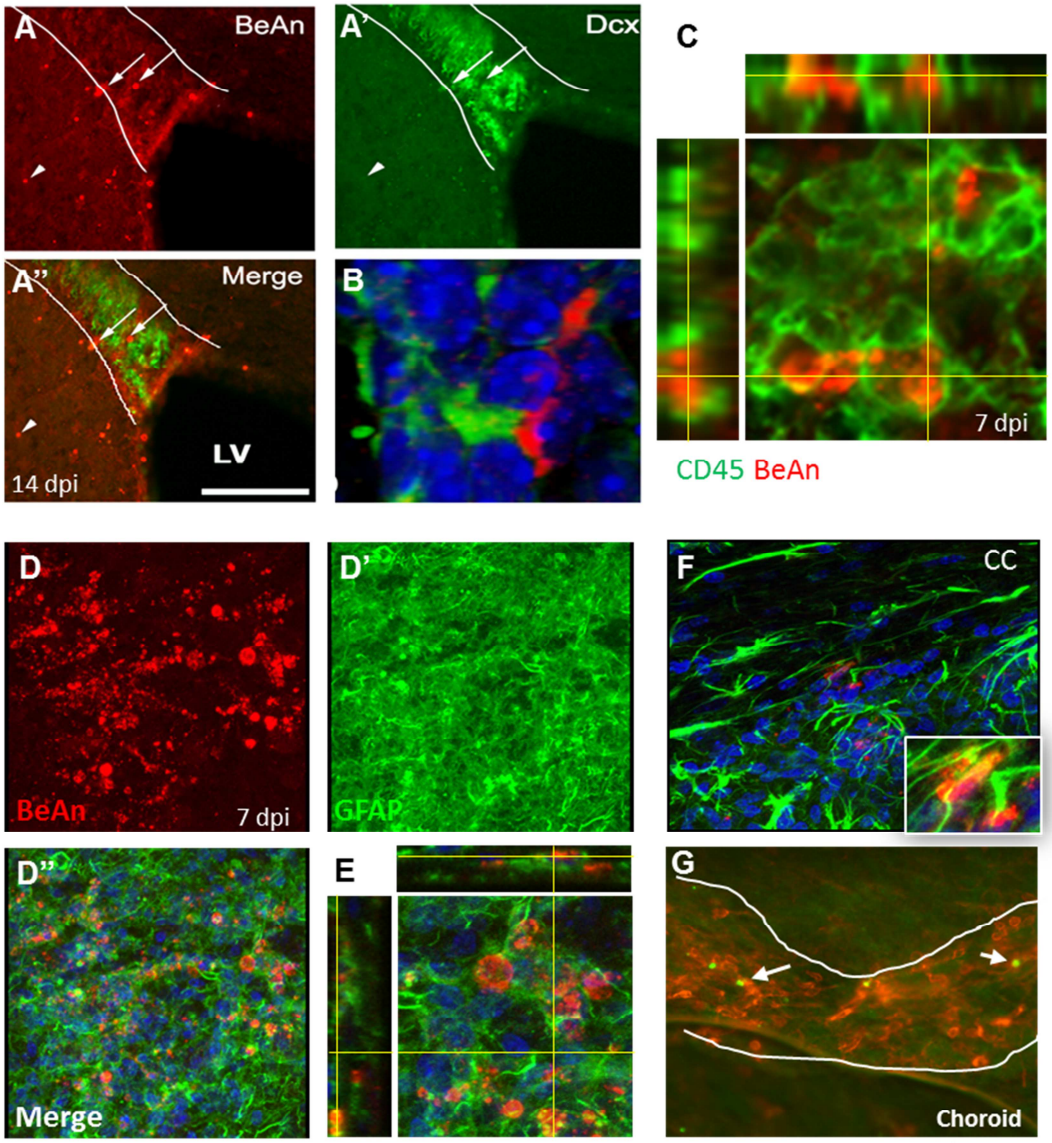


Figure 3.9 BeAn infection of cells of the CNS

(A) Dorsal SVZ labelled with anti-BeAn immunohistochemistry at 14 dpi. Viral labelling (arrows) in SVZ (outlined based on DAPI staining) and in surrounding parenchyma.

(B) Some viral particles were seen in Dcx+ cells.

(C) BeAn (red) infected CD45 (green) cells are present in the SVZ

(D) In striatum clusters of BeAn (red) is associated with GFAP+ (green) cells. Compressed z-stack.

(E) High mag compressed confocal stack showing infection of GFAP+ cells.

(F) In the corpus callosum BeAn+ cells are found that do no co-label with either CD45 or GFAP.

(G) BeAn infected (green) cells are visible in CD45+ (red) cells within the choroid plexus (BeAn particles shown by arrows)

3.2.6 Disruption of neuroblast chain integrity and changes in migration

Dcx is a microtubule associated protein and is an accepted readout for SVZ neurogenesis and emigration. In control mice, Dcx^+ neuroblasts are organised in tight arrays of cells (figure 3.10A). We had previously reported in Going et al, (Goings et al., 2008) that in TMEV infected SJL mice SVZ neuroblast cell-cell contacts were disrupted and their membranes exhibited a loss of integrity leading to an amorphous morphology in some cells at 21 dpi. (figure 3.10D). This disruption was also apparent from as early as 3 dpi and correlated with sections that contained high numbers of T-cells (figure 3.10B-C). Chain disruption was also present in the B6 mice (figure 3.12B). Similar results were found using PSA-NCAM, another neuroblast marker, the proposed target for TMEV (figure 3.10G-H). In order to quantify this apparent loss of neuroblasts the numbers of Dcx^+ cells as a percentage of total DAPI nuclei was quantified in the dorsal SVZ. Dcx^+ cell were significantly decreased at all time points in SJL/J ($n=7$, $p<0.001$, figure 3.11A) and at 3 and 7 dpi in C57BL/6 mice ($n=7$, $p<0.05$, figure 3.12A-B) although the total number of $DAPI^+$ cells remained similar. Naïve data has been included to exclude any influences due to the injection site as even very distant injuries can stimulate Dcx emigration in the SVZ.

Small numbers of Dcx^+ cells constitutively emigrate dorsally into the corpus callosum and septum and ventrally into the striatum (Yang et al., 2004). Increased numbers of Dcx^+ SVZ neuroblasts emigrated after a variety of insults such as stroke and traumatic brain injury (Young et al., 2011). Emigrated Dcx cells were counted to see if TMEV caused similar increases in emigration (figure 3.11B-E). In SJL mice there was a statistical increase in emigration into the dorsal striatum ($n=7$, $p<0.01$), septum ($n=7$, $p<0.05$) and ventral regions ($n=7$, $p<0.001$) at 21 dpi and at 45 dpi in the corpus callosum ($n=7$, $p<0.05$) (figure 3.11F). In B6 mice TMEV infection caused increase emigration of neuroblasts into the striatum at 7 dpi ($n=7$, $p<0.05$, figure 3.12C) but no change in

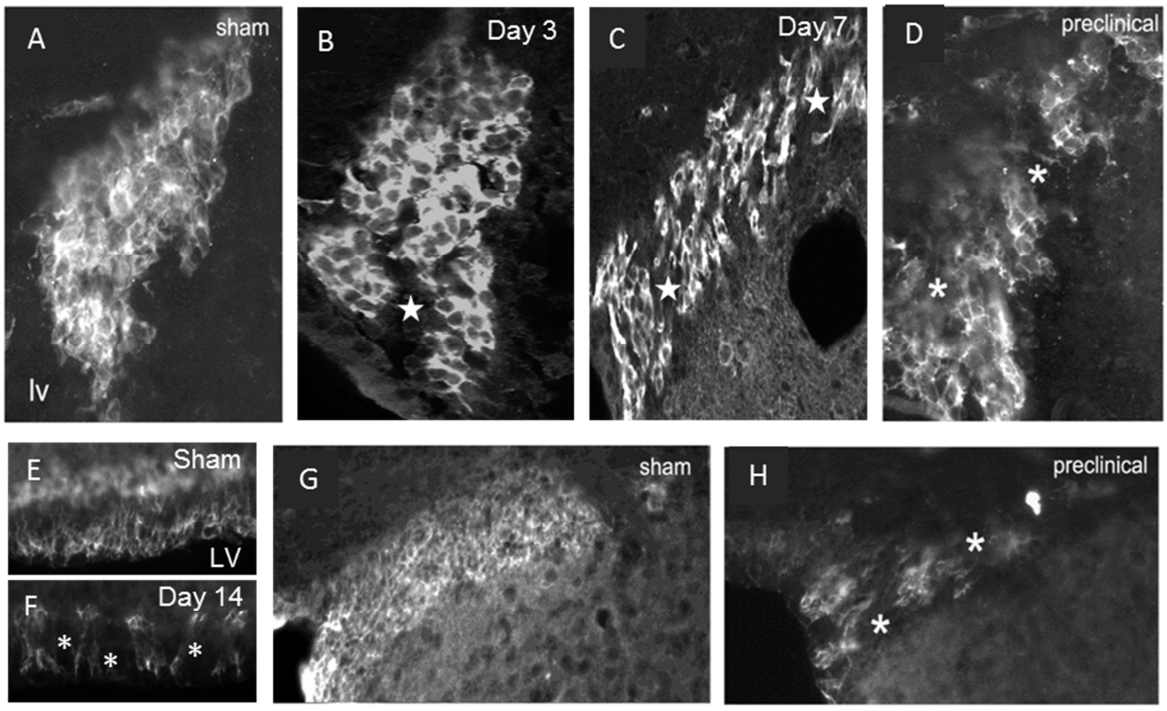


Figure 3.10 Loss of PSA-NCAM and disruption chains over time

(A) Cross section of Dcx+ chains in control SVZ

(B-D) Cell-cell contacts dissipate in SVZ at 3 dpi (B), 7 dpi (C) and 21 dpi (D) . Gaps in chains shown by *

(E-F) Gaps between chains in cross section of lateral ventral wall. Gaps shown by *

(G) PSA-NCAM immunohistochemistry in dorsolateral SVZ reveals contiguous chains of cells in sham controls

(H) Loss of PSA-NCAM+ cells in preclinical mice after TMEV. Gaps indicated by *

emigration into the corpus callosum (figure 3.12D). However, it should be noted that is only indirect evidence of migration from the SVZ. Other methods such as retroviral tracing or labelling by electroporation and tracking of positively labelled cells is needed to confirm these cells have derived from the SVZ.

3.2.7 TMEV infection leads to decreases in neural-lineage cell proliferation

The number of SVZ cells expressing phosphorylated histone H3 (Ph3), which is specifically phosphorylated during mitosis, was significantly decreased at all time points examined following TMEV infection in SJL/J mice (n=7, $p<0.01$, figure 3.13A). Only cells that were CD45- negative were counted to exclude haematopoietic lineage cells. To determine if different SVZ subregions were similarly affected the SVZ was split into 4 subregions. After TMEV infection significant decreases in proliferation was seen in dorsal striatal (n=7, $p<0.05$), middle (n=7, $p<0.01$) and ventral regions (n=7, $p<0.05$) (figure 3.13B). Ventral regions showed the greatest decreases at 14 dpi with an almost complete loss of proliferation. Proliferation in dorsal septal regions did not change.

Whilst C57BL/6 mice initially show the same decreases in proliferation as SJL/J mice at 3 and 7 dpi (n=7, $p< 0.01$, figure 3.14A) at 14 dpi there is a recovery in proliferation (not significant compared to sham). When SVZ proliferation is examined at the subregion level this recovery in proliferation at 14 dpi can be clearly seen in all regions (figure 3.14B). These results suggest that either clearance of virus from the B6 SVZ or the reduction in T-cell presence allows SVZ neural-lineage cells to recover levels of proliferation once more.

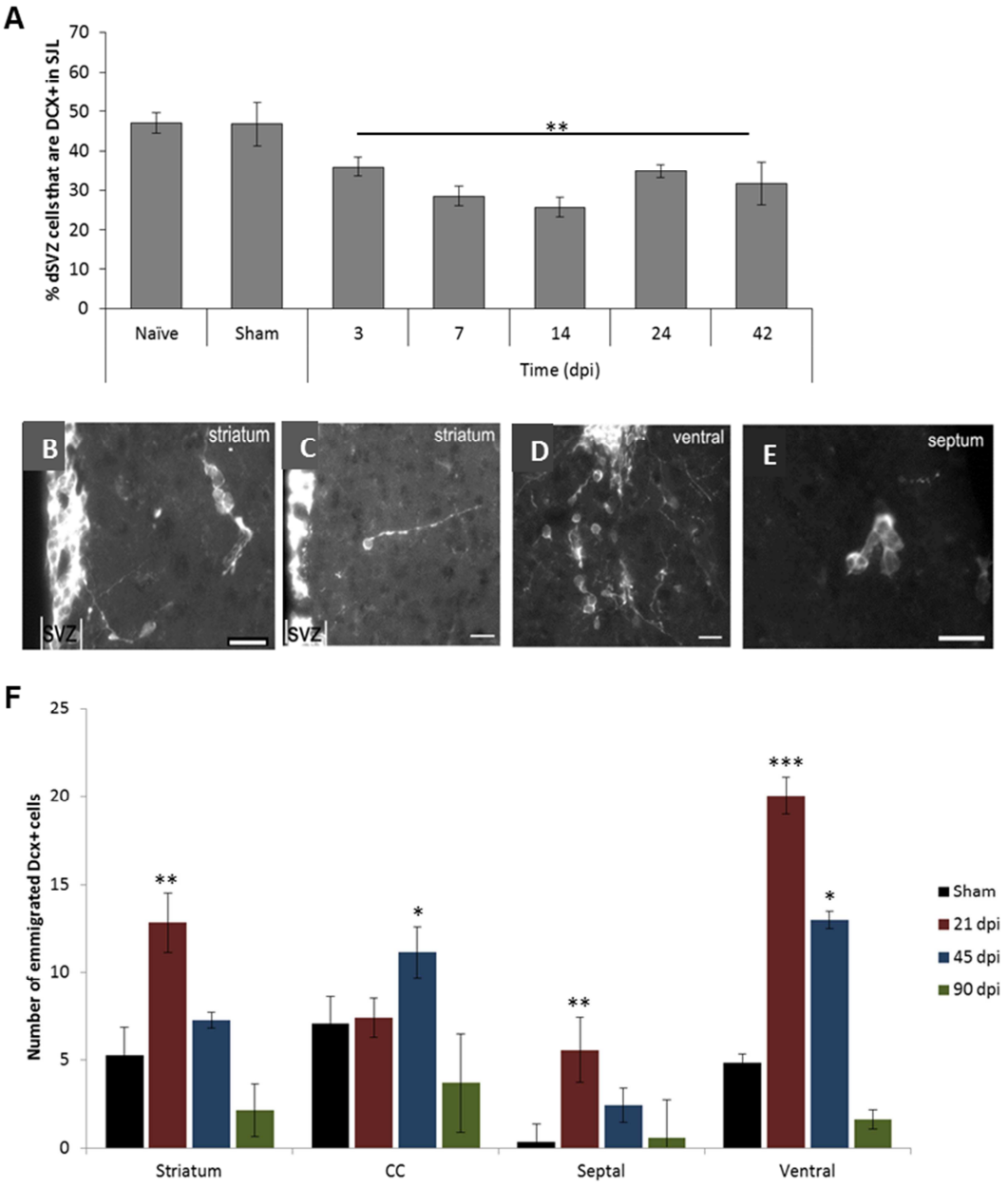


Figure 3.11 TMEV causes a transient increase in ectopic neuroblast emigration in SJL mice

(A) The numbers of Dcx+ cells as a percentage of total DAPI nuclei within the dorsal SVZ over TMEV progression.

(B-E) Examples of chains of Dcx+ cells and individual Dcx+ cells emigrating from SVZ into surrounding parenchyma

(F) Number of emigrating neuroblasts show a transient increase but decreases by the chronic stages. (Goings et al, 2008)

* p<0.05, ** p<0.01, *** p<0.001. Statistics compared to sham (ANOVA).

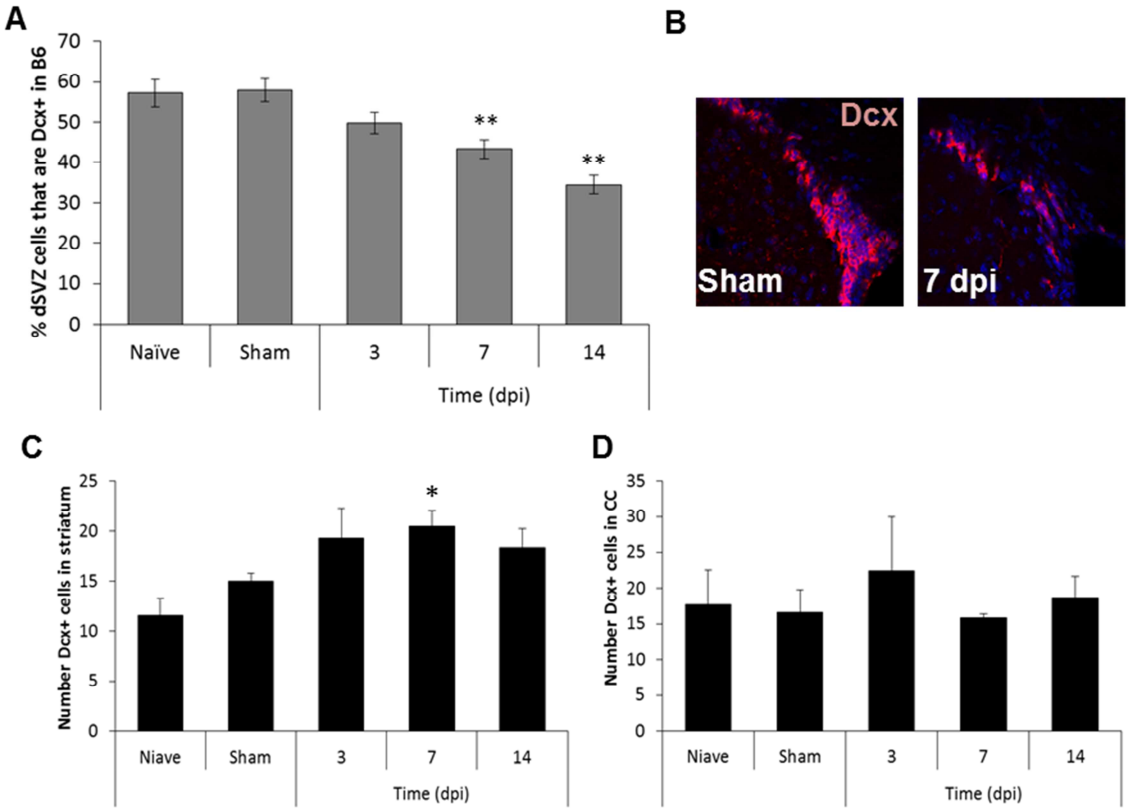


Figure 3.12 TMEV causes an increase in neuroblast emigration into the striatum in B6 mice

(A) The numbers of Dcx+ cells as a percentage of total DAPI nuclei within the dorsal SVZ after TMEV infection.

(B) Dcx staining in the dSVZ of sham and TMEV 7 dpi showing loss of neuroblasts

(C) Increase in neuroblasts emigration into the striatum at 7 dpi.

(D) TMEV infection does not change neuroblast emigration into the corpus callosum..

* $p<0.05$, ** $p<0.01$, Statistics compared to sham (ANOVA) n=7 all groups

3.2.8 TMEV leads to cell death *in vitro*

I have demonstrated that there the BeAn virus is capable of infecting cells, some of which may be SVZ cells and they infection may be direct or indirect through synaptic spreading. To further study the effects of TMEV infection, neurospheres were derived from the SVZ of B6 p4 mice and infected with increasing concentration of BeAn virus. Increasing the moiety of infection results in a significant decrease in both the numbers of neurospheres ($n=3$, $p<0.001$) and their size ($n=3$, $p<0.01$) over serial passages (figure 3.15A). At very high infections (MOI 100) neurospheres are no longer detected. Staining of infected cells shows labelling of some cells with cleaved caspase-3 at MOI 1 that is greatly increased at MOI 10 (figure 3.15B). Infected neurospheres lose their spheroid shape and gradually become fragmented with weak cell-cell contacts within the spheres (figure 3.15C-G). This can be clearly seen at high magnification (figure 3.15H). This suggests that TMEV is preventing the SVZ cells from proliferating, and at higher concentrations induces apoptosis. Whilst *in vitro* infection may lead to cell death this represents a heavy, acute infection that is not directly comparable with data from *in vivo* experiments.

One question that was of interest was whether neurospheres derived from TMEV infected adult mice would lead to changes in neurosphere cell fate after differentiation. Several attempts to produce spheres resulted in failure as the spheres were too unhealthy to grow properly and resulted in poor differentiation with high levels of cell death.

2.12.1 Profiles of SVZ inflammatory mediators varies between strains

Relative fold up-regulation of SVZ mRNA levels 7 dpi TMEV infection between the two strains was measured using an RT-PCR array for chemokines and cytokines related to autoimmunity. For a complete list of fold gene changes see table 2 in appendix 2. In

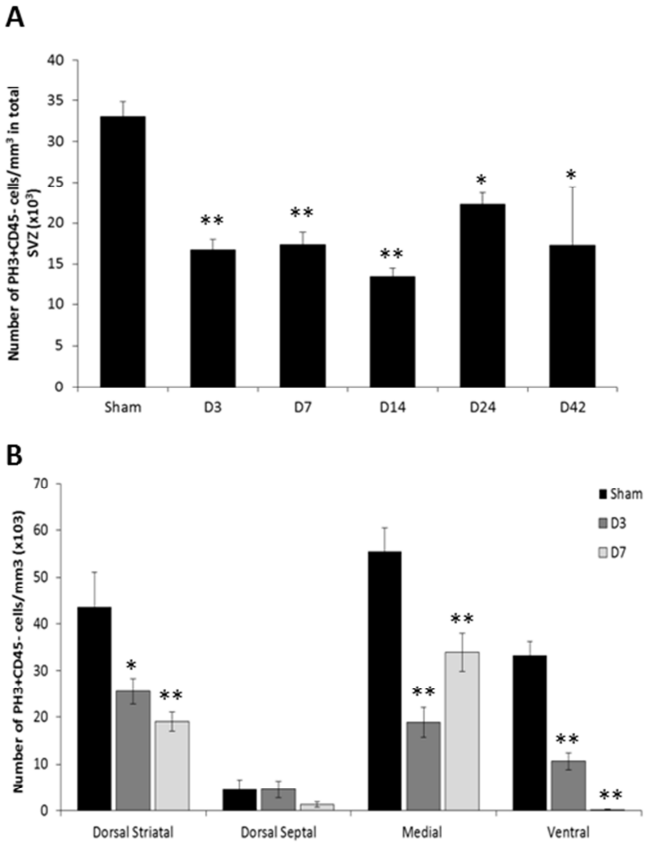


Figure 3.13 Decreases in SVZ proliferation after TMEV infection in SJL/J mice

(A) Number of PH3+ cells decreased after TMEV *P=0.05

(B) Different SVZ subregions show differences in Ph3+ cells. *$P<0.05$, ** $P<0.01$

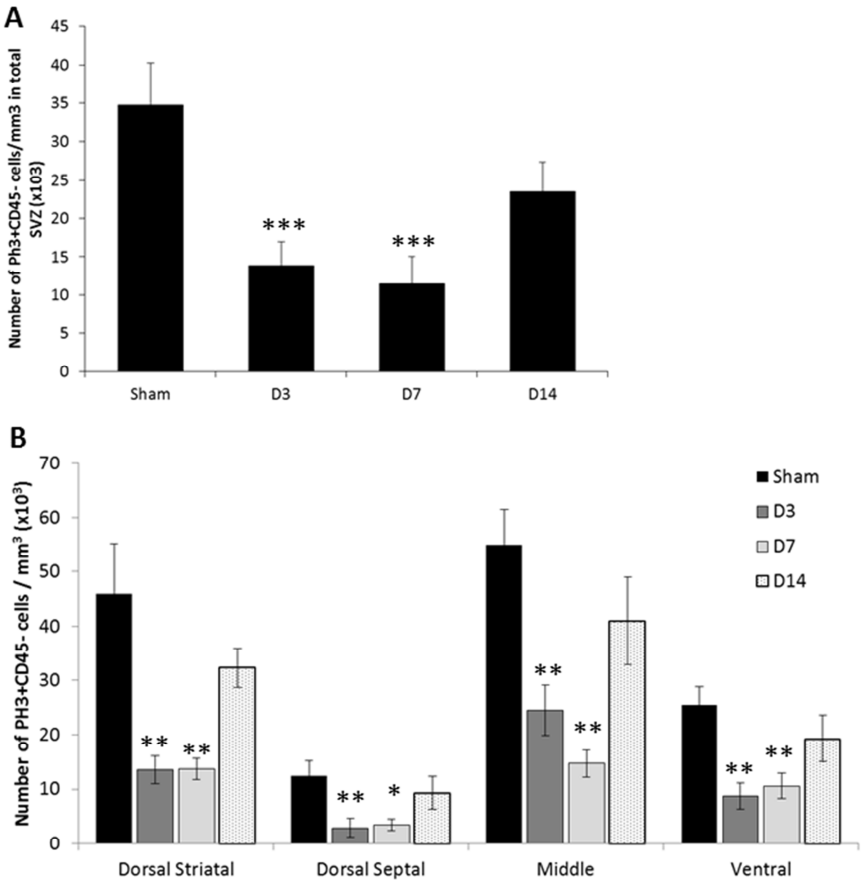


Figure 3.14 Proliferation in C57BL/6 shows sign of recovery at later time points

(A) Number of PH3+ cells after TMEV

(B) Different SVZ subregions show differences in PH3+ cells.

*p<0.05, ** p<0.01, *** p<0.001

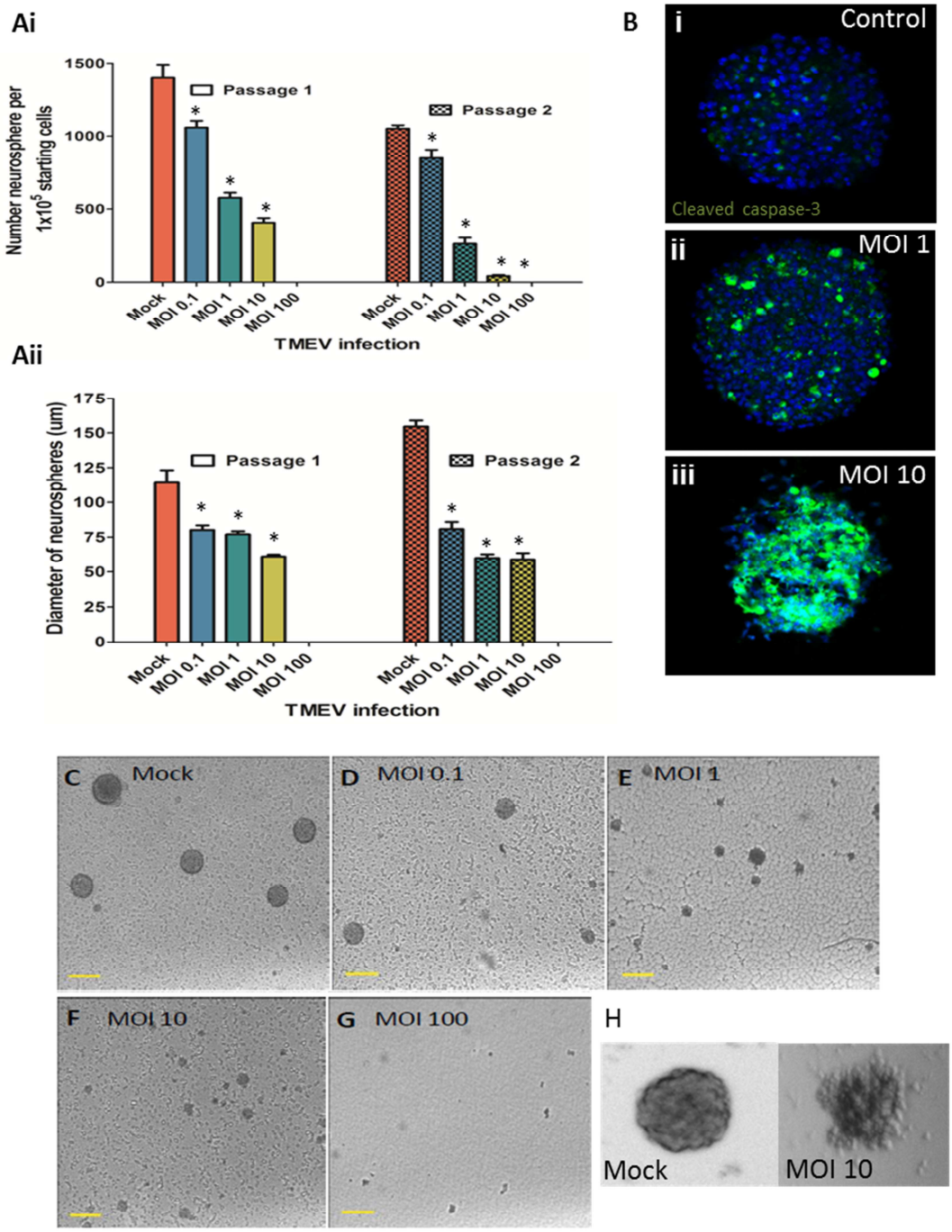


Figure 3.15 Infection of SVZ derived neurospheres inhibits cell growth

(A) Fewer neurospheres are produced in TMEV infected cultures. And they are smaller in size * $P < 0.05$

(B) TMEV infected neurospheres label for cleaved caspase-3 at high TMEV concentrations

(C-G) Infected spheres show 'unhealthy' morphology at high moieties.

(H) High magnification image of infected neurospheres (20X).

Scale bar 100 µm.

general more genes were unregulated in the B6 tissue (45%±1.06) compared to SJL tissue (28.9%±1.95). Several chemokines showed significantly greater up-regulation in the B6 mice compared to the SJL including CCL1, CCL11, CCL19, CCL2, CCL22, CCL7, CXCL1 and CXCL10 ($n=3$, $p<0.05$, figure 3.16A-C). Up-regulation of chemokine receptors was also lower in SJL mice (figure 3.16B). Only CCL5, CCL8 and CXCL11 showed greater increases in the SJL mice compared to B6. Many cytokines showed greater up-regulation in B6 mice including IFNγ, IL1β (figure 3.16D) and members of the tumour necrosis family (TNF) (figure 3.16E). Of particular interest is the finding that several components of the complement system are much less up-regulated in SJL mice compared to B6 mice (figure 3.16F). The complement system is important in recognising pathogens such as viruses and targeting them for destruction either by direct formation of a membrane attack complex or indirectly by recruiting phagocytic cells. Similarly, mRNA transcripts for several toll-like receptors were also less up-regulated in SJL mice (figure 3.16G). Toll-like receptors (TLR) are a family of pattern recognition receptors (PRRs) that allow for the recognition of pathogen-associated molecular patterns (PAMPs), motifs conserved across broad subclasses of bacteria, viruses, or fungi.

2.12.2 Chemokine protein levels in SVZ differ between strains

In order to confirm the differences in mRNA fold changes the protein levels of chemokines in SVZ and cortical tissue at 3 and 7 dpi were measured using ELISA. Four chemokines, CCL2, CCL5, CCL8 and CXCL10 were chosen as those that had shown the greatest differences in mRNA fold-change between strains (figure 3.16). For all four chemokines both constitutively and after TMEV infection protein levels were higher in SVZ tissue compared to cortical tissue. For CCL2, CCL5, CC8 and CXCL10 there were

no significant increases in proteins levels at 3 dpi compared to sham in either the SVZ or the cortex. This would suggest that even though T-cells are present in the SVZ at this time point infiltration may not be due to increases in chemokine expression. Consistent with the PCR data, levels of CCL2 (n=3, p=0.008, figure 3.17A) and CXCL10 (n=3, p=0.04, figure 3.17C) were significantly higher in the B6 compared to the SJL SVZ at 7 dpi. In contrast, SJL mice had higher levels of CCL5 (n=3, p=0.01, figure 3.17E) in SVZ tissue than B6 at 7 dpi, which is consistent with the array data. Both strains had similar protein levels of CCL8 in SVZ at 7 dpi (figure 3.17G). This does not match the PCR array data which showed a greater fold up-regulation of CCL8 mRNA in the SJL mice compared to the B6. However, constitutive CCL8 protein levels in sham SVZ are much lower for SJL mice. This would mean that if there are fewer mRNA transcripts present in normal SJL brain but levels are the same as in B6 after TMEV infection this would appear as a greater fold increase in mRNA levels but give equivalent levels of protein.

2.12.3 Cytokine profiles from primary astrocyte culture are similar to SVZ tissue

TMEV infection of primary SVZ astrocyte cultures derived from SJL mice caused the up-regulation of over 28/72 genes examined (figure 3.18A). Around half of these were chemokines (14/28) with the highest fold up-regulation for CCL12, CXCL10, CXCL5 and CCL4 (figure 3.18B). There was also up-regulation of the cytokines IL-6, IL1β and TNF. Similar to SVZ tissue complement component 3a receptor 1 was up-regulated along with mRNA for Toll-like receptors 2, 7 and 1. Interestingly, CD40 antigen also showed a 12xfold up-regulation. CD40 is a co-stimulatory molecule from the MHC class II complex that is critical for antigen presentation and T-cell activation.

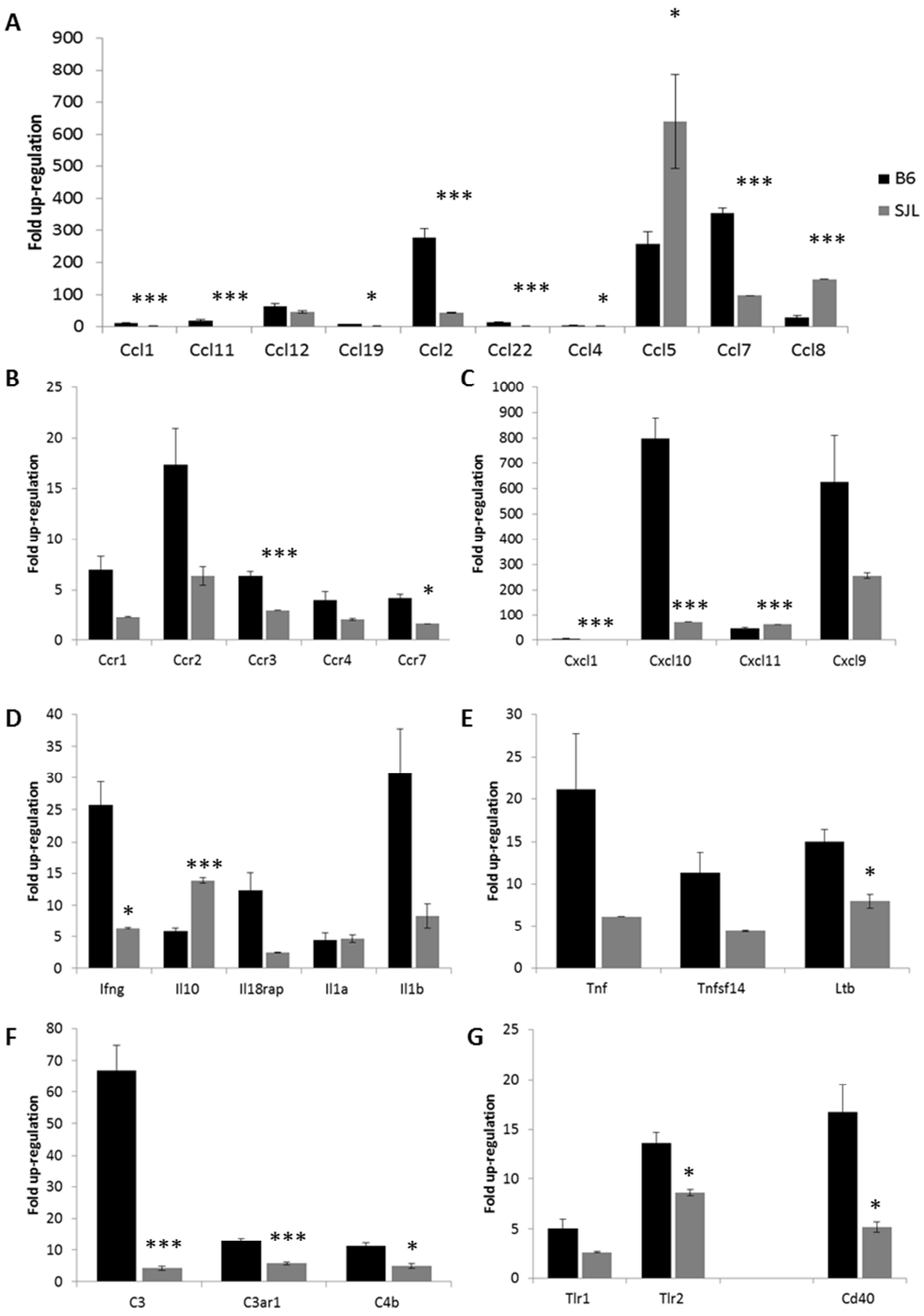


Figure 3.16 Levels of cytokine mRNA in SVZ tissue from B6 and SJL mice at 7 dpi
SVZ tissue is dissected naive mice and 7 dpi TMEV and run on a RT-PCR array for cytokines and chemokines. All numbers presented are fold change of TMEV infection tissue compared to control tissue. (A) Expression of C-C motif chemokines, (B) Expression C-C motif chemokine receptors, (C) Expression of C-X-C motif chemokines, (D) Expression of inflammatory cytokines, (E) Expression member of TNF family, (F) Members of complement system and (F) Mediators of antigen presentation

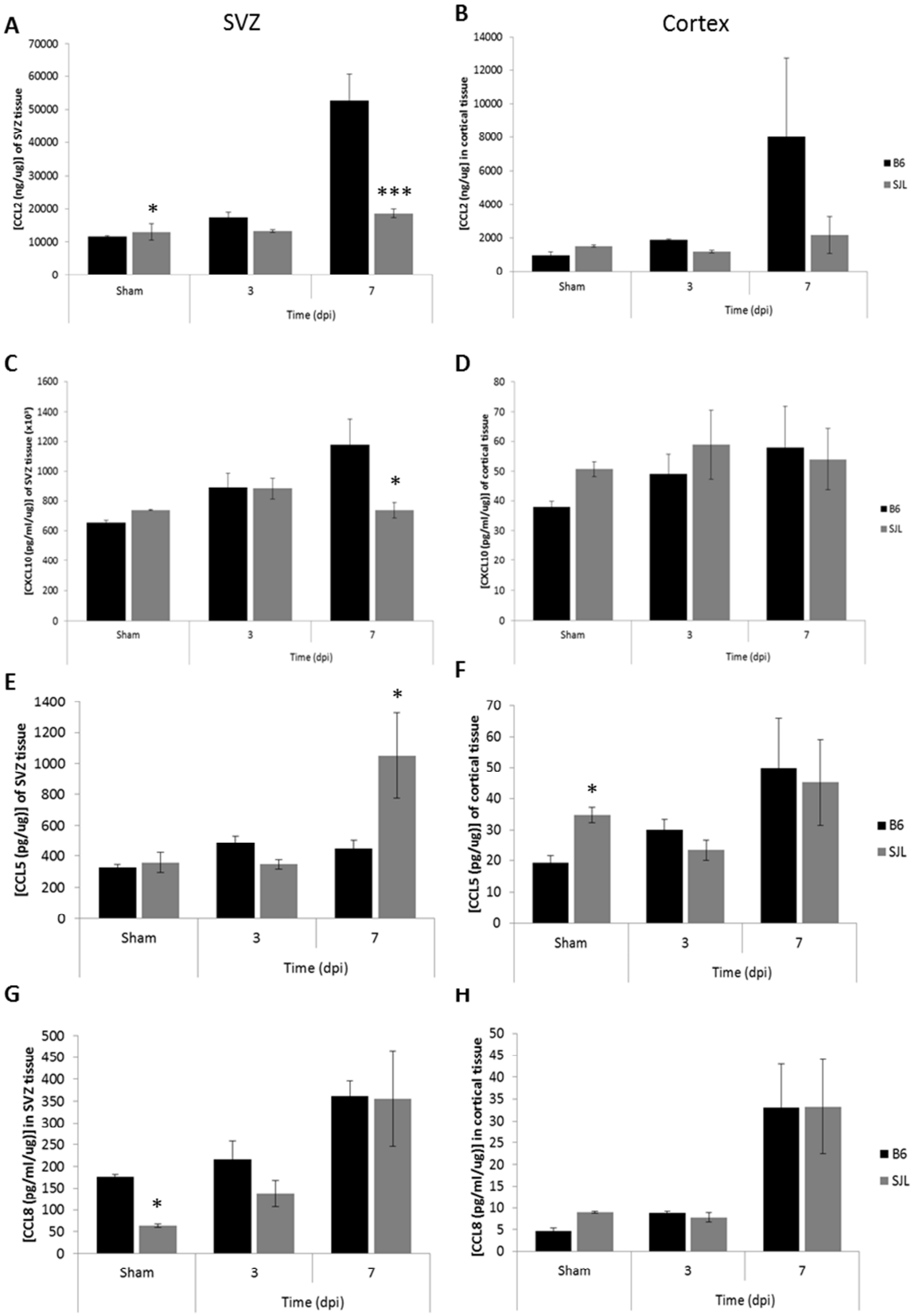
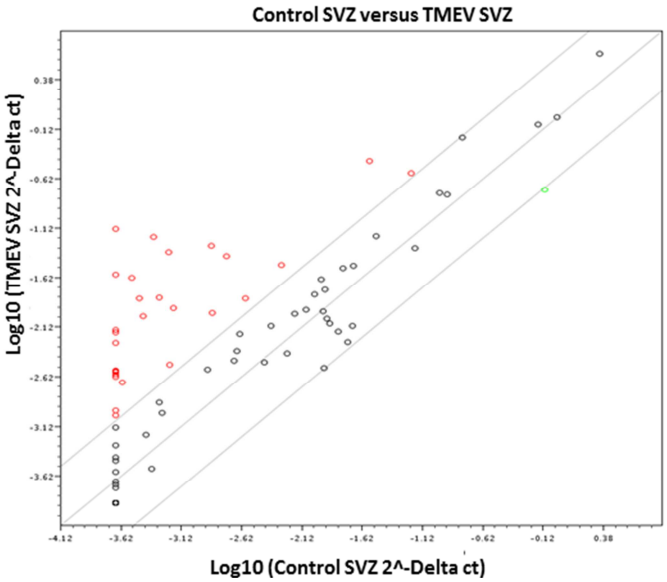


Figure 3.17 Protein levels of chemokines in SVZ tissue from B6 and SJL mice at 7 dpi

Measurement of protein levels of cytokines in tissue dissected from naïve, 3 and 7 dpi TMEV SVZ and cortex analysed by ELISA. * = $p<0.05$, ** $p<0.01$, *** $p<0.001$.

(A-B) CCL2, (C-D) CXCL10, (E-F) CCL5 and (G-H) CCL8

A



B

Gene	Gene symbol	Fold Change
Chemokine (C-C motif) 12	Ccl12	349.7063
Chemokine (C-X-C motif) 10	Cxcl10	139.1021
Chemokine (C-X-C motif) 5	Cxcl5	118.6033
Chemokine (C-C motif) 4	Ccl4	81.0084
Interleukin 6	Il6	73.0089
Complement component 3a receptor 1	C3ar1	43.1115
Chemokine (C-C motif) 5	Ccl5	37.2715
Chemokine (C-C motif) 3	Ccl3	32.8996
Chemokine (C-C motif) receptor 1	Ccr1	31.125
Integrin beta 2	Itgb2	29.8571
Chemokine (C-C motif) 8	Ccl8	26.7228
Toll like receptor 7	Tlr7	24.4201
Chemokine (C-X-C motif) 2	Cxcl2	22.3159
Chemokine (C-X-C motif) 11	Cxcl11	17.7531
Chemokine (C-C motif) 7	Ccl7	13.3614
Interleukin 1 alpha	Il1a	12.9063
Chemokine (C-X-C motif) 3	Cxcl3	12.6407
CD40 antigen	Cd40	12.3805
Tumour necrosis factor	Tnf	11.7942
Chemokine (C-X-C motif) 9	Cxcl9	11.0809
Interleukin 1 receptor antagonist	Il1rn	8.6338
Interleukin 8 receptor accessory protein	Il18rap	5.2054
Toll like receptor 2	Tlr2	7.6741
Receptor (TNFRSF)-interacting serine-threonine kinase 2	Ripk2	6.3203
Chemokine (C-X-C motif) 1	Cxcl1	5.6178
Toll like receptor 5.	Tlr5	5.0982
Chemokine (C-C motif) 2	Ccl2	4.5631
Interleukin 1 beta	Il1b	4.5631

Figure 3.18 Levels of cytokine mRNA in primary SVZ astrocytes cultures infected with TMEV MOI 10

Primary astrocytes cultures derived from SVZ were infected with TMEV at MOI 10 for 24 hours before measurement of cytokines mRNA levels by RT-PCR.

(A) Graph represents positive and negative fold changes in genes of control astrocytes versus TMEV infected astrocytes. Dots in black between the lines represent changes that were less than 4-fold. Red dots are gene changes that were greater than 4-fold.

(B) Table of all cytokines and chemokines that showed a fold change in mRNA greater then 4. Listed in order of most up-regulated first.

2.13 Discussion

This study has examined the effects that TMEV induced inflammation has upon the subventricular zone neurogenic niche. In this dissertation, I have shown that the BeAn strain of the TMEV virus infects cells of the SVZ *in vitro*. This causes long-term decreases in proliferation of SVZ cells and a disruption in neuroblast chain integrity and neuroblast numbers. I have also found that infiltrating T-cells target the SVZ over other forebrain regions from as early as 3 days post infection. In SJL mice occupation of the SVZ by T-cells continues right through to the chronic stages of the disease. By comparing between the susceptible SJL mice and resistant B6 mice I have demonstrated that in a resistant strain T-cell infiltration of the SVZ is largely gone by 14 dpi and this is accompanied by a recovery in SVZ proliferation. Differences in patterns in immune cell infiltration may be due to different cytokine profiles following infection.

3.3.1 The BeAn virus directly infects cells of the SVZ niche

BeAn virus was found to infect $CD45^+$ cells and neural progenitor cells in the subventricular zone from 7 days after infection. It is possible that infection of SVZ cells is a result of leakage of the virus from the cerebral hemispheres into the ventricular system. BeAn mRNA has previously been detected in cells isolated from cerebrospinal fluid at 60 dpi (Trottier et al., 2002). In my data BeAn antigen was detectable in the choroid plexus at 14 dpi suggesting the virus may be present in the CSF much earlier than has been previously published. As BeAn infected cells were detected in the SVZ at 7 dpi it would be worthwhile measuring viral load in the CSF at even earlier timepoints to confirm if this is a means of dissemination for the virus. Other groups have shown this may well be the case

as BeAn viral antigen can be detected in ependymal cells lining the fourth ventricle as early as 4 and 7 dpi in both SJL and B6 mice (Kummerfeld et al., 2012). TMEV infected neuroblasts cells were also detected throughout the RMS raising the intriguing possibility that infected neural progenitors may act as a viral conduit through the RMS to the OB allowing TMEV to disseminate through the CNS. Such a mechanism has been reported for coxsackievirus B3 (CVB3) where infected SVZ progenitor cells are no longer able to proliferate but are still capable of migrating to the OB where they differentiated into neurons causing CVB3 viral spread in the OB (Feuer et al., 2005). Afferent and efferent connections of the OB project to many brain regions, including the hippocampus, entorhinal area, insular cortex, and olfactory nuclei (Shipley and Adamek, 1984). CNS distribution of TMEV virus appears to be facilitated by intra-axonal transport of the virus (Dal Canto and Lipton, 1982; Tsunoda, 2008; Tsunoda et al., 2007) and TMEV virus carried to the OB by neuroblast cells could infect surrounding neurons in the OB and spread to other brain regions through axonal transport. This is a strong possibility as inoculation with TMEV into the olfactory bulb can disseminate throughout the limbic system to the hippocampus, entorhinal cortex, amygdaloid nuclei, mammillary body and olfactory nuclei (Wada and Fujinami, 1993).

The targeting of SVZ progenitor cells by the BeAn virus may relate to the receptor used by the virus. The BeAn strain has been shown to use sialic acid on N-linked glycoproteins for binding and entry into cells (Shah and Lipton, 2002; Tsunoda et al., 2009; Zhou et al., 2000). Three amino acids in the VP2 protein are directly involved in this interaction and are important in determining viral persistence by influencing virus attachment to a cellular receptor, such as sialyloligosaccharides (Zhou et al., 1997). Within the SVZ, sialic acid is expressed at very high levels as a polysialyated form that is attached to neural cell adhesion molecules (PSA-NCAM) on neural progenitor cells (Doetsch and

Alvarez-Buylla, 1996; Ono et al., 1994; Petridis et al., 2004). This high expression of PSA-NCAM on the surface of progenitor cells may provide a potential binding site for the BeAn virus. A similar effect has been reported for stem/progenitor cells in the lung where high expression of sialic acids allowed infection by influenza virus and reduced the potential for self-renewal of these cells (Khatri et al., 2012).

TMEV infected astrocytes were also present in the surrounding parenchyma and corpus callosum. Infection of cells in the corpus callosum has previously been reported as early as 4 dpi (Kummerfeld et al., 2012). Similar to my staining, the majority of infected cells were found to be $GFAP^+$ and the rest oligodendrocytes and microglia/macrophages. Within susceptible strains of mice it is thought that the induction of periventricular demyelination requires a switch in cell tropism from neuronal to glial cells. A very common finding in MS patients is development of characteristic periventricular lesions, with the lateral ventricles of the forebrain the most affected, followed by the fourth ventricle, third ventricle and aqueduct. Additionally, clinical MRI of these 'Dawson's fingers' demonstrates lesion progression from the lateral ventricle to surrounding brain areas in affected humans. Based on the findings with BeAn staining in subventricular regions this periventricular inflammation may could be a consequence of subependymal viral spread. The SVZ has been shown to be vulnerable to a wide range of different viral attacks (Das and Basu, 2008; Feuer et al., 2005; Krathwohl and Kaiser, 2004; Liu et al., 2005) and several other viruses that can infect the CNS have been reported to use sialic acid as a binding site (Leung et al., 2012; Puryear et al., 2012; Sanchez-Felipe et al., 2012; Zhang et al., 2012). Further work would identify if other viruses linked to MS susceptibility, like EBV, also infect SVZ cells. This is an important consideration if the SVZ is to be targeted for endogenous repair as therapies aimed at increasing ectopic migration may only serve to enhance viral spread.

3.3.2 T-cell infiltration targets the SVZ

Both susceptible and resistant strains of mice show targeted infiltration of $CD3^+$ T-cells into the SVZ that precedes inflammation in other forebrain regions. This inflammation shows a peak around 7 dpi. Infiltration of T-cells in the SVZ of susceptible mice continues right through to the chronic stages of the disease, whilst in the resistant mice inflammation decreased by day 14. This pattern is consistent with reported periventricular inflammation around the fourth ventricle that was most intense from 7 to 56 dpi in SJL/J mice and from 7 to 14 dpi in C57BL/6 mice (Kummerfeld et al., 2012).

Inflammation may target the SVZ due to the high presence of viral antigen. The SVZ may also be vulnerable to inflammation as several chemokines are constitutively expressed in the SVZ to regulate neuroblast migration and proliferation (Kokovay et al., 2010; Tran et al., 2004; Turbic et al., 2011). GFP^+CD3^+ cells injected into the lateral ventricles of mice migrate into the SVZ (Muzio et al., 2010) suggesting that the healthy SVZ may have chemo-attractant signals but T-cell immigration is normally prevented through an intact Blood Brain Barrier. Support for this may be found from my data where protein levels of chemokines were constitutively much higher in the SVZ when compared to the cortex. T-cells were not present in shams but T-cell infiltration into the SVZ could be detected as early as 3 dpi and was significantly higher than in other brain regions. Levels of the chemokines CCL2, CCL8, CCL5 and CXCL10 at 3 dpi were not different from sham mice. All of these chemokines are known to be chemoattractant to T-cells in the CNS (Glabinski et al., 1998; Huang et al., 2001; Karpus et al., 1995; Muzio et al., 2010; Tsunoda et al., 2004). This suggests that following TMEV induced expression of adhesion molecules on endothelial cells, allowing immune cells across the BBB (Mestre et al., 2011), constitutive chemokine levels were sufficient to attract T-cells to the SVZ.

Patterns of infiltration within different SVZ sub-regions varied between the strains with SJL dominated by dorsal infiltration and B6 mice by ventral infiltration. These differences may be due to differential spread of various chemokines throughout the ventricular wall. Alternatively, as blood vessels provide a main route of T-cell entry around the SVZ the vasculature may be unique for each strain and influence immigration patterns. The Szele lab have recently published a paper showing that wholemounts of the lateral wall can provide an excellent tool to study the vasculature in the lateral wall and subependymal layer (Young et al., 2011). This technique could be used to identify major strain differences in the location of blood vessels.

3.3.3 SVZ Cytokine profiles are different between SJL and B6 mice

In order to study cytokine expression in the SVZ I utilised a commercially available RT-PCR array with a variety of chemokines and cytokines related to autoimmunity. This approach was chosen as it allowed us to screen for a broad range of chemokines which may have been changed by TMEV infection. The array has limitations though in interpreting the data as it only provides a readout of relative gene fold-changes but not quantitative measurements of RNA copies. In order to confirm these differences I used ELISA to measure protein levels in tissue. Whilst this is a more accurate readout of levels of chemokines it still has several limitations. ELISA measurements of total tissue protein levels do not provide any indication of which cells are making the protein or whether the levels represent cellular or extracellularly secreted protein.

After TMEV infection many chemokines and cytokines are up-regulated in the SVZ. Other studies have also shown CNS expression of these chemokines after infection with BeAn virus (Hoffman et al., 1999; Murray et al., 2000) as well as with other viruses (Lane and Hosking, 2010; Nansen et al., 2000) suggesting a possible role for these molecules in viral pathogenesis. Many chemokine receptors are up-regulated by $CD4^+$ and $CD8^+$ T-cells when they are activated and are important in the accumulation of T-cells in the CNS to aid in the clearance of viral burden or drive immunpathologic responses. Within the SVZ, levels of several chemokines were significantly different between the resistant and susceptible strains after TMEV, with the majority displaying higher levels in the B6 mice compared to the SJLs. This may cause less efficient recruitment and infiltration of anti-viral $CD8^+$ T cells into the CNS in the SJL mice. The chemokines showing the highest expression within the SVZ after TMEV were CCL5, CCL2 and CXCL10. Genetic deficiency of CCR2 and its ligands CCL2, CCL5 or CXCL10 inhibits infiltration of T cells and is associated with increased viral loads after viral infection (Lane and Hosking, 2010; Nansen et al., 2000).

Very similar patterns of chemokine expression (CXCL10, CCL2 CXCL9, CXCL1, and CCL1) were reported in the SVZ after EAE (Muzio et al., 2010). CXCL10 showed the greatest up-regulation in both TMEV and EAE. In EAE overexpression of CXCL10 in the SVZ by lentivirus increased cellular infiltrate and enhanced demyelination (Muzio et al., 2010). Blockage of CXCL10 in EAE results in clinical improvement with suppression of antigen specific T-cell proliferation (Fife et al., 2001; Wildbaum et al., 2002). In contrast to this, treatment with anti-CXCL10 serum does not ameliorate clinical or pathological disease in TMEV infection (Tsunoda et al. 2004). This may be due to the different role CXCL10 plays in these diseases. In EAE $CD4^+$ Th1 cells are known to initiate demyelinating disease, whilst in TMEV their role is much less clear. The CXCL10

receptor, CXCR3 is expressed at much higher levels on $CD4^+$ Th1 cells than on Th2 cells (Fischer et al., 2000). Attraction of $CD4^+$ Th1 cells into the CNS is known to be important in producing resistance in B6 mice, as an increase in viral load was observed in B6 $CD4^{-/-}$ mice but not SJL $CD4^{-/-}$ mice (Murray et al., 1998). To the best of my knowledge this is the first report that CXCL10 mRNA and protein levels are up-regulated more in B6 mice than SJL mice after BeAn infection and this may be important in resistance to TMEV induced demyelination.

CXCL10 is made and secreted by neurospheres and IFNγ and TNFα can stimulate further expression (preliminary data, not included). Tissue protein levels of CXCL10 were high in the healthy SVZ of both B6 and SJL mice. It is likely that high expression of CXCL10 by SVZ NPCs initially attracts inflammatory cells from the blood, once recruited these secrete large amounts of pro-inflammatory cytokines including IFNγ and TNFα that further increase CXCL10 expression. Such a self-sustained loop could contribute to preferential periventricular localisation of inflammation and lesions.

3.3.4 The use of SVZ primary astrocytes cultures

Astrocytes are important in the development of TMEV inflammation. Elevated astrocyte proinflammatory responses are closely related to viral clearance and strain-dependant protection (Carpentier et al., 2008; Molina-Holgado et al., 2002b; Palma and Kim, 2004; Palma et al., 2003; Rubio and Sanz-Rodriguez, 2007; Rubio et al., 2006). Besides a direct effect on the CNS immune response, astrocytes may also trigger a proteolysis cascade initiated by MMPs and tissue inhibitors of matrix metalloproteinases (TIMPs) that could be responsible for opening of the blood brain barrier during TMEV progression (Ulrich et al., 2006). In order to study the role of SVZ astrocytes in TMEV induction I generated primary astrocytes cultures. Generation of primary cultures from cortical tissue is a widely

published technique (Carpentier et al., 2008; Carpentier et al., 2007; Kimelberg et al., 2000; Morga et al., 1998; Palma et al., 2003; van Neerven et al., 2010) but there are no papers so far published using primary SVZ cultures. An initial plan for the thesis had been to generate both cortical and SVZ cultures and compare their inflammatory responses and abilities to present antigen to T-cells. I found that microglial within SVZ cultures proliferated at much higher rates than in cortical cultures and were extremely difficult to eradicate. This may be related to the 'semi-activated' state of constitutive SVZ microglia that the Szele lab has previously published (Goings et al., 2006). Due to this issue I was only able to produce sufficient pure SVZ astrocyte numbers to run one RT-PCR so statistical analysis was not possible and I was unable to confirm changes at the protein level. Despite this, the RT-PCR array data still provides a good indicator of changes that may occur in SVZ astrocytes after TMEV infection.

3.3.5 SVZ astrocytes express TLR2 after TMEV infection

To initiate immune responses against foreign pathogens, host cells use Toll Like Receptors (TLRs) that can recognised specific molecular structures on pathogens. Ligation of distinct TLRs by pathogens induces specific downstream intracellular signalling cascades and initiates an inflammatory response. TLR2 is important for the production of pro-inflammatory cytokines in response to viral infection. In primary cortical astrocyte cultures TMEV activates innate immunity through a TLR-2 dependent pathway (So and Kim, 2009). In particular highly TLR2-dependent IL-6, IL-1β, CCL2 and CCL5 gene activation (Aravalli et al., 2005) is vigorously induced following TMEV infection (Palma et al., 2003) (Rubio and Capa, 1993). Primary astrocyte cultures from the SVZ also showed activation of the TLR2 gene and increased expression of IL-6 and IL-1β in my studies.

This suggests that SVZ astrocytes respond to TMEV infection through similar TLRs as cortical astrocytes. IL-6 is a key cytokine for promoting pathogenic T cells and modulating antigen processing and its expression by SVZ astrocytes may provide a key role in viral pathogenesis. SVZ astrocytes also expressed TLR5 and TLR7 but very little is known about their function in TMEV.

In the SVZ viral infection induces mRNA expression of pro-inflammatory cytokines such as IL-6 along with TLR2. It is a strong possibility that SVZ astrocytes utilise a TLR2-dependent signally pathway to regulate production of chemokines such as CCL2, CCL5 and CXCL10 which lead to T-cell recruitment in response to TMEV infection. Primary cortical astrocytes from B6 mice express increased levels of cytokines and chemokines including CXCL10, CC2 and CCL5, compared to SJL mice following TMEV infection (Carpentier et al., 2008). In my work SVZ TLR2 mRNA levels show greater increases in B6 mice which may be responsible for the increased expression of chemokines. Higher levels of CD40 antigen mRNA were also present in B6 versus SJL SVZ and up-regulated by TMEV infected SVZ astrocytes. CD40 is required to maintain resistance to demyelination in C57BL/6 mice (Drescher et al., 2000). CD40 is a co-stimulatory molecule for the MHC class II complex that is critical for antigen presentation and T-cell activation following TLR stimulation. These data suggest the possibility that enhanced astrocyte expression of members of the MHC complex may significantly contribute to the ability of the immune system to efficiently clear virus from resistant mice.

3.3.6 Complement system activation in TMEV

Complement system (C system) is part of the innate immune response, and similar to TLRs, functions to recognise and eliminate pathogens and can contribute to the release of

cytokines and induction of inflammation. In the classical pathway C4 binds to Ig-associated C1q enzyme that cleaves C4 to C4b and 4a. The C4b forms a complex called C3 convertase that converts C3 into an active form resulting in formation of a membrane-attack complex (MAC) which is able to lyse viruses. Members of the complement system (C3, C4b) are up-regulated in the SVZ after TMEV infection with higher levels in B6 mice. The DA strain of TMEV caused similar increases in C3 in B6 mice at 6 dpi that were important for regulation of TNF and IL-6 production (Libbey et al., 2010). In this study C3 levels were only measured for the whole brain and they did not identify which brain regions may be expressing it. In this study the role of complement has only been briefly touched upon in the RT-PCR arrays but previously published data on the role of complement in MS suggests it may warrant further investigation. If B6 mice have a greater C response in the SVZ they may be better able to initiate clearance of virally infected cells and prevent viral persistence.

Recent studies highlight that complement may play a predominant role in the pathogenesis of MS (Barnett and Prineas, 2004; Lucchinetti et al., 2000). Data implicates the complement system as an important contributor to the killing of oligodendrocytes and neurons through activation of caspase-3 (Rus et al., 2005a; Rus et al., 2005b). There is a wealth of data indicating that inhibition of complement activation at early stages of the pathways, particularly at the level of the C3 convertases, is effective in blocking or attenuating the course of EAE (Storch et al., 1998). Of particular note, $C3aR^{-/-}$ mice have attenuated EAE disease (Boos et al., 2004). C3aR expression is up-regulated on SVZ primary astrocytes and in SVZ tissue after TMEV and further investigation is needed to determine its role in TMEV pathogenesis. The impact of complement in MS remains poorly understood and these data suggest the TMEV model and differences between strains may prove a useful model to further elucidate its function.

3.3.7 TMEV infection decreases SVZ proliferation

Acute encephalomyelitis induced by TMEV infection results in decreased proliferation of SVZ cells that was present in both resistant and susceptible strains of mice. As I did not perform any co-labelling experiments, I am not able to say whether the decrease represents a loss of one specific cell type. This decrease could result from either cell death due to lytic infection or inhibition of cell proliferation due to a blockade of cell cycle progression caused by the virus or inflammatory mediators. Progressive infection of SVZ derived neurospheres *in vitro* caused an inhibition of growth and an increase in cleaved caspase-3 immunostaining suggesting initiation of apoptotic mechanisms (Sommer and Rao, 2002). However, caspase-3 staining of the SVZ *in vivo* identified very few cells (data not shown). This may suggest that *in vivo* infected cells are more resistant to TMEV induced apoptosis and the decrease in proliferation may represent a halting of the cell cycle. Indeed, in the B6 mice the decrease in T-cell infiltration seen at 14 dpi, which most likely represents clearance of the viral load within the CNS, allows rapid recovery of proliferation in the SVZ. Similar to TMEV, infection with Japenese Encephalomyelitis virus (JEV) also produced a high viral load in the SVZ and this decreased the NPC proliferative ability *in vivo* and *in vitro* (Das and Basu, 2008). Targeted infection of NPCs by both JEV and HIV lead to quiescence by inducing G1 phase arrest and elevated p21 and p27 levels (Das and Basu, 2008; Krathwohl and Kaiser, 2004). Further investigation will determine if TMEV affects the cell cycle in a similar manner.

As well as a direct influence on proliferation caused by viral infection, SVZ proliferation may be hampered by mediators involved in the inflammatory response. During TMEV infection the infiltrating T-cells are predominantly a Th1 phenotype and secrete pro-inflammatory cytokines such as IFNγ and TNFα. Pro-inflammatory cytokines

such as TNFα and IFNγ are able to regulate CD80 mediated cell death of neuronal stem cells *in vitro* (Imitola et al., 2004). In EAE Pluchino and colleagues (Pluchino et al., 2008) measured significant up-regulation of mRNA levels of TNFα and IFNγ at 20 and 30 dpi in the SVZ accompanied by a decrease in SVZ proliferation. EAE derived neurospheres cells show higher levels of lactate dehydrogenase activity, a measure of cell lysis, and increased caspase-3 activity (Sajad et al., 2011b). It is possible that these inflammatory signals drive NPCs into a quiescent state to block their proliferation or induce apoptotic mechanisms (Ben-Hur et al., 2003). Indeed, my RT-PCR array data shows that both IFNγ and TNF are up-regulated in the SVZ after TMEV infection. As these are most likely secreted by the infiltrating T-cells it is no surprise that the SVZ sub-regions with the greatest decreases in proliferation mirrored those with the highest numbers of infiltrates. This suggests that decreases in proliferation seen after both TMEV and EAE may share some common mechanisms related to the presence of T-cells and secreted inflammatory molecules.

3.3.8 Loss of neuroblast chain integrity and neuroblast numbers

Following TMEV infection there was a reduction in the percentage of neuroblasts within the SVZ that persisted in both strains for all times points examined. The BeAn virus was also strongly associated with Dcx^{+} neuroblasts and may induce changes in cell proliferation or differentiation. Accompanying this was a loss in neuroblast chain integrity and an increase the number of neuroblasts migrating individually. The reduction in proliferating cells may account for the decrease in neuroblast number. A paper by Tepavcevic (Tepavcevic et al., 2011) also reported a 3.3-fold reduction in neuroblast numbers with similar reduction in neuroblast chain length in EAE. They showed that a large number of neuroblasts co-labelled with cleaved caspase-3 suggesting specific cell

death within the neuroblast population. This purports that the loss of neuroblasts is more likely due to T-cell infiltration than direct viral infection. It would be intriguing to investigate whether this long-term decrease in neuroblast numbers leads to structural changes in the SVZ architecture where free gaps become occupied by astrocytes processes that could be inhibitory for reestablishment of normal cell migration.

The result of neuroblast loss in EAE was that fewer Dcx^{+} cells reached the OB causing a 50% decrease in BrdU labelled cells (Tepavcevic et al., 2011). They report that this resulted in an impairment in olfactory bulb memory although it could not be excluded that inflammation in other areas related to olfactory memory were responsible for the deficits. Further study would help to ascertain whether TMEV also reduced neuroblast migration to the OB and can cause similar olfactory impairments.

TMEV infection caused a transient increase in ectopic neuroblast emigration into the surrounding parenchyma. There are several possible reasons for this change in migration including chemokine up-regulation in inflamed areas, changes in blood vessels and modifications to astrocyte 'glial-tubes'. A strong potential candidate as a regulator of this migration is CCL2 and its receptor CCR2, both of which are strongly up-regulated in the SVZ after TMEV. CCR2 is expressed by migrating neuroblasts (Tran et al., 2004). However, I have shown that levels of several chemokines are higher in the SVZ compared to the cortex. Whilst I did not measure levels of chemokines in the corpus callosum, striatum or septum, they would have to be much higher than SVZ levels to overcome the strong chemoattraction from the SVZ. Another possibility, is that TMEV induces the expression of chemorepellant molecules such as Slits (Nguyen-Ba-Charvet et al., 2004) in the SVZ which may direct neuroblasts out into the parenchyma.

3.3.9 Conclusions

In this chapter, differences in the patterns of T-cell infiltration and cytokine profiles between resistant and susceptible strains in the SVZ were demonstrated. The differences in expression of several factors involved in the innate immune system, TLRs and complement system, suggest that using different strains may help elucidate the functions of these system in viral pathogenesis.

The data from the SJL mice raises some interesting questions. It would appear that prolonged inflammation within the SVZ leads to long-term changes in SVZ homeostasis. Does long-term inflammation in human MS also cause similar alterations in function? Are the periventricular lesions caused by persistent viral infection or through cellular infiltrates and inflammatory mediators, or possibly a combination of both? Even if we are able to regulate the inflammation through therapeutic approaches, are these changes in the SVZ homeostasis permanent? This could lead to irreversible failures in the repair capabilities of the SVZ and have serious implications when considering the use of the SVZ for repair through endogenous remyelination.

Chapter 4

Characterisation of Galectin-3 in the SVZ

4.1 Introduction **137**

4.2 Results **141**

4.3 Discussion **166**

4.1 Introduction

For many years the Szele lab has been interested in identifying novel molecules that may regulate neuroblast emigration (Goings et al., 2004; James et al., 2011; Kim et al., 2009; Ramaswamy et al., 2005). A search for in situ hybridisation data for Galectin genes in the Allen Brain Atlas (Lein et al., 2007) identifies that Galectin-3, Galectin-8 and Galectin-9 are expressed in the SVZ and RMS (figure 4.1). Gal-1 has been previously shown to be expressed by dividing SVZ astrocytes and promote cell proliferation (Sakaguchi et al., 2007; Sakaguchi et al., 2010; Sakaguchi et al., 2006).

Recently, a post-doctoral researcher in the lab showed that a β-galactoside binding protein called Galectin-3 was specifically expressed in the SVZ (Comte et al., 2011). Through several experiments they demonstrated that Gal-3 is able to regulate the migration of neuroblasts, as a loss of Gal-3 resulted in decreased speeds of migration with more exploratory behaviour using *ex vivo* imaging. *In vitro* functional blocking antibodies significantly inhibited neuroblast emigration from RMS explants. This was the first constitutive role found for Gal-3 in the brain but it had been shown to be up-regulated and influence the course of ischaemic lesions (Qu et al., 2010).

As discussed in chapter 1 there is an accumulating body of evidence to suggest that glycosylation and related molecules such as Gal-3 may play important roles in the pathogenesis of MS. Gal-3 has also been shown to be able to impact inflammation and may affect the differentiation of oligodendrocytes (Almkvist and Karlsson, 2004; Henderson and Sethi, 2009; Pasquini et al., 2011). So far though its role and function has not been studied comprehensively in models of MS and this was a goal of my thesis. In the TMEV model used throughout this thesis the vast majority of published work is conducted on two strains of mice: C57BL/6 and SJL/J. The Gal-$3^{-/-}$ mice used in the Comte study,

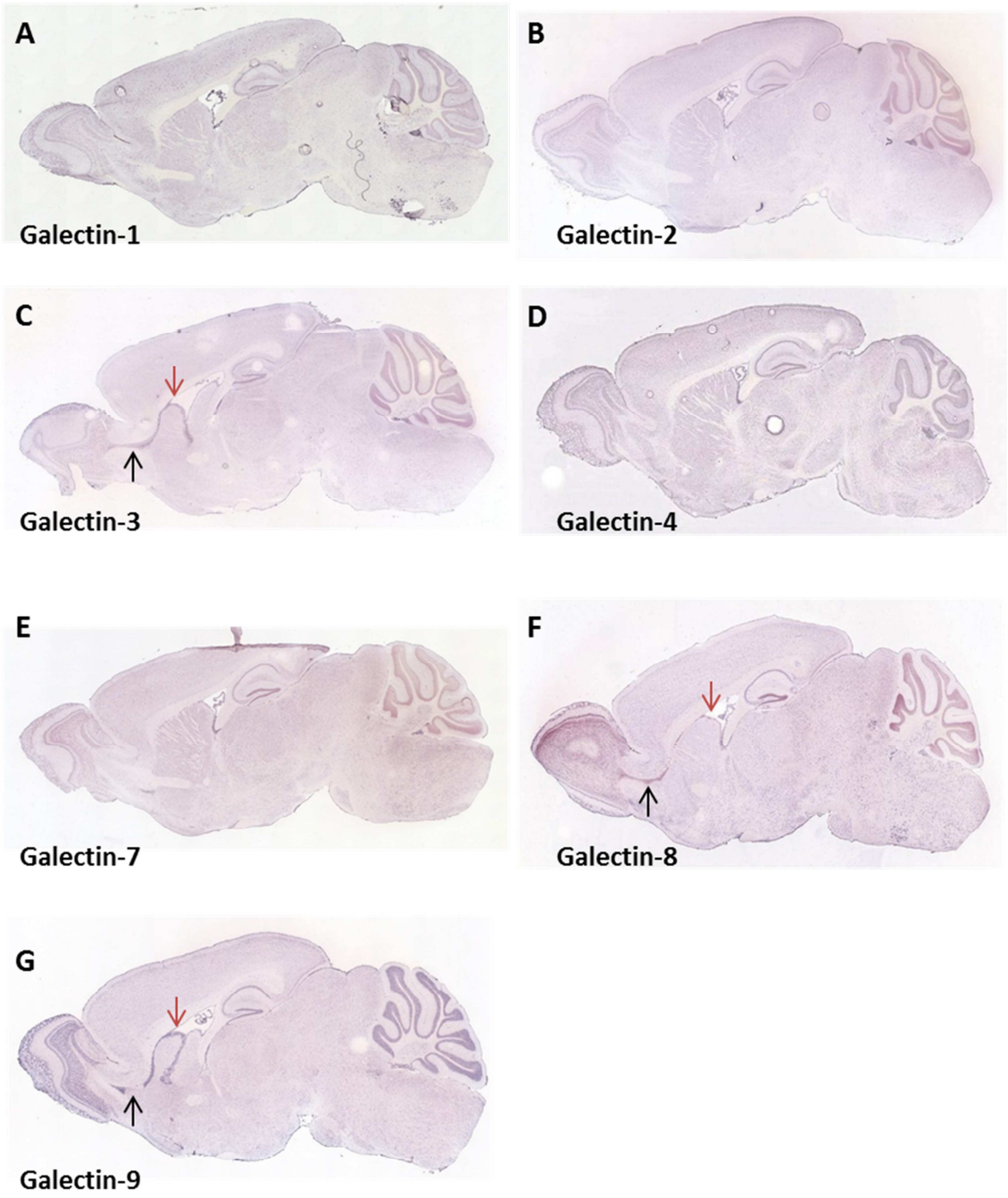


Figure 4.1 Expression of different galectins in Allen brain atlas

Red arrow identifies SVZ, black arrow identifies the RMS.

generated by the Poirier Laboratory were on a congenic 129sv background (Colnot et al., 1998). To the best of my knowledge there are no studies looking at TMEV in this particular strain of mice. In order to be able to relate my experiments to previously published data on TMEV I backcrossed the 129sv mice onto a SJL genetic background. The 129sv mice had previously been backcrossed onto a C57BL/6 background and were available for purchase.

Previous studies on the role of Gal-1 in the neurogenic niche have demonstrated the genetic background of a mouse can influence how galectins function. Deletion of Gal-1 from 129sv mice decreased DG neurogenesis (Kajitani et al., 2009) whilst deletion on a C57BL/6 background increased neurogenesis (Imaizumi et al., 2011). If Gal-1 regulates cytokine expression through the its C-terminal carbohydrate binding actions then these differences may be explained by variations in glycosylation levels between different strains of mice. Examination of N-glycan branching differences and golgi enzyme activity reveals different strains of mice have different levels of N-glycan branches on glycoproteins. Interestingly, susceptible strains of mice to both TMEV and EAE, like SJL mice, have lower levels of N-glycan branching than resistant strains, such as B6 (Lee et al., 2007). As glycoproteins display affinities for galectins in proportion to the number of N-glycans, the reduced number of N-glycans mean that Gal-3 binds with less affinity to its ligands and is less able to regulate function through formation of galectin-lattices.

Whilst the Comte study showed that Gal-3 could influence neuroblast migration and reported that there were no differences in proliferation between Gal-$3^{+/+}$ and Gal-$3^{-/-}$ mice. (Comte et al., 2011), the role of Gal-3 in ectopic emigration of neuroblasts, growth and proliferation of neurospheres and cell fate after differentiation were not investigated.

4.1. Research questions

I hypothesised that as different strains of mice show different levels of glycosylation Gal-3 expression and its function would differ between strains of mice. The aims of this chapter are therefore to: (1) quantify levels of Gal-3 in the two strains of mice, (2) characterise cellular Gal-3 expression both in adult and postnatal SVZ, (3) examine how Gal-3 deletion effects proliferation, neuroblast numbers and emigration and astrocyte function and (4) study the role of Gal-3 in the growth and differentiation of neurospheres.

4.2 Results

4.2.1 Genotyping of Gal-3 deficient mice

The Gal-3 null mutant mice were originally produced by Perrior lab through homozygous genetic deletion of exons II-IV of the Gal-3 gene locus (Colnot et al., 1998) (figure 4.2A). To confirm that backcrossing from the 129sv strain onto either the C57BL/6 or SJL/J strain had preserved the genetic deletion of exons II-IV of the Gal-3 gene locus genotyping PCR was performed to determine the genotype of offspring from Gal-3 heterozygote null (Gal-$3^{+/-}$) breeding pairs. For both strains wildtype mice (Gal-$3^{+/+}$) produced single DNA products -300 bp whilst Gal-3 homozygous null (Gal-$3^{-/-}$) mice produced single DNA products -500 bp (Doverhag et al., 2010). (figure 4.2B). To confirm the loss of immunodetectable Gal-3 protein an antibody against Gal-3 were used (figure 4.2C).

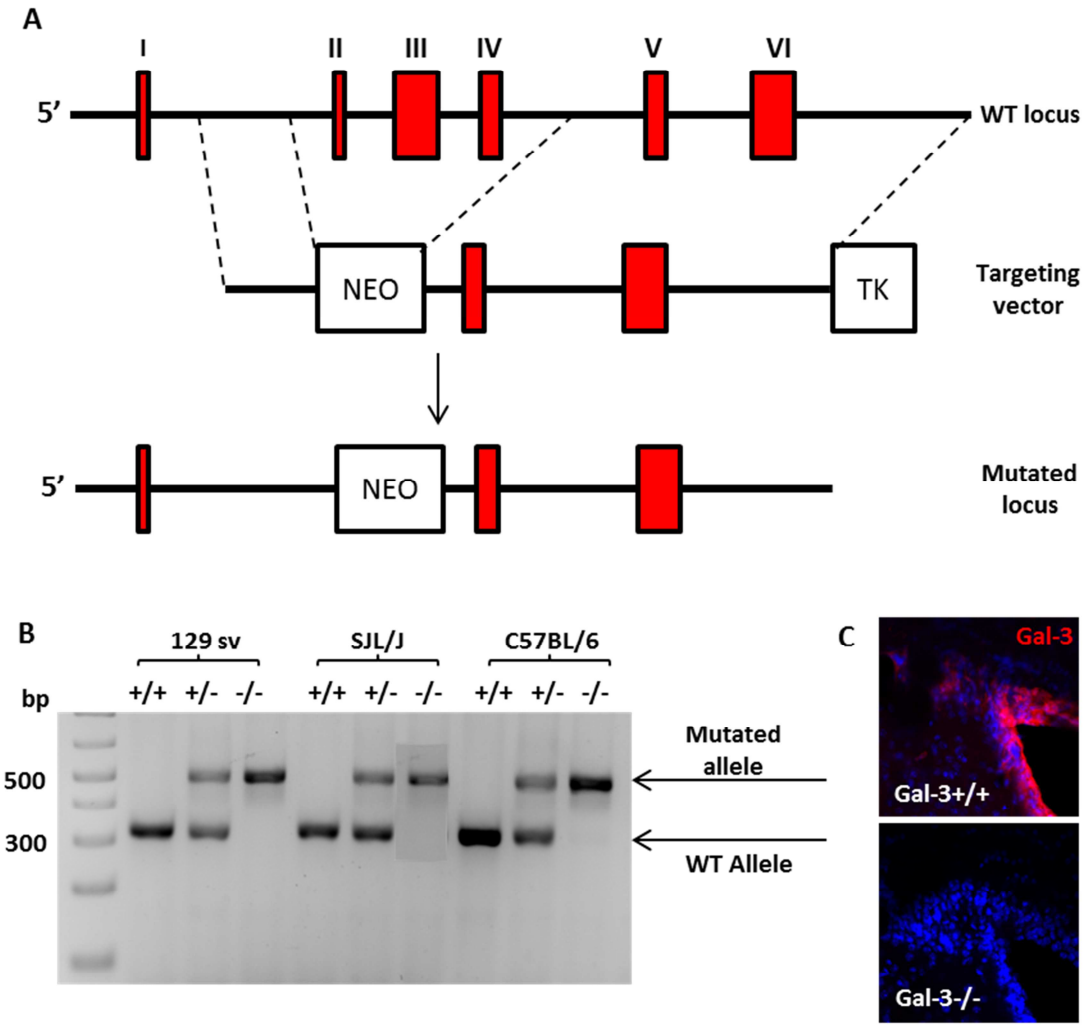


Figure 4.2 Galectin-3 homozygous null mutant mice

(A) Targeted deltion of exons II-IV of the LGal3 gene locus by homologous recombination. Modified from (Colnot et al, 1998).

(B) Gel electrophoresis of genotyping PCR products for each of the three strains of mice.

(C) Confirmation of Gal-3 deletion and a lack of postranslational product by immunohistochemistry.

4.2.2 SVZ expression of Galectin-3 differs between C57BL/6 and SJL/J mice

In agreement with *in-situ* hybridisation data from the Allen Brain Atlas, our lab have identified that Gal-3 was selectively expressed in the adult mouse brain in the SVZ, RMS and accessory OB (figure 4.3A) in the 129Sv mouse strain (Comte et al., 2011). Both SJL/J and C57BL/6 strains show the same general patterns of Gal-3 immunostaining to the 129 sv mice, with some subtle yet interesting differences. Whilst I cannot completely exclude the possibility that secreted Gal-3 from exogenous sources could theoretically bind to local niches the presence of Galectin-3 mRNA (figure 4.1C) suggest this is unlikely. Gal-3 immunoreactivity was not detected in the dentate gyrus of the hippocampus, the other neurogenic niche of the CNS in any of the strains examined (data not shown). Measurements of Gal-3 levels in SVZ tissue by ELISA revealed higher constitutive expression in the SJL/J mice compared to the B6 (figure 4.3B). Whilst Gal-3 immunoreactivity was absent in the main OB, cortex and the striatum ELISA data suggests that Gal-3 protein may be present in the cortex (figure 4.3B). It is possible that these levels are below the detection capability of our antibody in immunohistochemistry studies. In the dorsal SVZ of SJL/J mice Gal-3 is expressed throughout the dorsal extension, with significant overlap with GFAP expression (figure 4.3D). In contrast, C57BL/6 have much weaker Gal-3 staining in $GFAP^+$ cells in dorsal regions with higher staining more restricted to the ependymal layer (figure 4.3E). Using immunohistochemistry to further characterise these differences in cellular localisation confirmed that in B6 mice Gal-3 expression overlapped with $vimentin^+$ ependymal cells (data not shown).

SJL/J mice display diffuse Gal-3 expression in the cytoplasm and nucleus of $GFAP^+$ SVZ astrocytes (figure 4.4A). Comte et al (Comte et al., 2011) had previously reported that in 129sv mice Gal-3 is expressed in the nuclei of only a subset of $Gal\text{-}3^+$ astrocytes. In SJL/J mice the majority of $GFAP^+/Gal\text{-}3^+$ cells show Gal-3 immunostaining

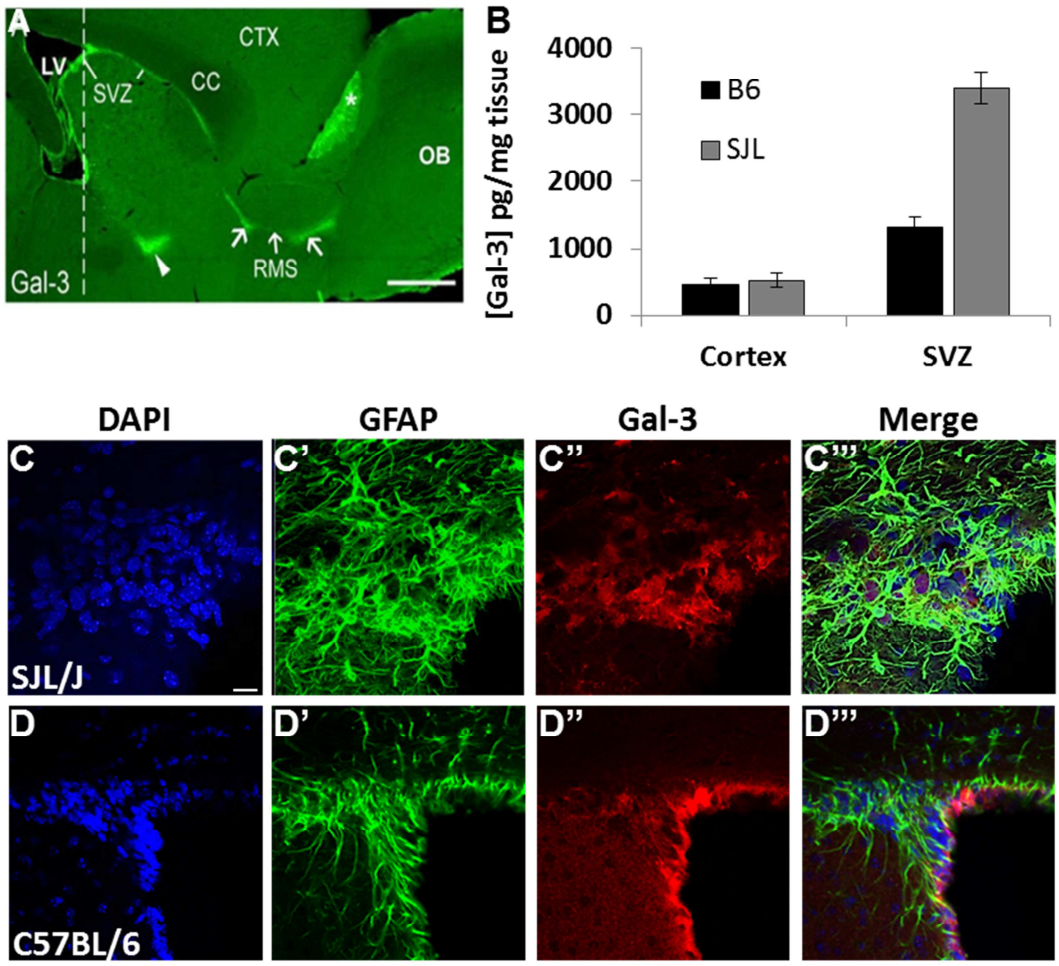


Figure 4.3 Gal-3 expression levels differ between strains of mice

(A) Gal-3 immunohistochemistry in an adult sagittal brain section. Gal-3 is specifically expressed in the SVZ, RMS (arrows) and accessory olfactory bulb (asterisk). CC, corpus callosum; CTX, cerebral cortex; LV, Lateral ventricle; OB, olfactory bulb.

(B) Gal-3 protein levels in SVZ and cortical tissue measured by ELISA. P = <0.005 measured by T-test (n=6, pooled data from three repeats).

(C) Gal-3 immunoreactivity in the dorsal SVZ of SJL /J mice. Scale bar 20 μm.

(D) Gal-3 immunoreactivity in the dorsal SVZ of C57BL/6 mice

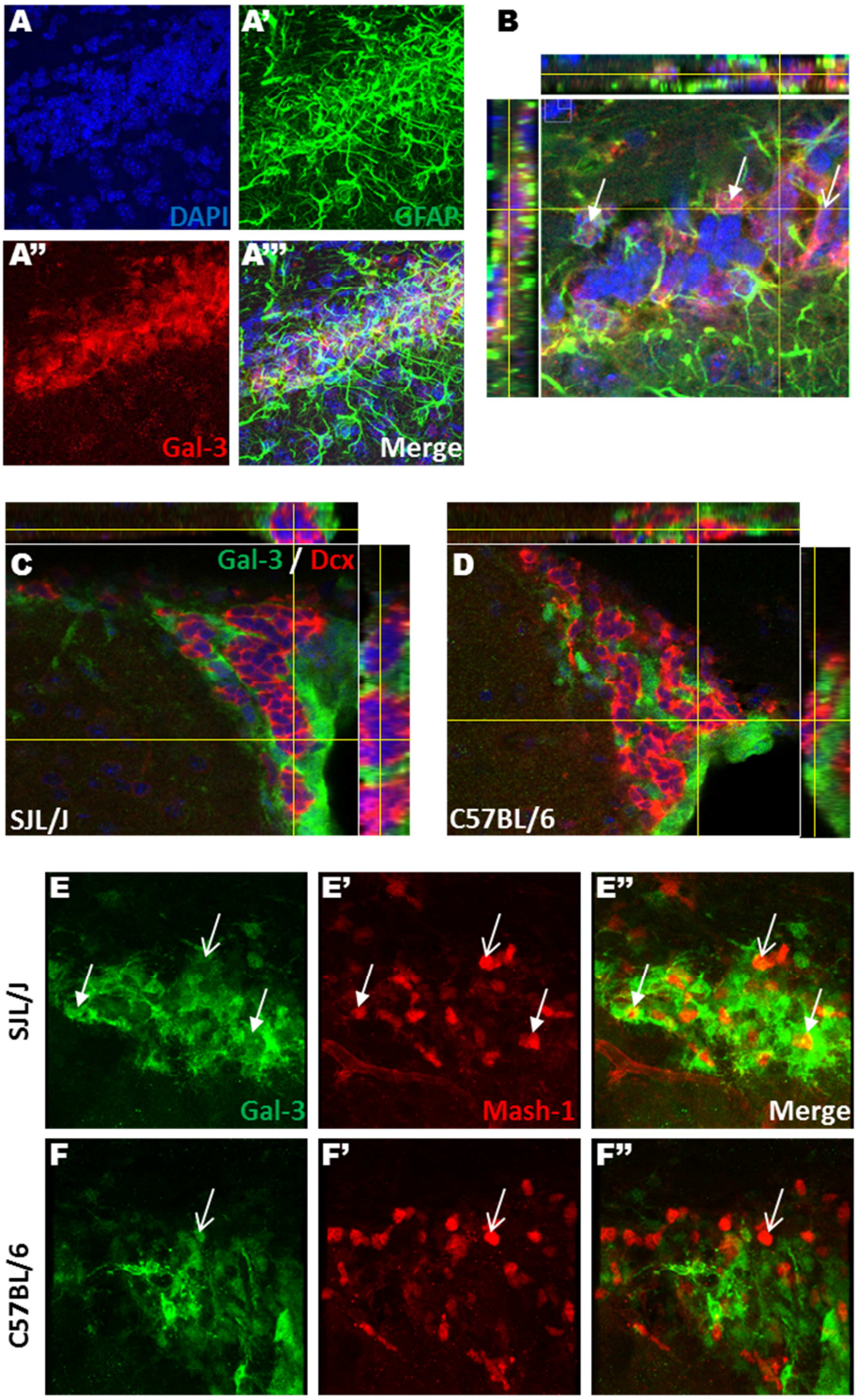


Figure 4.4 Gal-3 expression in SVZ cell types

(A) Diffuse Gal-3 expression in the cytoplasm and nucleus of GFAP+ SVZ astrocytes in SJL mice

(B) Compressed z-stack showing localisation of Gal-3 in the nucleus of GFAP+ cells (arrows).

(C-D) Gal-3 is not expressed by Dcx+ neuroblasts in either strains

(E-F) A subset of Mash1+ Gal-3+ cells seen in SJL mice that is not present in B6 mice

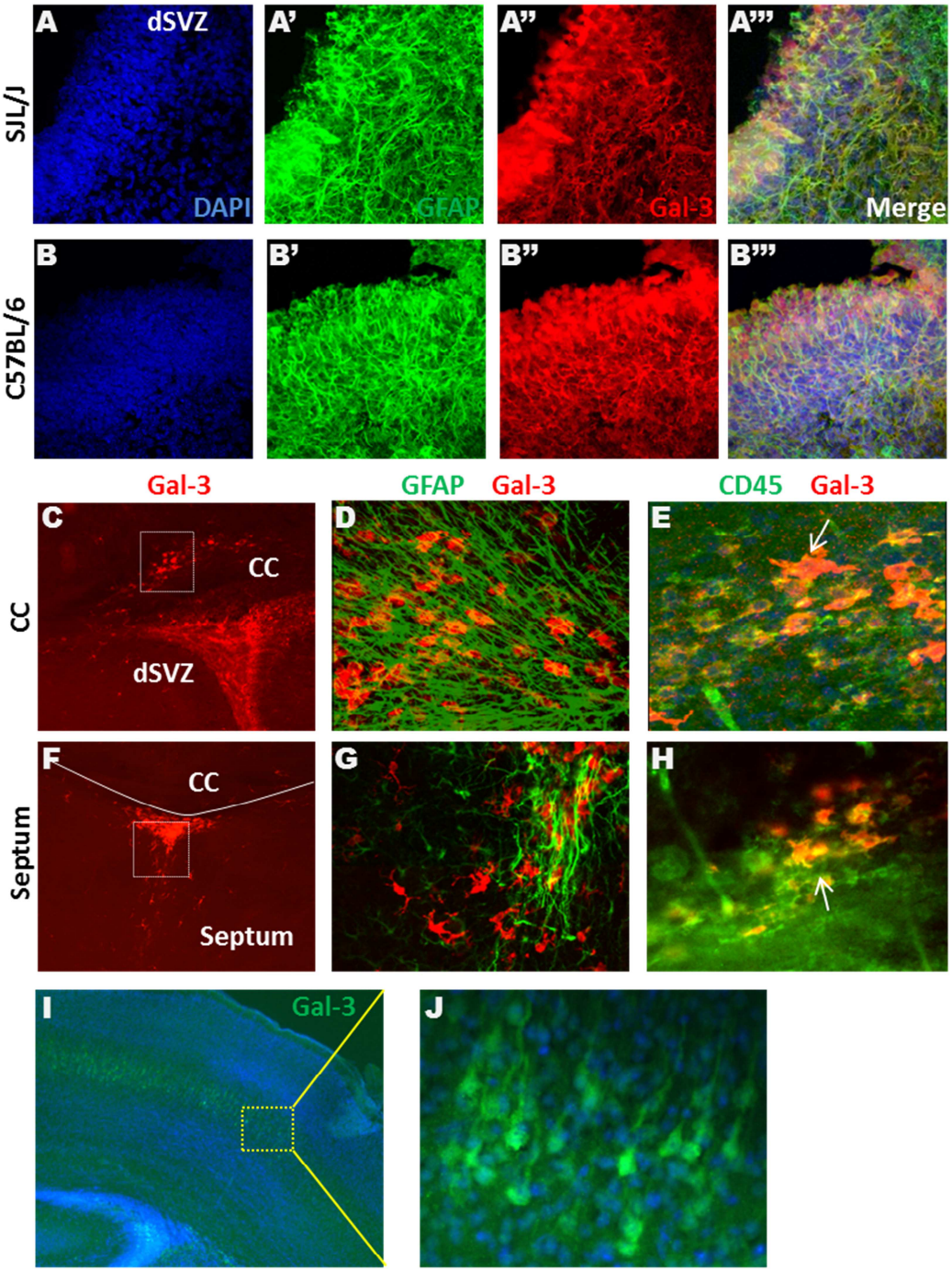


Figure 4.5 Expression of Gal-3 in postnatal mice

(A-B) Gal-3 (red) is associated with GFAP+ (green) astrocytes n the SVZ.

(C) Gal-3 labels a population of cells in the corpus callosum

(D-E) Higher mag image from white box in (C). Gal-3 positive cells are GFAP- (D) but CD45+ as indicated by arrow (E)

(F) Cells with a similar morphology are also found in the med septum region

(G-H) Higher mag images of white box in (F). Gal-3 (red) expression does not co-label with GFAP (green) (G) but does with CD45 (H).

(I-J) Gal-3+ cells are found in a distinct cortical layer (I) and have a neuronal morphology (J)

in the nuclei (figure 4.4B). In both SJL and B6 mice the Gal-3 staining formed a dense network that surrounded clusters of Dcx^+ neuroblasts but was not expressed inside these Dcx^+ chains (figure 4.4C-D). This pattern is reminiscent of the glial tubes surrounding neuroblasts. Further characterisation demonstrated that Gal-3 is expressed in the cytoplasm of a subset of $Mash1^+$ cells in SJL/J but not B6 mice (figure 4.4E^+F). $CD45^+$ SVZ microglia extremely rarely expressed Gal-3. These findings demonstrated the selective expression of Gal-3 by specific cell types of the adult neurogenic niche and that this expression may vary between different mouse strains.

4.2.3 Galectin-3 was expressed in postnatal mouse SVZ and cortex

As the SVZ is such an important stem cell niche in the development of the mouse brain the expression of Gal-3 at an earlier time point of postnatal day 4 was examined. This was also chosen as this is age when cells are harvested to make neurosphere cultures. At postnatal day 4 Gal-3 immunoreactivity showed that expression between SJL/J and B6 mice is much more similar than at later stages. In both strains Gal-3 is associated with $GFAP^+$ astrocytes in the SVZ (figure 4.5A-B). This expression was restricted to ventricular zone $GFAP^+$ cells and was not seen in radial processes that extended into the cortex and surrounding parenchyma. Surprisingly, in both strains Gal-3 labelling also identified a population of cells frequently found along the corpus callosum, in the mid septum region and more rarely in the cortex that were $CD45^+$/GFAP- (figure 4.5C-H). These cells had large somas with irregularly shaped, short thick processes, a morphology similar to that of activated/phagocytosing microglia. Within the cortex immunohistochemistry showed that both strains had Gal-3^+ neurons in layer IV of the cortex, no Gal-3^+ neurons were ever

detected in adult mice. These data suggest that the cellular expression of Galectin-3 may change at different stages of mouse development.

4.2.4 Deletion of Galectin-3 does not affect proliferation

To examine the effects of Gal-3 deletion on cell cycle we used BrdU and Phosphohistone H3 to distinguish between DNA replication in S phase and mitosis G2/M Phase cells respectively. Pulse labelling of proliferating cells with BrdU (50mg/kg) 2 hours before sacrifice showed comparable number of $BrdU^+$ cells in the SVZ of Gal-$3^{+/+}$ wildtypes and Gal-$3^{-/-}$ mutants in both SJL/J (figure 4.6A) and C57BL/6 (figure 4.6B) cells. Both strains showed the same trend to a decrease in the Gal-$3^{-/-}$ mice but this was not significant. Using PH3 revealed no change after Gal-3 deletion in the SJL/J mice (figure 4.6C) or B6 mice either (figure 4.6).

4.2.5 Emigration of neuroblasts into the parenchyma is altered in SJL/J mice

Previous experiments from the Szele laboratory reported that neuroblast migration in the SVZ-RMS-OB pathway was defective in Gal-$3^{-/-}$ mutants (Comte et al., 2011). To examine if a lack of Gal-3 resulted in changes in the number of neuroblasts or emigrating cells, neuroblasts were labelled with anti-doublecortin (Dcx) antibodies. The percentage of $DAPI^+$ cells that were Dcx^+ were quantified in the dSVZ and revealed a significant decrease in the percentage of neuroblasts within the SVZ of SJL/J Gal-$3^{-/-}$ compared to Gal-$3^{+/-}$ ($n=3$, $p=0.04$, figure 4.7A). These mice also displayed a disruption in the morphology of the chains of neuroblasts with a loss of integrity, causing smaller chain sizes and increased numbers of single Dcx^+ cells (figure 4.7E-H). In C57BL/6 there was

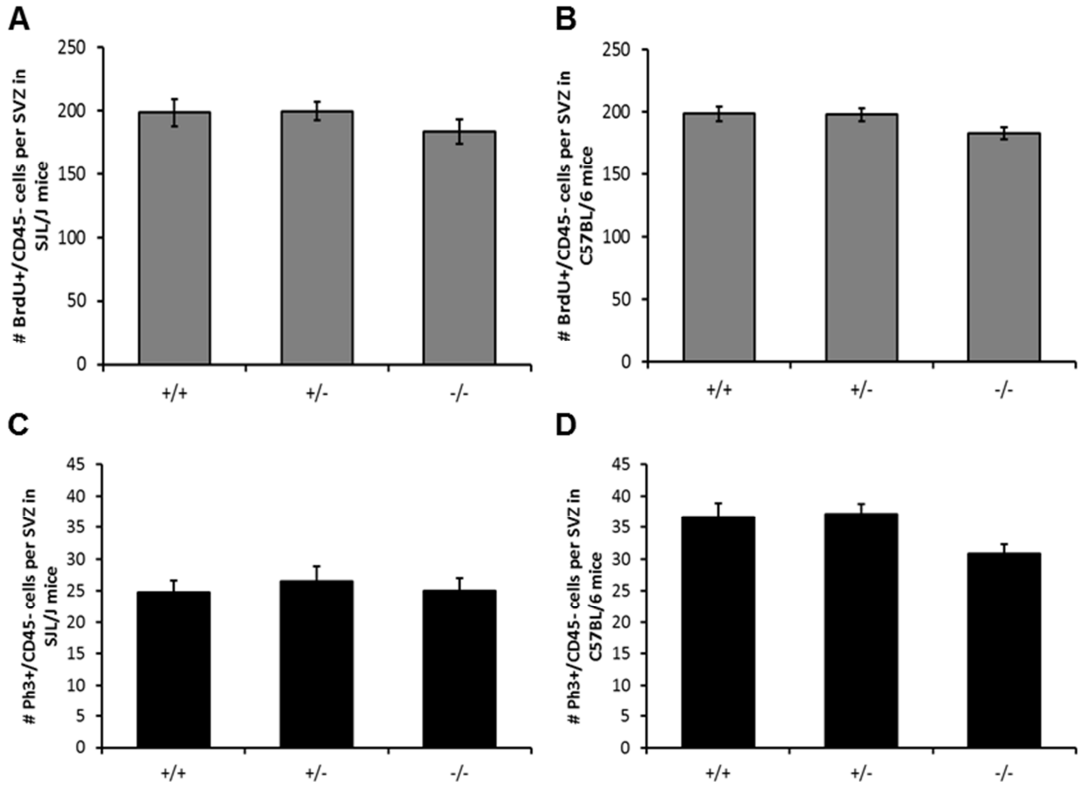


Figure 4.6 Proliferation does not change in the SVZ of Gal-3-/- mice

(A-B) A loss of Gal-3 does not alter the total number of proliferating cells per section labelled with BrdU in either SJL (A) or B6 (B) mice

(C-D) A loss of Gal-3 does not alter the total number of proliferating cells per section labelled with PH3 in either SJL (A) or B6 (B) mice

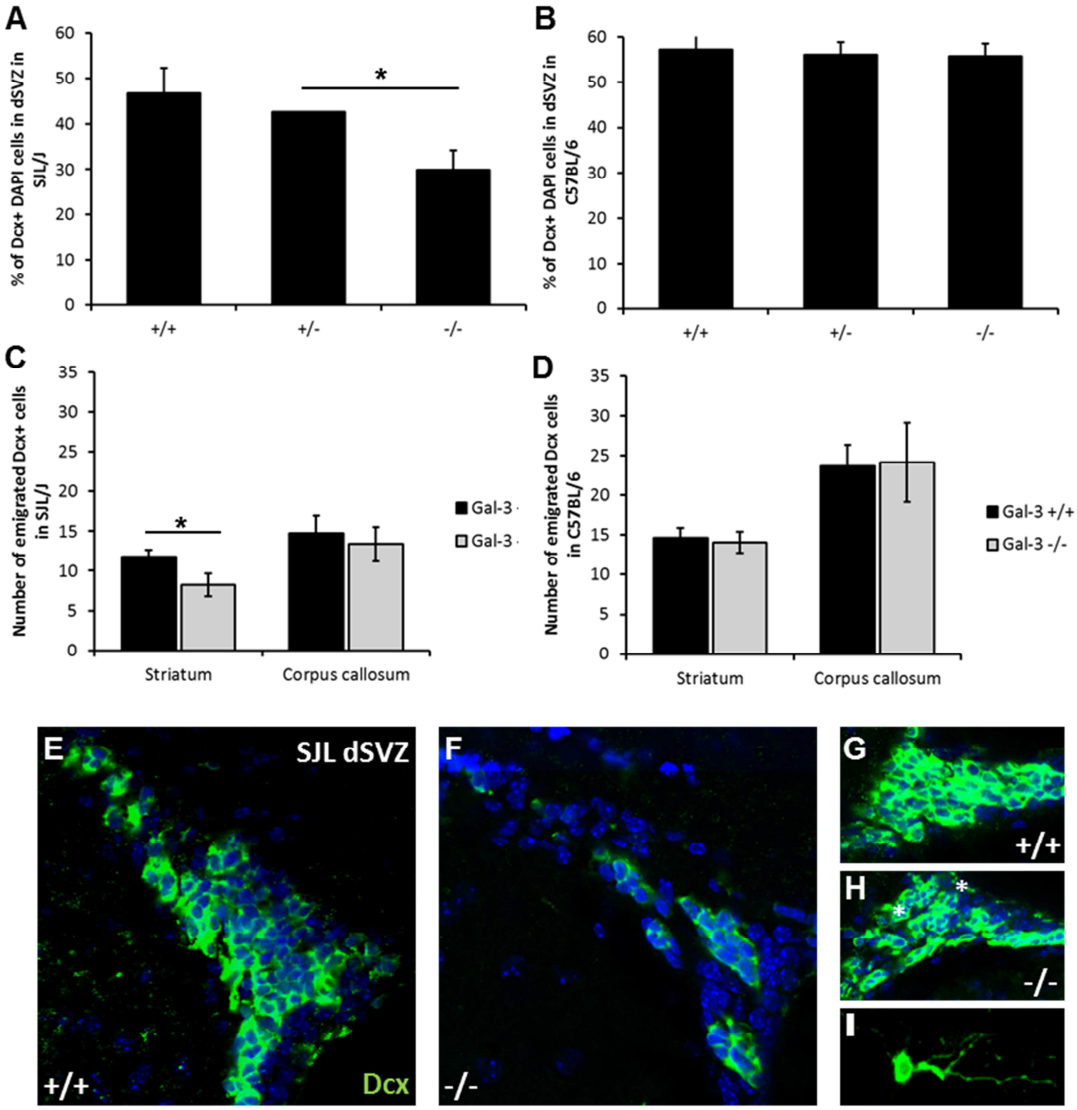


Figure 4.7 Gal-3 deletion causes loss of neuroblast number and chain integrity in SJL mice

(A) Percentage DCX+DAPI+ cells in dSVZ in SJL/J mice. * $p<0.01$, n=3, T-test

(B) Percentage DCX+DAPI+ cells in dSVZ in C57BL/6mice

(C) Fewer cells migrate into the striatum of SJL Gal-3 KO mice compared to WT . * $p<0.01$, n=3, T-test

(D) Lack of Gal-3 does not affect Dcx emigration in B6 mice

(E-F) Loss of Dcx+ cells in the dSVZ of SJL Gal-3-/-

(G-H) Disruption in chain morphology with smaller chains and higher numbers of single cells in SJL Gal-3-/-

(I) Typical morphology of Dcx+ emigrating neuroblast

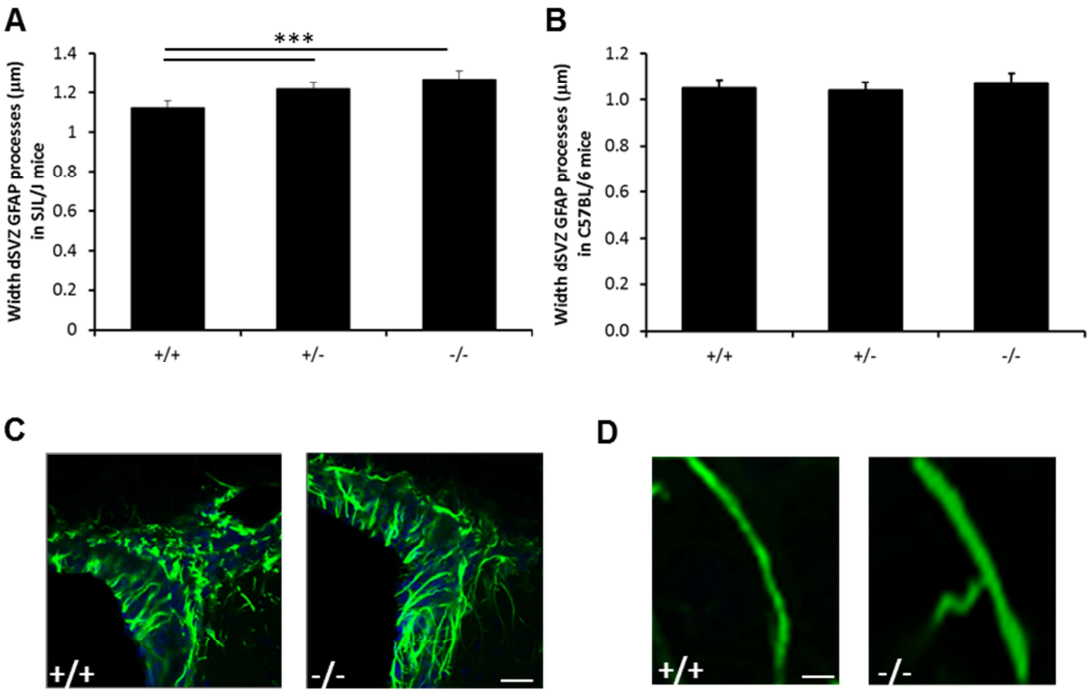


Figure 4.8 Gal-3 deletion increases GFAP process width in SJL astrocytes

(A) Quantification shows significant increases in the width of GFAP+ processes in the dorsal SVZ in SJL Gal-3-/-. *** p <0.001, n=3, students t-test

(B) Lack of Gal-3 does not effect GFAP+ process width in B6 mice

(C) Gal-3 null mice show slightly higher levels of GFAP immunofluorescence in dSVZ

(D) Example of increased GFAP process thickness in Gal3-/- mice

no significant change in the percentage of Dcx^+ cells (figure 4.7B). Small numbers of Dcx^+ cells constitutively emigrate dorsally into the corpus callosum and ventrally into the striatum. In SJL/J mice the numbers of Dcx^+ cells emigrating as individuals or in clusters of cells were decreased in the striatum of KO mice (n=3, p=0.04) but not in the corpus callosum (figure 4.7C). There were no significant changes in emigration in the C57BL/6 mice (figure 4.7D).

4.2.6 Gal-3 deletion increase astrocyte process width in SJL/J mice

Previously reported data from the lab showed that Gal-3 deletion in 129sv mice led to a significant increase in the width of GFAP processes and a distortion in morphology (Comte et al., 2011). This disruption in astrocyte morphology can contribute to altered migration. Measurement of SJL/J dlSVZ astrocyte process thickness showed a significant increase in width in both Gal-$3^{+/-}$ (P = 0.01, n=3) and in Gal-$3^{-/-}$ (P = 0.01, n=3) mice compared to $Gal3^{+/+}$ (figure 4.8A,C-D). There was no difference in C57BL/6 mice which is consistent with the data that Gal-3 levels are lower in SVZ astrocytes (figure 4.8B). GFAP immunoreactivity outside the SVZ and RMS was similar in all groups of mice. This is consistent with the immunohistochemistry data that showed that Gal-3 is only expressed by SJL but not by B6 SVZ astrocytes and so deletion would only affect astrocytes in this strain.

4.2.7 Galectin-3 is expressed in glial tubes in the RMS of SJL/J mice

Similar to the SVZ, Gal-3 immunostaining is high in astrocytes in the RMS of SJL/J mice (figure 4.9A) but only very weak in B6 mice (figure 4.9B). In SJLs, Gal-3 expression is

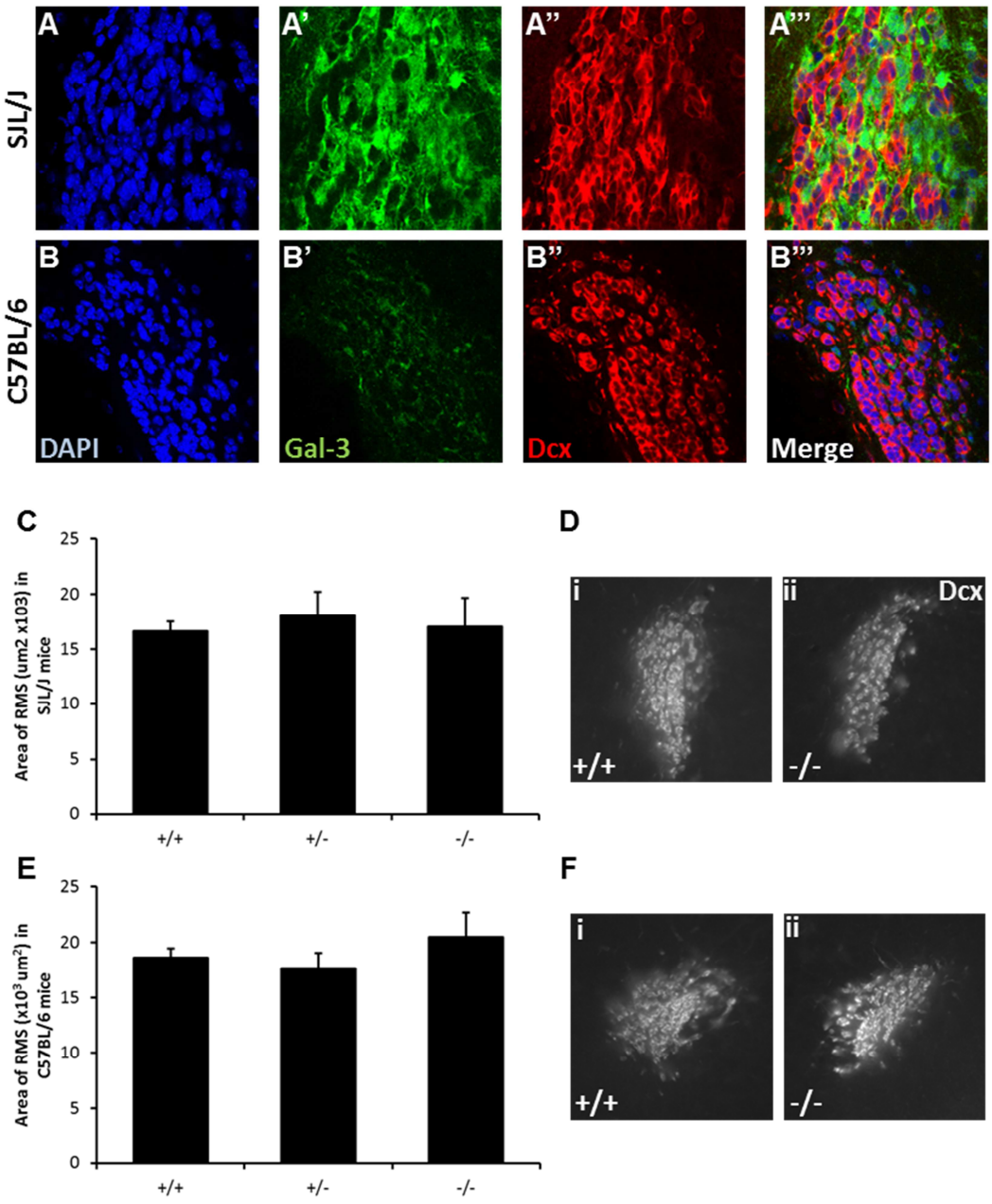


Figure 4.9 Loss of Gal-3 does not alter RMS surface area

(A) Diffuse Gal-3 expression in glial tubes surrounding Dcx+ neuroblasts in RMS in SJL

(B) Gal-3 staining is very weak in the B6 RMS

(C+E) The surface area of the RMS, measured by outlining the perimeter of Dcx immunofluorescence does not change in Gal-3 nulls

(D+F) Dcx immunohistohemistry in the RMS of a WT and Gal-3-/- mouse in SJL (D) and B6 (F)

Scale bar (A-B) 50μm (D, F) 100μm

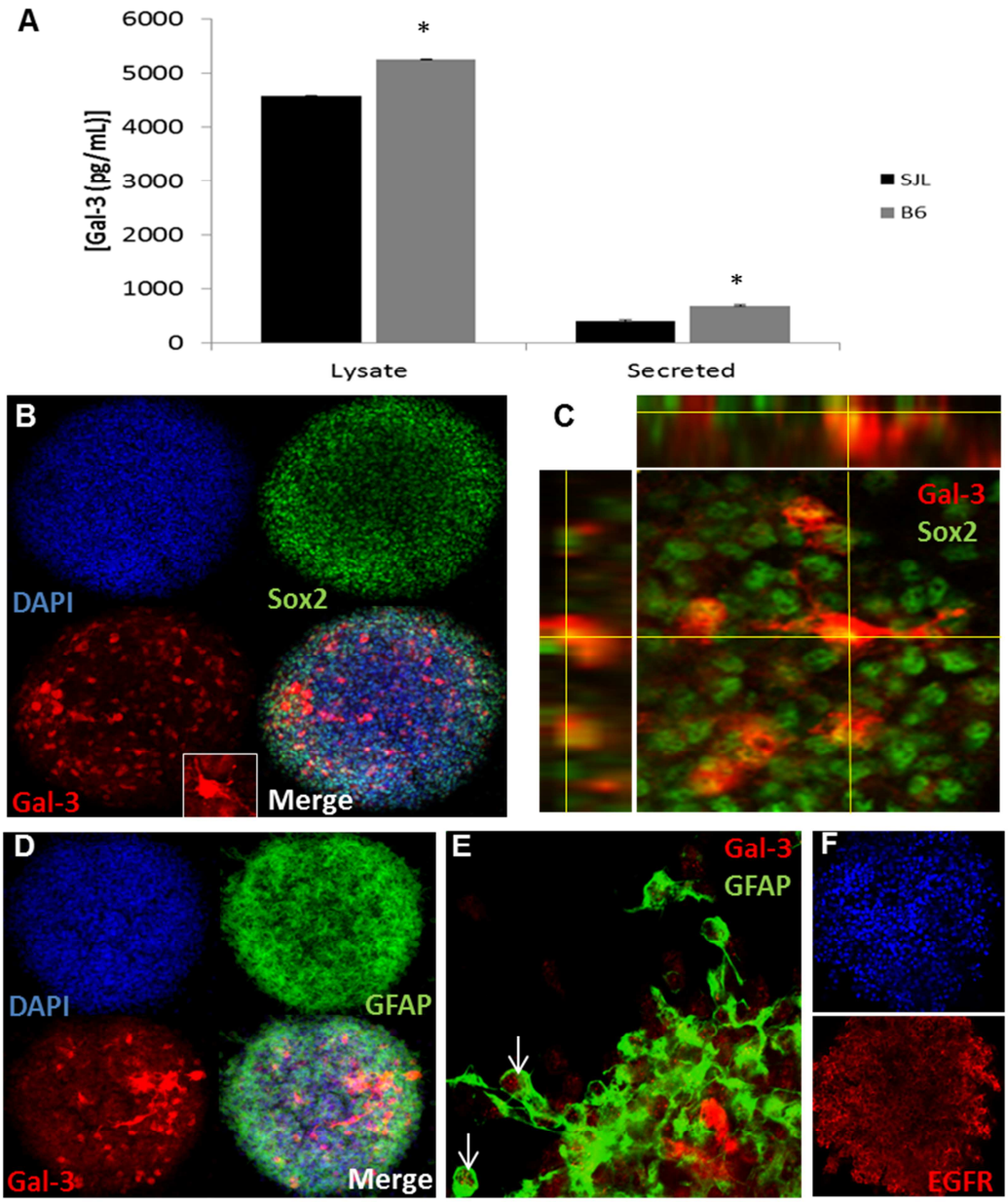


Figure 4.10 Galectin-3 is produced by a subset of cell within neurospheres and secreted extracellularly

(A) C57BL/6 derived neurospheres display higher levels of Gal-3 both in neurosphere cell lysate and secreted extracellularly. * p=0.01

(B) Immunohistochemistry identifies a subpopulation of cells in neurospheres that are Gal-3+.

(C) Confocal z-stacks though Gal-3+ cells in neurospheres shows expression both in the nucleus and in the cytoplasm.

(D) Gal-3 expression in a subset of GFAP+ cells that is expressed in the nucleus (E) as shown by arrow.

(F) Neurospheres express EGFR on the surface of majority of neurosphere cells

seen throughout the cytoplasm of astrocytes that form the glial tubes surrounding migrating chains of Dcx^+ neuroblasts. Comte et al (Comte et al., 2011) previously showed that deletion of Gal-3 from these cells decreased migration rates of neuroblast causing them to accumulate in the RMS resulting in increased RMS area. Measurement of RMS area, to see if similar effects may be occurring, revealed no changes in area in either strain (figure 4.9C-F).

4.2.8 Galectin-3 is expressed by a subset of cells within neurospheres

Given that Gal-3 is expressed so highly within SVZ cells I wanted to see whether this expression would be maintained when the SVZ stem cells were grown *in vitro* in the neurosphere assay. Galectin-3 protein levels within neurosphere cell lysate and secreted into supernatant were measured using ELISA. C57BL/6 neurospheres have statistically higher levels of Gal-3 in both the cell lysate (n=3, $P = 0.01$) and in supernatant (n=3, $P = 0.01$, figure 4.10A). This was unexpected since ELISA showed more in SJL's in vivo. Immunohistochemistry reveals that Gal-3 is expressed by a subset of cells within neurospheres (figure 4.10B) with expression in both the nucleus and cytoplasm (figure 4.10C). Labelling neurospheres with GFAP reveals that the majority of $Gal\text{-}3^+$ cells are $GFAP^+$ (figure 4.10D) in which Gal-3 is expressed in the nucleus (figure 4.10E, arrow). Gal-3 has been reported to form Galectin-lattices with EGFR (Lau et al., 2007). As high concentrations are used as a mitogen in neurospheres cultures it is not a surprise that EGFR is expressed by the vast majority of cells within the neurosphere (figure 4.10F). Whilst there doesn't seem to be any similarity between EGFR and Gal-3 expression this does not exclude the possibility that secreted Gal-3 can still bind to EGFR. Gal-3 staining

was present in both B6 and SJL derived neurospheres which suggests that in B6 SVZ astrocytes there is latent expression of Gal-3 than can be upregulated in certain conditions.

4.2.9 Recombinant Gal-3 decreases the proliferation of SJL/J neurospheres

The MTS assay is colormetric method for determining the number of viable cells in proliferation or cytotoxicity assays. The MTS reagent is reduced by metabolically active cells to give a formazan product that can be read as absorbance. The more metabolically active cells present the higher the absorbance reading. Using the MTS proliferation assay showed that there were no differences in the rate of cell growth between SJL Gal-$3^{+/+}$ and Gal-$3^{-/-}$ neurospheres (figure 4.11 A). To model whether exogenous Gal-3, such as would be secreted by neighbouring astrocytes *in vivo,* would affect cell growth I added exogenous recombinant Gal-3 (rGal-3). Interestingly, adding rGal-3 to the neurosphere cultures caused the spheres to adhere together (figure 4.11B) suggesting Gal-3 may affect cell adherence in cultures. In SJL Gal-$3^{+/+}$ cultures addition of rGal-3 led to a significant decrease in the number of neurospheres in a dose response effect that was further enhanced in Gal-$3^{-/-}$ cells (n=3, p=0.01,figure 4.11C). rGal-3 increased the diameter of Gal-$3^{-/-}$ but not Gal-$3^{+/+}$ neurospheres (figure 4.11D). This may be due to the adherence effect described above rather than a change in proliferation *per se*. The MTS assay was used to see if the reduced neurosphere numbers was due to alterations in proliferation. rGal-3 led to small decrease in proliferation in Gal-$3^{+/+}$ cells at 24 and 48 hours that recovered by 72 hours (figure 4.11E). In contrast, in the Gal-$3^{-/-}$ cells rGal-3 proliferation continued to decrease over time (n=3, p=0.01, figure 4.11F). There did not seem to be a dose response effect.

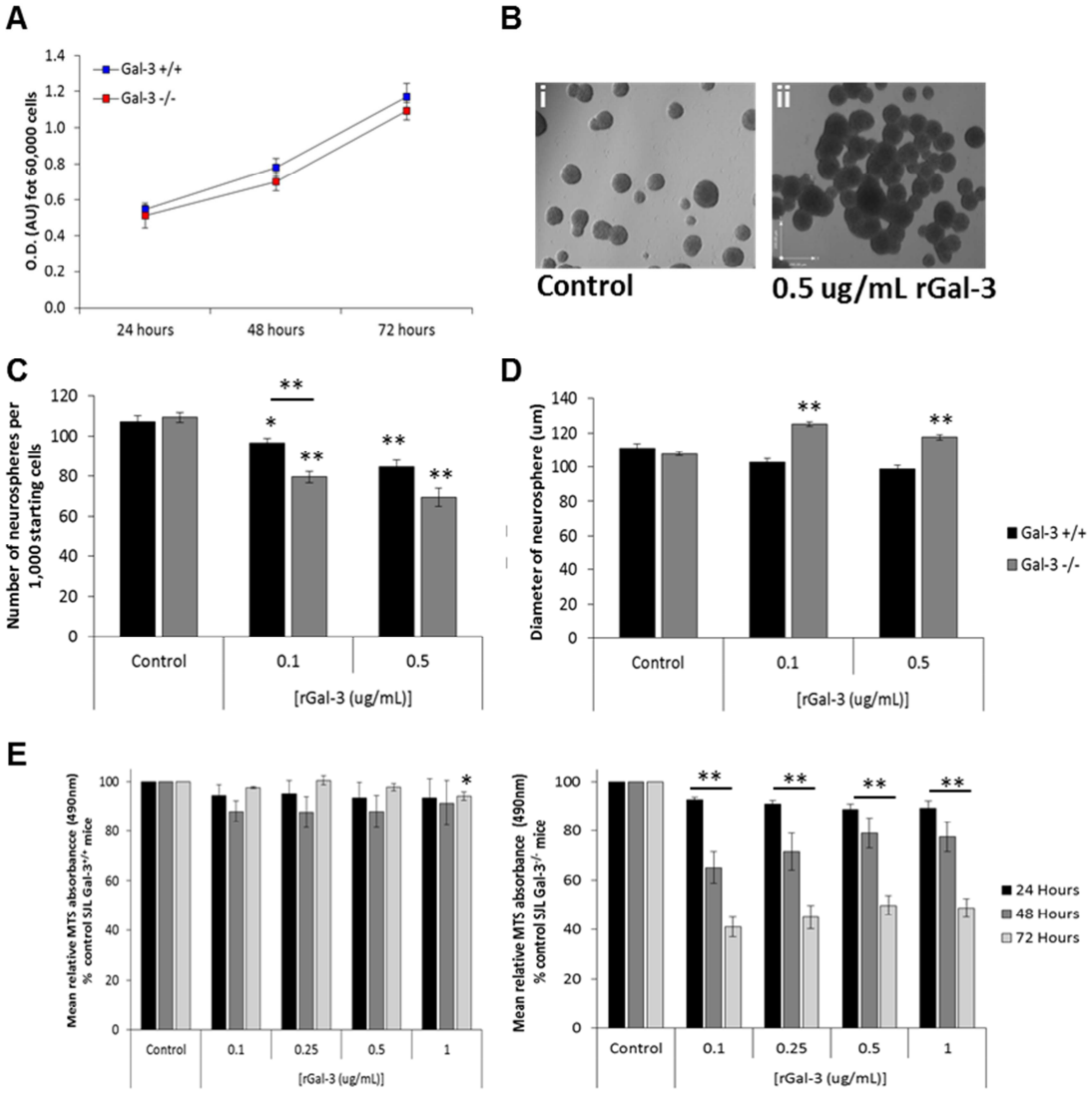


Figure 4.11 Exogenous rGal-3 alters SJL/J neurosphere growth

(A) MTS absorbance on 50,000 starting cells shows there is no difference in rates of growth between Gal-3+/+ and Gal-3-/- cells.

(B) Addition of exogenous Gal-3 causes neurospheres to adhere together

(C) Exogenous rGal-3 decreases the number of neurospheres from 1,000 starting cells. Compared to control except for bar compared between WT and KO. *p<0.01, ** p<0.01

(D) Diameter of Gal-3-/- and Gal-3+/+ in presence of rGal-3

(E) For 50,000 Gal3+/+ cells rGal-3 causes a transient decrease in MTS absorbance at 24 and 48 hours .

(F) rGal-3 causes gradual loss of MTS absorbance in Gal3-/- cells over 72 hours for 50,000 cells. ** p<0.01. Representative of three independent experiments.

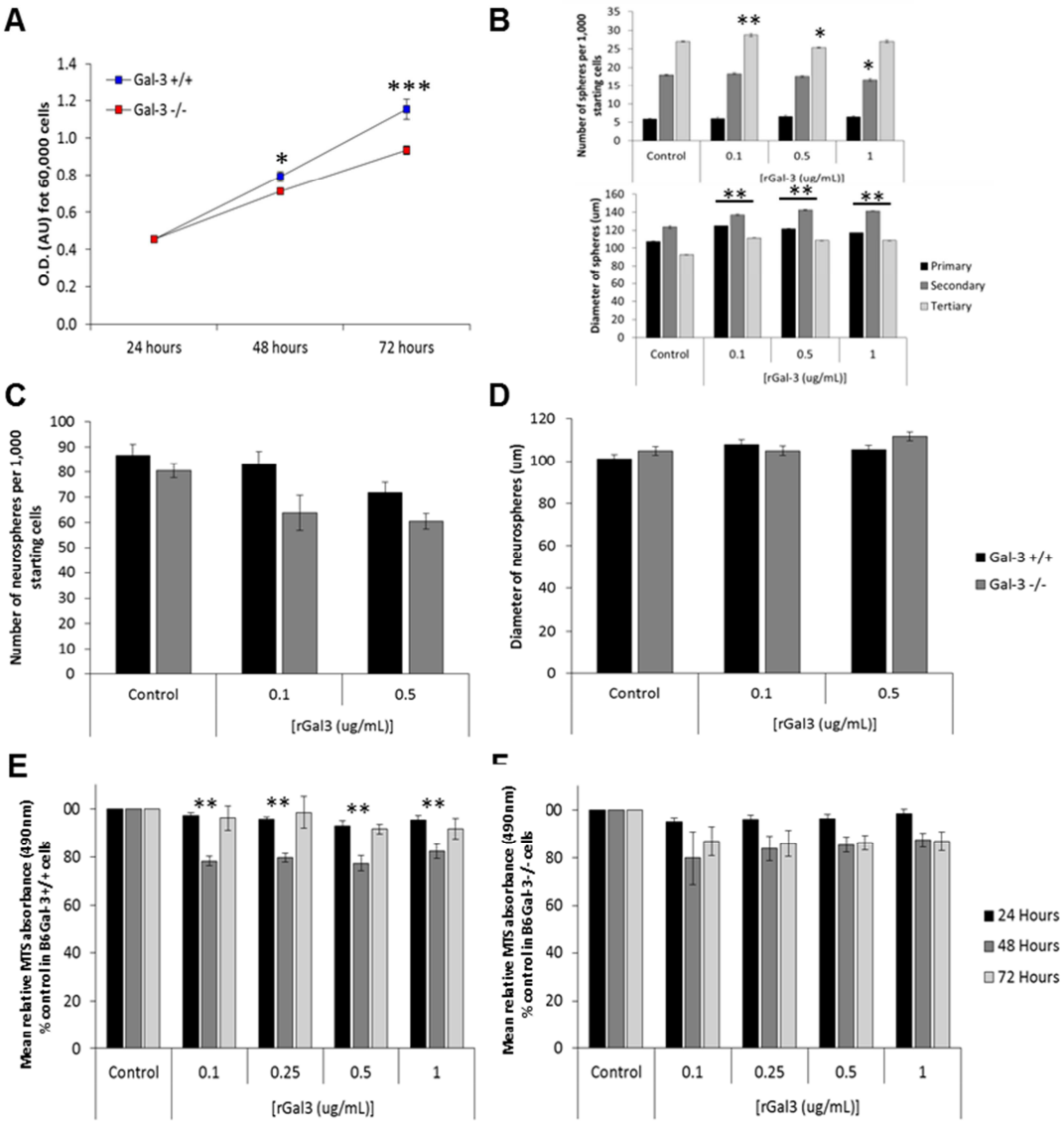


Figure 4.12 Effects of exogenous rGAl-3 on C57BL/6 neurosphere growth

(A) MTS absorbance on 50,000 starting cells shows a statistical decrease in rates of growth between Gal-3+/+ and Gal-3-/- cells over 48 and 72 hours. * $p<0.05$, ** $p<0.001$, ANOVA. N=3

(B) Growth of Gal-3 WT cells over serial passages in the presence of rGal-3.

(C) Number of KO and WT neurospheres per 1,00 0 starting cells grown in rGal-3.

(D) Diameter of KO and WT neurospheres grown in rGal-3.

(E) MTS absorbance of 50,000 B6 Gal-3+/+ cells over 72 hours period in presence of rGal-3 at different concentrations. ** $p<0.01$. n=3.

(F) MTS absorbance of 50,000 B6 Gal-3+/+ cells over 72 hours period in presence of rGal-3 at different concentrations .

All representative of three independent experiments.

4.2.10 Recombinant Gal-3 has less of an effect on C57BL/6 neurosphere proliferation

In C57BL/6 derived cultures the MTS assay shows that Gal-$3^{-/-}$ neurospheres grow at a slower rate than Gal-$3^{+/+}$ neurospheres (figure 4.12A). Growing WT neurospheres in rGal-3 over several passages causes a significant increase in diameter and at higher concentrations increased the number of spheres (figure 4.12B). When neurospheres are grown in rGal-3 for shorter periods of time (48 hours) rGal-3 showed a trend to decrease the number of spheres for both Gal-$3^{+/+}$ and Gal-$3^{-/-}$ but it was not significant (figure 4.12C) and did not affect neurosphere size (figure 4.12D). The MTS assay showed a significant decrease in proliferation at 48 hrs that had recovered by 72 hours for Gal-$3^{+/+}$ cells (figure 4.12E). Gal-$3^{-/-}$ cells showed a trend to decrease in proliferation but it was not significant (figure 4.12F).

4.2.11 Gal-3 blocking antibodies stimulate proliferation of neurospheres

Secreted Gal-3 can bind to receptors on the surfaces of cells such as EGFR and ECM proteins such as laminin, collagen and fibronectin to regulate both cell proliferation and adherence. To attempt to block the carbohydrate binding activity of Gal-3 a functional blocking antibody was added to the neurosphere media to attempt to distinguish extracellular from intracellular functions. The same antibody had previously been validated and shown to block SVZ neuroblast migration from explants (Comte et al., 2011). For both the WT and Gal-$3^{-/-}$ cells addition of the blocking antibody led to significant increases in absorbance using the MTS assay (figure 4.13A and B) and decreases in the number (figure 4.13 C and E) and size (figure 4.13 D and F) of neurospheres that were equal to those seen with the IgG2a antibody control. By 72 hours the MTS assays shows that the metabolic activity of the cells has dramatically decreased,

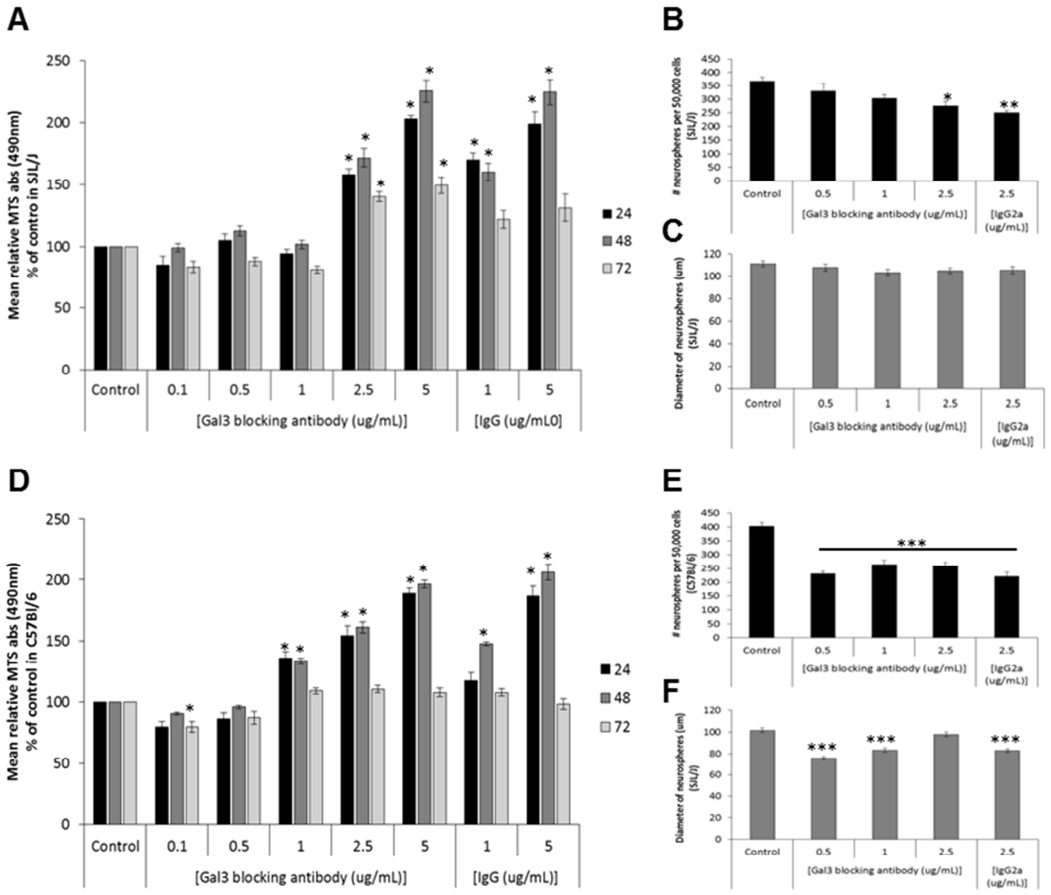


Figure 4.13 Functional blocking antibody and IgG stimulate proliferation

(A) MTS absorbance on 50,000 starting SJL cells that anti-Gal-3 blocking antibody and the IgG matched control stimulate equivalent increases in absorbance

(B-C) Number and size of SJL neurospheres in functional blocking antibody and IgG control

(D) MTS absorbance on 50,000 starting B6 cells that anti-Gal-3 blocking antibody and the IgG matched control stimulate equivalent increases in absorbance

(E-f) Number and size of B6 neurospheres in functional blocking antibody and IgG control

sometimes below that of the control (figure 3.13 A,C). As the MTS assay is a measure of metabolic activity of cells this increase could be due to the same number of cells being more metabolically active after stimulation with IgG. This showed that IgGs are able to stimulate cells within neurosphere cultures and so I was unable to conduct any further experiments using this blocking antibody.

4.2.12 Gal-3 is expressed by all cell types in differentiating neurospheres

The expression of Gal-3 by cells in undifferentiated neurospheres called for an examination to see whether this expression was maintained after differentiation. Co-labelling with Gal-3 and GFAP shows that Gal-3 is expressed highly in the cytoplasm (open arrow) and at lower levels in the nucleus (closed arrow) of the vast majority of $GFAP^+$ cells (figure 4.14A). Cells with a neuronal phenotype also appear to express Gal-3 (figure 4.14F). A previously published study demonstrated that Gal-3 was expressed in primary oligodendrocyte cultures and had a role in oligodendrocyte differentiation and myelination (Pasquini et al., 2011). During the early stages of $O4^+$ oligodendrocyte differentiation in neurospheres Gal-3 is expressed in the nucleus (figure 4.14E) and in the numerous fine processes that give the $O4^+$ cells their typical stellate appearance (figure 4.14B, closed arrows). As the oligodendrocytes further differentiate the primary processes form secondary and tertiary connections to form the ‘myelin membrane sheath’. During this stage Gal-3 expression is lost from the ‘myelin sheath’ (figure 4.14C, closed arrow) but is maintained in the nucleus (figure 4.14C, open arrow). There are no obvious differences in morphology between $O4^+$ cells from $Gal3^{+/+}$ and $Gal3^{-/-}$ neurospheres (figure 4.14D and D’). Quantification of C57BL/6 neurospheres showed there are no differences in the fate of $Gal\text{-}3^{+/+}$ and $Gal^{-/-}$ cells after differentiation (figure 4.14G).

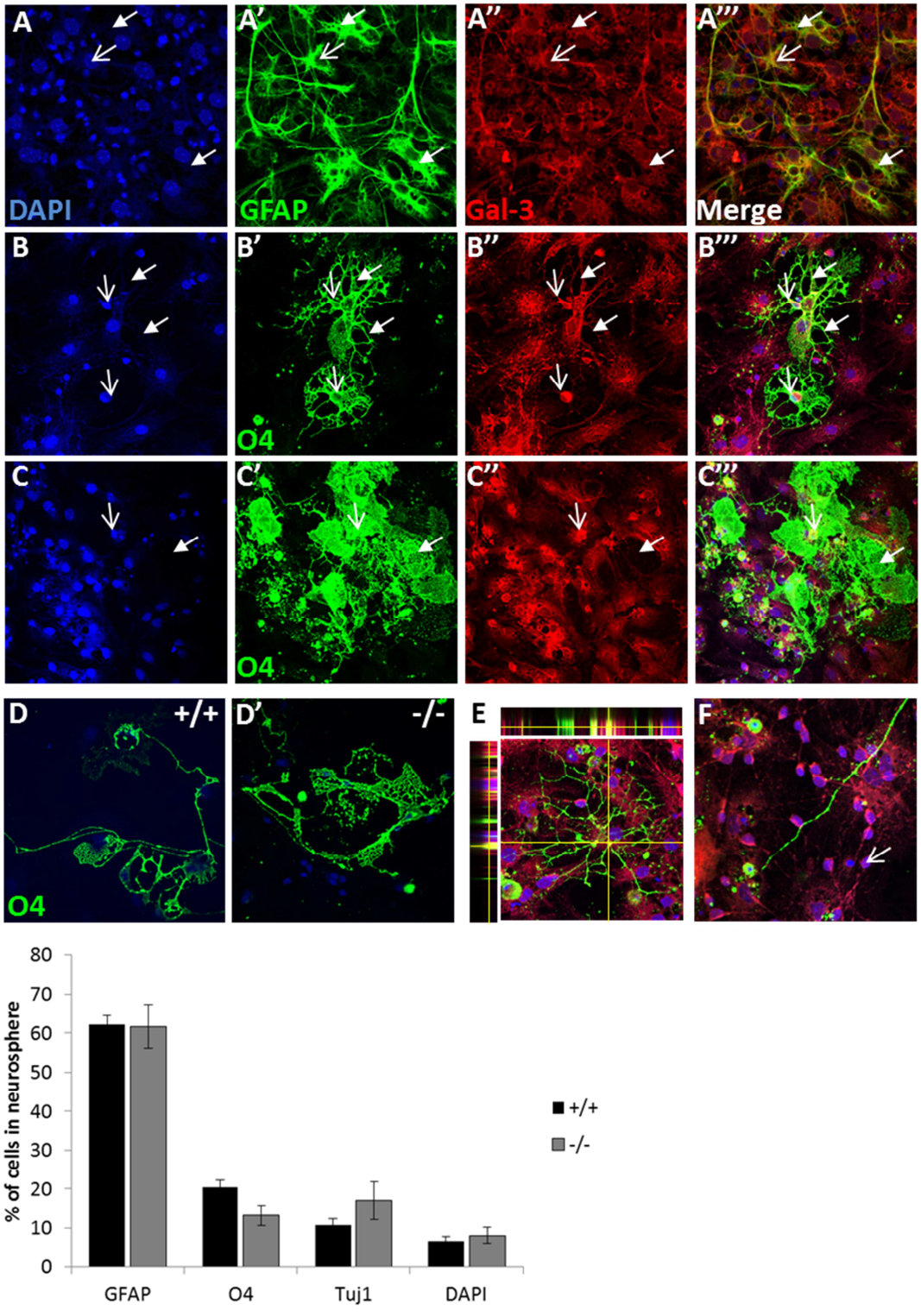


Figure 4.14 Gal-3 is expressed by all cell types in differentiated neurosphere cultures but does not change cell fate

Figure 4.14 Gal-3 is expressed by all cell types in differentiated neurosphere cultures

(A) Gal-3 (red) is expressed in both the nucleus (open arrow) and diffusely through the cytoplasm (closed arrow) of GFAP+ cells (green) . Inset box shows higher mag image of GFAP+Gal3+ nucleus

(B) O4+ cells (green) label for Gal-3 (red) in the nucleus (open arrow) and numerous fine processes (closed arrow).

(C) O4+ cells (green) that have a more mature differentiated phenotype no longer express Gal-3 (red) in the 'myelin membranes' (closed arrow) but retain expression in the nucleus (open arrow).

(D) O4+ cells from Gal-3+/+ (D) or Gal-3-/- (D') cultures have no noticeable differences in morphology.

(E) Confocal z-stack showing Gal-3 expression in the nucleus of an O4+ cell

(F) Cells with a neuronal phenotype show Gal-3 immunostaining in the cytoplasm and long processes (arrow).

4.3 Discussion

4.3.1 Only select Galectins are expressed in the CNS

Using the Allen Brain Atlas to investigate which Galectins are expressed in mouse CNS identified that galectin-3, galectin-8 and galectin-9 are present in the SVZ and RMS by *in situ* hybridisation. This is very interesting as Stancic (Stancic et al., 2011) using qPCR on post mortem human tissue has shown that galectin-1 was the most prominently expressed in cortical white matter but that galectins-3, -8 and -9 were also significantly expressed at the mRNA level. Protein expression of these galectins was confirmed by western blot. Whilst not in the same brain region this suggests that there may be parallels between galectin expression profiles in mouse and human CNS. Whilst the Allen Brain Atlas *in situ* data did not show Gal-1 expression in the SVZ, a study by Sakaguchi and colleagues (Sakaguchi et al., 2006) showed Gal-1 immunostaining in SVZ astrocytes suggesting it most probably is present. The striking similarities between galectin expression in humans and mice provides some strength to the idea that manipulation of these proteins could prove a valuable new therapeutic tool. It would be of particular interest to look at levels of Galectins in the human SVZ.

4.3.2 Expression of Galectin-3 in the SVZ differs depending on genetic background

Galectin-3 expression within cells of the SVZ differs depending on the genetic background of the mouse. SJL/J mice have higher tissue protein levels of Gal-3 in the SVZ than B6 mice. Also, whilst Gal-3 expression is high in SVZ astrocytes in the SJL/J mice it is almost undetectable in the B6 astrocytes which display a more ependymal distribution. Whilst this is the only study to date examining differences in Gal-3 expression in the CNS, similar differences in cellular distribution between strains has been described in the colon.

Mathieu (Mathieu et al., 2008) showed that in colonic crypt epithelium the number of cells showing cytoplasmic and/or nuclear Gal-3 expression was lower in the 129Sv/Ev strain compared to either C57BL/6 or BALB/c strains. Gal-3 deletion in SJL mice leads to decreases in neuroblast number and reduces ectopic emigration with no effect in the B6 mice. This suggests that mouse phenotypes may differ depending on genetic background. Studies on another member of the galectin family, galectin-1, have shown that the genetic background of a mouse can dramatically influence how galectin-1 regulates neurogenesis in the adult dentate gyrus (DG). Kajitani (Kajitani et al., 2009) observed that on the 129sv background Gal-1 null mice had fewer $BrdU^+$ cells compared to wildtypes in the DG. When the same BrdU labelling protocol was used on Gal-1 KO mice that had been backcrossed from the 129sv to a C57BL/6 background the opposite result was seen in the DG with an increase in $BrdU^+$ cells (Imaizumi et al., 2011). It is possible that levels of Galectin-1 also show differences between the strains and the opposite effects on neurogenesis could represent a dose-dependent effect.

Both Gal-1 and Gal-3, bind to the carbohydrate chains of signalling molecules and modulate signal transduction (Karmakar et al., 2008; Song et al., 2009; Toscano et al., 2011; Walzel et al., 2006). Binding of Galectins is directly proportional to the levels of glycosylation of a glycoprotein and the expression of many glycosyltransferases and glycosidases, which add or remove specific carbohydrate resides respectively (Lowe and Marth, 2003), could change during the differentiation and proliferation of neural stem/progenitor cells. Differences in genetic regulation of glycosylation between mouse strains could alter the binding affinity of Galectin-3 for different glycoproteins and produce different functional effects. One example of this is the regulation of sialylation, where sialic acids are added onto the ends of branched glycans on receptors which can significantly alter cellular sensitivity toward Gal-3 or Gal-1 (Stowell et al., 2008) (Crocker

and Varki, 2001; Rabinovich et al., 2002). Polysialic acid (PSA) is a linear homopolymer containing 8–100 a2–8-linked sialic acid residues (SAa2-8SAa2-) (Rutishauser and Landmesser, 1996) that is exclusively carried by NCAM (PSA-NCAM) expressed on neural stem/progenitor cells both in the SVZ and the dentate gyrus (Angata and Fukuda, 2003; Cremer et al., 2000; Doetsch et al., 1997). Depending on the levels and timing of PSA-NCAM expression on neural progenitors this could affect galectin binding and sialylation-related masking of Gal-3 ligands could be important in regulating its effects. This may also explain why Gal-3 is not associated with PSA-NCAM^{+}Dcx^{+} neuroblast cells as the high levels of sialylation may be inhibitory to binding.

The precise mechanisms of how Galectin-3 expression is regulated are poorly understood. However the presence of CRE and NF-κB-like sites in the *LGAL3* gene promoter region implies that the activation of Gal-3 expression could be regulated through signalling pathways involving the cAMP response element binding protein (CREB) or the NF-κB transcription factor (Dumic et al., 2000b; Kim et al., 2003). Nf-κB family members are expressed in the SVZ (Denis-Donini et al., 2005) and TNFα (Widera et al., 2006a; Widera et al., 2006b), VEGF (Wada et al., 2006) and glutamate (Brazel et al., 2005; Guerrini et al., 1995) have all been shown to regulate NSC proliferation and survival through NF-κB activation. It is possible that external stimulation of SVZ cells by a wide variety of growth factors, cytokines or neurotransmitters may initiate and regulate the transcription of Gal-3. It has been shown in other systems that Gal-3 and its ligands can work together in a feedback loop to regulate the expression of each other (de Oliveira et al., 2011; Merlin et al., 2011). In the SVZ increased levels of a ligand, such as EGFR, may regulate levels of Gal-3 and vice versa.

Recent studies on other members of the galectin family, including galectin-1 and galectin-7 suggest that methylation is important for the regulation of galectin expression

(Benvenuto et al., 1996; Moisan et al., 2003). A recent study has shown expression of the Gal-3 proteins is regulated in part by promoter methylation of the *LGALS3* gene (Ruebel et al., 2005). Gal-3 protein was only expressed in pituitary tumour cells when the *LGALS3* gene was unmethylated and methylation of the promoter silenced gene expression. The role of methylation is currently being further studied by the Szele lab.

It is also possible that Gal-3 expression is partially regulated through peripheral hormones that enter the CNS from the bloodsteam. Several hormones have been shown to induce the expression of Gal-3 in various cells including oestradiol, progesterone, oestrogen, glucocorticoids and human chorionic gonadotropin (hCG), (Abu-Amer and Bar-Shavit, 1994; Maldonado et al., 2011; Yang et al., 2011). Although relatively little is known about the role of hormones in the SVZ, oestradiol, oestrogen and glucocorticoids have all been shown to regulate rates of neurogenesis (Brock et al., 2010; Kanagawa et al., 2006; Suzuki et al., 2007; Veyrac and Bakker, 2011; Zhang et al., 2010). Further work would show if these hormones can induce Gal-3 expression in the SVZ. For my thesis I focused only on female mice, as sex hormones can regulate both Gal-3 expression and neurogenesis. It would be interesting to see if Gal-3 expression is different in male mice.

Regulation of the expression of Gal-3 during both transcription and translation is a complex, fine-tuned mechanism which involves several different transcription factors and signalling pathways which are dependent on cell type, levels of glycosylation, external stimuli and environmental conditions (Dumic et al., 2006). This means that determining the exact mechanism for the differential regulation of galectin-3 expression in various genetic backgrounds may prove challenging as genetic background could affect any of these factors and thereby alter the function of Gal-3 in adult neurogenesis.

4.3.3 Gal-3 expression in the SVZ neurogenic niche

Within the healthy neural stem cell niche Gal-3 is specifically expressed by ependymal cells, astrocytes and, in the SJL/J strain only, by a subset of progenitor cells. However, neuroblasts and differentiated interneuron progenies in the adult SVZ do not express Gal-3. In the dentate gyrus, the only other adult neurogenic niche, Gal-3 expression was not detected in any strain. This would suggest that expression of Gal-3 is not a general feature of adult neural stem cells but is unique to the SVZ. Interestingly, striatal and cortical astrocytes do not express Gal-3. Because both ependymal cells and astrocytes lining the lateral ventricles arise from radial glia it was not surprising that postnatal SVZ radial glia also expressed Gal-3. What was more interesting, was that at postnatal day 4 the expression profile was indistinguishable between the SJL and C57BL/6 mice, in stark contrast to the differences seen in the adult mice. This might imply that at different developmental stages the cellular expression and possibly the function of Galectin-3 may change. Ongoing experiments in the lab are determining potential embryonic expression and function of Gal-3.

A recent study used fluorescence-activated cell sorting in C57BL/6 mice to isolate $GFAP^+$/$prominin^+$ adult NSCs in the SVZ, and proposed that the *LGal3* gene was highly enriched in the adult NSC population compared to $GFAP^+$/prominin1- SVZ niche astrocytes (Beckervordersandforth et al., 2010). Whilst in the B6 mice with fewer $Gal\text{-}3^+$ $GFAP^+$ cells this idea may have some validity it can't explain why in the SJL/J mice the vast majority of both SVZ and RMS $GFAP^+$ cells express high levels of Gal-3. Maybe different levels between strains represent different percentages of active stem cells. However, it is imperative to point out that although Gal-3 is expressed by astrocyte-like stem cells, it is not an exclusive marker for adult NSCs, and is also robustly expressed by

other SVZ cell types and parenchymal astrocytes in other brain regions during inflammation (chapter 6).

SVZ $Gal3^{+}GFAP^{+}$ cells demonstrated great variability in the intensity of Gal-3 staining in the nucleus versus the cytoplasm. Indeed immuno-electron microscopy in the 129svGal-3 KO mice has shown that SVZ astrocytes could be divided into two subsets where one contained only nuclear Gal-3 immunoprecipitates versus the other where Gal-3 was both nuclear and cytoplasmic (Comte et al., 2011). Within the $Gal\text{-}3^{+}$ stem/progenitor cells in floating neurospheres expression was always both nuclear and cytoplasmic. Phosphorylation of Gal-3 is important in determining its location within a cell as phosphorylated galectin-3 (pI 8.2) was found in both the cytoplasm and the nucleus, whereas the unphosphorylated form (pI 8.7) was found exclusively in the cytoplasm (Cowles et al., 1990). Phosphorylation at position of Ser6, by an as yet unknown enzyme, of Gal-3 strongly affects its sugar binding affinity and has been proposed to be an 'on/off' biological switch of its downstream biological effects (Mazurek et al., 2000). This raises an intriguing possibility that differential cellular distribution may be linked to different states of activation, certainly in other cell types Gal-3 localisation is related to proliferative states. In quiescent fibroblast cultures Gal-3 was predominantly cytoplasmic but during proliferation in the same cells expression shifted to intense nuclear staining (Moutsatsos et al., 1987). Nuclear Gal-3 participates in pre-mRNA splicing regulation of cell growth, cell cycle progression and apoptosis (Dagher et al., 1995; Wang et al., 2004) but it remains to be seen whether the differential cell compartment expression in the SVZ may distinguish active from quiescent astrocyte-like stem cells or stem cells from niche astrocytes.

Interestingly, only a subset of cells within the neurospheres expressed Gal-3. It should be noted that neurospheres are not truly 'stem cell' cultures and the detection of sphere forming cells is not equivalent to that of stem cells. Studies show at best they may

only contain a few per cent of stem cells. *In vitro* assays have had great difficulties in differentiating between transit amplifying progenitors and stem cells within the neurospheres and this makes it difficult to draw unambiguous conclusions. The low levels of Gal-3 expression in neurosphere cells may reflect the fact that *in vivo* Gal-3 did not label any Mash-1 progenitor cells in B6 mice and only a very small subset in the SJL mice. If neurospheres have a high composition of progenitor cells this could explain the sparse nature of the staining.

4.3.4 Decreased neuroblast number and ectopic migration in SJL Gal3 null mice

Previous studies from the laboratory have shown that Gal-3 is required to maintain specific dynamic features of neuroblast migration and the pro-migratory environment in the SVZ-RMS-OB axis. With such an important role in migration I examined how the loss of Gal-3 affects neuroblast numbers and emigration. Gal-3 deletion in SJL/J mice results in a dramatic decrease in the numbers of Dcx^+ cells and a loss of neuroblast chain integrity in the SVZ demonstrated by smaller chain sizes and increased numbers of individually migrating cells, a phenotype very similar to that seen after TMEV infection (chapter 3). In the Gal-$3^{-/-}$ mice fewer Dcx^+ cells emigrated as individuals or in clusters into the striatum compared to wildtypes. This phenotype was not seen in the B6 Gal-$3^{-/-}$ mice.

One possibility to explain this difference would be if Gal-3 regulated neuroblast chain integrity and migration via maintenance of the glial tube scaffold. Only in the SJL mice is Gal-3 expressed by the SVZ and RMS astrocytes which form the glial tubes enveloping the migrating neuroblast chains. In these mice, deletion of Gal-3 resulted in hypertrophied astrocyte processes, although this was not accompanied by changes in RMS area. This phenotype has been previously associated with abnormal neuroblast migration

(Ghashghaei et al., 2006; Kaneko et al., 2010). Alternatively, Gal-3 secreted extracellularly by astrocytes within the tubes may maintain neuroblast chain integrity through direct interactions with extracellular matrix (ECM) proteins. Extracellular Gal-3 acts as an adhesion molecule by cross-linking adjacent cells and cells with ECM by binding to ECM proteins like laminin, elastin, fibronectin and others (Dumic et al., 2006). Indeed, Comte et al showed that in acute *in vitro* RMS explants, where the glial tubes are not present, anti-Gal-3 functional blocking antibodies decreased Dcx chain formation and increased the number of cells migrating as individuals (Comte et al., 2011). This is a similar phenotype to that resulting from a loss of Gal-3 in the SJL/J mice.

It would be interesting to investigate whether these differences in phenotype would also be present when measuring more dynamic features of migration using multiphoton technology (James et al., 2011; Nam et al., 2007; Zhao and Nam, 2007). If deficits were only seen in the SJL/J strain this could provide an excellent means to elucidate the mechanisms through which Gal-3 is regulating migration.

4.3.5 Gal-3 deletion does not alter proliferation *in vivo*.

Previous studies in the laboratory reported that deletion of Gal-3 in 129sv mice did not have any effect upon proliferation of SVZ cells (Comte et al., 2011). Similarly in this thesis, a short term BrdU labelling protocol or staining with Ph3 showed deletion of Gal-3 produced no changes in the number of cells in S phase or M phase respectively in either strain. Gal-1 is also expressed by astrocytes in the SVZ and may be a key regulator of proliferation of cells both in the healthy brain and in stroke (Sakaguchi et al., 2006). This suggests that Gal-1 and Gal-3 may have distinct functions within the SVZ, whereby Gal-3 regulates migration and Gal-1 regulates proliferation. As there is minimal migration by DG

cells compared to SVZ cells Gal-3 may not be required and so is not expressed. It still remains to be answered what the role of the other galectins, Gal-8 and Gal-9, expressed in the SVZ may be.

4.3.6 Gal-3 influences proliferation of neurosphere cells.

Interestingly, neurospheres derived from SJL Gal-$3^{-/-}$ mice had lower MTS absorbances over 72 hours compared to SJL Gal-$3^{+/+}$ neurospheres. This could be due to fewer cells in the culture actively proliferating at a given time or that the same number of cells were taking longer to progress through the cell cycle. Cells from B6 mice showed only transient decreases in MTS readings with Gal-3. Gal-$3^{-/-}$ cells from B6 mice did grow slower over a 72 hour period and addition of rGAl-3 increased both size and number of spheres. To investigate further how Gal-3 may regulate proliferation and growth neurospheres were grown in the presence of exogenous recombinant Gal-3. For both strains exogenously added rGal-3 decreased the number of neurospheres in a dose-dependent manner, although this was only significant for SJL mice. Intriguingly, addition of rGal-3 to Gal-$3^{-/-}$ cultures led to even greater decreases in proliferation that that of the wildtypes, particularly in the SJL neurosphere cells. This is most strikingly seen using the MTS assay which showed that doses from 0.1 to 1 μg/mL of rGal-3 led to a 60% decrease in number of metabolically active cells compared to 0 ug rGal-3.

Galectin-3 is secreted from neurospheres, most likely through the same non-classical, ER/Golgi-independent secretory pathway that has been reported for several other cell types (Hughes, 1999). The main galectin ligands on the surface of cells are branched N-glycans found on transmembrane proteins such as EGFR, FGFR, and PDGFR. In neurospheres I have shown that EGFR is expressed on the surface of the majority of cells.

Galectin-3 is able to cross-link Mgat5-modified N-glycans on EGFR inducing the endocytosis and intracellular accumulation of EGFR (Furtak et al., 2001). In wildtype cells addition of exogenous rGal-3 may stimulate the endocytosis of EGFR and decrease their responsiveness to the mitogenic effects of EGF. One possible reason that the Gal-3 null mice show greater decreases in proliferation may be due to a greater availability of receptors to which the galectin can bind. Comte et al (Comte et al., 2011) showed that levels of phosphorylated EGFR (active form) in Gal-$3^{-/-}$ mice are increased. This has also been reported in pancreatic cancer cells where silencing of galectin-3 also increased EGF-induced EGFR phosphorylation and p42/44 ERK activation which strongly increased the cell surface expression of EGFR (Merlin et al., 2011). This would mean that addition of rGal-3 would cause greater endocytosis of EGFR and larger effects on proliferation.

A possible reason that I do not see any huge differences in the proliferation between the Gal-$3^{+/+}$ and Gal-$3^{-/-}$ cells may be due to the fact that only a small subset of cells in the neurosphere actually express Gal-3 so deletion only has a limited effect on growth. This may also be part of the reason exogenous Gal-3 has such a strong effect, as addition will affect all cells in the neurosphere. Something else to consider is that how galectins are presented to cells affects their interaction with N-glycans leading to different functional outputs. Studies have shown that Gal-3 can have different effects depending on whether the galectin is immobilised or soluble, for example immobilised Gal-3 promotes neurite outgrowth whereas soluble Gal-3 does not (Pesheva et al., 1998). It is possible that the soluble exogenous Gal-3 functions differently than endogenous protein which is more likely to be immobilised on the cell surface. These data support the notion that Galectin-carbohydrate lattices regulate the decision between cell growth and arrest by regulating receptor turnover.

4.3.7 Galectins and neuronal growth

Expression of Gal-3 was demonstrated in discrete cortical layers during development and in differentiating neurons in the neurosphere cultures and suggests it may have a role in neuronal differentiation. Subsets of DRG neurons projecting to laminae I and II or dorsal horn display Gal-3 expression that is mediated by nerve growth factor (NGF) (Pesheva et al., 2000). In phaeochromocytoma (PC12) cells, a model for sympathetic neurons, it was shown that Gal-3 can be induced by bFGF and NGF via the Ras- and mitogen-activated protein kinase (MAPK)-dependent and independent signalling pathways and its expression correlated with NGF mediated neuronal differentiation (Kuklinski et al., 2003). Interestingly Gal-3 levels gradually decreased as the cells developed. Gal-3 at the cell surface may participate in axon guidance and fasciculation of neuronal projections (Pesheva et al., 1998) as neurons grown on Gal-3 produce longer, more complex axons (Diez-Revuelta et al., 2010). These effects could be due to Gal-3 binding to several different neural recognition molecules involved in cell-matrix interactions including NCAM, cell adhesion molecule L1 and myelin associated glycoprotein (MAG) (Probstmeier et al., 1995). Transient expression of Gal-3 by neurons both in culture and *in vivo* during their development could be involved in the regulation of axon growth. Further study of various timepoints during development would highlight whether Gal-3 was selectively switched ‘on’ or ‘off’ at discrete stages of formation of each cortical layer.

4.3.8 Galectin and oligodendrocytes.

A possible role for Galectin-3 in oligodendrocyte function has been previously reported. Pasquini and colleagues (Pasquini et al., 2011) showed that Gal-3 was up-regulated during oligodendrocyte differentiation and exposure to Gal-3 promoted oligodendrocyte

differentiation in a dose dependant manner. They reported that morphometric analysis showed a significant decrease in the frequency of myelinated axons, myelin turns (lamellae) and g-ratio in the corpus callosum and striatum of Lgals3($^{-/-}$) compared with wild-type mice. Whilst I found that Gal-3 was expressed by differentiating oligodendrocytes in the neurospheres, loss of Gal-3 did not alter the fate of these cells or result in any noticeable changes in morphology. Further experiments growing neurospheres in increasing concentrations of recombinant Gal-3 did not affect the fate of oligodendrocytes either, although it did change ratios of neurons to astrocytes (data not shown). It is possible the presence of other cells, such as astrocytes and neurons, could explain the differences between these findings. Alternatively, it could be that because the other researchers used an immortalised OLG line for the experiments this may have altered the functions of the cells.

Another galectin, Gal-4, has been shown to act as a neuronal regulator of myelination (Stancic et al., 2012). Non-myelinated axons express and release substantial amounts of Gal-4. OLGs transiently expose Gal-4 binding sites at their surfaces just before MBP synthesis begins and these remain until the onset of myelin-like membrane formation. When OLGs are exposed to Gal-4 it impedes their maturation and causes dedifferentiation and proliferation. This could be a mechanism for neurons to regulate the numbers of OLGs and the timing of myelination. I have shown in this chapter that differentiating neurons both in culture in cortical layers of postnatal mice express Gal-3. Given the above findings by Pasquini et al (2011) it would be worthwhile to question whether Gal-3 serves as a similar means for neurons to regulate myelination.

4.3.9 Conclusion

Despite high levels of expression within the SVZ Gal-3 only shows subtle effects on proliferation, emigration and fate of neurospheres. Given the previous findings that Gal-3 deletion is important in regulating migration this would be worthwhile to study in further experiments. In this chapter I have shown that depending on the mouse strain levels of Galectin-3 can vary significantly and deletion of Gal-3 can have different effects. These data demonstrate that when performing studies on Gal-3 it is important to consider the strain chosen as this may influence the outcome of the experiments.

Chapter 5

Role of Galectin-3 in regulation of neuroinflammation

5.1 **Introduction** **178**

5.2 **Results** **180**

5.3 **Discussion** **207**

5.1 Introduction

Lesions in multiple sclerosis are often characterised by a disturbance in the blood-brain barrier, local oedema and demyelination. These findings indicate that early in the disease on-going inflammatory activity is present and is responsible for the relapsing-remitting course that most patients experience. There is also considerable heterogeneity in terms of the pathological and clinical changes, which are reflected in the polygenic nature of the disease. The difficulties that researchers have faced in identifying the trigger for these relapses, together with disappointing results from clinical trials and treatment with IFNβ, glatiramer acetate or immunosuppressive agents, show that there is still a long way to go in understanding inflammation in MS. Curtailing immune infiltration in the CNS through targeting chemokine-receptors and MMPs with antagonists, or through novel therapeutic targets, might produce more promising results. The ideal scenario is a compound that can ablate the aberrant immune response, protect axons and allow remyelination and repair (Hemmer et al., 2002).

Galectin-3 may be good potential candidate molecule. The links between multiple sclerosis and defects in glycosylation and galectin related pathways were discussed in detail in chapter 1. Deletion of Gal-3 has been shown to be able to dampen immune responses and improve clinical outcome in a variety of different inflammatory disease models (Brand et al., 2012; Forsman et al., 2011; Toscano et al., 2012; Wang et al., 2010a). EAE induced in Gal-3 deficient mice is markedly attenuated compared to WT mice (Jiang et al., 2009). This attenuation was accompanied by reduced cellular infiltration of monocytes and macrophages in the CNS, alterations in cytokine levels and increased apoptosis of CNS infiltrates.

In chapter 3 I found that TMEV induced inflammation had a detrimental impact on several processes in the SVZ including proliferation and survival. In chapter 4, Gal-3 was found to be specifically expressed in the cells of the SVZ. Studying the role of Gal-3 in TMEV induced inflammation in the SVZ would be beneficial in furthering our understanding of the role Gal-3 in MS pathology. As constitutive levels of Galectin-3 were different between resistant and susceptible strains of mice it may have differential roles in inflammation in these strains. Given that Gal-3 is able to regulate the expression of cytokines, chemokines and adhesion molecules and modulate T-cell activities it is possible that Gal-3 may have a role in providing resistance in B6 mice.

5.1.2 Research questions

I hypothesised that Gal-3 is up-regulated in the TMEV brain and is a regulator of the immune response to viral infection. In addition, it is put forward that modulation of the immune response through deletion of Gal-3 may infer beneficial effects on the SVZ neurogenic niche. Also, it is postulated that varying levels of expression of Gal-3 in different strains of mice would produce different inflammatory patterns. The aims of this chapter are therefore to: (1) determine the cellular localisation and levels of Gal-3 expression after TMEV infection, (2) examine changes in immune cell infiltration after Gal-3 deletion, (3) determine if loss of Gal-3 results in changes in SVZ processes, and (4) determine if Gal-3 deletion influences levels of chemokines in the SVZ.

5.2 Results

5.2.1 Galectin-3 is up-regulated after TMEV infection

Measurement of tissue Gal-3 protein levels showed that after TMEV Gal-3 expression is increased in the SVZ in both strains but only up-regulated in the cortex of B6 mice (figure 5.1A). In the SVZ, B6 mice had greater up-regulation of Gal-3 at both 3 DPI and 7 DPI compared to SJL mice ($n=3$, $p<0.0001$, figure 5.1A). In confirmation of the ELISA data immunohistochemistry showed there were increases in Gal-3 expression in the SVZ, and in surrounding periventricular regions that did not normally express Gal-3, including the septum and striatum (figure 5.1B). The corpus callosum showed much lower levels of expression. Gal-3 expression correlated strongly with areas of CD3 infiltration in both strains (figure 5.1C-D).

5.2.2 TMEV infection stimulated Gal-3 expression in CNS astrocytes

Immunohistochemistry showed that the cellular localisation of Galectin-3 expression in the SVZ did not change following TMEV infection. As in naïve animals Gal-3 is expressed by astrocytes, ependymal cells and in SJL/J a subset of Mash-1^+ progenitor cells but not by Dcx^+ neuroblasts. Following TMEV infection Gal-3 expression was increased in $GFAP^+$ cells in dorsal and ventral SVZ regions (figure 5.2A-B). $GFAP^+$ astrocytes in the corpus callosum medial to the SVZ only express Gal-3 weakly. In the dorsal and ventral SVZ, Gal-3 was expressed in the cytoplasm and nucleus of the majority of astrocytes, with little expression in fine cellular processes (figure 5.2A-B'). There are clear differences in the expression profile of Gal-3 between SVZ astrocytes compared to

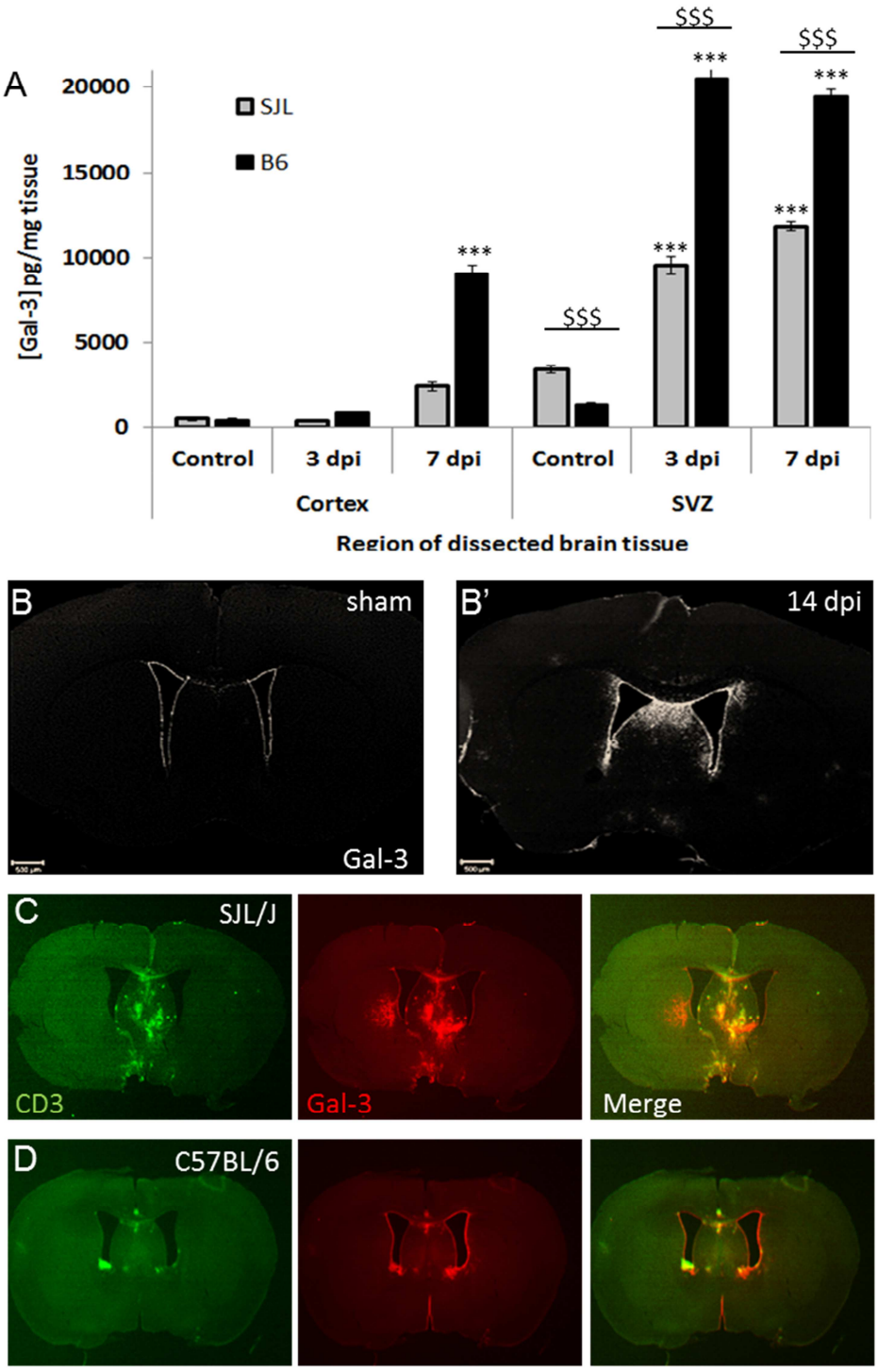


Figure 5.1 Galectin-3 is up-regulated after TMEV infection

(A) Gal-3 tissue protein levels measured using ELISA. ***p<0.001 compared to control. $$$ p<0.001 compared between SJL and B6.

(B) TMEV infection causes upregulation of Gal-3 in periventricular regions. Gal-3 expression in meninges shown by red arrow. Scale bar 500 μm.

(C-D) CD3 (green) and Gal-3 (red) expression overlaps in SJL (C) and C57BL/6 (D) mice at 7 dpi

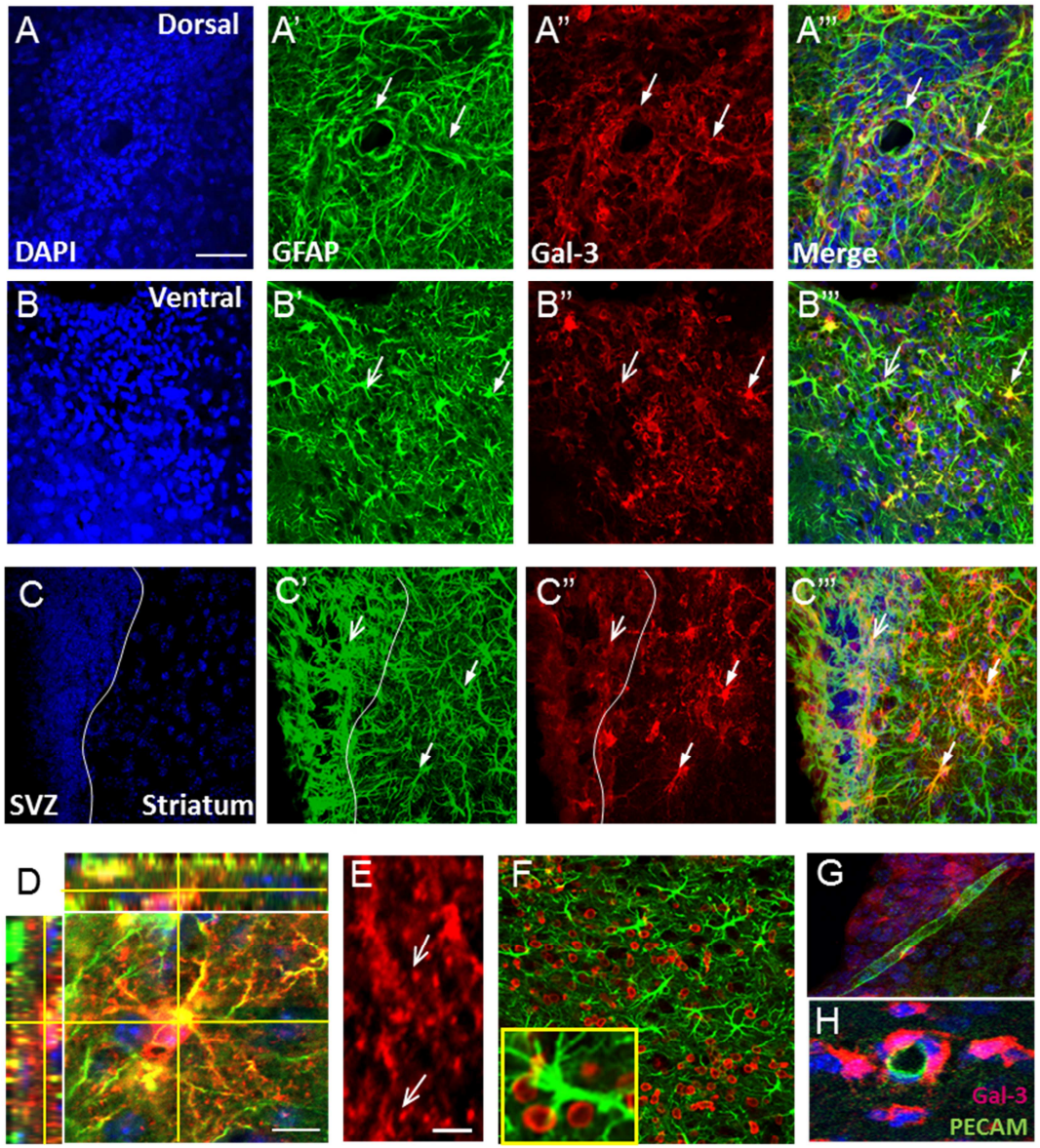


Figure 5.2 Gal-3 is expressed by SVZ and periventricular astrocytes

(A) Expression of Gal-3 (red) by GFAP+ (green) cells in dorsal SVZ regions 7dpi. Arrows indicate Gal-3+ GFAP+ cells forming the basement membrane around blood vessels.

(B) GFAP+ (green) and Gal-3+ (red) in ventral SVZ regions

(C) GFAP+ (green) cells in the SVZ and striatum show different expression profiles of Gal-3 (red). SVZ boundary outlined.

(D) Compressed confocal z-stack of astrocyte in striatum. Scale bar 5 μm

(E) Punctate appearance of Gal-3 (red) in fine processes (shown by arrow) Scale bar 2.5μm

(F) Cortical astrocytes show little expression of Gal-3

(G-H) Endothelial cells (PECAM+) (green) do not label for Gal-3 (red)

striatal astrocytes. In the SVZ Gal-3 is localised mainly in the nucleus with diffuse cytoplasmic localisation in thick GFAP$^+$ processes (figure 5.2C, open arrow). In comparison, in striatal astrocytes Gal-3 was also found in the nucleus (figure 5.2D, closed arrow) but immunostaining showed a more punctate appearance in the processes, suggesting a possible vesicular localisation (figure 5.2E). Gal-3$^+$ striatal astrocytes were generally only found in close proximity to ventricular regions. In contrast to the SVZ, Gal-3$^+$ astrocytes in cortex were quite rare, even in areas of high T cell infiltration (figure 5.2E), but they were most commonly found in contact with meningeal wall. High Gal-3 expression in meningeal layer can be seen in figure 5.1B' (indicated by red arrow).

After infection GFAP$^+$Gal-3$^+$ astrocytes are found making up the glial basement membrane of the meninges, lateral ventricles and midline in infected animals. A greater intensity of Gal-3 immunoreactivity was seen in astrocytes whose end feet were associated with blood vessels surrounded by perivascular inflammatory infiltrates (Fig 5.2A', closed arrow and figure 5.2H). Previous studies on active human MS lesions have suggested that endothelial cells may express Gal-1 and Gal-9 but not Gal-3 (Stancic et al., 2011). CD31 staining confirmed that blood vessel endothelial cells were not Gal-3$^+$ in TMEV (figure 5.2G-H). It is plausible therefore, that a key role for Gal-3 in astrocytes is in control or regulation of immune cell infiltration given its high expression at main sites of immigration.

5.2.3 SVZ primary astrocytes cultures make more Gal-3 than cortical cultures

Immunostaining showed that Gal-3$^+$ astrocytes were very rarely found in the cortex, unlike the high expression in periventricular regions. To determine whether SVZ astrocytes are more disposed to produce high levels of Gal-3 compared to cortical

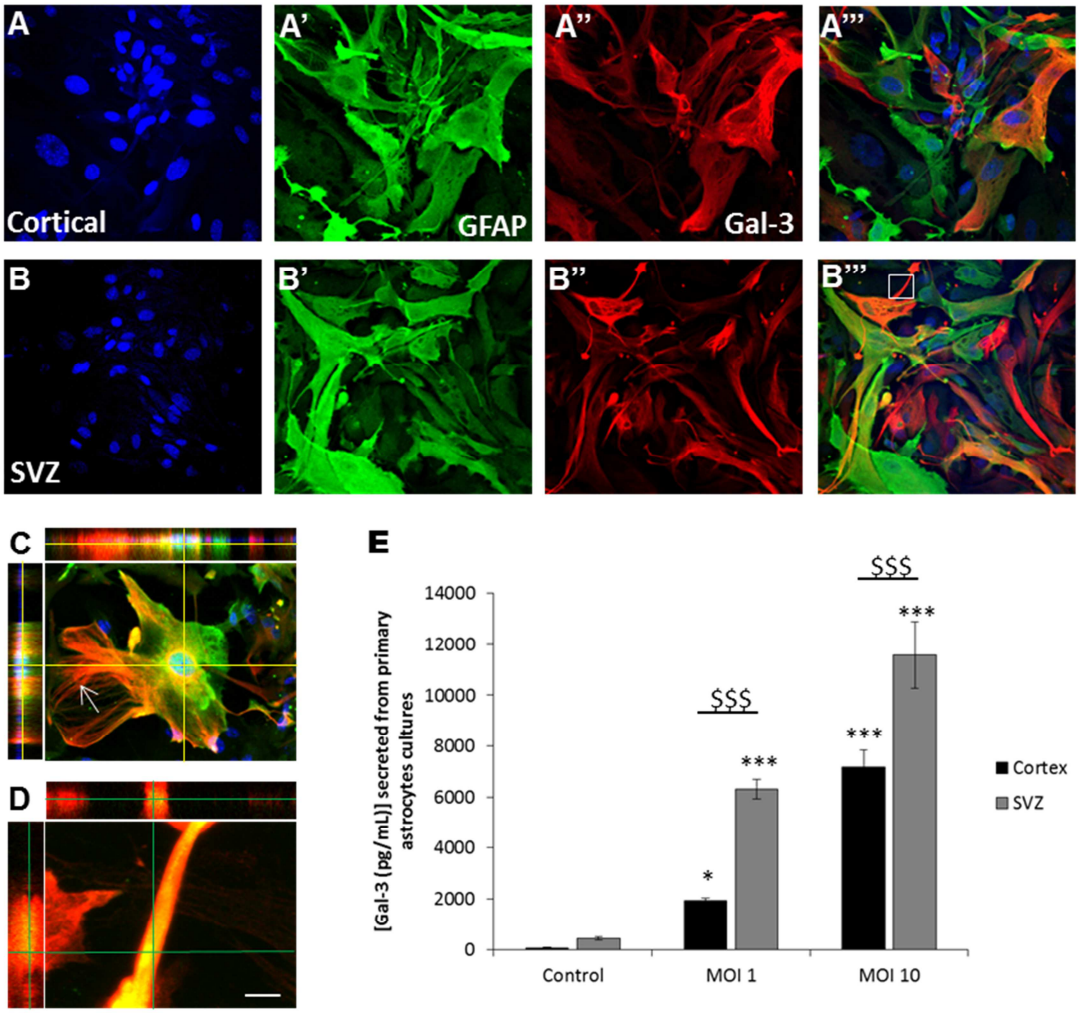


Figure 5.3 Gal-3 up-regulation in TMEV infected astrocytes

(A-B) Primary cultures derived from cortex (A) and SVZ (B). Gal-3 (red) labelling of GFAP (green) cells.

(C) Compressed z-stack shows perinuclear localisation of Gal-3 (red) in GFAP+ (green) cells.

(D) In GFAP+ processes Gal-3 (red) surrounds GFAP (green) in a 'tube' like structure. Scale bar 5 μm. High mag image of boxed are in (B''').

(E) Measurement of secretion of Gal-3 after TMEV infection. * $p<0.05$, *** $p<0.001$ compared to control, $$$ $p<0.001$ SVZ compared to control. N=3. Representative of three independent experiments.

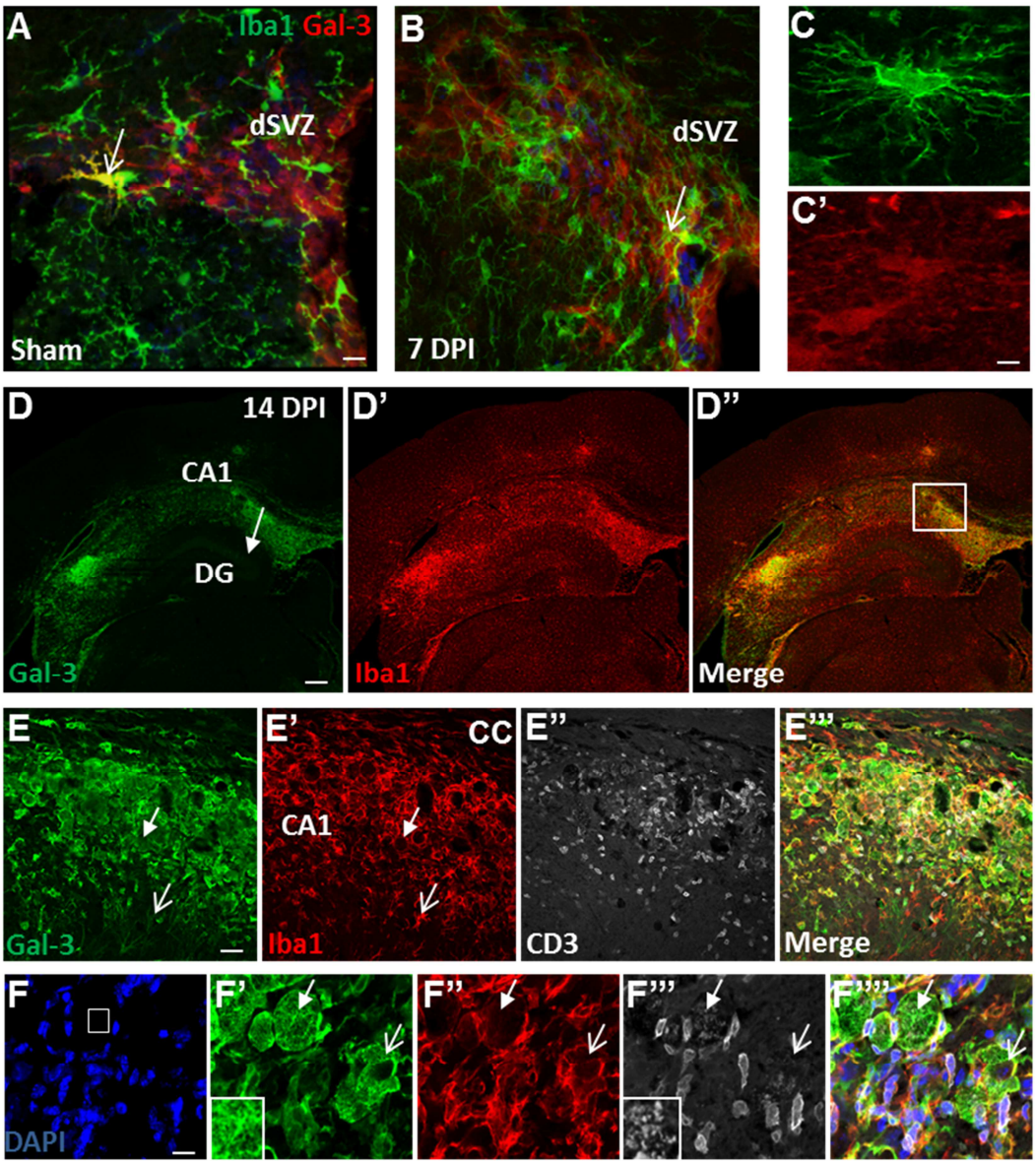


Figure 5.4 Phagocytosing microglia in the hippocampus express Gal-3

(A) Gal-3 (red) labelled microglia (green) are rare in the healthy SVZ.

(B) At 7dpi microglia (green) are activated but do not express Gal-3 (red).

(C) Expression of Gal-3 (red) in Iba1+ cell (green) in corpus callosum.

(D) In the hippocampus there is a strong correlation between Gal-3 (green) and Iba1 (red) immunoreactivity.

(E) Microglia/macrophages (red) with a phagocytosing 'foamy' appearance label with Gal-3 (green)

(F) Gal-3 (green) expression in phagocytosing Iba1+ cells (red) containing digested CD3+ T-cells (grey).

astrocytes I produced primary cultures from these regions. Constitutively, immunostaining did not reveal any major differences in expression of Gal-3 between the two cultures (figure 5.3A-B). In both cultures expression is in the cytoplasm of a subset of astrocytes, with strong perinuclear localisation (figure 5.3C). It is highly expressed in processes that did not always express GFAP (figure 5.3C, arrow). In $GFAP^+$ processes that did stain for Gal-3 it formed a 'tube' surrounding the GFAP (figure 5.3D). Secretion of Gal-3 was significantly increased in SVZ and cortical cultures by both concentrations of TMEV (figure 5.3E). Primary SVZ astrocytes secreted significantly higher levels of Gal-3 then cortical astrocytes at both MOI 1 and MOI 10 ($n=3$, $p<0.001$, figure 5.3E).

5.2.4 Phagocytosing microglia in the hippocampus express Gal-3

Gal-3 has been shown to be expressed highly in microglial cells surrounding areas of tissue damage in models of stroke and ischemia (Fernandes Bertocchi et al., 2008; Lalancette-Hebert et al., 2012; Yan et al., 2009). I wanted to see if TMEV also induced Gal-3 expression in microglia. Within healthy SVZ very few microglia constitutively express Gal-3 (figure 5.4A, arrow) and there is no obvious increase in the number of Gal-3^+iba1^+ cells after TMEV infection (figure 5.4B, arrow). More commonly, microglia in the corpus callosum express Gal-3^+ in their nucleus, cytoplasm and in fine processes (figure 5.4C). In contrast, immunohistochemistry on the hippocampus at 14 dpi shows there is strong correlation between iba1 and Gal-3 up-regulation (figure 5.4D-D''). During the chronic stages of TMEV infection, autoreactive pathogenic lymphocytes undergo phagocytosis and are subsequently phagocytosed by resident CNS microglia. This is an important mechanism of elimination, in order to maintain homeostasis, which otherwise could lead to tissue destruction. During phagocytosis, microglia evolve from a ramified

morphology with multiple rough processes (figure 5.4C $^{+}$ E, open arrow) to an enlarged soma with shorter, less numerous prolongations (figure 5.4E, closed arrow). This strongly suggests that Gal-3 plays an important role in the clearance of lymphocytes by microglia phagocytosis in TMEV infection.

5.2.5 Galectin-3 expression by CD3^{+} cells

A subpopulation of CD3^{+} T-cells co-label for Gal-3 at 7 dpi and 14 dpi (figure 5.5A). The percentage labelled was consistent across several different brain regions examined (figure 5.5C-F). Within the dorsal SVZ, fewer T-cells express Gal-3 compared to middle and ventral regions (27±4% vs 67±4% and 52±3% respectively, figure 5.5B). Within the spleen clusters of Gal-3+ cells are seen at 7dpi TMEV infection in SJL mice. Brightly labelled Gal-3+ cells show no overlap with CD3+ cells seen in the spleen at this time point suggesting up-regulation may occur during migration into the CNS (figure 5.6D).

A subset of the CD3^{+}Gal3^{+} cells are cytotoxic CD8^{+} T cells (fig 5.6A-A’’’) but CD8^{-}Gal3^{+}CD3^{+} cells can be seen which are most probably CD4^{+} T cells (yellow arrow). Unfortunately, I have been unable to achieve consistent staining with CD4 antibodies to confirm this due to the fact that the anti-CD4 antibodies require acetone fixation which is not compatible with my other experiments. The cytoplasmic location of Gal-3 in T-cells can be clearly seen in figure 5.6B.

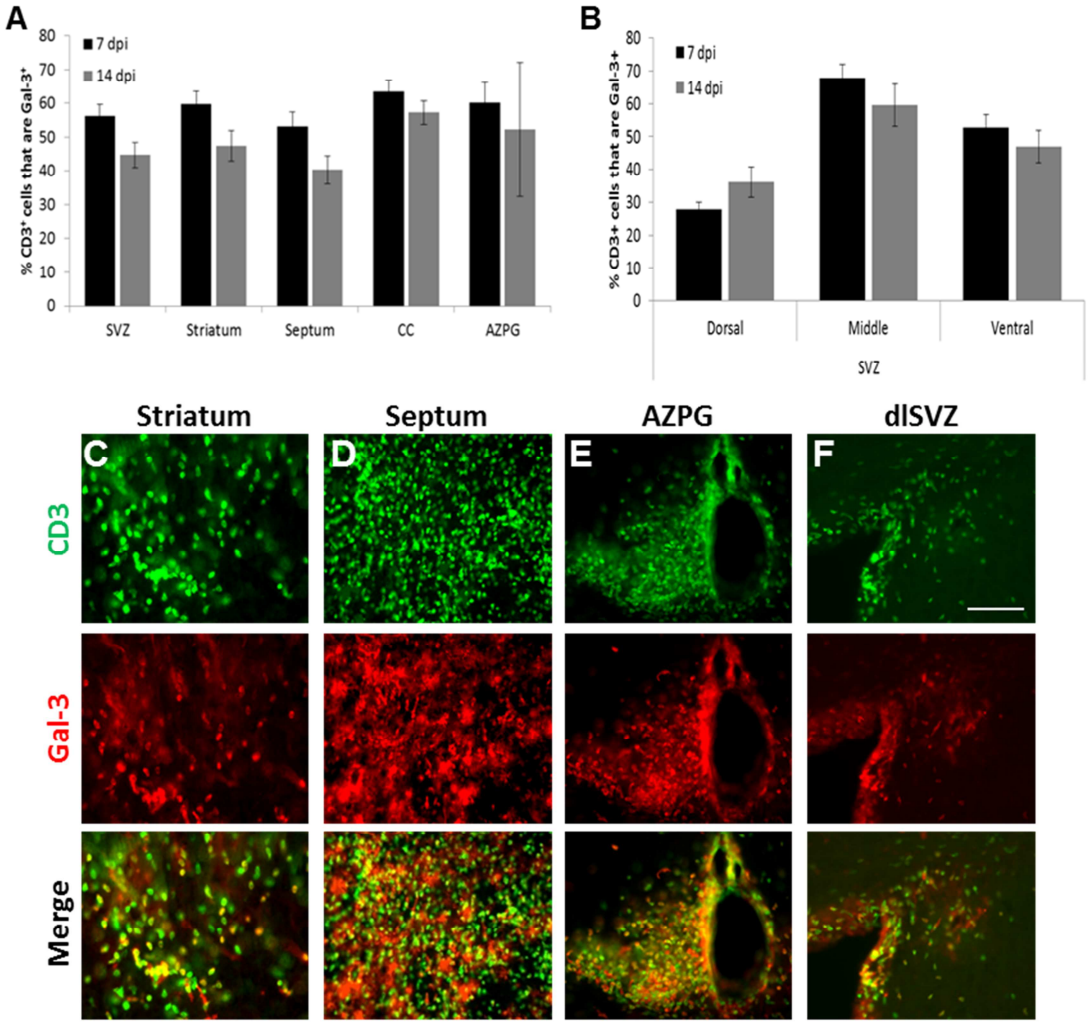


Figure 5.5 A subset of T-cells co-label for Gal-3

(A) The percentage of CD3+ that co-label for Gal-3 in several brain regions

(B) Percentage CD3 and Gal-3 co-labelled cells in SVZ subregions.

(C-E) Immunohisitochemistry showing the strong overlap between Gal-3 (red) and CD3 (green) in different brain regions. Scale bar 100 μm

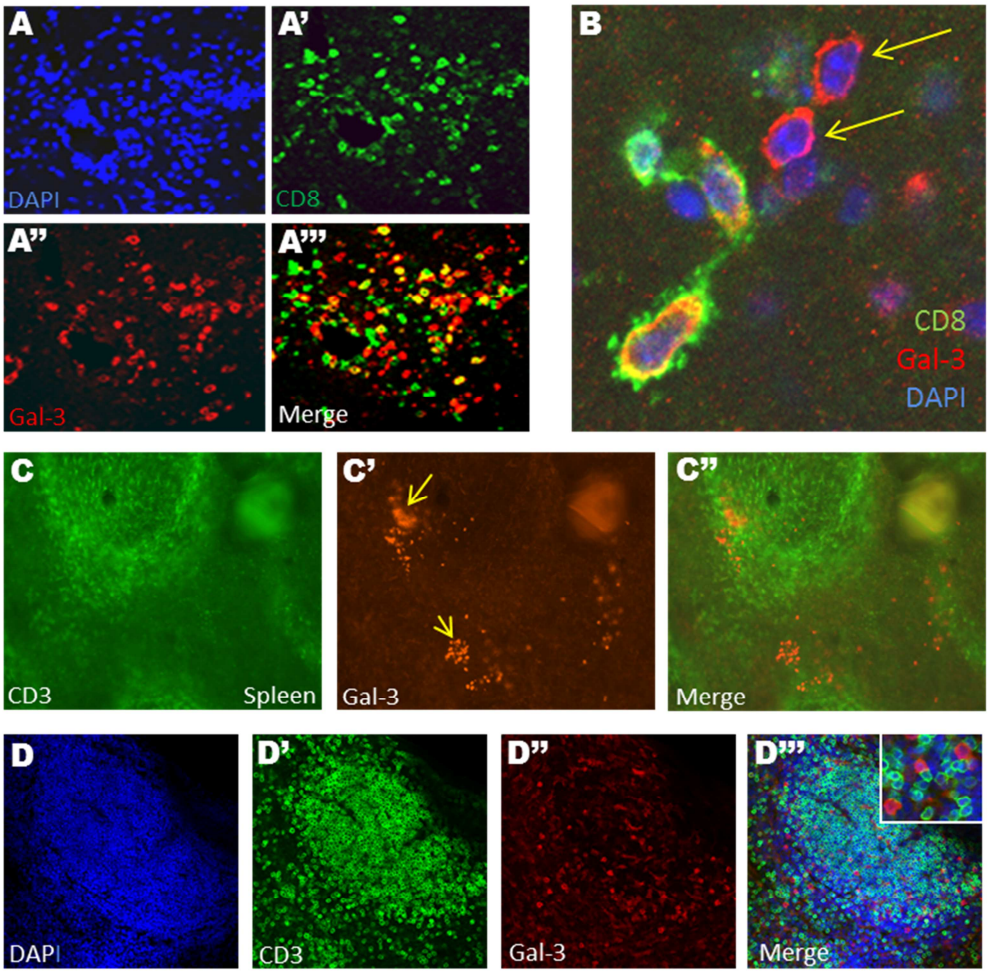


Figure 5.6 A subset of T-cells are Gal-3+

(A) A subset of $CD3^{+}Gal3^{+}$ cells infiltrating into the brain are cytotoxic $CD8^{+}$ T cells

(B) Gal-3 is expressed in the cytoplasm of T-cells. Yellow arrows indicate cells that are CD8+Gal-3-.

(C) Immunohistochemistry on the spleen from 7dpi TMEV SJL mice. (5x)

(D) CD3+ and Gal-3 immunohistochemistry in 7 dpi SJL spleen from SJL mice. Inset box shows lack of overlap between CD3+ and Gal-3+ cells.

5.2.6 Deletion of Galectin-3 reduced haematopoietic cell infiltration after TMEV

In chapter 2 I showed that infiltrating T-cells preferentially targeted the SVZ. In order to see if deletion of Gal-3 from the SVZ affected this infiltration I quantified the numbers of amoeboid $CD45^+$ cells in the SVZ and other brain regions. The CD3 antibody utilised in chapter 2 was no longer commercially available. Co-labelling between CD45 and Iba1 found very minimal presence of amoeboid macrophage cells in forebrain regions at the time points quantified. Therefore, by counting amoeboid $CD45^+$ with a morphology consistent with T-cells, numbers are most likely to represent T-cell infiltration. Numbers were also very consistent with those found for T-cells in the previous cohorts of mice used for chapter 2. Deletion of Gal-3 in SJL mice caused a significant decrease in amoeboid $CD45^+$ cells present into the striatum, septum and dorsal and ventral SVZ at 3 dpi ($n=5$, $p<0.001$, figure 5.7A-B). Amoeboid $CD45^+$ cells were also decreased in the striatum, cortex, dorsal SVZ and ventral SVZ at 14 dpi in SJL mice ($n=5$, $p<0.001$, figure 5.7A-B). At 7 dpi there was no change in $CD45^+$ in numbers in any brain region examined for the SJL mice. This is in stark contrast to B6 mice, who showed little change in $CD45^+$ numbers at 3 and 14 dpi (figure 5.8 A-B). At 7 dpi there was a dramatic decrease in the number of amoeboid $CD45^+$ cells present in all regions of SVZ as well as the striatum and septum ($n=5$, $p<0.001$, figure 5.8A-B).

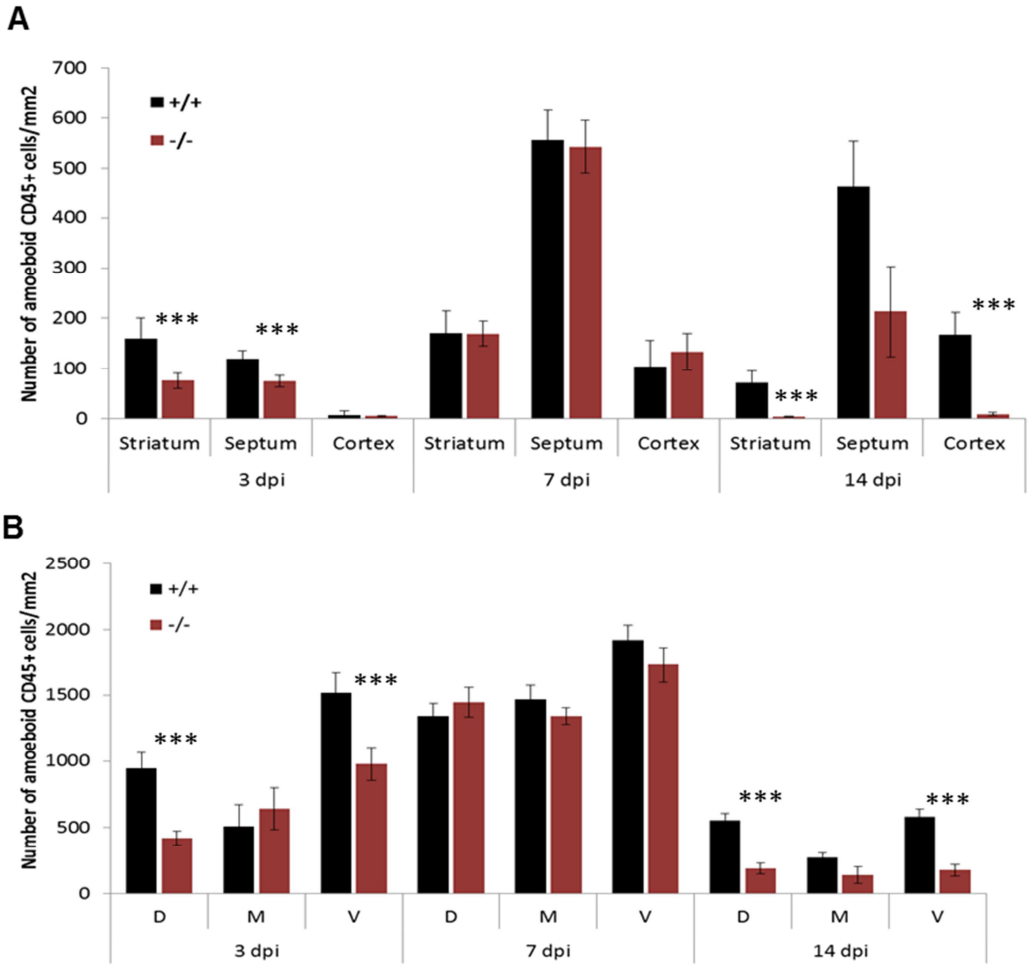


Figure 5.7 Decreases in amoeboid CD45+ infiltration in SJL mice at 3 and 13 dpi

(A) Numbers of infiltrating amoeboid CD45+ cells in Gal3+/+ and Gal-3-3 mice in cortical and periventricular regions

(B) Numbers of infiltrating amoeboid CD45+ cells in Gal3+/+ and Gal-3-/3 mice in SVZ subregions

* p<0.05, *** p<0.001. ANOVA Gal3-+/+ to Gal-3-/- N=5 all groups

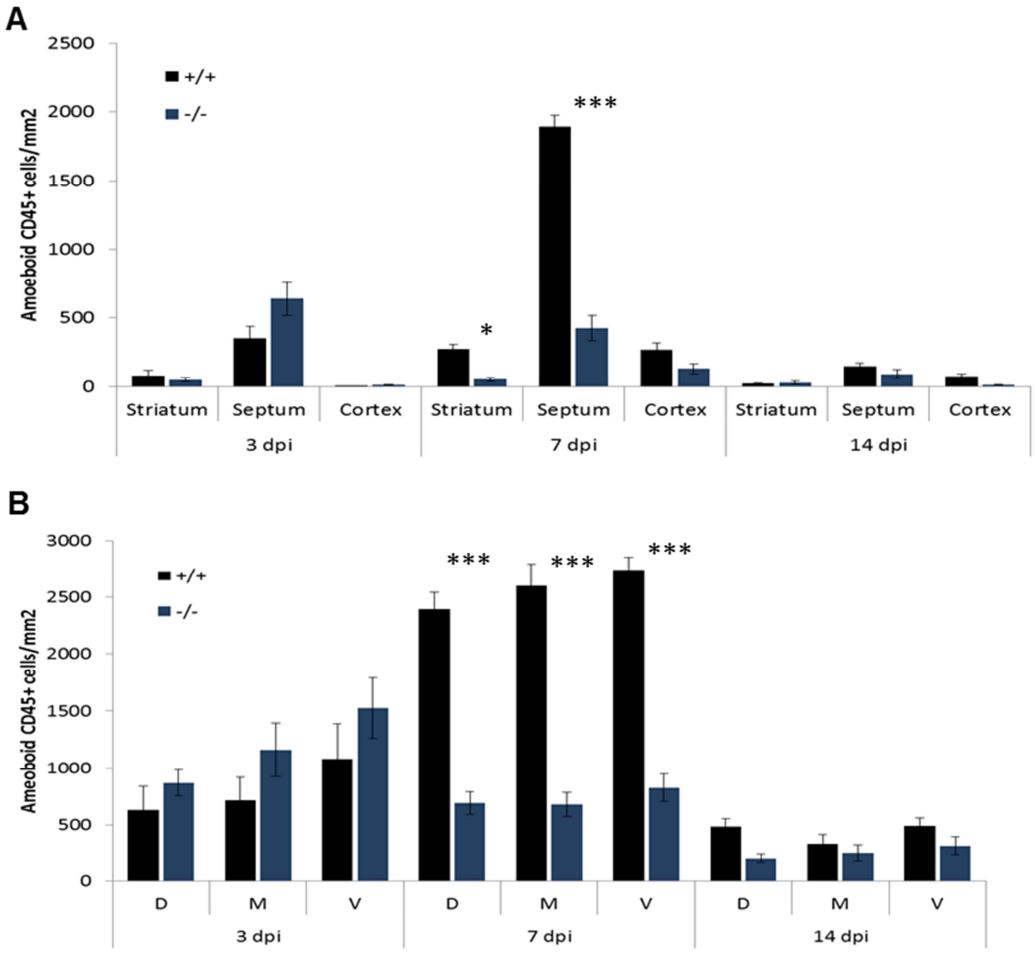


Figure 5.8 Fewer Infiltrating amoeboid CD45+ cells in periventricular regions in B6 Gal-3-/-

(A) Numbers of infiltrating amoeboid CD45+ cells in B6 Gal3+/+ and Gal-3-/- mice in cortical and periventricular regions

(B) Numbers of infiltrating amoeboid CD45+ cells in Gal3+/+ and Gal-3 mice in SVZ subregions

* $p<0.05$, *** $p<0.001$ ANOVA Gal3-+/+ to Gal-3-/- N=5 all groups

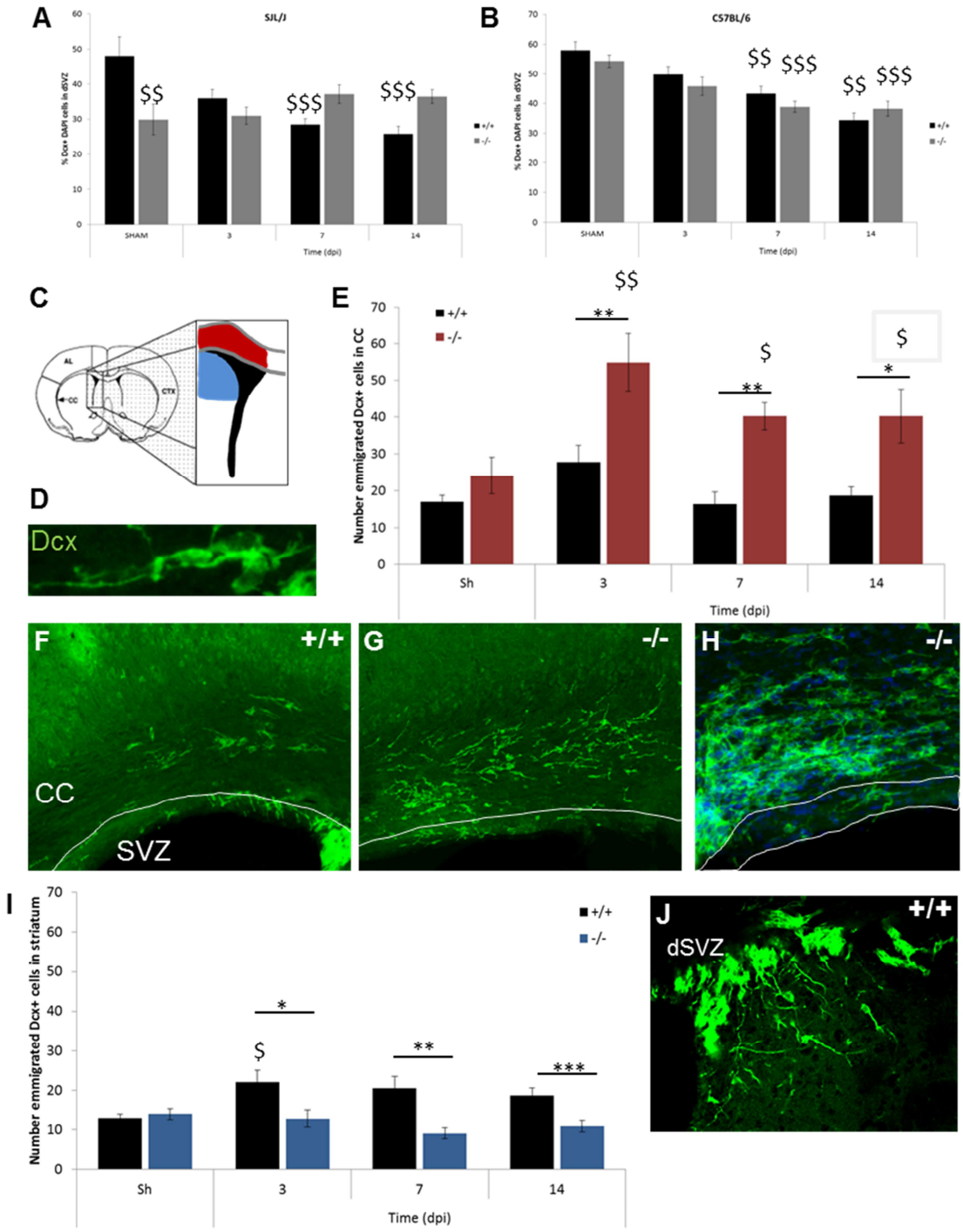


Figure 5.9 Loss of Gal-3 increase ectopic neuroblast migration

(A-B) Percentage of Dcx+ DAPI+ in dlSVZ in SJL (A) and B6 mice (B).

(C) Schematic depicting division of brain regions for quantification.

All images and graphs D-J from C57BL/6 mice.

(D) Example morphology of Dcx+ cell quantified in migration measurements.

(E) Quantification of neuroblast emigration into the corpus callosum. * $p<0.05$, ** $p<0.01$, ANOVA WT vs KO. $ $p<0.05$, $$ $P<0.001$ ANOVA control vs TMEV. n=5 all groups. Example of typical morphology of migrating Dcx+ neuroblast shown in (D)

(F-G) Dcx+ migration into CC at 7dpi in Gal-3+/+ (F) and Gal-3-/- mice (G).

(H) In some sections Dcx+ neuroblasts can be found leaving the SVZ 'en-masse '

(I) Gal-3 loss prevents the transient increase in emigration into the SVZ after TMEV

(J) Quantification of neuroblast emigration into the corpus callosum

5.2.7 Loss of Gal-3 increases ectopic neuroblast emigration

Deletion of Gal-3 from SJL mice prevents the decrease in neuroblast numbers in the dorsal SVZ seen at 7 and 14 dpi in Gal-$3^{+/+}$ mice (figure 5.9A). Deletion of Gal-3 from B6 mice did not prevent this loss of neuroblast cells (figure 5.9B). Quantification of Dcx^{+} cells that emigrated into the corpus callosum showed that B6 Gal-$3^{-/-}$ mice had significantly higher numbers of emigrating cells than Gal-$3^{+/+}$ mice at all time points ($n=5$, $p<0.01$, figure 5.9E-G). There was no detectable increase in emigration of cells into the corpus callosum after TMEV infection in WT mice compared to constitutive levels (figure 5.9F). In some sections Dcx^{+} neuroblasts could be found migrating 'en-masse' out of the SVZ (figure 5.9H). It is likely that there is no apparent recovery of neuroblasts numbers in the SVZ of Gal-$3^{-/-}$ mice due to the increased emigration. Gal-$3^{+/+}$ mice showed a transient increase in emigration into the striatum at 3dpi compared to controls ($n=5$, $p=0.04$, figure 5.9J). At all time points Gal-$3^{-/-}$ mice had reduced levels of emigration into the striatum compared to Gal-$3^{+/+}$ mice ($n=5$, $p<0.05$, figure 5.9J). Processes of Dcx^{+} cells extended from the dSVZ into the striatum (figure 5.9J).

5.2.8 $Ph3^{+}$ proliferation after Gal-3 KO

As reported in chapter 3 TMEV infection decreased proliferation in the SVZ. As this may be due to an inhibitory effect of the presence of lymphocytes I considered the possibility that reduced haematopoietic cell infiltration due to the lack of Gal-3 may lead to a recovery in proliferation. Deletion of Gal-3 in SJL/J mice restored proliferation back to sham level at 14 dpi for both BrdU (figure 5.10A) and Ph3 labelled cells (figure 5.10B). Similarly, in B6 Gal-$3^{-/-}$ mice the decrease in proliferation at 7 dpi was prevented shown by both Ph3 (figure 5.11A) and BrdU (figure 5.11B). Intriguingly, B6 Gal-$3^{-/-}$ showed a

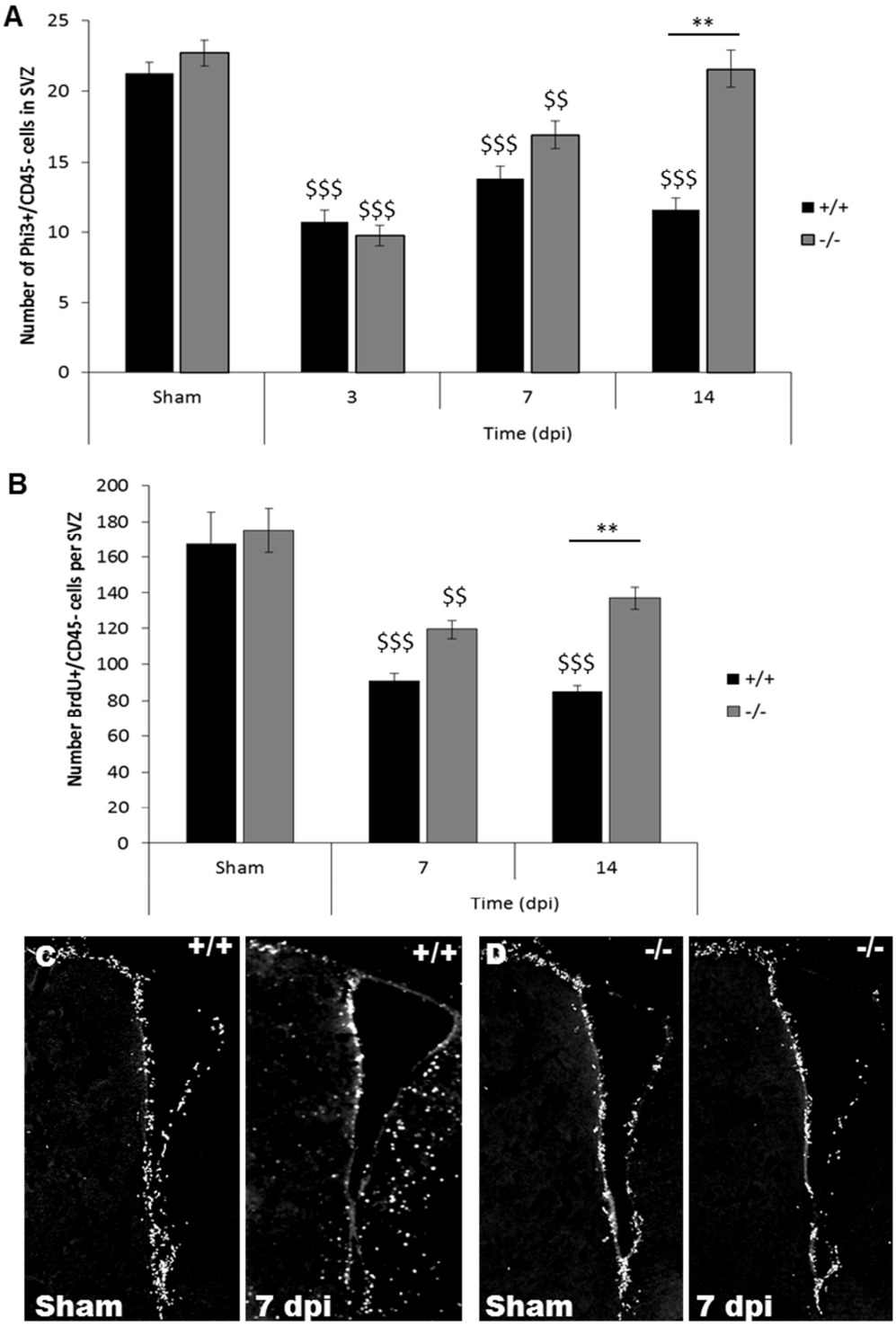


Figure 5.10 Gal-3 deletion restores proliferation in SJL/J mice

(A) Quantification of PH3+ cells in entire SVZ wall in WT and KO mice.

(B) Quantification of BrdU+ cells in entire SVZ wall in WT and KO mice. $$ $p<0.01$, $$$ $p<0.001$ ANOVA compared to control. ** $p<0.01$ ANOVA compared WT vs KO. N=5 all groups

(C) BrdU+ cells in SVZ in Gal-3+/+ mice. BrdU+ cells can be seen in surrounding periventricular regions

(D) BrdU+ cells in SVZ in Gal-3-/- mice..

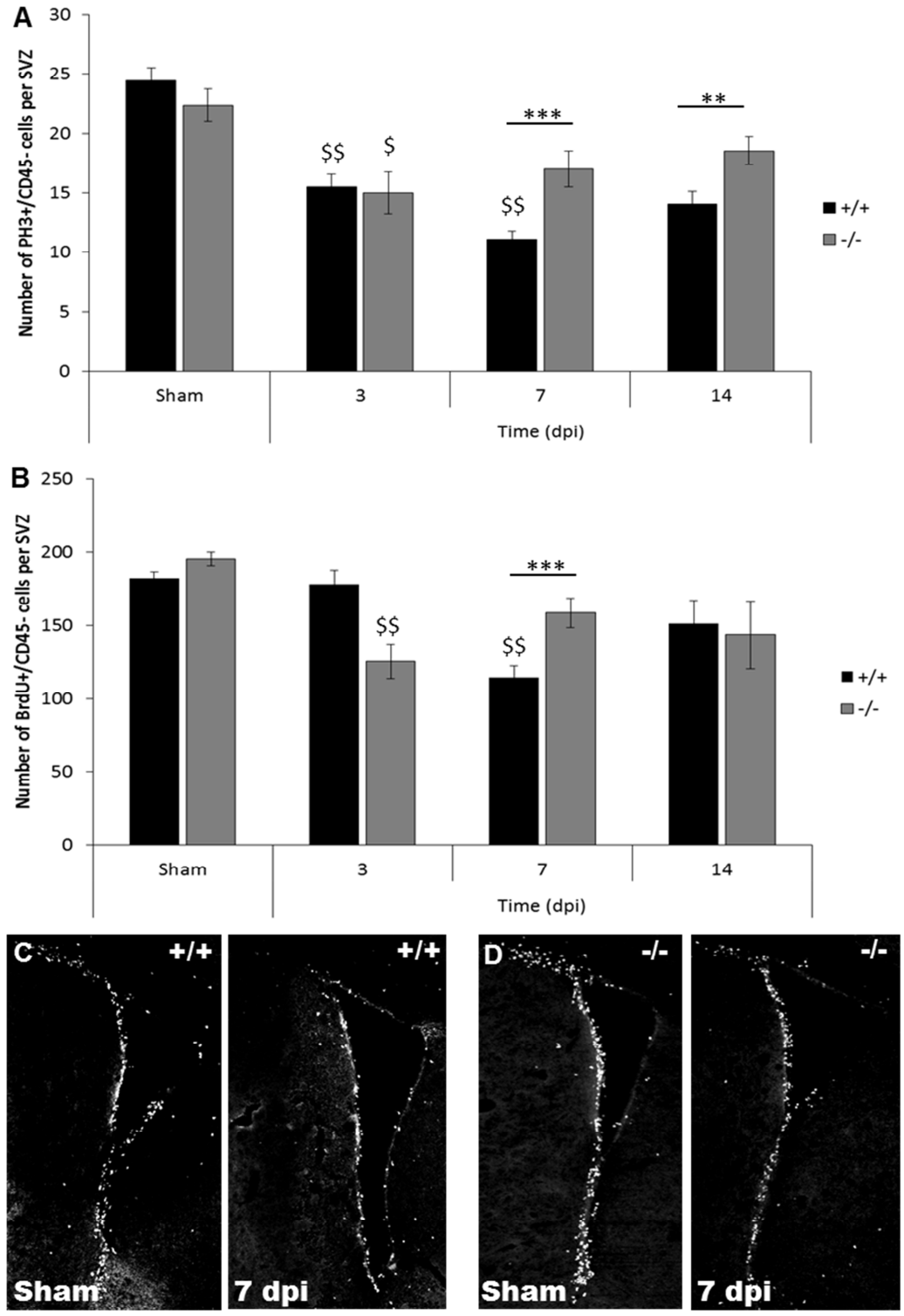


Figure 5.11 Gal-3 deletion restores proliferation in B6 mice

(A) Quantification of PH3+ cells in entire SVZ wall in WT and KO mice.

(B) Quantification of BrdU+ cells in entire SVZ wall in WT and KO mice. $$ p<0.01, $$$ p<0.001 ANOVA compared to control. ** p<0.01 ANOVA compared WT vs KO. N=5 all groups.

(C) BrdU+ cells in SVZ in Gal-3+/+ mice.

(D) BrdU+ cells in SVZ in Gal-3-/- mice..

significant decrease in BrdU cells compared to Gal-$3^{+/+}$ mice at 3 dpi (n=5, p=0.01, figure 5.11B). This may be a result of KO mice having slightly higher numbers of $CD45^{+}$ cells at this time point compared to WT mice (figure 5.8A-B). Levels of proliferation in Gal-$3^{-/-}$ mice at 7 dpi were not significantly different from sham, unlike Gal-$3^{+/+}$ mice that had significant decreases in proliferation (figure 5.11A-B).

High numbers of $BrdU^{+}$CD45- labelled cells were present in the cortex but $Ph3^{+}$CD45- cells were very rare. Induction of apoptosis can be preceded by an abortive attempt of the cell to enter into cell cycle and damaged neurons initiate abortive DNA synthesis. In Alzheimer's mature neurons attempt to divide and activate the machinery for cell division (Neve, 2000). As completion of cell cycle not possible in postmitotic cells the neuron dies instead and is difficult to exclude the possibility that neurons incorporate BrdU during abortive S phase (Kuan, 2004). As apoptosis of neurons is a key feature of TMEV the disparity between BrdU and Ph3 labelling may due to infected neurons undergoing apoptosis label with BrdU but not Ph3. This could be confirmed by TUNEL staining.

5.2.9 TMEV infection of neurospheres stimulates secretion of Gal-3

As immunostaining levels of Gal-3 were so high in SVZ astrocytes I wanted to see whether expression was induced by direct infection by BeAn virus or from activation by infiltrating immune cells. Secondary neurospheres were infected with TMEV at concentrations of MOI 1 and MOI 10, or treated with IFNγ/TNFα to model proinflamamtory cytokines from microglia/T-cells. After 4 hours Gal-3 was significantly up-regulated in the MOI 10 condition for both B6 and SJL neurospheres (n=3, $p<0.001$, figure 5.12A). IFNγ/TNFα stimulated an increase in Gal-3 secretion at 4 hours from B6

cells that was gone by 24 hours (figure 5.12A). At 24 hours B6 cells secreted significantly higher levels of Gal-3 than SJL neurospheres (n=3, p<0.00001, figure 5.12B).

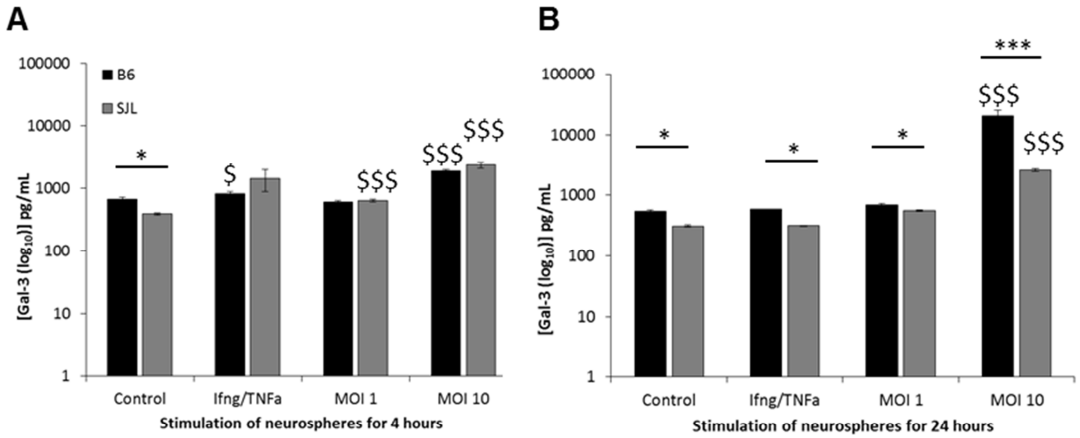


Figure 5.12 TMEV infection of neurospheres stimulates secretion of Gal-3

Secondary neurospheres were stimulated with IFNg/TNFa, or infected with TMEV at either MOI 1 or MOI 10 and supernatant was collected at 4 (A) and 24 (B) hours. Gal-3 levels were measured by ELISA.

* p<0.05 ANOVA WT vs KO, $$$ p<0.001 ANOVA control vs treated. N-3 all groups. Representative of three independent experiments.

5.2.10 Gal-3 deletion protects from TMEV cytotoxicity in neurospheres

In Chapter 3, I demonstrated that TMEV infection of neurospheres cells led to a decrease in neurosphere number and size. Using the MTS assay confirmed there is a significant decrease in the numbers of metabolically active cells compared to controls over 48 hours that is similar for both SJL Gal3$^{+/+}$ (figure 5.13A) and Gal-3$^{-/-}$ (figure 5.13B). At 72 hours both B6 and SJL Gal-3$^{+/+}$ cells show an increase in metabolic activity that is not seen in the Gal-3$^{-/-}$ cells. A lactate dehydrogenase assay confirmed that the TMEV virus causes

cytotoxicity in neurospheres cells (figure 5.13C-E). Gal-3 deletion in SJL cells seemed to provide protection as Gal-$3^{-/-}$ cells showed significantly less TMEV induced death 72 hours post infection (n=3, $p<0.05$, figure 5.13E). B6 neurospheres showed the same decrease in proliferation over 72 hours with the MTS assay in both Gal-$3^{+/+}$ (figure 5.14A) and Gal-$3^{-/-}$ cells (figure 5.14B). The LDH assay showed that Gal-3 KO in B6 cells provided the same protection from cytotoxicity at 72 hours (figure 5.14F) and at 48 hours at the highest concentrations of Gal-3 (figure 5.14D).

5.2.11 Role IFNγ on regulation of Galectin-3 secretion

Jeon et al (Jeon et al., 2010) reported that stimulation by IFNγ led to an up-regulation of galectin-3 in microglial cultures. Interestingly IFNγ mRNA up-regulation was significantly higher in B6 SVZ tissue compared to SJL tissue as shown in chapter 3. Attempts to confirm these differences with ELISA were unsuccessful as IFNγ levels were too low for reliable analysis. In order to assess whether IFNγ caused a similar effect in neurospheres cells were stimulated with increasing concentrations of recombinant IFNγ. IFNγ did not stimulate the secretion of Gal-3 from either B6 (figure 5.15B) or SJL (figure 5.15C) derived neurospheres. In B6 neurosphere cell lysate rIFNγ did not increase total Gal-3 protein levels within the cells (figure 5.15A). Immunostaining for Gal-3 after IFNγ stimulation did not show any changes in Gal-3 expression (figure 3.15D). This suggest that Gal-3 may be differently regulated in different systems.

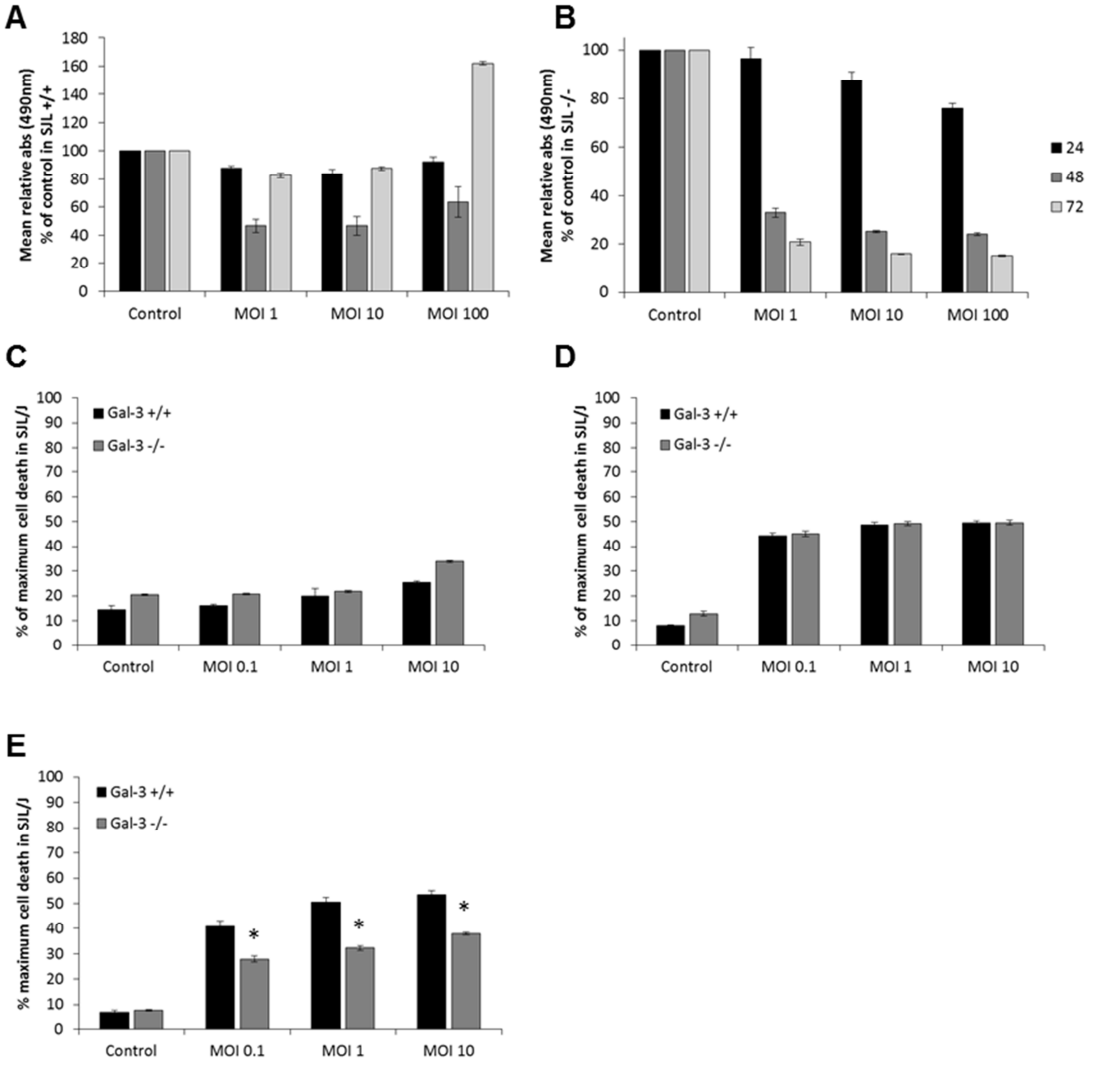


Figure 5.13 Loss of Gal-3 decreases TMEV induced cell lysis in SJL neurospheres

(A-B) Measure of MTS absorbancy over a 72 hours period for TMEV infected Gal-3+/+ (A) and Gal-3-/- cells (B).

(C-E) Measurement of lactate dehydrogenase levels following TMEV infection of WT and KO neurospheres . * $p<0.01$, n=3 ANOVA wt vs ko. Representative of three independent experiments.

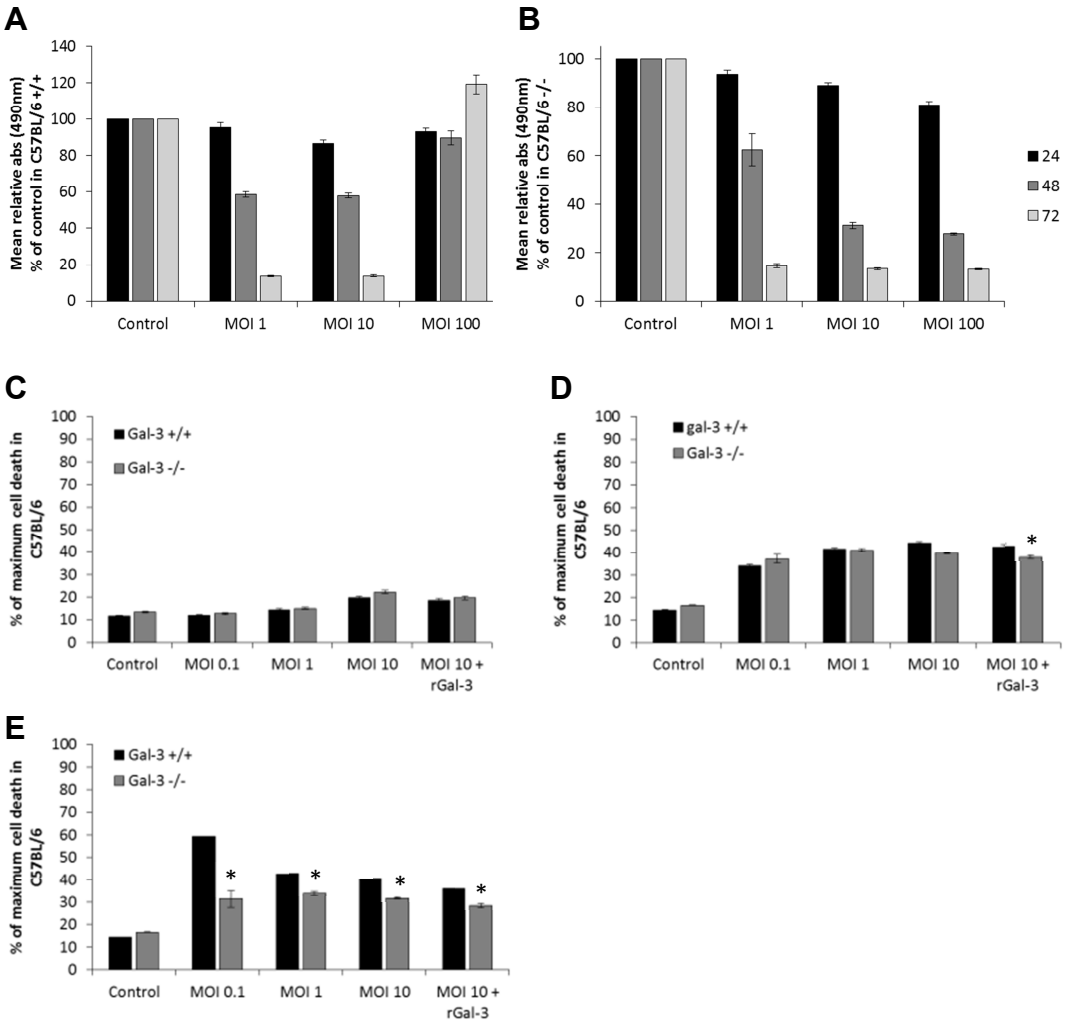


Figure 5.14 Loss of Gal-3 decreases TMEV induced cell lysis in B6 neurospheres

(A-B) Measure of MTS absorbency over a 72 hours period for TMEV infected Gal-3+/+ (A) and Gal-3-/- cells (B).

(C-E) Measurement of lactate dehydrogenase levels following TMEV infection of WT and KO neurospheres . * $p<0.01$, n=3 ANOVA wt vs ko. Representative of three independent experiments.

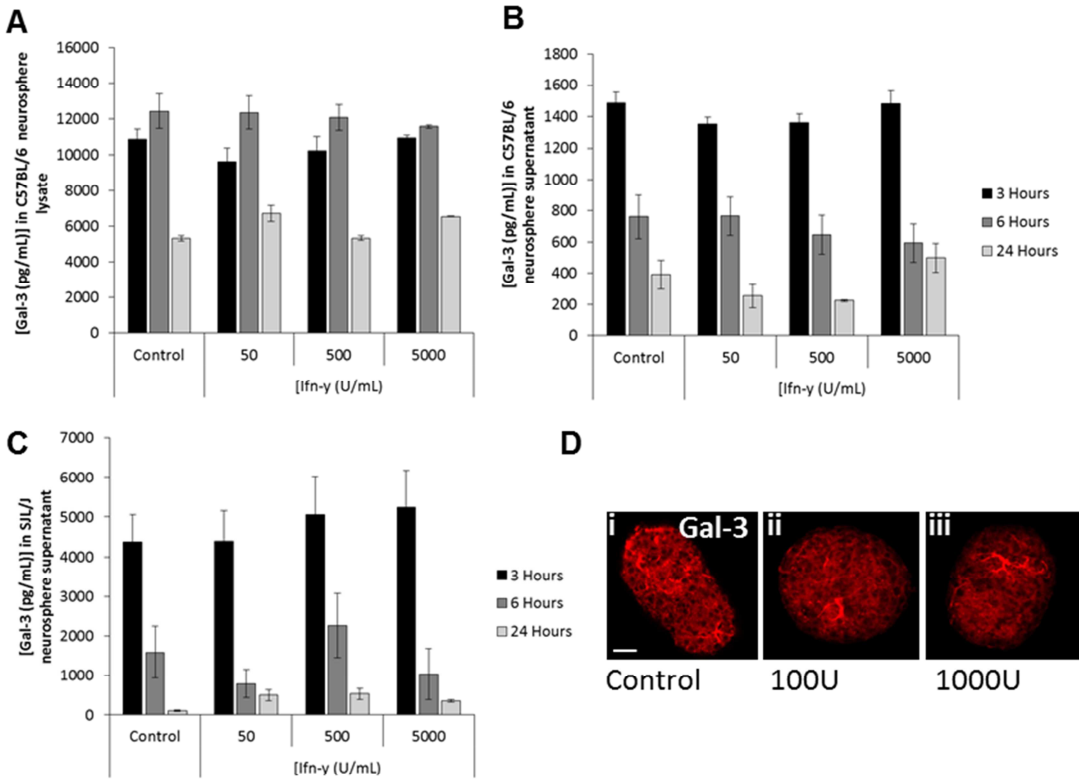


Figure 5.15 IFNγ does not stimulate the secretion of Gal-3 from neurospheres

(A-C) Treatment of teritary neurospheres with IFNγ did not increase Gal-3 levels in either cell lysate (A) or supernatant (B) of B6 cells or SJL (C) cells.

(D) Gal-3 immunostaining does not noticeably increase in the presence of IFNγ. Scale bar 20 μm.

5.2.12 Loss of Gal-3 in B6 mice alters chemokines mRNA levels in the SVZ

Galectin-3 has been shown to act in most cases as a 'pro-inflammatory cytokine', and can directly or indirectly regulate the transcription of several different cytokines and chemokines (Cortegano et al., 2000; Jeon et al., 2010; Mackinnon et al., 2012; Ruas et al., 2009; Saegusa et al., 2009; Silverman et al., 2012). To investigate whether a loss of Gal-3 affected expression of inflammatory molecules, tissue was dissected from the SVZ of naïve and 7 dpi TMEV infected mice and run on the same RT-PCR array used in chapter 2. Gal-$3^{-/-}$ mice had significantly lower levels of several chemokines compared to Gal-$3^{+/+}$, including CCL1, CCL11, CCL7 and CXCL10 (figure 5.16A-C). Both CCL5 and CCL8 mRNA levels showed greater up-regulation after Gal-3 deletion (figure 5.16A, B). For the full list of cytokines examined please see Table 2 in the appendix.

5.2.13 Chemokine ELISAs on SVZ tissue (D3 and D7)

The measurements of fold changes in mRNA levels were not quantitative and can be greatly influenced by the starting levels of mRNA within a cell. To confirm that Gal-3 altered levels of inflammatory molecules the protein levels of the chemokines that showed the greatest changes were measured using ELISA. The chemokines CCL2, CCL5, CXCL10 and CCL8 were chosen as they showed the greatest changes at the mRNA levels. As reported in chapter 2 cytokine levels were higher in SVZ compared to cortex for all chemokines examined. Deletion of Gal-3 did not alter chemokine levels in the cortex in either strain (figure 5.17). This is not surprising as levels of Gal-3 are relatively low in cortical tissue. In both B6 and SJL mice SVZ chemokines levels were significantly lower in the Gal-$3^{-/-}$ compared to Gal-$3^{+/+}$ mice (n=3 pooled tissue samples with 6 mice per group). The greatest difference was seen for CCL8 where Gal-3 deletion produced a

dramatic decrease in levels after TMEV infection for both B6 and SJL mice (figure 5.17G-H). For the B6 Gal-3$^{-/-}$ there were differences between the mRNA levels and the protein levels, as both CCL5 (figure 5.17A and 5.18C) and CCL8 (figure 5.16A and 5.17G) showed increases in mRNA but decreases in protein when KOs are compared to WTs. Both CXCL10 mRNA and proteins levels were decreased in B6 Gal-3$^{-/-}$ versus Gal-3$^{+/+}$ mice.

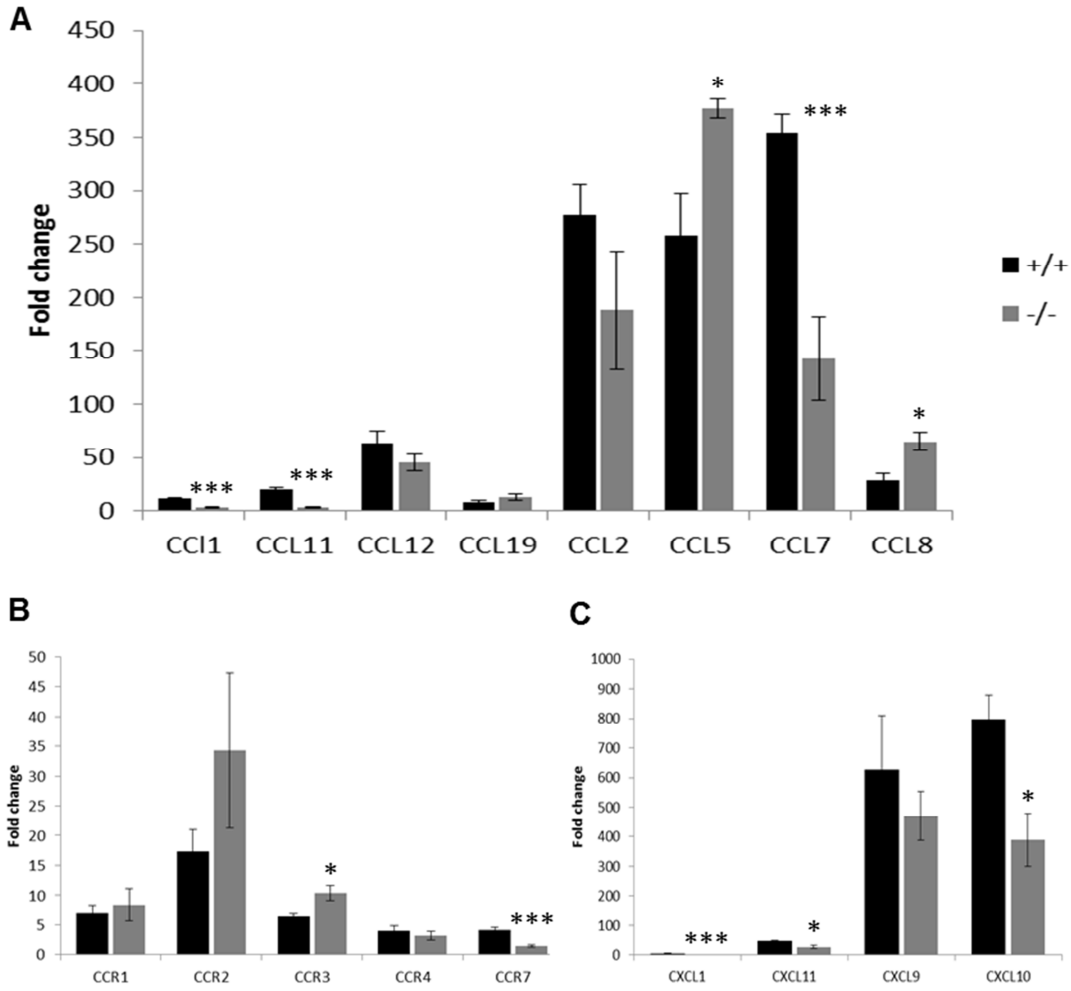


Figure 5.16 Loss of Gal-3 in B6 mice alters chemokines mRNA levels in the SVZ
SVZ tissue is dissected naive and 7 dpi TMEV mice and run on a RT-PCR array for cytokines and chemokines. All numbers presented are fold change of TMEV infection tissue compared to control tissue.

(A) Expression of C-C motif chemokines,

(B) Expression C-C motif chemokine receptors,.

(C) Expression of C-X-C motif chemokines.

* p<0.05, ** p<0.001, *** p<0.001. WT vs KO, ANOVA n=3.

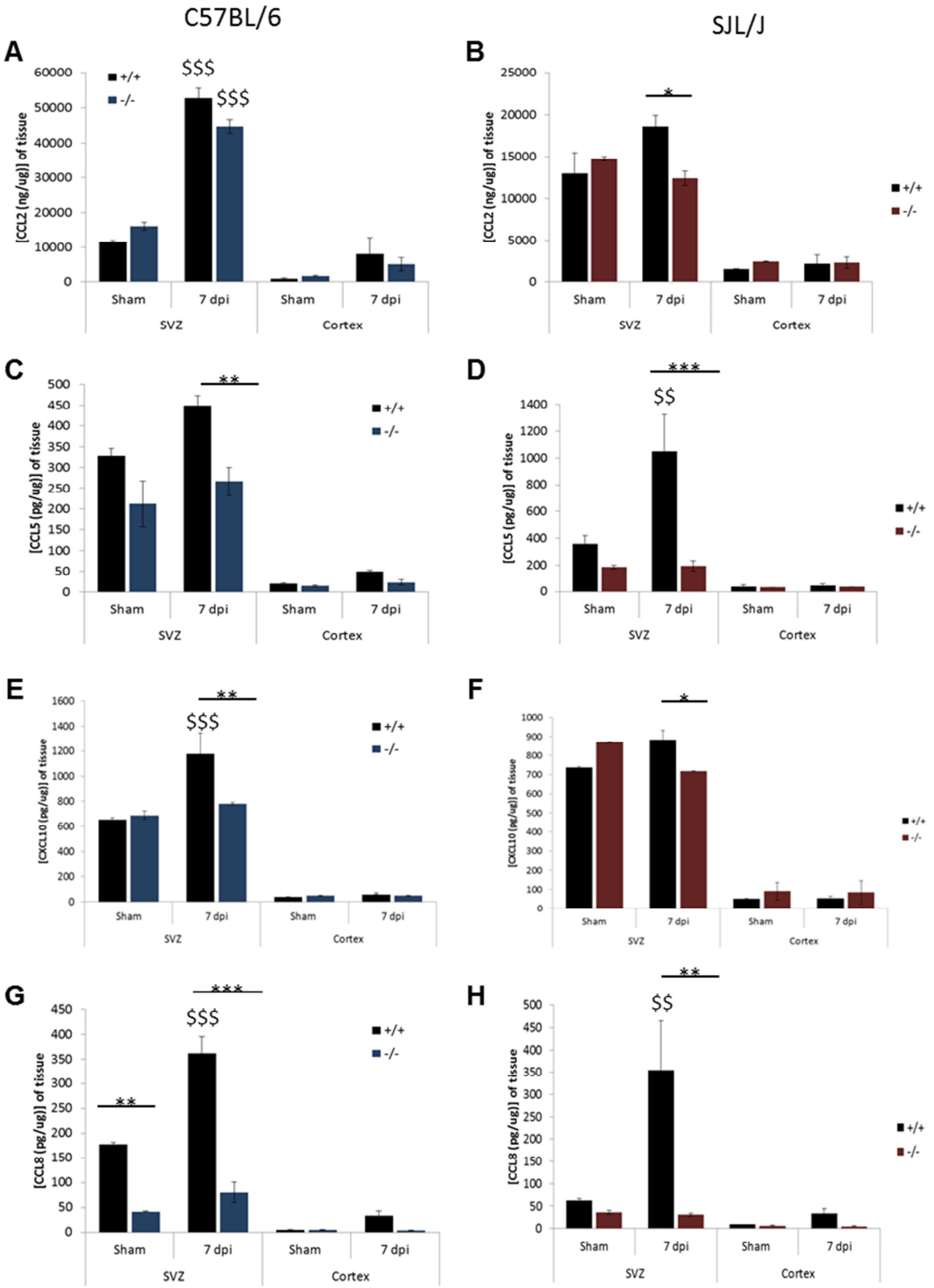


Figure 5.17 Protein levels of chemokines in SVZ and cortical tissue from B6 and SJL Gal-3-/- and Gal-3+/+ mice at 7 dpi TMEV

Measurement of protein levels of cytokines in tissue dissected from naïve and 7 dpi TMEV SVZ and cortex analysed by ELISA.

(A-B) CCL2, (C-D) CCL5, (E-F) CXCL10 and (G-H) CCL8

* p<0.05, ** p<0.01, *** p<0.001 ANOVA WT vs KO. $$ p<0.05, $$$ p<0.001, control vs TMEV ANOVA. N=3 all groups

5.3 Discussion

Following TMEV infection Gal-3 expression is up-regulated in periventricular regions and levels of Gal-3 are much higher in resistant compared to susceptible strains of mice. In the forebrain Gal-3 is expressed by both SVZ and striatal astrocytes, as well as a subset of $CD3^+$ cells. Neurosphere cultures of SVZ stem/progenitor cells secrete Gal-3 after TMEV infection, with levels much higher in B6 derived spheres compared to SJL spheres. In the hippocampus at later disease stages, Gal-3 is expressed by phagocytosing macrophages. Deletion of Gal-3 decreased the protein levels of CCL2, CCL5, CCL8 and CXCL10 in the SVZ but not the cortex. SJLGal-$3^{-/-}$ mice had decreased amoeboid $CD45^+$ cell numbers at 3 and 14 dpi in several brain regions but in B6 Gal-$3^{-/-}$ mice $CD45^+$ cell numbers were dramatically reduced at 7 dpi. Gal-3 deficiency in B6 mice caused a huge expansion in the emigration of neuroblasts into the corpus callosum and in both strains allowed a recovery in proliferation. Together these data show that the Gal-3 may regulate several inflammatory processes that are distinct between different mouse strains.

5.3.1 Galectin-3 and its involvement with multiple sclerosis

A particularly interesting study looking at expression of Galectin-3 in human post mortem sections from MS patients found that Gal-3 was expressed highly in both the cytoplasm of microglia and hypertrophic astrocytes in sites of active lesions (Stancic et al., 2011). Together with the TMEV data this suggests that Gal-3 may have an important role in the pathogenesis of multiple sclerosis. Induction of EAE in Gal-3 deficient mice results in a significantly milder EAE, with fewer infiltrating leukocytes and monocytes supporting this idea (Jiang et al., 2009). Unfortunately, the researchers did not perform any

immunohistochemistry in this study and so they were unable to identify which cell types expressed Gal-3 during EAE and mediated this disease attenuation in the CNS. The only study that has directly looked at Gal-3 expression in EAE focused solely on the spinal cord and optic nerve (Reichert and Rotshenker, 1999). It would be fascinating to study Gal-3 expression in forebrain regions after EAE to see any similarities to TMEV that may suggest common mechanisms important for MS pathogenesis.

5.3.2 Galectin-3 levels are different between resistant and susceptible strains

TMEV infection induced significantly higher levels of Gal-3 in both the cortex and SVZ of B6 compared to SJL mice. To the best of my knowledge, these are the first data to show that in the CNS the same disease model can induce different levels of Gal-3 in different mouse strains. Only one other study has shown that Gal-3 levels vary between strains in a model of experimental colitis but do not demonstrate any functional outcome from these differences in the colon (Mathieu et al., 2008). Infection of neurospheres with TMEV resulted in greater secretion of Gal-3 from B6 derived compared to SJL derived spheres. As there is very little work about the mechanisms of induction of Gal-3 and as various stimuli can affect expression at both a transcriptional and translational level it is hard to say what may be responsible for the differences between the strains. The presence of 5 CRE and 2 NF-κB-like sites in the *LGal3* promoter region implies that signalling pathways involving the cAMP-response element-binding protein (CREB) or the NF-κB transcription factor may regulate activation of Gal-3 (Kadrofske et al., 1998). TMEV infection of astrocytes can quickly activate NF-κB pathways (Palma and Kim, 2004; Palma et al., 2003) (Molina-Holgado et al., 2002a) and this may directly up-regulate Gal-3 levels. This could also induce transcription of other cytokines which, together with secreted Gal-3,

may act in a feedback loop to further stimulate Gal-3 secretion. It has been reported that in the liver, different mouse strains have different levels of activation of NF-κB and CCL2 levels are considerably higher in mice with high levels of NF-κB activation than those with low activation (Liao et al., 1993). Strain differences in the responses of NF-κB after TMEV infection would induce different levels of Gal-3 and cytokine expression, and if Gal-3 functions in a feedback loop, this could lead to greater enhancement of further expression.

5.3.3 Galectin-3 up-regulation in the SVZ

Galectin-3 has been shown to be expressed in experimental models of adult stroke (Lalancette-Hebert et al., 2007; Lalancette-Hebert et al., 2012; Walther et al., 2000; Yan et al., 2009), a model of neonatal hypoxic-ischaemic brain injury (Doverhag et al., 2010) and prion infections of the CNS (Mok et al., 2007). Gal-3 expression was also reported in a Junin virus-induced disease (De Giusti et al., 2011). In a model of EAE Gal-3 expression was reported in the spinal cord and optic nerve in areas of demyelination (Reichert and Rotshenker, 1999). In all of these studies Gal-3 was reported to be expressed mainly in microglia/macrophages with very few $GFAP^{+}Gal\text{-}3^{+}$ cells detected. This is in contrast to TMEV infection where in forebrain regions $Gal\text{-}3^{+}$ microglia are rare and the vast majority of cells expressing Gal-3 were astrocytes. Gal-3 has a critical role in phagocytosis by microglia/macrophages (Sano et al., 2003). Whilst there is substantial cell death in cortical regions in models of stroke (Lalancette-Hebert et al., 2007) after TMEV very little caspase-3 staining was detected in forebrain regions at these early stages. However, at later stages of TMEV Gal-3 was expressed by microglia in areas of significant cell death in the hippocampus, which I shall cover in more detail later in this discussion.

Another possible reason few Gal-3$^+$ astrocytes were detected could be the brain regions that these studies focused on. For stroke and ischaemic models the researchers examined cortical regions in proximity to the infarct. In TMEV Gal-3 labelled astrocytes were fairly sparse in the cortex, when compared to periventricular regions, even in areas of higher T-cell infiltration. Similarly, SVZ primary cultures produced much high levels of Gal-3 after TMEV infection than cortical primary cultures. This suggests that to up-regulate Gal-3 expression in cortical astrocytes the type or concentrations of stimuli needed may be different than for SVZ astrocytes.

5.3.4 Gal-3 is expressed by astrocytes

Following TMEV infection almost all astrocytes expressed Gal-3 within the SVZ and large numbers were present in the surrounding periventricular regions. Direct viral infection of primary SVZ astrocyte and floating neurosphere cultures was sufficient to up-regulate Gal-3 secretion. This is the first example of viral stimulation of Gal-3 expression in astrocytes and neural stem cells but virally induced expression and secretion in other cell types has been reported (Fogel et al., 1999; Hsu et al., 1996; King et al., 2009). Whilst TMEV infection may be sufficient to stimulate Gal-3 expression in cells, it is unlikely that *in vivo* all Gal-3$^+$ astrocytes are directly infected with BeAn virus. Gal-3 staining of periventricular astrocytes identified vesicle like formations on multiple processes and suggests secretion of Gal-3 into ECM. Secreted Gal-3 from infected cells may stimulate Gal-3 expression in neighbouring non-infected cells in a paracrine fashion, although such a mechanism has not yet been reported for Gal-3. It is more probable that an inflammatory mediator secreted by virally-infected CNS cells or infiltrating immune cells stimulates Gal-3 expression.

A group previously demonstrated that IFNγ could stimulate Gal-3 secretion from rat primary microglia, primary cortical astrocytes and B35 rat glioma cells cultures measured by western blot (Jeon et al., 2010). In contrast, my data shows that stimulation of floating neurospheres, composed of stem-cell like astrocytes and progenitor cells, with IFNγ did not stimulate Gal-3 secretion or increase the amount in the cell lysate, even at concentrations 100xfold higher than those used by Jeong and colleagues. These differences may be due to several reasons: cortical cells versus SVZ cells, different cell types, rat cells versus mouse cells or the influence of contaminating cells such as microglia. No microglia were shown to be present in the neurospheres by immunohistochemistry, consistent with previous reports (Welser and Milner, 2012). It is notoriously difficult to completely remove microglia from astrocyte cultures (Crocker et al., 2008; Hamby et al., 2006; Saura, 2007; Uliasz et al., 2012) and Jeong and colleagues provide no data to demonstrate complete removal of microglia. This could influence the results as secreted Gal-3 levels were much higher from microglia than astrocytes in their experiments. Similar caution must be applied to the primary SVZ and astrocyte cultures used in this thesis. Immunohistochemistry demonstrated around 5% microglia remained and SVZ and cortical microglia may respond differently to TMEV infection. Of note, even in cortical regions with high numbers infiltrating T-cells, most likely secreting IFNγ, few Gal-3^{+} astrocytes were detected.

5.3.5 Regulation of inflammatory molecule expression by Galectin-3

Recent findings suggest that galectins have cytokine-like properties that could modulate inflammatory processes (Chen et al., 2006; Hsu et al., 2000). Treatment of cultured microglia and astrocytes with galectin-3 considerably increased expression of pro-

inflammatory cytokines in particular TNFα, CCL2 and CXCL10 but not anti-inflammatory mediators (Jeon et al., 2010). Gal-3 induced secretion of TNFα, CCL2, CCL3 and CCL5 in synovial fibroblasts (Filer et al., 2009). The chemokines previously reported to be increased by Gal-3 (CCL2, CCL5, CXCL10) are all highly expressed in both SVZ tissue and SVZ astrocyte primary cultures after TMEV infection. Deletion of Gal-3 reduced SVZ mRNA levels of these chemokines and other cytokines in B6 mice and decreased proteins levels in both B6 and SJL mice. Based on the findings reported in chapter 3 these dampened inflammatory responses may reflect reduced cytokine transcription in Gal-3 deficient astrocytes. Gal-3 may mediate these effects by enhancing the binding of nuclear factors (NFs) to the NF-κB binding site, as galectin-3–deficient astrocytes exhibited reduced NF-κB responses (Filer et al., 2009; Jeon et al., 2010). Lippert et al (Lippert et al., 2007) identified galectin 3 as a protein present in conditioned media from colonic epithelial cells that is responsible for lamina propria fibroblast IL-8 secretion and NF-κB activation. Direct TMEV infection of astrocytes can activate NF-κB within 5 minutes of infection and directly induce selective pro-inflammatory cytokines (Palma et al., 2003). Cytokine gene expression induced by TMEV can be completely abolished by inhibitors specific for the NF-κB pathway, indicating that this pathway is critical for the expression of all of these cytokine genes. If Gal-3 null mice have reduced NF-κB activity this could account for the reduced expression of chemokines. Further investigation would identify whether Gal-3 null mice exhibit reduced NF-κB activation in SVZ cells and if there are variations between the strains.

Gal-3 was consistently associated with basement membrane astrocytes that formed the meninges and surrounded perivascular cuffs of lymphocytes around blood vessels. These cuffs are a hallmark of MS and this breakdown in the blood brain barrier may be a

prerequisite for lesion formation (Tonra et al., 2001). Restricting mononuclear infiltrates to these perivascular cuffs may attenuate disease progression (McCandless et al., 2006). Pro-inflammatory cytokines such as IL-1β, TNF and IL-17 can induce chemokine sets that recruit leukocytes into vascular cuffs of EAE and MS lesions. If Gal-3 functions in a similar manner to these cytokines to initiate chemokine transcription it could be a novel therapeutic target to regulate vascular cuffing.

A function for Gal-3 in regulation of chemokine expression in astrocytes could also help to explain the constitutive expression of the protein in healthy SVZ. Several chemokines are expressed in the SVZ and influence the proliferation, migration and differentiation of SVZ niche cells (Gordon et al., 2012). Galectin-3 expression by astrocytes may serve to regulate the transcription of these chemokines. Whether gal-3 functions in an autocrine or paracrine manner or a combination of both requires further verification.

5.3.6 Gal-3 may mediate differences in cytokine levels between strains

mRNA and protein levels of several cytokines and chemokines differ between the two strains in the SVZ. If Gal-3 regulates cytokine expression through its C-terminal carbohydrate binding actions then these differences may be explained by variations in glycosylation levels between different strains of mice. Examination of N-glycan branching differences and golgi enzyme activity reveals different strains of mice have different levels of N-glycan branches on glycoproteins, with lower levels in SJL mice than B6 (Lee et al., 2007). Glycoproteins display affinities for galectins in proportion to the number of N-glycans. The reduced number of N-glycans in SJL mice may mean that Gal-3 binds with less affinity to its ligands. Binding of Gal-3 to its ligand allows ligand cross-linking

through oligomerisation and the formation of galectin-lattices that can regulate the lateral movement and/or recycling of cell surface receptors (Nieminen et al., 2007). As most of its functions are thought to depend on oligomerisation, alterations in extracellular concentrations of Gal-3 may affect levels of certain receptors at the cell surface important in regulating the immune response.

5.3.7 Galectin-3 expression by phagocytosing microglia

By 14-21 dpi massive $CD3^+$ infiltration was apparent in the hippocampus. This was accompanied by activation of phagocytic microglia/macrophages that could be seen engulfing $CD3^+$ cells. In TMEV, apoptosis is an important mechanism of elimination of autoreactive pathogenic lymphocytes to maintain homoeostasis which otherwise could leads to tissue destruction and to autoimmune disease. During the acute stages of TMEV infection around 20-30% of $CD3^+$ T-cells are undergoing apoptosis in the spinal cord (Oleszak et al., 2003). In resting macrophages Gal-3 was diffuse throughout the cytoplasm. During phagocytosis Gal-3 appeared to be expressed in the phagocytic cups and associated with phagosomes, which are formed from the internalised cells. This accumulation of Gal-3 in macrophage phagosomes has been reported previously in bacterial infections (Beatty et al., 2002). Galectin-3–deficient macrophages also exhibit reduced phagocytosis of IgG opsonized erythrocytes (Sano et al., 2003). In EAE, Galactin-3/MAC-2 expression, as well as that of complement and Fc receptors, was up-regulated in demyelinating areas, and Gal-3^+ microglia and macrophages were found to be engaged in myelin phagocytosis (Reichert and Rotshenker, 1999). How Galectin-3 contributes to phagocytosis remains to be elucidated but it is known that Gal-3 does not participate in the rearrangement of the active cytoskeleton (Sano et al., 2003). As I have shown that Gal-3^+ phagocytosing macrophages

contain $CD3^+$ cell debris Gal-3 may play an important role in contributing to clearance of cytotoxic T-cells in TMEV. Study of the chronic stages of TMEV in Gal-3 deficient mice would show a lack of Gal-3 alters clearance of T-cells and whether this would have long term effects on disease progression.

5.3.8 Gal-3 expressed by subpopulation of immigrating T-cells

In SJL mice expression of Gal-3 in the cytoplasm of a subpopulation of $CD3^+$ T-cells was consistently seen across several brain regions and more cells expressed Gal-3 at 7 dpi than at 14 dpi. Gal-3 was not restricted to either $CD4^+$ or $CD8^+$ cell types. Expression of Gal-3 in T-cells has been linked to many different functions which could be related to TMEV pathogenesis. As discussed above apoptosis of T-cells is an important mechanism of T-cell clearance and galectin-3 is able to regulate apoptosis in activated T-cells . I have shown that around 50% of SJL T-cells express Gal-3 at 7 dpi. The numbers of T-cells expressing Gal-3 in my data are higher than reported levels of apoptotic $CD3^+$ cells in the spinal cord at similar time points (24% of cells) but this difference most likely relates to use of the DA strain of TMEV used by the authors (Oleszak et al., 2003). Levels of apoptosis in the early stages of BeAn infection have not yet been quantified. In susceptible strains of mice a lack of apoptosis in chronic disease leads to the accumulation of $CD3^+$ cells in the CNS that are responsible for demyelination (Oleszak et al., 2003). Initiation of T-cell apoptosis is typically thought to occur through extracellular stimulation by Gal-3. In contrast, intracellular expression of galectin-3, as seen in TMEV, can confer resistance to apoptosis through interactions with the apoptosis repressor Bcl-2 (Yang et al., 1996). Accumulated T-cells in the chronic stages show high levels of Bcl-2 (Oleszak et al., 2003). It is possible that if the intracellular expression of Gal-3 reported here continues through to chronic

disease stages it could provide protection from apoptosis and be related to T-cell accumulation. If this was true it would be expected that fewer T-cells would express Gal-3 in B6 mice. Given that Gal-3 levels are also higher in B6 mice it is possible that extracellular Gal-3 initiates apoptosis in B6 T-cells. High levels of Bcl-2 have also been found in T-cells infiltrating the CNS of patients with chronic progressive MS (Zettl et al., 1998). Galectin-3 expression has been reported in human T-cells (Demotte et al., 2010; Liu et al., 2009; Ocklenburg et al., 2006) and expression has been shown to correlate with apoptosis of tumour associated T-cells (Zubieta et al., 2006).

5.3.9 Reduced haematopoietic cell infiltration after Gal-3 deletion in B6 mice

Amoeboid $CD45^+$ cell infiltration into the SVZ, striatum septum and cortex was significantly reduced in Gal-3 deficient B6 mice at both 7 and 14 dpi. Based on my findings from chapter 2 these are most likely to be T-cells. Galectin-3 is not known to be chemoattractant to T-cells so the effect is unlikely to relate directly to the loss of Gal-3 (Sano et al., 2000). Deletion of Gal-3 significantly decreased SVZ protein levels of CCL2, CCL5, CXCL10 and CCL8. These chemokines are key for the immigration of peripheral $CD4^+$ and $CD8^+$ T-cells into the CNS after TMEV infection (Ransohoff et al., 2002) and decreased levels could account for reduced T-cell immigration. For example, anti-CCL2 treatment reduces numbers of CNS-infiltrating $CD4^+$ T-cells in TMEV (Karpus et al., 2006). As mentioned above the loss of Gal-3 from astrocytes surrounding perivascular cuffs may also be involved in the decreased number of infiltrating cells if it normally functions to facilitate haematopoietic cell entry into the CNS (Sato et al., 2002). In contrast, Gal-3 deletion from SJL mice only decreased T-cell infiltration at 3 dpi and 14

dpi. This supports the notion that Gal-3 plays an important role in the regulation of the immune response in resistant strains of mice.

5.3.10 The role of other Galectins

The differential profiles between the strains of T-cell infiltration and changes in chemokines levels may be related to the functions of other Galectins. There are several studies showing that Galectin-1 can have strong anti-inflammatory effects in viral disease (Poisa-Beiro et al., 2009). Treatment of herpes simplex virus infected mice with recombinant Gal-1 decreased numbers of infiltrating IFNγ producing $CD4^+$ T cells in the cornea and disease severity was much greater in Gal-1 null mice (Rajasagi et al., 2012). *In vitro* exposure to Galectin-1 inhibited the proliferation and expression of IFNγ in Epstein-Barr virus specific T-cells (Gandhi et al., 2007). Similar to Gal-3, Gal-1 is also made and secreted in mouse astrocytic cell lines (Yin et al., 2012a) and expression by SVZ astrocytes has been previously reported (Ishibashi et al., 2007; Sakaguchi et al., 2007; Sakaguchi et al., 2006). In stroke reactive astrocytes within and around the infarcted area express Gal-1 and stable delivery of human Gal-1from transplanted human NSPCs can reduce ischaemic volume (Yamane et al., 2011). This suggests Gal-1 expression in NPCs could regulate anti-inflammatory responses. TMEV may also induce the expression Gal-1 in SVZ astrocytes that, in Gal-3 null mice, is able to have an anti-inflammatory effect and decrease $CD45^+$ infiltration and dampen cytokine expression. For example, Gal-1 can target the activation of p38MAPK-, CREB and NF-kB-dependent signalling pathways and suppress downstream pro-inflammatory mediators (Starossom et al., 2012). If Gal-1 was expressed at higher levels in B6 mice than SJL, similar to the profile for Gal-3, this would produce the larger decreases in inflammation seen in the B6 mice. Gal-1 can also suppress

autoimmune disease by promoting a Th2 and Treg mediated anti-inflammatory response (Toscano et al., 2006). It has been proposed that deletion of Gal-3 promotes a Th2 response in inflammation (Bernardes et al., 2006; Saegusa et al., 2009; Zuberi et al., 2004) most likely through the functions of Gal-1. It would of particular importance to study T-cell polarisation in TMEV after Gal-3 deletion. Microglia activated by Th2 cytokines are able to bias SVZ cells to an oligodendrocyte fate (Butovsky et al., 2006b), suggesting regulation of T-cell polarisation by Gal-3 could prove useful in supporting cell renewal from adult stem cells.

5.3.11 Gal-3 effects on proliferation and cell death in neurospheres cultures.

Using the MTS assay to measure cell viability after TMEV infection I found an increase in absorbance at 72 hours post infection, which was unexpected as the LDH assay showed high levels of cell death. MTS is a tetrazolium salt that is reduced to purple formazan crystals mainly by mitochondrial succinate dehydrogenase (O'Toole et al., 2003). Theoretically, the colour intensity of the formazan dye produced correlates to the numbers of viable cells in the assay. However, metabolic activity may be changed by many different conditions, including pH and mitochondrial activity and it is hard to say what may be the cause of these increases (Plumb et al., 1989). The anti-apoptotic protein of TMEV contains a mitochondrial targeting signal that may interfere with mitochondrial function (Himeda et al., 2011; Sorgeloos et al., 2011; Stavrou et al., 2011) and enable the injured cells to reduce MTS and increase the production of formazan by the same numbers of cells.

Neurospheres derived from Gal-$3^{-/-}$ mice had lower levels of lactate dehydrogenase, a measure of cell lysis, compared to Gal-$3^{+/+}$ cell after TMEV infection.

This suggests that deletion of Gal-3 may have a protective effect upon neurospheres from TMEV induced apoptosis. Intracellular Gal-3 usually protects from apoptosis (Akahani et al., 1997; Matarrese et al., 2000b; Yang et al., 1996) so if it has the opposite in neurospheres this would be a very novel finding. More likely, is that deletion of Gal-3 reduced the secretion of cytokines from infected neurospheres cells that are cytotoxic in large doses.

5.3.12 SVZ proliferation preserved in Gal-3 null mice

As discussed in chapter 2 TMEV infection results in decreased proliferation of SVZ cells in both strains of mice. During TMEV infection the infiltrating T-cells are predominantly a Th1 phenotype and secrete pro-inflammatory cytokines such as IFNγ and TNFα. IFNγ has been shown to have detrimental effects on neurogenesis as progenitor cells from IFNγ$^{-/-}$ mice exhibit increased self-renewal ability (Li et al., 2010). The RT-PCR array data showed B6 Gal-3$^{-/-}$ mice had decreased mRNA levels of IFNγ and TNF compared to B6 Gal-3$^{+/+}$ mice and this may account for the improvements in neurogenesis. Also, Gal-1 can promote proliferation of SVZ cells (Ishibashi et al., 2007) and increased levels in Gal-3 null mice may increase neurogenesis.

5.3.13 Increased neuroblast migration in Gal-3 KO mice

Deletion of Gal-3 in the B6 mice greatly enhanced emigration of Dcx^{+} neuroblasts into the corpus callosum after TMEV. Neuroblasts migrating as single cells or in clusters of cells travelled sometimes hundreds of microns. In contrast, deletion of Gal-3 in healthy B6 Gal-3 KO mice did not alter neuroblast emigration. It is likely that increases in emigration are

not seen in control mice as it is modulated by an inflammatory mediator not normally present in healthy tissue. After TMEV Dcx^+ neuroblasts migrated to the boundary of the corpus callosum and cortex but I did not find any that had migrated into the cerebral cortex. This discrepancy suggests that the cerebral cortex produces a chemorepellant specific for SVZ neuroblasts (Sundholm-Peters et al., 2005).

Neuroblasts could also be seen migrating en masse in large numbers into the corpus callosum after Gal-3 deletion. A similar 'migratory-ridge' was described following TGFα infusion in rat, possibly related to increased EGFR mRNA levels (Fallon et al., 2000). EGF increases in a spatiotemporal pattern overlapping with SVZ cell emigration into the corpus callosum following a cortical injury model (Sundholm-Peters et al., 2005). EGF secreted by reactive corpus callosal astrocytes after TMEV infection may form a chemoattractant gradient for $EGFR^+$ neuroblasts in the SVZ. Our lab have previously shown that exposure to TGFα decreases the percentage of motile neuroblasts within the RMS by targeting a subpopulation of $EGFR^+$ neuroblasts (Kim et al., 2009). Reductions in migration speeds of neuroblasts through the RMS may give cells a greater capacity to respond to signals that stimulate emigration. Similar to $EGFR^+$ neuroblasts in 129sv mice a loss of Gal-3 decreased the speed and increased migration complexity accompanied by an increase in phosphorylated EGFR (Comte et al., 2011). Increased EGFR phosphorylation strongly increased the cell surface expression of EGFR (Merlin et al., 2011). Overexpression of EGFR has been shown to increase ectopic migration by conferring migratory properties to non-migratory postnatal neural progenitors (Aguirre et al., 2007; Aguirre et al., 2005; Gonzalez-Perez et al., 2009). I propose that a lack of Gal-3 may increase EGFR expression on neural progenitors and enhance migratory responses to secreted EGF from sites of injury. Further study is needed to confirm this proposed mechanism.

Another possibility is that increased levels of chemokines within the SVZ after TMEV infection may produce such a strong chemoattractant gradient that neuroblasts are unable to exit the SVZ into surrounding parenchymal regions. Decreased chemokine expression after Gal-3 deletion may allow neuroblasts to overcome this restraint and emigrate out of the SVZ. Similarly, secreted Gal-3 is chemoattractant to other cell types (Nangia-Makker et al., 2000; Sano et al., 2000). By *in vivo* and *in vitro* studies it was shown that higher concentrations of galectin-3 (1 μM) are necessary for chemotactic effects, while lower concentrations (10–100 nM) induce increased non-directional cell movements (chemokinesis). Further experiments may elucidate if Gal-3 has a chemoattract effect on neural progenitors and if so whether high SVZ Gal-3 levels hamper ectopic neuroblast emigration and deletion overcomes this. Gal-3 may contribute to migration through its well documented negative modulation of cell adhesion to ECM proteins such as integrins and laminin (Lagana et al., 2006; Matarrese et al., 2000a). A loss of Gal-3 may allow interactions with the ECM more suited to emigration.

5.3.14 Conclusions

Recent studies have highlighted that glycosylation and galectins may have a role in the pathogenesis of multiple sclerosis. In the TMEV model of MS Galectin-3 has roles in the regulation of immune responses in the SVZ following viral infection. Deletion of Gal-3 allowed recovery of SVZ function that is normally lost after TMEV infection and, in the case of neuroblast emigration, greatly enhanced the number of ectopic neuroblasts in the corpus callosum. Expression of galectin-3 is different in resistant and susceptible strains and may be important in regulating mechanisms of viral clearance that prevent demyelination. This study has demonstrated that targeting of Gal-3 could be a novel

candidate for regulation of inflammation in neurogenic niches. There are still many questions that are unanswered which further work would help to clarify. How does Gal-3 deletion affect T-cell activation or polarisation in TMEV? What are the relative contributions of the other galectins present in the CNS? Does Gal-3 deletion alter resistance or susceptibility in mice in the longer term?

Chapter 6

Discussion

6.1 Overall view 224

6.2 Limitations 230

6.3 Future directions 233

For many years, research has focused on whether endogenous neural stem cells from the SVZ could be utilised for remyelination and neuronal replacement in MS. However, despite several studies in EAE our understanding of how inflammation in the SVZ may impact on SVZ niche homeostasis is poorly understood. The central focus of this thesis has been to try to understand how acute inflammation impacts upon the adult neural stem cell niche. Using the Theiler's murine encephalomyelitis viral model of Multiple Sclerosis the first detailed study of changes in SVZ homeostasis during high levels of inflammation was carried out. Infiltrating T-cells were seen to accumulate in the SVZ due to targeted infection of SVZ cells by the BeAn virus and high levels of chemokine expression. The high presence of immigrated immune cells in susceptible mice caused disruptions in neuroblast numbers and chain integrity and resulted in a long term decrease in proliferating SVZ cells. Viral clearance by resistant B6 mice and dissolution of T-cell immigration allowed a recovery in proliferation. It was demonstrated that differences between the strains may be due to different cytokine expression profiles. It was shown that deletion of Gal-3, which is highly up-regulated by astrocytes within the SVZ after TMEV infection, was able to dampen the inflammatory response and reduce haematopoietic-cell infiltration into the SVZ in B6 mice. Gal-3 deficiency in B6 mice caused a huge expansion in the emigration of neuroblasts into the corpus callosum and in both strains allowed a recovery in proliferation. Levels of Gal-3 expression are much higher in resistant compared to the susceptible SJL strains of mice Together these data show that the SVZ as a neural stem cell niche undergoes significant changes during TMEV pathogenesis and Gal-3 may regulate several inflammatory processes that are distinct between different mouse strains.

6.1 Overall view

6.1.1 Persistent viral infections in the SVZ

There is strong evidence for a viral etiology to MS and several candidates have been proposed, including EBV, herpes simplex virus 6 and the measles virus. The SVZ is vulnerable to viral attacks and the characteristic periventricular lesion development may relate to subependymal viral spread (Das and Basu, 2008; Feuer et al., 2005; Krathwohl and Kaiser, 2004; Liu et al., 2005). Viral infection of migrating progenitors via the RMS could also serve to spread the virus to the olfactory bulb and other cortical areas (Feuer et al., 2005). A growing body of literature indicates that MS relapses can be triggered by viral infections (D'Hooghe M et al., 2010). The resulting inflammation response during a viral infection may aggravate latent viral infections in the CNS and lead to development of new lesions. I have shown here that TMEV is present in NPCs in the SVZ during early chronic stages of the disease and another study has shown that TMEV infection can persist in subependymal regions for the entire duration of the disease (Kummerfeld et al., 2012) showing NPCs are capable of harbouring latent viruses for long periods of time. Models of persistent viral infection of HIV in NSPCs show that diminished viral production can be revived through stimulation by cytokines such as TNFα (Krathwohl and Kaiser, 2004; Rothenaigner et al., 2007). Treatment of MS patients with natalizumub can cause activation of JC virus from sites of latency in the brain and patients develop PML. Similar to TMEV, JC virus requires sialic acid to infect cells (Dugan et al., 2008) and infection has been reported in PSA-NCAM expressing human progenitor cells (Hou et al., 2006). If MS candidate viruses, such as EBV, can also infect human SVZ cells then NPCs could act as a reservoir for viral persistence. Reactivation of these viruses by cytokines during illness could produce further axonal loss and produce new periventricular lesions.

TMEV infection resulted in decreased proliferation of SVZ cells. Direct TMEV infection of neurosphere cultures prevented proliferation and at higher concentrations induced apoptosis. A characteristic feature of virus induced cytopathic effects on NSPCs is the arrest in proliferative ability of these cells (Das and Basu, 2011). Detrimental effects on neurogenesis are brought about through activated microglia and astrocytes via the release of pro-inflammatory mediators such as IL-1β, IL-6, IFNγ, and TNFα (Ben-Hur et al., 2003). The various chemokines released upon HIV-1 infection acting via their chemokine receptors on the NSPCs induce quiescence in these cells (Krathwohl and Kaiser, 2004). Binding of CXCL12 to its receptor CXCR4 promotes the survival and proliferation of NSPCs (Peng et al., 2004). Binding of HIV to CXCR4 triggered signalling events that antagonise those of CXCL12 and prevent proliferation. The BeAn virus was able to infect SVZ cells and induced up-regulation of many cytokines and chemokines at levels much higher than in the cortex. Differential distribution of cytokines has been reported after JEV infection, with the SVZ the most affected area (Das et al., 2011). Whilst CXCL12 has so far not been implicated in TMEV other chemokines may have a similar effect in decreasing proliferation.

6.1.2 Regulation of inflammation in TMEV

Chemokines that might recruit T-cells to the CNS after TMEV infection have been a focus of research for several years. Pro-inflammatory cytokines (TNFα and IL-6) are produced early in the brain after viral infections and stimulate transcription of a wide array of chemokines. Many chemokine receptors are up-regulated by $CD4^+$ and $CD8^+$ T-cells when they are activated and are important in their accumulation in the CNS. TMEV infection stimulated chemokine production in the SVZ, notably of CXCL10, CCL5 and CCL2, for which astrocytes may be the primary source suggested by similar chemokine patterns

expressed in TMEV infected SVZ primary astrocytes. In the SVZ TMEV most likely leads to the expression of chemoattractants through activation of TLR2 receptors, similar to in the cortex (So and Kim, 2009). Whilst most viruses result in distinct chemokine signature patterns, chemokines such as CXCL10 and CCL5 are often expressed independently of either cellular tropism or viral genetics, suggesting some responses to infection are shared between many viruses (Hosking and Lane, 2010). The patterns of chemokine expression I have reported here are very similar to previously reported patterns for EAE (CXCL10, CCL2, CXCL9, CXCL1 and CCL1). The use of similar inflammatory pathways for many pathologies could mean that novel therapeutic targets to regulate inflammation used in models such as TMEV may have a broader application.

One such novel candidate molecule as a regulator of inflammation within the SVZ is Galectin-3. In the healthy brain expression is largely restricted to the SVZ but after TMEV it is highly expressed by astrocytes in periventricular regions. Deletion of Gal-3 dampened the expression of many cytokines and chemokines in the SVZ in both strains of mice. Reduced levels of TLR2 in the SVZ after Gal-3 deletion may cause decreased levels of chemokine transcription. Gal-3 deficiency in resistant B6 mice caused reduced T-cell trafficking into the SVZ. The effect of Gal-3 deletion is similar to that reported for minocycline treatment after JEV infection which dramatically reduced peripheral immune infiltrates (Das et al., 2011). This effect was mediated through reduced production of inflammatory molecules, particularly CCL2, and maintenance of the BBB integrity. As Gal-3 is expressed by both T-cells and astrocytes it is difficult to know whether the loss of Gal-3 from either population alone or both is required for the decreased T-cell infiltration. The relative contribution of Gal-3 from CNS resident cells and infiltrating T-cells could be addressed by using irradiated bone marrow chimeras. Lethal irradiation of recipient mice destroys the bone marrow which can then be reconstituted through adoptive transfer of

bone marrow from a suitable donor. Gal-$3^{-/-}$ cells can be transferred in Gal-$3^{+/+}$ mice and vice versa. Similarly, migration of exogenously labelled T-cells with fluorescent dyes injected into infected mice could be tracked using *in vivo* imaging techniques such multiphoton microscopy (James et al., 2011).

6.2.3 Susceptibility in TMEV

To understand the underlying mechanisms of differential susceptibility I analysed cytokine and chemokine production in the SVZ of virus-infected resistant B6 and susceptible SJL mice. Messenger levels of several cytokines and chemokines with consistently higher in B6 mice than SJL mice. Analysis of levels of Gal-3 showed that B6 mice had significantly higher levels of Gal-3 than SJL in both the SVZ and the cortex. To investigate whether Gal-3 may be responsible for the differential expression of chemokines between the strains I measured the proteins levels of CCL2, CCL5, CCL8 and CXCL10 and found that Gal-$3^{-/-}$ mice on both backgrounds had lower levels. Studies on Gal-1 have shown that the genetic background of a mouse can influence how Gal-1 regulates neurogenesis. Deletion of Gal-1 from 129sv mice decreased DG neurogenesis (Kajitani et al., 2009) whilst deletion on a C57BL/6 background increased neurogenesis (Imaizumi et al., 2011). If Gal-3 regulates cytokine expression through the its C-terminal carbohydrate binding actions then these differences may be explained by variations in glycosylation levels between different strains of mice. Examination of N-glycan branching differences and golgi enzyme activity reveals different strains of mice have different levels of N-glycan branches on glycoproteins, with T-cells displaying lower levels in SJL mice than B6 (Lee et al., 2007). Regulated glycosylation of T-cells controls many processes including activation, differentiation and homing by creating ligands for galectins (Toscano et al., 2007). As

glycoproteins display affinities for galectins in proportion to the number of N-glycans the reduced number of N-glycans on SJL T-cells may mean that Gal-3 binds with less affinity to its ligands and is less able to regulate T-cell function.

These results strongly suggest that different levels of intrinsic susceptibility may relate to Gal-3 regulation of cytokine production, and T-cell activation ability by microglia and astrocytes that contributes to the levels of viral persistence and antiviral T-cell responses in the CNS. Differences in these responses are critical for the differential susceptibility to TMEV-induced demyelinating disease between SJL and B6 mice. Genome wide association studies have identified SNPs in Mgat5, a enzyme critical in regulating glycosylation and N-glycan branching, in patients with MS that are linked to disease progression and susceptibility (Brynedal et al., 2010; Esposito et al., 2011). High expression levels of Galectin-3 in are also found in active MS lesions (Stancic et al., 2011). Together this role of Gal-3 in MS immunopathogenesis warrants further investigation.

The increases in proliferation and emigration seen after Gal-3 deletion imply Gal-3 could be a novel therapeutic target to regulate endogenous cell replacement. Selective inhibitors of Gal-3 are available and currently undergoing clinical testing (Cumpstey et al., 2005; Salameh et al., 2010). One current MS treatment may partially work by modulating Gal-3 expression (Reichert and Rotshenker, 1999). However, galectin-3 has been shown to be anti-inflammatory in several disease models. A large part of this beneficial role can be attributed to the role Gal-3 plays in activation and phagocytosis by microglia. Selective ablation of microglia expressing Gal-3 after an ischemic injury resulted in a larger infarct volume, increased apoptosis and worsened recovery (Lalancette-Hebert et al., 2007). Similarly, ischemic lesions are larger in Gal-$3^{-/-}$ mice due to defective microglial activation/proliferation (Lalancette-Hebert et al., 2012). A greater understanding of the

role of this protein in inflammation is required before it can be considered for therapeutic targeting.

6.2 Limitations

The main target in cell replacement therapies for MS has been looking at mechanisms of remyelination. One reason that TMEV may not be the model of choice for studying the role of endogenous stem cells for remyelination is that no alterations in myelin integrity in the forebrain grey and white matter including the corpus callosum have been detected in either SJL or C57BL/6 mice (Kummerfeld et al., 2012). In TMEV, demyelination largely occurs in the spinal cord in the chronic stages of the disease (Drescher and Tracy, 2007). However, besides myelin loss, axonal damage has attracted attention in demyelinating disease because it is supposed to account for permanent functional deficits in MS patients. Whilst TMEV may not be a suitable model to study the role of SVZ in remyelination I have shown here that ectopic emigration of neurons is seen after TMEV infection and this can be greatly enhanced by deletion of Gal-3. This suggests that TMEV could be an excellent tool to study mechanisms of neuronal loss and replacement in inflammatory lesions. In this thesis study of changes in neuroblast emigration after Gal-3 deletion was only performed up to 14 dpi. Therefore, the eventual fate of the large numbers of emigrated neuroblasts is unknown. Further study would need to examine if these cells survive, differentiate and integrate as functioning neurons. As Dcx^+ cells are vulnerable to BeAn infection it cannot be ruled out that infection of emigrating cells has a detrimental impact on their long term survival.

Gal-3 is a highly promiscuous molecule (Kim et al., 2007) that can have different functions depending on its localisation and the surrounding environment with which it

interacts. In the SVZ Gal-3 is found in extracellular, cytoplasmic and nuclear compartments and this, combined with its ability to be monomeric or form oligomers depending on its concentration, makes it extremely difficult to identify how Gal-3 mediates its immunoregulatory properties. This is particularly true after TMEV infection as astrocytes, microglia and T-cells all express Gal-3 and it is impossible to say how Gal-3 deletion in each cell type contributes to the alterations seen in the inflammatory response. Further studies using acute gain- and loss- of function strategies such as over-expression vectors, siRNA and infusion of Gal-3 recombinant protein or functional blocking antibodies may help to further elucidate Gal-3 function.

Whilst the data in this thesis has demonstrated Gal-3 deficiency dampens inflammatory responses in the SVZ, and this is accompanied by increases in proliferation and emigration, a direct causal link between the two has not been proven. In the healthy brain Gal-3 deletion had little effect upon the SVZ supporting the notion that factors directly relating to the inflammation mediated these changes. However, the neural stem cell niche can be influenced by many factors including disruption of the glial tube migratory scaffold, blood-borne molecules, disturbances in normal CSF flow and changes in the vasculature (Ihrie and Alvarez-Buylla, 2011), any of which Gal-3 deletion may alter. For instance, Gal-3 has been shown to result in failure to mount an angiogenic response following stroke through modulation of vascular endothelial growth factor expression (VEGF) (Markowska et al., 2011) (unpublished data from Szele lab). Gal-3 is ubiquitously expressed throughout many different organs and is important in the regulation of inflammatory processes in immune organs such as the spleen, lymph tissue and liver (Breuilh et al., 2007; Dragomir et al., 2012; Oliveira et al., 2011). For example, Gal-3 expression in dendritic cells in the spleen is pivotal to control the magnitude of T-cell priming (Breuilh et al., 2007), an important prerequisite for T-cell infiltration into the

CNS. Gal-3 deletion can reduce levels of hepatic derived chemokines (Dragomir et al., 2012) and these chemokines may normally serve to amplify the CNS response to injury (Campbell et al., 2005). It may be possible to refine the expression of Gal-3 to specific cells within the CNS through conditional gene deletions by a promoter-specific tamoxifen inducible Cre system. Deletion of Gal-3 can be temporally controlled and targeted to neural progenitors using a nestin promoter (Burns et al., 2007) or in astrocytes with a GFAP promoter (Hirrlinger et al., 2006).

The use of conditional knock-out mice would also overcome problems of redundancy with the Gal-3 KO mice. In the mice used in this thesis Gal-3 is absent from the point of conception and it is possible that the development of redundant pathways by other galectins might have disguised processes normally regulated by Gal-3. The Allen Brain Atlas identifies Gal-8 and Gal-9 as present constitutively in the SVZ. Expression of Gal-1 by SVZ astrocytes promotes cell proliferation through interactions with β1-integrin (Sakaguchi et al., 2010). Peptidomic analysis of mouse astrocyte cell lines show that Gal-1 is both produced and secreted by astrocytes (Yin et al., 2012b). Gal-1 and Gal-3 exhibit functional redundancy as nuclear pre-mRNA splicers and either alone is sufficient to reconstitute the activity of the other (Vyakarnam et al., 1997; Vyakarnam et al., 1998). Gal-1 and Gal-9 have redundant roles in promoting plasma cell formation (Tsai et al., 2011).

Gal-1 and Gal-9 have been implicated in many similar biological processes as Gal-3, such as cell proliferation, cell adhesion and inflammation, with shared molecular partners. Following ischemic stroke Gal-1 is expressed by reactive and SVZ astrocytes and promotes functional recovery (Ishibashi et al., 2007). In a study looking at Galectin expression in MS lesions, along with Gal-3, both Galectin-1 and Galectin-9 were highly

expressed (Stancic et al., 2011). Gal-1 treatment significantly inhibited disease progression of EAE in C57BL/6 mice (Wang et al., 2009) and Gal-1-deficient mice showed enhanced susceptibility to EAE (Toscano et al., 2007). In EAE Gal-1 works to temper microglial activation and deletion of Gal-1 during the acute phase of EAE resulted in pronounced inflammation-induced neurodegeneration (Starossom et al., 2012). Generally, Gal-1 is considered to have anti-inflammatory effects and bias T-cells towards a Th2 phenotype as levels of TNFα and IFNγ are markedly reduced when T-cells are incubated with recombinant Gal-1 (Rabinovich et al., 1999). The presence of Gal-1 was shown to inhibit T-cell adhesion to intact ECM, laminin and fibronectin. In contrast to the anti-apoptoic activity of Gal-3, in T-cells Gal-1 is pro-apoptotic and has an inhibitory role on T-cell proliferation and survival. Further work is needed to identity the presence and proportions of specific galectins after TMEV and if they are responsible for the anti-inflammatory effects seen after Gal-3 deletion.

6.3 Future directions

This thesis has focused on the acute encephalomyelitis induced by TMEV and its effects on the SVZ. A big question remains as to what are the long term effects of Gal-3 deletion on TMEV pathogenesis. Resistant B6 mice do not develop the chronic demyelinating disease seen in SJL mice as they mount an efficient and targeted $CD8^+$ and $CD4^+$ T-cell response that clears the virus (Karls et al., 2002; Tsunoda et al., 2002). Viral persistence is a prerequisite to drive proinflammatory cytokine expression and lead to the chronic demyelinating disease (Trottier et al., 2004). A lack of Gal-3 suppresses this T-cell response in B6 mice, while it preserves some SVZ function, may impact on viral clearance. T-cell entry into the CNS can have beneficial effects. Following West Nile

Virus (WNV) infection of the CNS, CXCL12 retains antigen-sensitized lymphocytes within the perivascular space. Antagonism of CXCR4, the receptor for CXCL12, enhances T lymphocyte entry into the CNS parenchyma, and this correlates with reduced WNV burden, enhanced survival, and limited neuropathology (McCandless et al., 2006; McCandless et al., 2008). CXCL10, which is prominently expressed within the SVZ after TMEV and greatly decreased after Gal-3 deletion functions to attract activated T lymphocytes bearing the receptor CXCR3. Neutralization or genetic silencing of CXCL10 following infection with HSV, JHMV, and WNV dramatically reduces T-cell trafficking into the CNS, thus preventing efficient viral control resulting in poor resolution (Klein et al., 2005; Liu et al., 2000; Wuest and Carr, 2008). Measurement of levels of viral titres and active replication through RT-PCR and viral plaque assays in B6 and SJL mice following Gal-3 deletion would be beneficial. If viral titres are altered after Gal-3 deletion measurements of demyelination in the spinal cord and cerebellum and clinical deficit scores would identify if Gal-3 deletion renders B6 mice ‘susceptible’ or SJL mice ‘susceptible’.

Stressful life events have been associated with the onset and/or exacerbation of multiple sclerosis (MS). Studies have indicated that restraint stress (RS) and social stress reduces inflammation and virus-induced chemokine expression in TMEV (Johnson et al., 2006; Mi et al., 2006a; Mi et al., 2006b). This facilitated the acute viral infection, and even induced dissemination of the virus to other organs such as the heart and the subsequent demyelination phase of the disease was exacerbated (Sieve et al., 2004). These results indicated an immunosuppressive effect of stress during early TMEV infection causing impaired viral clearance, which may be a potential exacerbating factor for later demyelination. Interestingly, immobilisation stress in mice reduces tissue levels of Gal-3 by as much as 50% (Dumic et al., 2000a). Given the similarities between Gal-3 deletion

and stress induced changes it would be interesting to investigate whether Gal-3 plays a role in the immunosuppressive effect of stress on TMEV.

It has been recently shown that systemic injection of both aNCPs and mesenchymal stem cells (MSCs) can have therapeutic effects on EAE in rodent and primates. Neural stem cells represent an endogenous source of cells for brain repair that circumvents immune rejection (Goldman et al., 2006). Pluchino et al (Pluchino et al., 2003) found that SVZ derived NSCs injected into mice with EAE induced by MOG35-55 inoculation, were found in close proximity to lesion sites, many expressing markers for oligodendrocyte differentiation. In general, transplanted MSCs and aNSCs reveal little evidence of remyelinating capacity but rather improved clinical outcome appears to result from bystander immunomodulatory and neuroprotective effects exerted by NSCs in response to signals from the surrounding microenvironment, which collectively dampen inflammation, inhibit glial scar formation and enhance neurogenesis (Einstein et al., 2003). SVZ derived NSCs are able to engage in dialogue with immune cells (Martino and Pluchino, 2007) and show a greater capacity to suppress T-cell proliferation and reduce pro-inflammatory cytokine production than MSC or embryonic derived cells (Payne et al., 2012). Experiments have found that Galectins seem to be crucial for immunomodulation by MSCs. Galectins-1, and Gal-3 are secreted and displayed on cell surface of MSC when in co-culture with T-cells (Najar et al., 2010; Sioud et al., 2011). Inhibition of Gal-3 and Gal-1 gene expression together in MSCs abrogated their immunosuppressive capacity (Sioud et al., 2011) but Gal-3 KO alone using siRNA reduced their inhibitory effects on T-cell proliferation but did not eliminate their immunosuppressive capacity (Sioud et al., 2010). Given the high levels of expression of Gal-3 by SVZ cells both *in vivo* and *in vitro* the potential role of Gal-3 in mediating the immunosuppressive effects of transplanted NSC will be a worthy topic for further research.

REFERENCES

Abu-Amer, Y., and Z. Bar-Shavit. 1994. Modulation of vitamin D increased H2O2 production and MAC-2 expression in the bone marrow-derived macrophages by estrogen. *Calcified tissue international* 55:29-32.

Aguirre, A., J.L. Dupree, J.M. Mangin, and V. Gallo. 2007. A functional role for EGFR signaling in myelination and remyelination. *Nature neuroscience* 10:990-1002.

Aguirre, A., and V. Gallo. 2007. Reduced EGFR signaling in progenitor cells of the adult subventricular zone attenuates oligodendrogenesis after demyelination. *Neuron glia biology* 3:209-220.

Aguirre, A., T.A. Rizvi, N. Ratner, and V. Gallo. 2005. Overexpression of the epidermal growth factor receptor confers migratory properties to nonmigratory postnatal neural progenitors. *The Journal of neuroscience : the official journal of the Society for Neuroscience* 25:11092-11106.

Aharoni, R., R. Arnon, and R. Eilam. 2005a. Neurogenesis and neuroprotection induced by peripheral immunomodulatory treatment of experimental autoimmune encephalomyelitis. *The Journal of neuroscience : the official journal of the Society for Neuroscience* 25:8217-8228.

Aharoni, R., R. Eilam, H. Domev, G. Labunskay, M. Sela, and R. Arnon. 2005b. The immunomodulator glatiramer acetate augments the expression of neurotrophic factors in brains of experimental autoimmune encephalomyelitis mice. *Proceedings of the National Academy of Sciences of the United States of America* 102:19045-19050.

Aharoni, R., A. Herschkovitz, R. Eilam, M. Blumberg-Hazan, M. Sela, W. Bruck, and R. Arnon. 2008. Demyelination arrest and remyelination induced by glatiramer acetate treatment of experimental autoimmune encephalomyelitis. *Proceedings of the National Academy of Sciences of the United States of America* 105:11358-11363.

Ahmed, H., S.J. Du, N. O'Leary, and G.R. Vasta. 2004. Biochemical and molecular characterization of galectins from zebrafish (Danio rerio): notochord-specific expression of a prototype galectin during early embryogenesis. *Glycobiology* 14:219-232.

Akahani, S., P. Nangia-Makker, H. Inohara, H.R. Kim, and A. Raz. 1997. Galectin-3: a novel antiapoptotic molecule with a functional BH1 (NWGR) domain of Bcl-2 family. *Cancer research* 57:5272-5276.

Alley, J., S. Khasabov, D. Simone, A. Beitz, M. Rodriguez, and M.K. Njenga. 2003. More severe neurologic deficits in SJL/J male than female mice following Theiler's virus-induced CNS demyelination. *Experimental neurology* 180:14-24.

Almkvist, J., and A. Karlsson. 2004. Galectins as inflammatory mediators. *Glycoconjugate journal* 19:575-581.

Alonso, A., and M.A. Hernan. 2008. Temporal trends in the incidence of multiple sclerosis: a systematic review. *Neurology* 71:129-135.

Alvarez-Buylla, A., M. Kohwi, T.M. Nguyen, and F.T. Merkle. 2008. The heterogeneity of adult neural stem cells and the emerging complexity of their niche. *Cold Spring Harbor symposia on quantitative biology* 73:357-365.

Angata, K., and M. Fukuda. 2003. Polysialyltransferases: major players in polysialic acid synthesis on the neural cell adhesion molecule. *Biochimie* 85:195-206.

Aravalli, R.N., S. Hu, T.N. Rowen, J.M. Palmquist, and J.R. Lokensgard. 2005. Cutting edge: TLR2-mediated proinflammatory cytokine and chemokine production by microglial cells in response to herpes simplex virus. *Journal of immunology* 175:4189-4193.

Arnon, R., and R. Aharoni. 2004. Mechanism of action of glatiramer acetate in multiple sclerosis and its potential for the development of new applications. *Proceedings of the National Academy of Sciences of the United States of America* 101 Suppl 2:14593-14598.

Ascherio, A., K.L. Munger, E.T. Lennette, D. Spiegelman, M.A. Hernan, M.J. Olek, S.E. Hankinson, and D.J. Hunter. 2001. Epstein-Barr virus antibodies and risk of multiple sclerosis: a prospective study. *JAMA : the journal of the American Medical Association* 286:3083-3088.

Ashton-Chess, J., S. Brouard, and J.P. Soulillou. 2006. Is clinical tolerance realistic in the next decade? *Transplant international : official journal of the European Society for Organ Transplantation* 19:539-548.

Banisadr, G., T.J. Frederick, C. Freitag, D. Ren, H. Jung, S.D. Miller, and R.J. Miller. 2011. The role of CXCR4 signaling in the migration of transplanted oligodendrocyte progenitors into the cerebral white matter. *Neurobiology of disease* 44:19-27.

Barker, R.A., and H. Widner. 2004. Immune problems in central nervous system cell therapy. *NeuroRx : the journal of the American Society for Experimental NeuroTherapeutics* 1:472-481.

Barnett, M.H., and J.W. Prineas. 2004. Relapsing and remitting multiple sclerosis: pathology of the newly forming lesion. *Annals of neurology* 55:458-468.

Barondes, S.H., V. Castronovo, D.N. Cooper, R.D. Cummings, K. Drickamer, T. Feizi, M.A. Gitt, J. Hirabayashi, C. Hughes, K. Kasai, and et al. 1994. Galectins: a family of animal beta-galactoside-binding lectins. *Cell* 76:597-598.

Beatty, W.L., E.R. Rhoades, D.K. Hsu, F.T. Liu, and D.G. Russell. 2002. Association of a macrophage galactoside-binding protein with Mycobacterium-containing phagosomes. *Cellular microbiology* 4:167-176.

Beckervordersandforth, R., P. Tripathi, J. Ninkovic, E. Bayam, A. Lepier, B. Stempfhuber, F. Kirchhoff, J. Hirrlinger, A. Haslinger, D.C. Lie, J. Beckers, B. Yoder, M. Irmler, and M. Gotz. 2010. In vivo fate mapping and expression analysis reveals molecular hallmarks of prospectively isolated adult neural stem cells. *Cell stem cell* 7:744-758.

Bellizzi, A., C. Nardis, E. Anzivino, D. Rodio, D. Fioriti, M. Mischitelli, F. Chiarini, and V. Pietropaolo. 2012. Human polyomavirus JC reactivation and pathogenetic mechanisms of progressive multifocal leukoencephalopathy and cancer in the era of monoclonal antibody therapies. *Journal of neurovirology* 18:1-11.

Belmadani, A., P.B. Tran, D. Ren, and R.J. Miller. 2006. Chemokines regulate the migration of neural progenitors to sites of neuroinflammation. *The Journal of neuroscience : the official journal of the Society for Neuroscience* 26:3182-3191.

Ben-Hur, T., O. Ben-Menachem, V. Furer, O. Einstein, R. Mizrachi-Kol, and N. Grigoriadis. 2003. Effects of proinflammatory cytokines on the growth, fate, and motility of multipotential neural precursor cells. *Molecular and cellular neurosciences* 24:623-631.

Benvenuto, G., M.L. Carpentieri, P. Salvatore, L. Cindolo, C.B. Bruni, and L. Chiariotti. 1996. Cell-specific transcriptional regulation and reactivation of galectin-1 gene expression are controlled by DNA methylation of the promoter region. *Molecular and cellular biology* 16:2736-2743.

Bernardes, E.S., N.M. Silva, L.P. Ruas, J.R. Mineo, A.M. Loyola, D.K. Hsu, F.T. Liu, R. Chammas, and M.C. Roque-Barreira. 2006. Toxoplasma gondii infection reveals a novel regulatory role for galectin-3 in the interface of innate and adaptive immunity. *The American journal of pathology* 168:1910-1920.

Billiau, A. 1977. Effect of interferon on RNA tumor viruses. *Texas reports on biology and medicine* 35:406-419.

Bitsch, A., T. Kuhlmann, C. Da Costa, S. Bunkowski, T. Polak, and W. Bruck. 2000. Tumour necrosis factor alpha mRNA expression in early multiple sclerosis lesions: correlation with demyelinating activity and oligodendrocyte pathology. *Glia* 29:366-375.

Bjartmar, C., R.P. Kinkel, G. Kidd, R.A. Rudick, and B.D. Trapp. 2001. Axonal loss in normal-appearing white matter in a patient with acute MS. *Neurology* 57:1248-1252.

Bjartmar, C., and B.D. Trapp. 2003. Axonal degeneration and progressive neurologic disability in multiple sclerosis. *Neurotoxicity research* 5:157-164.

Bjartmar, C., J.R. Wujek, and B.D. Trapp. 2003. Axonal loss in the pathology of MS: consequences for understanding the progressive phase of the disease. *Journal of the neurological sciences* 206:165-171.

Blakemore, W.F., and R.J. Franklin. 2000. Transplantation options for therapeutic central nervous system remyelination. *Cell transplantation* 9:289-294.

Blakemore, W.F., P.M. Smith, and R.J. Franklin. 2000. Remyelinating the demyelinated CNS. *Novartis Foundation symposium* 231:289-298; discussion 298-306.

Bo, L., J.J. Geurts, S.J. Mork, and P. van der Valk. 2006. Grey matter pathology in multiple sclerosis. *Acta neurologica Scandinavica. Supplementum* 183:48-50.

Boos, L., I.L. Campbell, R. Ames, R.A. Wetsel, and S.R. Barnum. 2004. Deletion of the complement anaphylatoxin C3a receptor attenuates, whereas ectopic expression of C3a in the brain exacerbates, experimental autoimmune encephalomyelitis. *Journal of immunology* 173:4708-4714.

Borson, N.D., C. Paul, X. Lin, W.K. Nevala, M.A. Strausbauch, M. Rodriguez, and P.J. Wettstein. 1997. Brain-infiltrating cytolytic T lymphocytes specific for Theiler's virus recognize H2Db molecules complexed with a viral VP2 peptide lacking a consensus anchor residue. *Journal of virology* 71:5244-5250.

Boscher, C., J.W. Dennis, and I.R. Nabi. 2011. Glycosylation, galectins and cellular signaling. *Current opinion in cell biology* 23:383-392.

Brahic, M., J.F. Bureau, and T. Michiels. 2005. The genetics of the persistent infection and demyelinating disease caused by Theiler's virus. *Annual review of microbiology* 59:279-298.

Brand, C., F.L. Oliveira, C.M. Takiya, A. Palumbo, Jr., D.K. Hsu, F.T. Liu, R. Borojevic, R. Chammas, and M.C. El-Cheikh. 2012. The involvement of the spleen during chronic phase of Schistosoma mansoni infection in galectin-3-/- mice. *Histology and histopathology* 27:1109-1120.

Brazel, C.Y., J.L. Nunez, Z. Yang, and S.W. Levison. 2005. Glutamate enhances survival and proliferation of neural progenitors derived from the subventricular zone. *Neuroscience* 131:55-65.

Breuilh, L., F. Vanhoutte, J. Fontaine, C.M. van Stijn, I. Tillie-Leblond, M. Capron, C. Faveeuw, T. Jouault, I. van Die, P. Gosset, and F. Trottein. 2007. Galectin-3 modulates immune and inflammatory responses during helminthic infection: impact of galectin-3 deficiency on the functions of dendritic cells. *Infection and immunity* 75:5148-5157.

Brill, M.S., J. Ninkovic, E. Winpenny, R.D. Hodge, I. Ozen, R. Yang, A. Lepier, S. Gascon, F. Erdelyi, G. Szabo, C. Parras, F. Guillemot, M. Frotscher, B. Berninger, R.F. Hevner, O. Raineteau, and M. Gotz. 2009. Adult generation of glutamatergic olfactory bulb interneurons. *Nature neuroscience* 12:1524-1533.

Brock, O., M. Keller, A. Veyrac, Q. Douhard, and J. Bakker. 2010. Short term treatment with estradiol decreases the rate of newly generated cells in the subventricular zone and main olfactory bulb of adult female mice. *Neuroscience* 166:368-376.

Bruck, W. 2005. Inflammatory demyelination is not central to the pathogenesis of multiple sclerosis. *Journal of neurology* 252 Suppl 5:v10-15.

Brynedal, B., J. Wojcik, F. Esposito, V. Debailleul, J. Yaouanq, F. Martinelli-Boneschi, G. Edan, G. Comi, J. Hillert, and H. Abderrahim. 2010. MGAT5 alters the severity of multiple sclerosis. *Journal of neuroimmunology* 220:120-124.

Burns, K.A., A.E. Ayoub, J.J. Breunig, F. Adhami, W.L. Weng, M.C. Colbert, P. Rakic, and C.Y. Kuan. 2007. Nestin-CreER mice reveal DNA synthesis by nonapoptotic neurons following cerebral ischemia hypoxia. *Cerebral cortex* 17:2585-2592.

Butovsky, O., G. Landa, G. Kunis, Y. Ziv, H. Avidan, N. Greenberg, A. Schwartz, I. Smirnov, A. Pollack, S. Jung, and M. Schwartz. 2006a. Induction and blockage of oligodendrogenesis by differently activated microglia in an animal model of multiple sclerosis. *The Journal of clinical investigation* 116:905-915.

Butovsky, O., Y. Ziv, A. Schwartz, G. Landa, A.E. Talpalar, S. Pluchino, G. Martino, and M. Schwartz. 2006b. Microglia activated by IL-4 or IFN-gamma differentially induce neurogenesis and oligodendrogenesis from adult stem/progenitor cells. *Molecular and cellular neurosciences* 31:149-160.

Campbell, S.J., V.H. Perry, F.J. Pitossi, A.G. Butchart, M. Chertoff, S. Waters, R. Dempster, and D.C. Anthony. 2005. Central nervous system injury triggers hepatic CC and CXC chemokine expression that is associated with leukocyte mobilization and recruitment to both the central nervous system and the liver. *The American journal of pathology* 166:1487-1497.

Carlson, N.G., M.A. Rojas, J.W. Redd, P. Tang, B. Wood, K.E. Hill, and J.W. Rose. 2010. Cyclooxygenase-2 expression in oligodendrocytes increases sensitivity to excitotoxic death. *Journal of neuroinflammation* 7:25.

Carpentier, P.A., M.T. Getts, and S.D. Miller. 2008. Pro-inflammatory functions of astrocytes correlate with viral clearance and strain-dependent protection from TMEV-induced demyelinating disease. *Virology* 375:24-36.

Carpentier, P.A., B.R. Williams, and S.D. Miller. 2007. Distinct roles of protein kinase R and toll-like receptor 3 in the activation of astrocytes by viral stimuli. *Glia* 55:239-252.

Cate, H.S., J.K. Sabo, D. Merlo, D. Kemper, T.D. Aumann, J. Robinson, T.D. Merson, B. Emery, V.M. Perreau, and T.J. Kilpatrick. 2010. Modulation of bone morphogenic protein signalling alters numbers of astrocytes and oligodendroglia in the subventricular zone during cuprizone-induced demyelination. *Journal of neurochemistry* 115:11-22.

Chang, A., M.C. Smith, X. Yin, R.J. Fox, S.M. Staugaitis, and B.D. Trapp. 2008. Neurogenesis in the chronic lesions of multiple sclerosis. *Brain : a journal of neurology* 131:2366-2375.

Chang, J.R., E. Zaczynska, C.D. Katsetos, C.D. Platsoucas, and E.L. Oleszak. 2000. Differential expression of TGF-beta, IL-2, and other cytokines in the CNS of Theiler's murine encephalomyelitis virus-infected susceptible and resistant strains of mice. *Virology* 278:346-360.

Chen, H.Y., B.B. Sharma, L. Yu, R. Zuberi, I.C. Weng, Y. Kawakami, T. Kawakami, D.K. Hsu, and F.T. Liu. 2006. Role of galectin-3 in mast cell functions: galectin-3-deficient mast cells exhibit impaired mediator release and defective JNK expression. *Journal of immunology* 177:4991-4997.

Chen, J.T., D.L. Collins, H.L. Atkins, M.S. Freedman, D.L. Arnold, and M.S.B.M.T.S.G. Canadian. 2008. Magnetization transfer ratio evolution with demyelination and remyelination in multiple sclerosis lesions. *Annals of neurology* 63:254-262.

Chen, L., Z. Li, M. Ping, R. Li, J. Liu, X. Xie, X. Song, and L. Guo. 2012. Regulation of Olig2 during astroglial differentiation in the subventricular zone of a cuprizone-induced demyelination mouse model. *Neuroscience*

Chittajallu, R., Y. Chen, H. Wang, X. Yuan, C.A. Ghiani, T. Heckman, C.J. McBain, and V. Gallo. 2002. Regulation of Kv1 subunit expression in oligodendrocyte progenitor cells and their role in G1/S phase progression of the cell cycle. *Proceedings of the National Academy of Sciences of the United States of America* 99:2350-2355.

Chiu, C.Y., A.L. Greninger, K. Kanada, T. Kwok, K.F. Fischer, C. Runckel, J.K. Louie, C.A. Glaser, S. Yagi, D.P. Schnurr, T.D. Haggerty, J. Parsonnet, D. Ganem, and J.L. DeRisi. 2008. Identification of cardioviruses related to Theiler's murine encephalomyelitis virus in human infections. *Proceedings of the National Academy of Sciences of the United States of America* 105:14124-14129.

Cohen, J.A., and J. Chun. 2011. Mechanisms of fingolimod's efficacy and adverse effects in multiple sclerosis. *Annals of neurology* 69:759-777.

Colnot, C., D. Fowlis, M.A. Ripoche, I. Bouchaert, and F. Poirier. 1998. Embryonic implantation in galectin 1/galectin 3 double mutant mice. *Developmental dynamics : an official publication of the American Association of Anatomists* 211:306-313.

Comte, I., Y. Kim, C.C. Young, J.M. van der Harg, P. Hockberger, P.J. Bolam, F. Poirier, and F.G. Szele. 2011. Galectin-3 maintains cell motility from the subventricular zone to the olfactory bulb. *Journal of cell science* 124:2438-2447.

Connick, P., M. Kolappan, C. Crawley, D.J. Webber, R. Patani, A.W. Michell, M.Q. Du, S.L. Luan, D.R. Altmann, A.J. Thompson, A. Compston, M.A. Scott, D.H. Miller, and S. Chandran. 2012. Autologous mesenchymal stem cells for the treatment of secondary progressive multiple sclerosis: an open-label phase 2a proof-of-concept study. *Lancet neurology* 11:150-156.

Conover, J.C., and R.Q. Notti. 2008. The neural stem cell niche. *Cell and tissue research* 331:211-224.

Cortegano, I., V. Pozo, B. Cardaba, I. Arrieta, S. Gallardo, M. Rojo, E. Aceituno, T. Takai, S. Verbeek, P. Palomino, F.T. Liu, and C. Lahoz. 2000. Interaction between galectin-3 and FcgammaRII induces down-regulation of IL-5 gene: implication of the promoter sequence IL-5REIII. *Glycobiology* 10:237-242.

Cowles, E.A., N. Agrwal, R.L. Anderson, and J.L. Wang. 1990. Carbohydrate-binding protein 35. Isoelectric points of the polypeptide and a phosphorylated derivative. *The Journal of biological chemistry* 265:17706-17712.

Cremer, H., G. Chazal, P.M. Lledo, G. Rougon, M.F. Montaron, W. Mayo, M. Le Moal, and D.N. Abrous. 2000. PSA-NCAM: an important regulator of hippocampal plasticity. *International journal of developmental neuroscience : the official journal of the International Society for Developmental Neuroscience* 18:213-220.

Crocker, P.R., and A. Varki. 2001. Siglecs, sialic acids and innate immunity. *Trends in immunology* 22:337-342.

Crocker, S.J., R.F. Frausto, J.L. Whitton, and R. Milner. 2008. A novel method to establish microglia-free astrocyte cultures: comparison of matrix metalloproteinase expression profiles in pure cultures of astrocytes and microglia. *Glia* 56:1187-1198.

Cumpstey, I., A. Sundin, H. Leffler, and U.J. Nilsson. 2005. C2-symmetrical thiodigalactoside bis-benzamido derivatives as high-affinity inhibitors of galectin-

3: efficient lectin inhibition through double arginine-arene interactions. *Angewandte Chemie* 44:5110-5112.

D'Aversa, T.G., E.A. Eugenin, L. Lopez, and J.W. Berman. 2012. Myelin Basic Protein Induces Inflammatory Mediators from Primary Human Endothelial Cells and Blood-Brain-Barrier Disruption: Implications for the Pathogenesis of Multiple Sclerosis. *Neuropathology and applied neurobiology*

D'Hooghe M, B., G. Nagels, V. Bissay, and J. De Keyser. 2010. Modifiable factors influencing relapses and disability in multiple sclerosis. *Multiple sclerosis* 16:773-785.

D'Intino, G., G. Perretta, A. Taglioni, M. Calistri, C. Falzone, M. Baroni, L. Giardino, and L. Calza. 2006. Endogenous stem and precursor cells for demyelinating diseases: an alternative for transplantation? *Neurological research* 28:513-517.

Dagher, S.F., J.L. Wang, and R.J. Patterson. 1995. Identification of galectin-3 as a factor in pre-mRNA splicing. *Proceedings of the National Academy of Sciences of the United States of America* 92:1213-1217.

Dal Canto, M.C., and H.L. Lipton. 1982. Ultrastructural immunohistochemical localization of virus in acute and chronic demyelinating Theiler's virus infection. *The American journal of pathology* 106:20-29.

Das, S., and A. Basu. 2008. Japanese encephalitis virus infects neural progenitor cells and decreases their proliferation. *Journal of neurochemistry* 106:1624-1636.

Das, S., and A. Basu. 2011. Viral infection and neural stem/progenitor cell's fate: implications in brain development and neurological disorders. *Neurochemistry international* 59:357-366.

Das, S., K. Dutta, K.L. Kumawat, A. Ghoshal, D. Adhya, and A. Basu. 2011. Abrogated inflammatory response promotes neurogenesis in a murine model of Japanese encephalitis. *PloS one* 6:e17225.

Das Sarma, J., L.C. Kenyon, S.T. Hingley, and K.S. Shindler. 2009. Mechanisms of primary axonal damage in a viral model of multiple sclerosis. *The Journal of neuroscience : the official journal of the Society for Neuroscience* 29:10272-10280.

De Giusti, C.J., L. Alberdi, J. Frik, M.F. Ferrer, E. Scharrig, M. Schattner, and R.M. Gomez. 2011. Galectin-3 is upregulated in activated glia during Junin virus-induced murine encephalitis. *Neuroscience letters* 501:163-166.

de Oliveira, J.T., A.J. de Matos, A.L. Santos, R. Pinto, J. Gomes, V. Hespanhol, R. Chammas, A. Manninen, E.S. Bernardes, C. Albuquerque Reis, G. Rutteman, and F. Gartner. 2011. Sialylation regulates galectin-3/ligand interplay during mammary tumour progression--a case of targeted uncloaking. *The International journal of developmental biology* 55:823-834.

Decker, L., N. Picard-Riera, F. Lachapelle, and A. Baron-Van Evercooren. 2002. Growth factor treatment promotes mobilization of young but not aged adult subventricular zone precursors in response to demyelination. *Journal of neuroscience research* 69:763-771.

DeLuca, G.C., G.C. Ebers, and M.M. Esiri. 2004. Axonal loss in multiple sclerosis: a pathological survey of the corticospinal and sensory tracts. *Brain : a journal of neurology* 127:1009-1018.

DeLuca, G.C., K. Williams, N. Evangelou, G.C. Ebers, and M.M. Esiri. 2006. The contribution of demyelination to axonal loss in multiple sclerosis. *Brain : a journal of neurology* 129:1507-1516.

Demarquay, G., P. Ryvlin, and J.P. Royet. 2007. [Olfaction and neurological diseases: a review of the literature]. *Revue neurologique* 163:155-167.

Demetriou, M., M. Granovsky, S. Quaggin, and J.W. Dennis. 2001. Negative regulation of T-cell activation and autoimmunity by Mgat5 N-glycosylation. *Nature* 409:733-739.

Demotte, N., G. Wieers, P. Van Der Smissen, M. Moser, C. Schmidt, K. Thielemans, J.L. Squifflet, B. Weynand, J. Carrasco, C. Lurquin, P.J. Courtoy, and P. van der Bruggen. 2010. A galectin-3 ligand corrects the impaired function of human CD4 and CD8 tumor-infiltrating lymphocytes and favors tumor rejection in mice. *Cancer research* 70:7476-7488.

Denic, A., A.J. Johnson, A.J. Bieber, A.E. Warrington, M. Rodriguez, and I. Pirko. 2011. The relevance of animal models in multiple sclerosis research. *Pathophysiology : the official journal of the International Society for Pathophysiology / ISP* 18:21-29.

Denis-Donini, S., A. Caprini, C. Frassoni, and M. Grilli. 2005. Members of the NF-kappaB family expressed in zones of active neurogenesis in the postnatal and adult mouse brain. *Brain research. Developmental brain research* 154:81-89.

Dethlefs, S., M. Brahic, and E.L. Larsson-Sciard. 1997. An early, abundant cytotoxic T-lymphocyte response against Theiler's virus is critical for preventing viral persistence. *Journal of virology* 71:8875-8878.

Diez-Revuelta, N., S. Velasco, S. Andre, H. Kaltner, D. Kubler, H.J. Gabius, and J. Abad-Rodriguez. 2010. Phosphorylation of adhesion- and growth-regulatory human galectin-3 leads to the induction of axonal branching by local membrane L1 and ERM redistribution. *Journal of cell science* 123:671-681.

Doetsch, F., and A. Alvarez-Buylla. 1996. Network of tangential pathways for neuronal migration in adult mammalian brain. *Proceedings of the National Academy of Sciences of the United States of America* 93:14895-14900.

Doetsch, F., I. Caille, D.A. Lim, J.M. Garcia-Verdugo, and A. Alvarez-Buylla. 1999. Subventricular zone astrocytes are neural stem cells in the adult mammalian brain. *Cell* 97:703-716.

Doetsch, F., J.M. Garcia-Verdugo, and A. Alvarez-Buylla. 1997. Cellular composition and three-dimensional organization of the subventricular germinal zone in the adult mammalian brain. *The Journal of neuroscience : the official journal of the Society for Neuroscience* 17:5046-5061.

Doetsch, F., L. Petreanu, I. Caille, J.M. Garcia-Verdugo, and A. Alvarez-Buylla. 2002. EGF converts transit-amplifying neurogenic precursors in the adult brain into multipotent stem cells. *Neuron* 36:1021-1034.

Doverhag, C., M. Hedtjarn, F. Poirier, C. Mallard, H. Hagberg, A. Karlsson, and K. Savman. 2010. Galectin-3 contributes to neonatal hypoxic-ischemic brain injury. *Neurobiology of disease* 38:36-46.

Dragomir, A.C., R. Sun, V. Mishin, L.B. Hall, J.D. Laskin, and D.L. Laskin. 2012. Role of galectin-3 in acetaminophen-induced hepatotoxicity and inflammatory mediator production. *Toxicological sciences : an official journal of the Society of Toxicology* 127:609-619.

Drescher, K.M., and S. Tracy. 2007. Establishment of a model to examine the early events involved in the development of virus-induced demyelinating lesions. *Annals of the New York Academy of Sciences* 1103:152-156.

Drescher, K.M., L.J. Zoecklein, K.D. Pavelko, C. Rivera-Quinones, D. Hollenbaugh, and M. Rodriguez. 2000. CD40L is critical for protection from demyelinating disease and development of spontaneous remyelination in a mouse model of multiple sclerosis. *Brain pathology* 10:1-15.

Dugan, A.S., M.L. Gasparovic, and W.J. Atwood. 2008. Direct correlation between sialic acid binding and infection of cells by two human polyomaviruses (JC virus and BK virus). *Journal of virology* 82:2560-2564.

Dumic, J., K. Barisic, M. Flogel, and G. Lauc. 2000a. Galectin-3 decreases in mice exposed to immobilization stress. *Stress* 3:241-246.

Dumic, J., S. Dabelic, and M. Flogel. 2006. Galectin-3: an open-ended story. *Biochimica et biophysica acta* 1760:616-635.

Dumic, J., G. Lauc, and M. Flogel. 2000b. Expression of galectin-3 in cells exposed to stress-roles of jun and NF-kappaB. *Cellular physiology and biochemistry : international journal of experimental cellular physiology, biochemistry, and pharmacology* 10:149-158.

Einstein, O., D. Karussis, N. Grigoriadis, R. Mizrachi-Kol, E. Reinhartz, O. Abramsky, and T. Ben-Hur. 2003. Intraventricular transplantation of neural precursor cell spheres attenuates acute experimental allergic encephalomyelitis. *Molecular and cellular neurosciences* 24:1074-1082.

Endo, K., and T. Tsukamoto. 1997. Experimental bystander encephalitis induced by immunization with HTLV-I-producing T cells in mice. *Acta neurologica Scandinavica* 96:106-113.

Esposito, F., J. Wojcik, M. Rodegher, M. Radaelli, L. Moiola, A. Ghezzi, R. Capra, P. Brambilla, M. Sorosina, G. Giacalone, V. Martinelli, G. Comi, H. Abderrahim, and F. Martinelli Boneschi. 2011. MGAT5 and disease severity in progressive multiple sclerosis. *Journal of neuroimmunology* 230:143-147.

Fallon, J., S. Reid, R. Kinyamu, I. Opole, R. Opole, J. Baratta, M. Korc, T.L. Endo, A. Duong, G. Nguyen, M. Karkehabadhi, D. Twardzik, S. Patel, and S. Loughlin. 2000. In vivo induction of massive proliferation, directed migration, and differentiation of neural cells in the adult mammalian brain. *Proceedings of the National Academy of Sciences of the United States of America* 97:14686-14691.

Fancy, S.P., C. Zhao, and R.J. Franklin. 2004. Increased expression of Nkx2.2 and Olig2 identifies reactive oligodendrocyte progenitor cells responding to demyelination in the adult CNS. *Molecular and cellular neurosciences* 27:247-254.

Fernandes Bertocchi, A.P., G. Campanhole, P.H. Wang, G.M. Goncalves, M.J. Damiao, M.A. Cenedeze, F.C. Beraldo, V. de Paula Antunes Teixeira, M.A. Dos Reis, M. Mazzali, A. Pacheco-Silva, and N.O. Camara. 2008. A Role for galectin-3 in renal tissue damage triggered by ischemia and reperfusion injury. *Transplant international : official journal of the European Society for Organ Transplantation* 21:999-1007.

Feuer, R., R.R. Pagarigan, S. Harkins, F. Liu, I.P. Hunziker, and J.L. Whitton. 2005. Coxsackievirus targets proliferating neuronal progenitor cells in the neonatal CNS. *The Journal of neuroscience : the official journal of the Society for Neuroscience* 25:2434-2444.

Fife, B.T., K.J. Kennedy, M.C. Paniagua, N.W. Lukacs, S.L. Kunkel, A.D. Luster, and W.J. Karpus. 2001. CXCL10 (IFN-gamma-inducible protein-10) control of encephalitogenic CD4+ T cell accumulation in the central nervous system during experimental autoimmune encephalomyelitis. *Journal of immunology* 166:7617-7624.

Filer, A., M. Bik, G.N. Parsonage, J. Fitton, E. Trebilcock, K. Howlett, M. Cook, K. Raza, D.L. Simmons, A.M. Thomas, M. Salmon, D. Scheel-Toellner, J.M. Lord, G.A. Rabinovich, and C.D. Buckley. 2009. Galectin 3 induces a distinctive pattern of cytokine and chemokine production in rheumatoid synovial fibroblasts via selective signaling pathways. *Arthritis and rheumatism* 60:1604-1614.

Filippi, M., M. Rovaris, M.A. Rocca, M.P. Sormani, J.S. Wolinsky, G. Comi, and G. Eurpoean/Canadian Glatiramer Acetate Study. 2001. Glatiramer acetate reduces the proportion of new MS lesions evolving into "black holes". *Neurology* 57:731-733.

Fischer, F.R., L. Santambrogio, Y. Luo, M.A. Berman, W.W. Hancock, and M.E. Dorf. 2000. Modulation of experimental autoimmune encephalomyelitis: effect of altered peptide ligand on chemokine and chemokine receptor expression. *Journal of neuroimmunology* 110:195-208.

Fogel, S., M. Guittaut, A. Legrand, M. Monsigny, and E. Hebert. 1999. The tat protein of HIV-1 induces galectin-3 expression. *Glycobiology* 9:383-387.

Forsman, H., U. Islander, E. Andreasson, A. Andersson, K. Onnheim, A. Karlstrom, K. Savman, M. Magnusson, K.L. Brown, and A. Karlsson. 2011. Galectin 3 aggravates joint inflammation and destruction in antigen-induced arthritis. *Arthritis and rheumatism* 63:445-454.

Fuller, A., H. Yahikozawa, E.Y. So, M. Dal Canto, C.S. Koh, C.J. Welsh, and B.S. Kim. 2007. Castration of male C57L/J mice increases susceptibility and estrogen treatment restores resistance to Theiler's virus-induced demyelinating disease. *Journal of neuroscience research* 85:871-881.

Furtak, V., F. Hatcher, and J. Ochieng. 2001. Galectin-3 mediates the endocytosis of beta-1 integrins by breast carcinoma cells. *Biochemical and biophysical research communications* 289:845-850.

Gandhi, M.K., G. Moll, C. Smith, U. Dua, E. Lambley, O. Ramuz, D. Gill, P. Marlton, J.F. Seymour, and R. Khanna. 2007. Galectin-1 mediated suppression of Epstein-Barr virus specific T-cell immunity in classic Hodgkin lymphoma. *Blood* 110:1326-1329.

Gean-Marton, A.D., L.G. Vezina, K.I. Marton, G.K. Stimac, R.G. Peyster, J.M. Taveras, and K.R. Davis. 1991. Abnormal corpus callosum: a sensitive and specific indicator of multiple sclerosis. *Radiology* 180:215-221.

Gensert, J.M., and J.E. Goldman. 1997. Endogenous progenitors remyelinate demyelinated axons in the adult CNS. *Neuron* 19:197-203.

Gerety, S.J., M.K. Rundell, M.C. Dal Canto, and S.D. Miller. 1994. Class II-restricted T cell responses in Theiler's murine encephalomyelitis virus-induced demyelinating disease. VI. Potentiation of demyelination with and characterization of an immunopathologic CD4+ T cell line specific for an immunodominant VP2 epitope. *Journal of immunology* 152:919-929.

Ghashghaei, H.T., J. Weber, L. Pevny, R. Schmid, M.H. Schwab, K.C. Lloyd, D.D. Eisenstat, C. Lai, and E.S. Anton. 2006. The role of neuregulin-ErbB4 interactions on the proliferation and organization of cells in the subventricular zone. *Proceedings of the National Academy of Sciences of the United States of America* 103:1930-1935.

Glabinski, A.R., V.K. Tuohy, and R.M. Ransohoff. 1998. Expression of chemokines RANTES, MIP-1alpha and GRO-alpha correlates with inflammation in acute experimental autoimmune encephalomyelitis. *Neuroimmunomodulation* 5:166-171.

Goektas, O., F. Schmidt, G. Bohner, K. Erb, L. Ludemann, B. Dahlslett, L. Harms, and F. Fleiner. 2011. Olfactory bulb volume and olfactory function in patients with multiple sclerosis. *Rhinology* 49:221-226.

Goings, G.E., A. Greisman, R.E. James, L.K. Abram, W.S. Begolka, S.D. Miller, and F.G. Szele. 2008. Hematopoietic cell activation in the subventricular zone after Theiler's virus infection. *Journal of neuroinflammation* 5:44.

Goings, G.E., D.A. Kozlowski, and F.G. Szele. 2006. Differential activation of microglia in neurogenic versus non-neurogenic regions of the forebrain. *Glia* 54:329-342.

Goings, G.E., V. Sahni, and F.G. Szele. 2004. Migration patterns of subventricular zone cells in adult mice change after cerebral cortex injury. *Brain research* 996:213-226.

Goldman, S.A., J. Lang, N. Roy, S.J. Schanz, F.S. Sim, S. Wang, V. Washco, and M.S. Windrem. 2006. Progenitor cell-based myelination as a model for cell-based therapy of the central nervous system. *Ernst Schering Research Foundation workshop* 195-213.

Goldschmidt, T., J. Antel, F.B. Konig, W. Bruck, and T. Kuhlmann. 2009. Remyelination capacity of the MS brain decreases with disease chronicity. *Neurology* 72:1914-1921.

Gonzalez-Perez, O., and A. Alvarez-Buylla. 2011. Oligodendrogenesis in the subventricular zone and the role of epidermal growth factor. *Brain research reviews* 67:147-156.

Gonzalez-Perez, O., and A. Quinones-Hinojosa. 2010. Dose-dependent effect of EGF on migration and differentiation of adult subventricular zone astrocytes. *Glia* 58:975-983.

Gonzalez-Perez, O., R. Romero-Rodriguez, M. Soriano-Navarro, J.M. Garcia-Verdugo, and A. Alvarez-Buylla. 2009. Epidermal growth factor induces the progeny of subventricular zone type B cells to migrate and differentiate into oligodendrocytes. *Stem cells* 27:2032-2043.

Gordon, R.J., N.F. Mehrabi, C. Maucksch, and B. Connor. 2012. Chemokines influence the migration and fate of neural precursor cells from the young adult and middle-aged rat subventricular zone. *Experimental neurology* 233:587-594.

Gourraud, P.A., H.F. Harbo, S.L. Hauser, and S.E. Baranzini. 2012. The genetics of multiple sclerosis: an up-to-date review. *Immunological reviews* 248:87-103.

Grigorian, A., and M. Demetriou. 2011. Mgat5 deficiency in T cells and experimental autoimmune encephalomyelitis. *ISRN neurology* 2011:374314.

Grigorian, A., S.U. Lee, W. Tian, I.J. Chen, G. Gao, R. Mendelsohn, J.W. Dennis, and M. Demetriou. 2007. Control of T Cell-mediated autoimmunity by metabolite flux to N-glycan biosynthesis. *The Journal of biological chemistry* 282:20027-20035.

Guerrini, L., F. Blasi, and S. Denis-Donini. 1995. Synaptic activation of NF-kappa B by glutamate in cerebellar granule neurons in vitro. *Proceedings of the National Academy of Sciences of the United States of America* 92:9077-9081.

Guo, J., H. Li, C. Yu, F. Liu, Y. Meng, W. Gong, H. Yang, X. Shen, G. Ju, Z. Li, and J. Wang. 2010. Decreased neural stem/progenitor cell proliferation in mice with chronic/nonremitting experimental autoimmune encephalomyelitis. *Neuro-Signals* 18:1-8.

Hack, M.A., M. Sugimori, C. Lundberg, M. Nakafuku, and M. Gotz. 2004. Regionalization and fate specification in neurospheres: the role of Olig2 and Pax6. *Molecular and cellular neurosciences* 25:664-678.

Hamby, M.E., T.F. Uliasz, S.J. Hewett, and J.A. Hewett. 2006. Characterization of an improved procedure for the removal of microglia from confluent monolayers of primary astrocytes. *Journal of neuroscience methods* 150:128-137.

Hammond, S.R., D. English, C. de Wytt, I.C. Maxwell, K.S. Millingen, E.G. Stewart-Wynne, J.G. McLeod, and M.G. McCall. 1988. The clinical profile of MS in Australia: a comparison between medium- and high-frequency prevalence zones. *Neurology* 38:980-986.

Hemmer, B., J.J. Archelos, and H.P. Hartung. 2002. New concepts in the immunopathogenesis of multiple sclerosis. *Nature reviews. Neuroscience* 3:291-301.

Henderson, N.C., and T. Sethi. 2009. The regulation of inflammation by galectin-3. *Immunological reviews* 230:160-171.

Hill, K.E., M. Pigmans, R.S. Fujinami, and J.W. Rose. 1998. Gender variations in early Theiler's virus induced demyelinating disease: differential susceptibility and effects of IL-4, IL-10 and combined IL-4 with IL-10. *Journal of neuroimmunology* 85:44-51.

Himeda, T., and Y. Ohara. 2012. Saffold virus, a novel human Cardiovirus with unknown pathogenicity. *Journal of virology* 86:1292-1296.

Himeda, T., T. Okuwa, M. Nojiri, Y. Muraki, and Y. Ohara. 2011. The anti-apoptotic protein L(*) of Theiler's murine encephalomyelitis virus (TMEV) contains a mitochondrial targeting signal. *Virus research* 155:381-388.

Hiremath, M.M., Y. Saito, G.W. Knapp, J.P. Ting, K. Suzuki, and G.K. Matsushima. 1998. Microglial/macrophage accumulation during cuprizone-induced demyelination in C57BL/6 mice. *Journal of neuroimmunology* 92:38-49.

Hirrlinger, P.G., A. Scheller, C. Braun, J. Hirrlinger, and F. Kirchhoff. 2006. Temporal control of gene recombination in astrocytes by transgenic expression of the tamoxifen-inducible DNA recombinase variant CreERT2. *Glia* 54:11-20.

Hoffman, L.M., B.T. Fife, W.S. Begolka, S.D. Miller, and W.J. Karpus. 1999. Central nervous system chemokine expression during Theiler's virus-induced demyelinating disease. *Journal of neurovirology* 5:635-642.

Hosking, M.P., and T.E. Lane. 2010. The role of chemokines during viral infection of the CNS. *PLoS pathogens* 6:e1000937.

Hou, J., P. Seth, and E.O. Major. 2006. JC virus can infect human immune and nervous system progenitor cells: implications for pathogenesis. *Advances in experimental medicine and biology* 577:266-273.

Hsu, D.K., S.R. Hammes, I. Kuwabara, W.C. Greene, and F.T. Liu. 1996. Human T lymphotropic virus-I infection of human T lymphocytes induces expression of the beta-galactoside-binding lectin, galectin-3. *The American journal of pathology* 148:1661-1670.

Hsu, D.K., R.Y. Yang, Z. Pan, L. Yu, D.R. Salomon, W.P. Fung-Leung, and F.T. Liu. 2000. Targeted disruption of the galectin-3 gene results in attenuated peritoneal inflammatory responses. *The American journal of pathology* 156:1073-1083.

Huang, D.R., J. Wang, P. Kivisakk, B.J. Rollins, and R.M. Ransohoff. 2001. Absence of monocyte chemoattractant protein 1 in mice leads to decreased local macrophage recruitment and antigen-specific T helper cell type 1 immune response in experimental autoimmune encephalomyelitis. *The Journal of experimental medicine* 193:713-726.

Hughes, R.C. 1999. Secretion of the galectin family of mammalian carbohydrate-binding proteins. *Biochimica et biophysica acta* 1473:172-185.

Ihrie, R.A., and A. Alvarez-Buylla. 2011. Lake-front property: a unique germinal niche by the lateral ventricles of the adult brain. *Neuron* 70:674-686.

Ilarregui, J.M., D.O. Croci, G.A. Bianco, M.A. Toscano, M. Salatino, M.E. Vermeulen, J.R. Geffner, and G.A. Rabinovich. 2009. Tolerogenic signals delivered by dendritic cells to T cells through a galectin-1-driven immunoregulatory circuit involving interleukin 27 and interleukin 10. *Nature immunology* 10:981-991.

Imaizumi, Y., M. Sakaguchi, T. Morishita, M. Ito, F. Poirier, K. Sawamoto, and H. Okano. 2011. Galectin-1 is expressed in early-type neural progenitor cells and down-regulates neurogenesis in the adult hippocampus. *Molecular brain* 4:7.

Imitola, J., M. Comabella, A.K. Chandraker, F. Dangond, M.H. Sayegh, E.Y. Snyder, and S.J. Khoury. 2004. Neural stem/progenitor cells express costimulatory molecules

that are differentially regulated by inflammatory and apoptotic stimuli. *The American journal of pathology* 164:1615-1625.

International Multiple Sclerosis Genetics, C., C. Wellcome Trust Case Control, S. Sawcer, G. Hellenthal, M. Pirinen, C.C. Spencer, N.A. Patsopoulos, L. Moutsianas, A. Dilthey, Z. Su, C. Freeman, S.E. Hunt, S. Edkins, E. Gray, D.R. Booth, S.C. Potter, A. Goris, G. Band, A.B. Oturai, A. Strange, J. Saarela, C. Bellenguez, B. Fontaine, M. Gillman, B. Hemmer, R. Gwilliam, F. Zipp, A. Jayakumar, R. Martin, S. Leslie, S. Hawkins, E. Giannoulatou, S. D'Alfonso, H. Blackburn, F. Martinelli Boneschi, J. Liddle, H.F. Harbo, M.L. Perez, A. Spurkland, M.J. Waller, M.P. Mycko, M. Ricketts, M. Comabella, N. Hammond, I. Kockum, O.T. McCann, M. Ban, P. Whittaker, A. Kemppinen, P. Weston, C. Hawkins, S. Widaa, J. Zajicek, S. Dronov, N. Robertson, S.J. Bumpstead, L.F. Barcellos, R. Ravindrarajah, R. Abraham, L. Alfredsson, K. Ardlie, C. Aubin, A. Baker, K. Baker, S.E. Baranzini, L. Bergamaschi, R. Bergamaschi, A. Bernstein, A. Berthele, M. Boggild, J.P. Bradfield, D. Brassat, S.A. Broadley, D. Buck, H. Butzkueven, R. Capra, W.M. Carroll, P. Cavalla, E.G. Celius, S. Cepok, R. Chiavacci, F. Clerget-Darpoux, K. Clysters, G. Comi, M. Cossburn, I. Cournu-Rebeix, M.B. Cox, W. Cozen, B.A. Cree, A.H. Cross, D. Cusi, M.J. Daly, E. Davis, P.I. de Bakker, M. Debouverie, B. D'Hooghe M, K. Dixon, R. Dobosi, B. Dubois, D. Ellinghaus, I. Elovaara, F. Esposito, C. Fontenille, S. Foote, A. Franke, D. Galimberti, A. Ghezzi, J. Glessner, R. Gomez, O. Gout, C. Graham, S.F. Grant, F.R. Guerini, H. Hakonarson, P. Hall, A. Hamsten, H.P. Hartung, R.N. Heard, S. Heath, J. Hobart, M. Hoshi, C. Infante-Duarte, G. Ingram, W. Ingram, T. Islam, M. Jagodic, M. Kabesch, A.G. Kermode, T.J. Kilpatrick, C. Kim, N. Klopp, K. Koivisto, M. Larsson, M. Lathrop, J.S. Lechner-Scott, M.A. Leone, V. Leppa, U. Liljedahl, I.L. Bomfim, R.R. Lincoln, J. Link, J. Liu, A.R. Lorentzen, S. Lupoli, F. Macciardi, T. Mack, M. Marriott, V. Martinelli, D. Mason, J.L. McCauley, F. Mentch, I.L. Mero, T. Mihalova, X. Montalban, J. Mottershead, K.M. Myhr, P. Naldi, W. Ollier, A. Page, A. Palotie, J. Pelletier, L. Piccio, T. Pickersgill, F. Piehl, S. Pobywajlo, H.L. Quach, P.P. Ramsay, M. Reunanen, R. Reynolds, J.D. Rioux, M. Rodegher, S. Roesner, J.P. Rubio, I.M. Ruckert, M. Salvetti, E. Salvi, A. Santaniello, C.A. Schaefer, S. Schreiber, C. Schulze, R.J. Scott, F. Sellebjerg, K.W. Selmaj, D. Sexton, L. Shen, B. Simms-Acuna, S. Skidmore, P.M. Sleiman, C. Smestad, P.S. Sorensen, H.B. Sondergaard, J. Stankovich, R.C. Strange, A.M. Sulonen, E. Sundqvist, A.C. Syvanen, F. Taddeo, B. Taylor, J.M. Blackwell, P. Tienari, E. Bramon, A. Tourbah, M.A. Brown, E. Tronczynska, J.P. Casas, N. Tubridy, A. Corvin, J. Vickery, J. Jankowski, P. Villoslada, H.S. Markus, K. Wang, C.G. Mathew, J. Wason, C.N. Palmer, H.E. Wichmann, R. Plomin, E. Willoughby, A. Rautanen, J. Winkelmann, M. Wittig, R.C. Trembath, J. Yaouanq, A.C. Viswanathan, H. Zhang, N.W. Wood, R. Zuvich, P. Deloukas, C. Langford, A. Duncanson, J.R. Oksenberg, M.A. Pericak-Vance, J.L. Haines, T. Olsson, J. Hillert, A.J. Ivinson, P.L. De Jager, L. Peltonen, G.J. Stewart, D.A. Hafler, S.L. Hauser, G. McVean, P. Donnelly, and A. Compston. 2011. Genetic risk and a primary role for cell-mediated immune mechanisms in multiple sclerosis. *Nature* 476:214-219.

Ishibashi, S., T. Kuroiwa, M. Sakaguchi, L. Sun, T. Kadoya, H. Okano, and H. Mizusawa. 2007. Galectin-1 regulates neurogenesis in the subventricular zone and promotes functional recovery after stroke. *Experimental neurology* 207:302-313.

Ishii, A., K. Ikenaka, and S.E. Pfeiffer. 2007. The N-glycan profile of mouse myelin, a specialized central nervous system membrane. *Journal of neurochemistry* 103 Suppl 1:25-31.

Ivkovic, S., P. Canoll, and J.E. Goldman. 2008. Constitutive EGFR signaling in oligodendrocyte progenitors leads to diffuse hyperplasia in postnatal white matter. *The Journal of neuroscience : the official journal of the Society for Neuroscience* 28:914-922.

Jablonska, B., A. Aguirre, M. Raymond, G. Szabo, Y. Kitabatake, K.A. Sailor, G.L. Ming, H. Song, and V. Gallo. 2010. Chordin-induced lineage plasticity of adult SVZ neuroblasts after demyelination. *Nature neuroscience* 13:541-550.

James, R., Y. Kim, P.E. Hockberger, and F.G. Szele. 2011. Subventricular zone cell migration: lessons from quantitative two-photon microscopy. *Frontiers in neuroscience* 5:30.

Jeon, S.B., H.J. Yoon, C.Y. Chang, H.S. Koh, S.H. Jeon, and E.J. Park. 2010. Galectin-3 exerts cytokine-like regulatory actions through the JAK-STAT pathway. *Journal of immunology* 185:7037-7046.

Jiang, H.R., Z. Al Rasebi, E. Mensah-Brown, A. Shahin, D. Xu, C.S. Goodyear, S.Y. Fukada, F.T. Liu, F.Y. Liew, and M.L. Lukic. 2009. Galectin-3 deficiency reduces the severity of experimental autoimmune encephalomyelitis. *Journal of immunology* 182:1167-1173.

Jin, K., M. LaFevre-Bernt, Y. Sun, S. Chen, J. Gafni, D. Crippen, A. Logvinova, C.A. Ross, D.A. Greenberg, and L.M. Ellerby. 2005. FGF-2 promotes neurogenesis and neuroprotection and prolongs survival in a transgenic mouse model of Huntington's disease. *Proceedings of the National Academy of Sciences of the United States of America* 102:18189-18194.

Jin, Y.H., B. Kang, and B.S. Kim. 2009. Theiler's virus infection induces a predominant pathogenic CD4+ T cell response to RNA polymerase in susceptible SJL/J mice. *Journal of virology* 83:10981-10992.

Johnson, K.P., and B.J. Nelson. 1977. Multiple sclerosis: diagnostic usefulness of cerebrospinal fluid. *Annals of neurology* 2:425-431.

Johnson, R.R., T.W. Prentice, P. Bridegam, C.R. Young, A.J. Steelman, T.H. Welsh, C.J. Welsh, and M.W. Meagher. 2006. Social stress alters the severity and onset of the chronic phase of Theiler's virus infection. *Journal of neuroimmunology* 175:39-51.

Jones, M.S., V.V. Lukashov, R.D. Ganac, and D.P. Schnurr. 2007. Discovery of a novel human picornavirus in a stool sample from a pediatric patient presenting with fever of unknown origin. *Journal of clinical microbiology* 45:2144-2150.

Kadrofske, M.M., K.P. Openo, and J.L. Wang. 1998. The human LGALS3 (galectin-3) gene: determination of the gene structure and functional characterization of the promoter. *Archives of biochemistry and biophysics* 349:7-20.

Kajitani, K., H. Nomaru, M. Ifuku, N. Yutsudo, Y. Dan, T. Miura, D. Tsuchimoto, K. Sakumi, T. Kadoya, H. Horie, F. Poirier, M. Noda, and Y. Nakabeppu. 2009. Galectin-1 promotes basal and kainate-induced proliferation of neural progenitors in the dentate gyrus of adult mouse hippocampus. *Cell death and differentiation* 16:417-427.

Kaltner, H., D. Kubler, L. Lopez-Merino, M. Lohr, J.C. Manning, M. Lensch, J. Seidler, W.D. Lehmann, S. Andre, D. Solis, and H.J. Gabius. 2011. Toward comprehensive analysis of the galectin network in chicken: unique diversity of galectin-3 and comparison of its localization profile in organs of adult animals to the other four members of this lectin family. *Anatomical record* 294:427-444.

Kanagawa, T., T. Tomimatsu, S. Hayashi, M. Shioji, H. Fukuda, K. Shimoya, and Y. Murata. 2006. The effects of repeated corticosteroid administration on the neurogenesis in the neonatal rat. *American journal of obstetrics and gynecology* 194:231-238.

Kaneko, N., O. Marin, M. Koike, Y. Hirota, Y. Uchiyama, J.Y. Wu, Q. Lu, M. Tessier-Lavigne, A. Alvarez-Buylla, H. Okano, J.L. Rubenstein, and K. Sawamoto. 2010. New neurons clear the path of astrocytic processes for their rapid migration in the adult brain. *Neuron* 67:213-223.

Kang, B.S., M.A. Lyman, and B.S. Kim. 2002. Differences in avidity and epitope recognition of CD8(+) T cells infiltrating the central nervous systems of SJL/J mice infected with BeAn and DA strains of Theiler's murine encephalomyelitis virus. *Journal of virology* 76:11780-11784.

Kang, B.S., J.P. Palma, M.A. Lyman, M. Dal Canto, and B.S. Kim. 2005. Antibody response is required for protection from Theiler's virus-induced encephalitis in C57BL/6 mice in the absence of CD8+ T cells. *Virology* 340:84-94.

Kappel, C.A., R.W. Melvold, and B.S. Kim. 1990. Influence of sex on susceptibility in the Theiler's murine encephalomyelitis virus model for multiple sclerosis. *Journal of neuroimmunology* 29:15-19.

Karls, K.A., P.W. Denton, and R.W. Melvold. 2002. Susceptibility to Theiler's murine encephalomyelitis virus-induced demyelinating disease in BALB/cAnNCr mice is related to absence of a CD4+ T-cell subset. *Multiple sclerosis* 8:469-474.

Karmakar, S., S.R. Stowell, R.D. Cummings, and R.P. McEver. 2008. Galectin-1 signaling in leukocytes requires expression of complex-type N-glycans. *Glycobiology* 18:770-778.

Karpus, W.J., K.J. Kennedy, B.T. Fife, J.L. Bennett, M.C. Dal Canto, S.L. Kunkel, and N.W. Lukacs. 2006. Anti-CCL2 treatment inhibits Theiler's murine encephalomyelitis virus-induced demyelinating disease. *Journal of neurovirology* 12:251-261.

Karpus, W.J., N.W. Lukacs, B.L. McRae, R.M. Strieter, S.L. Kunkel, and S.D. Miller. 1995. An important role for the chemokine macrophage inflammatory protein-1 alpha in the pathogenesis of the T cell-mediated autoimmune disease, experimental autoimmune encephalomyelitis. *Journal of immunology* 155:5003-5010.

Katakowski, M., J. Chen, Z.G. Zhang, M. Santra, Y. Wang, and M. Chopp. 2007. Stroke-induced subventricular zone proliferation is promoted by tumor necrosis factor-alpha-converting enzyme protease activity. *Journal of cerebral blood flow and metabolism : official journal of the International Society of Cerebral Blood Flow and Metabolism* 27:669-678.

Khatri, M., S.M. Goyal, and Y.M. Saif. 2012. Oct4+ stem/progenitor swine lung epithelial cells are targets for influenza virus replication. *Journal of virology* 86:6427-6433.

Kim, H., J. Lee, J.W. Hyun, J.W. Park, H.G. Joo, and T. Shin. 2007. Expression and immunohistochemical localization of galectin-3 in various mouse tissues. *Cell biology international* 31:655-662.

Kim, K., E.P. Mayer, and M. Nachtigal. 2003. Galectin-3 expression in macrophages is signaled by Ras/MAP kinase pathway and up-regulated by modified lipoproteins. *Biochimica et biophysica acta* 1641:13-23.

Kim, Y., I. Comte, G. Szabo, P. Hockberger, and F.G. Szele. 2009. Adult mouse subventricular zone stem and progenitor cells are sessile and epidermal growth factor receptor negatively regulates neuroblast migration. *PloS one* 4:e8122.

Kimelberg, H.K., Z. Cai, G. Schools, and M. Zhou. 2000. Acutely isolated astrocytes as models to probe astrocyte functions. *Neurochemistry international* 36:359-367.

King, R.D., J.M. Lubinski, and H.M. Friedman. 2009. Herpes simplex virus type 1 infection increases the carbohydrate binding activity and the secretion of cellular galectin-3. *Archives of virology* 154:609-618.

Klein, R.S., E. Lin, B. Zhang, A.D. Luster, J. Tollett, M.A. Samuel, M. Engle, and M.S. Diamond. 2005. Neuronal CXCL10 directs CD8+ T-cell recruitment and control of West Nile virus encephalitis. *Journal of virology* 79:11457-11466.

Kobelt, G., J. Berg, P. Lindgren, J. Kerrigan, N. Russell, and R. Nixon. 2006. Costs and quality of life of multiple sclerosis in the United Kingdom. *The European journal of health economics : HEPAC : health economics in prevention and care* 7 Suppl 2:S96-104.

Kokovay, E., S. Goderie, Y. Wang, S. Lotz, G. Lin, Y. Sun, B. Roysam, Q. Shen, and S. Temple. 2010. Adult SVZ lineage cells home to and leave the vascular niche via differential responses to SDF1/CXCR4 signaling. *Cell stem cell* 7:163-173.

Krathwohl, M.D., and J.L. Kaiser. 2004. HIV-1 promotes quiescence in human neural progenitor cells. *The Journal of infectious diseases* 190:216-226.

Kreuzberg, M., E. Kanov, O. Timofeev, M. Schwaninger, H. Monyer, and K. Khodosevich. 2010. Increased subventricular zone-derived cortical neurogenesis after ischemic lesion. *Experimental neurology* 226:90-99.

Kuhlmann, T., G. Lingfeld, A. Bitsch, J. Schuchardt, and W. Bruck. 2002. Acute axonal damage in multiple sclerosis is most extensive in early disease stages and decreases over time. *Brain : a journal of neurology* 125:2202-2212.

Kuhn, H.G., J. Winkler, G. Kempermann, L.J. Thal, and F.H. Gage. 1997. Epidermal growth factor and fibroblast growth factor-2 have different effects on neural progenitors in the adult rat brain. *The Journal of neuroscience : the official journal of the Society for Neuroscience* 17:5820-5829.

Kuklinski, S., V. Vladimirova, A. Waha, H. Kamata, P. Pesheva, and R. Probstmeier. 2003. Expression of galectin-3 in neuronally differentiating PC12 cells is regulated both via Ras/MAPK-dependent and -independent signalling pathways. *Journal of neurochemistry* 87:1112-1124.

Kummerfeld, M., F. Seehusen, S. Klein, R. Ulrich, R. Kreutzer, I. Gerhauser, V. Herder, W. Baumgartner, and A. Beineke. 2012. Periventricular Demyelination and Axonal Pathology Is Associated with Subependymal Virus Spread in a Murine Model for Multiple Sclerosis. *Intervirology*

Lagana, A., J.G. Goetz, P. Cheung, A. Raz, J.W. Dennis, and I.R. Nabi. 2006. Galectin binding to Mgat5-modified N-glycans regulates fibronectin matrix remodeling in tumor cells. *Molecular and cellular biology* 26:3181-3193.

Lalancette-Hebert, M., G. Gowing, A. Simard, Y.C. Weng, and J. Kriz. 2007. Selective ablation of proliferating microglial cells exacerbates ischemic injury in the brain. *The Journal of neuroscience : the official journal of the Society for Neuroscience* 27:2596-2605.

Lalancette-Hebert, M., V. Swarup, J.M. Beaulieu, I. Bohacek, E. Abdelhamid, Y.C. Weng, S. Sato, and J. Kriz. 2012. Galectin-3 is required for resident microglia activation and proliferation in response to ischemic injury. *The Journal of neuroscience : the official journal of the Society for Neuroscience* 32:10383-10395.

Lane, T.E., and M.P. Hosking. 2010. The pathogenesis of murine coronavirus infection of the central nervous system. *Critical reviews in immunology* 30:119-130.

Lau, K.S., E.A. Partridge, A. Grigorian, C.I. Silvescu, V.N. Reinhold, M. Demetriou, and J.W. Dennis. 2007. Complex N-glycan number and degree of branching cooperate to regulate cell proliferation and differentiation. *Cell* 129:123-134.

Lee, S.U., A. Grigorian, J. Pawling, I.J. Chen, G. Gao, T. Mozaffar, C. McKerlie, and M. Demetriou. 2007. N-glycan processing deficiency promotes spontaneous inflammatory demyelination and neurodegeneration. *The Journal of biological chemistry* 282:33725-33734.

Lein, E.S., M.J. Hawrylycz, N. Ao, M. Ayres, A. Bensinger, A. Bernard, A.F. Boe, M.S. Boguski, K.S. Brockway, E.J. Byrnes, L. Chen, L. Chen, T.M. Chen, M.C. Chin, J. Chong, B.E. Crook, A. Czaplinska, C.N. Dang, S. Datta, N.R. Dee, A.L. Desaki, T. Desta, E. Diep, T.A. Dolbeare, M.J. Donelan, H.W. Dong, J.G. Dougherty, B.J. Duncan, A.J. Ebbert, G. Eichele, L.K. Estin, C. Faber, B.A. Facer, R. Fields, S.R. Fischer, T.P. Fliss, C. Frensley, S.N. Gates, K.J. Glattfelder, K.R. Halverson, M.R. Hart, J.G. Hohmann, M.P. Howell, D.P. Jeung, R.A. Johnson, P.T. Karr, R. Kawal, J.M. Kidney, R.H. Knapik, C.L. Kuan, J.H. Lake, A.R. Laramee, K.D. Larsen, C. Lau, T.A. Lemon, A.J. Liang, Y. Liu, L.T. Luong, J. Michaels, J.J. Morgan, R.J. Morgan, M.T. Mortrud, N.F. Mosqueda, L.L. Ng, R. Ng, G.J. Orta, C.C. Overly, T.H. Pak, S.E. Parry, S.D. Pathak, O.C. Pearson, R.B. Puchalski, Z.L. Riley, H.R. Rockett, S.A. Rowland, J.J. Royall, M.J. Ruiz, N.R. Sarno, K. Schaffnit, N.V. Shapovalova, T. Sivisay, C.R. Slaughterbeck, S.C. Smith, K.A. Smith, B.I. Smith, A.J. Sodt, N.N. Stewart, K.R. Stumpf, S.M. Sunkin, M. Sutram, A. Tam, C.D. Teemer, C. Thaller, C.L. Thompson, L.R. Varnam, A. Visel, R.M. Whitlock, P.E. Wohnoutka, C.K. Wolkey, V.Y. Wong, M. Wood, M.B. Yaylaoglu, R.C. Young, B.L. Youngstrom, X.F. Yuan, B. Zhang, T.A. Zwingman, and A.R. Jones. 2007. Genome-wide atlas of gene expression in the adult mouse brain. *Nature* 445:168-176.

Lemire, J.M., and D.C. Archer. 1991. 1,25-dihydroxyvitamin D3 prevents the in vivo induction of murine experimental autoimmune encephalomyelitis. *The Journal of clinical investigation* 87:1103-1107.

Leung, H.S., O.T. Li, R.W. Chan, M.C. Chan, J.M. Nicholls, and L.L. Poon. 2012. The virus entry of influenza A virus with a alpha2,6-linked sialic acid binding preference requires host fibronectin. *Journal of virology*

Levin, L.I., K.L. Munger, M.V. Rubertone, C.A. Peck, E.T. Lennette, D. Spiegelman, and A. Ascherio. 2005. Temporal relationship between elevation of epstein-barr virus antibody titers and initial onset of neurological symptoms in multiple sclerosis. *JAMA : the journal of the American Medical Association* 293:2496-2500.

Li, L., T.L. Walker, Y. Zhang, E.W. Mackay, and P.F. Bartlett. 2010. Endogenous interferon gamma directly regulates neural precursors in the non-inflammatory brain. *The Journal of neuroscience : the official journal of the Society for Neuroscience* 30:9038-9050.

Liang, Z., A.S. Kumar, M.S. Jones, N.J. Knowles, and H.L. Lipton. 2008. Phylogenetic analysis of the species Theilovirus: emerging murine and human pathogens. *Journal of virology* 82:11545-11554.

Liao, F., A. Andalibi, F.C. deBeer, A.M. Fogelman, and A.J. Lusis. 1993. Genetic control of inflammatory gene induction and NF-kappa B-like transcription factor activation in response to an atherogenic diet in mice. *The Journal of clinical investigation* 91:2572-2579.

Libbey, J.E., N.J. Kirkman, K.S. Wilcox, H.S. White, and R.S. Fujinami. 2010. Role for complement in the development of seizures following acute viral infection. *Journal of virology* 84:6452-6460.

Lincoln, M.R., A. Montpetit, M.Z. Cader, J. Saarela, D.A. Dyment, M. Tiislar, V. Ferretti, P.J. Tienari, A.D. Sadovnick, L. Peltonen, G.C. Ebers, and T.J. Hudson. 2005. A predominant role for the HLA class II region in the association of the MHC region with multiple sclerosis. *Nature genetics* 37:1108-1112.

Lippert, E., W. Falk, F. Bataille, T. Kaehne, M. Naumann, M. Goeke, H. Herfarth, J. Schoelmerich, and G. Rogler. 2007. Soluble galectin-3 is a strong, colonic epithelial-cell-derived, lamina propria fibroblast-stimulating factor. *Gut* 56:43-51.

Lipton, H.L., A.S. Kumar, and M. Trottier. 2005. Theiler's virus persistence in the central nervous system of mice is associated with continuous viral replication and a difference in outcome of infection of infiltrating macrophages versus oligodendrocytes. *Virus research* 111:214-223.

Liu, G., I.H. Martins, J.A. Chiorini, and B.L. Davidson. 2005. Adeno-associated virus type 4 (AAV4) targets ependyma and astrocytes in the subventricular zone and RMS. *Gene therapy* 12:1503-1508.

Liu, M.T., B.P. Chen, P. Oertel, M.J. Buchmeier, D. Armstrong, T.A. Hamilton, and T.E. Lane. 2000. The T cell chemoattractant IFN-inducible protein 10 is essential in host defense against viral-induced neurologic disease. *Journal of immunology* 165:2327-2330.

Liu, T.Y., C.Y. Chen, H.F. Tien, and C.W. Lin. 2009. Loss of CD7, independent of galectin-3 expression, implies a worse prognosis in adult T-cell leukaemia/lymphoma. *Histopathology* 54:214-220.

Lois, C., and A. Alvarez-Buylla. 1994. Long-distance neuronal migration in the adult mammalian brain. *Science* 264:1145-1148.

Lowe, J.B., and J.D. Marth. 2003. A genetic approach to Mammalian glycan function. *Annual review of biochemistry* 72:643-691.

Lublin, F.D., and S.C. Reingold. 1996. Defining the clinical course of multiple sclerosis: results of an international survey. National Multiple Sclerosis Society (USA) Advisory Committee on Clinical Trials of New Agents in Multiple Sclerosis. *Neurology* 46:907-911.

Lucchinetti, C., W. Bruck, J. Parisi, B. Scheithauer, M. Rodriguez, and H. Lassmann. 1999. A quantitative analysis of oligodendrocytes in multiple sclerosis lesions. A study of 113 cases. *Brain : a journal of neurology* 122 (Pt 12):2279-2295.

Lucchinetti, C., W. Bruck, J. Parisi, B. Scheithauer, M. Rodriguez, and H. Lassmann. 2000. Heterogeneity of multiple sclerosis lesions: implications for the pathogenesis of demyelination. *Annals of neurology* 47:707-717.

Luo, M., C. He, K.S. Toth, C.X. Zhang, and H.L. Lipton. 1992. Three-dimensional structure of Theiler murine encephalomyelitis virus (BeAn strain). *Proceedings of the National Academy of Sciences of the United States of America* 89:2409-2413.

Lutterotti, A., M. Vedovello, M. Reindl, R. Ehling, F. DiPauli, B. Kuenz, C. Gneiss, F. Deisenhammer, and T. Berger. 2011. Olfactory threshold is impaired in early, active multiple sclerosis. *Multiple sclerosis* 17:964-969.

Lyman, M.A., J. Myoung, M. Mohindru, and B.S. Kim. 2004. Quantitative, not qualitative, differences in CD8(+) T cell responses to Theiler's murine encephalomyelitis virus between resistant C57BL/6 and susceptible SJL/J mice. *European journal of immunology* 34:2730-2739.

Mackinnon, A.C., M.A. Gibbons, S.L. Farnworth, H. Leffler, U.J. Nilsson, T. Delaine, A.J. Simpson, S.J. Forbes, N. Hirani, J. Gauldie, and T. Sethi. 2012. Regulation of transforming growth factor-beta1-driven lung fibrosis by galectin-3. *American journal of respiratory and critical care medicine* 185:537-546.

Magalon, K., C. Cantarella, G. Monti, M. Cayre, and P. Durbec. 2007. Enriched environment promotes adult neural progenitor cell mobilization in mouse demyelination models. *The European journal of neuroscience* 25:761-771.

Maire, C.L., A. Wegener, C. Kerninon, and B. Nait Oumesmar. 2010. Gain-of-function of Olig transcription factors enhances oligodendrogenesis and myelination. *Stem cells* 28:1611-1622.

Maldonado, C.A., V. Sundblad, M. Salatino, J. Elia, L.N. Garcia, C. Leimgruber, D.O. Croci, and G.A. Rabinovich. 2011. Cell-type specific regulation of galectin-3

expression by glucocorticoids in lung Clara cells and macrophages. *Histology and histopathology* 26:747-759.

Markowska, A.I., K.C. Jefferies, and N. Panjwani. 2011. Galectin-3 protein modulates cell surface expression and activation of vascular endothelial growth factor receptor 2 in human endothelial cells. *The Journal of biological chemistry* 286:29913-29921.

Martino, G., and S. Pluchino. 2006. The therapeutic potential of neural stem cells. *Nature reviews. Neuroscience* 7:395-406.

Martino, G., and S. Pluchino. 2007. Neural stem cells: guardians of the brain. *Nature cell biology* 9:1031-1034.

Matarrese, P., O. Fusco, N. Tinari, C. Natoli, F.T. Liu, M.L. Semeraro, W. Malorni, and S. Iacobelli. 2000a. Galectin-3 overexpression protects from apoptosis by improving cell adhesion properties. *International journal of cancer. Journal international du cancer* 85:545-554.

Matarrese, P., N. Tinari, M.L. Semeraro, C. Natoli, S. Iacobelli, and W. Malorni. 2000b. Galectin-3 overexpression protects from cell damage and death by influencing mitochondrial homeostasis. *FEBS letters* 473:311-315.

Mathieu, A., N. Nagy, C. Decaestecker, L. Ferdinande, K. Vandenbroucke, P. Rottiers, C.A. Cuvelier, I. Salmon, and P. Demetter. 2008. Expression of galectins-1, -3 and -4 varies with strain and type of experimental colitis in mice. *International journal of experimental pathology* 89:438-446.

Mazurek, N., J. Conklin, J.C. Byrd, A. Raz, and R.S. Bresalier. 2000. Phosphorylation of the beta-galactoside-binding protein galectin-3 modulates binding to its ligands. *The Journal of biological chemistry* 275:36311-36315.

McCandless, E.E., Q. Wang, B.M. Woerner, J.M. Harper, and R.S. Klein. 2006. CXCL12 limits inflammation by localizing mononuclear infiltrates to the perivascular space during experimental autoimmune encephalomyelitis. *Journal of immunology* 177:8053-8064.

McCandless, E.E., B. Zhang, M.S. Diamond, and R.S. Klein. 2008. CXCR4 antagonism increases T cell trafficking in the central nervous system and improves survival from West Nile virus encephalitis. *Proceedings of the National Academy of Sciences of the United States of America* 105:11270-11275.

McCrone, P., M. Heslin, M. Knapp, P. Bull, and A. Thompson. 2008. Multiple sclerosis in the UK: service use, costs, quality of life and disability. *PharmacoEconomics* 26:847-860.

Menn, B., J.M. Garcia-Verdugo, C. Yaschine, O. Gonzalez-Perez, D. Rowitch, and A. Alvarez-Buylla. 2006. Origin of oligodendrocytes in the subventricular zone of the adult brain. *The Journal of neuroscience : the official journal of the Society for Neuroscience* 26:7907-7918.

Merkle, F.T., Z. Mirzadeh, and A. Alvarez-Buylla. 2007. Mosaic organization of neural stem cells in the adult brain. *Science* 317:381-384.

Merkler, D., T. Ernsting, M. Kerschensteiner, W. Bruck, and C. Stadelmann. 2006. A new focal EAE model of cortical demyelination: multiple sclerosis-like lesions with rapid resolution of inflammation and extensive remyelination. *Brain : a journal of neurology* 129:1972-1983.

Merlin, J., L. Stechly, S. de Beauce, D. Monte, E. Leteurtre, I. van Seuningen, G. Huet, and P. Pigny. 2011. Galectin-3 regulates MUC1 and EGFR cellular distribution and EGFR downstream pathways in pancreatic cancer cells. *Oncogene* 30:2514-2525.

Mestre, L., P.M. Inigo, M. Mecha, F.G. Correa, M. Hernangomez-Herrero, F. Loria, F. Docagne, J. Borrell, and C. Guaza. 2011. Anandamide inhibits Theiler's virus induced VCAM-1 in brain endothelial cells and reduces leukocyte transmigration

in a model of blood brain barrier by activation of CB(1) receptors. *Journal of neuroinflammation* 8:102.

Mi, W., T.W. Prentice, C.R. Young, R.R. Johnson, A.N. Sieve, M.W. Meagher, and C.J. Welsh. 2006a. Restraint stress decreases virus-induced pro-inflammatory cytokine mRNA expression during acute Theiler's virus infection. *Journal of neuroimmunology* 178:49-61.

Mi, W., C.R. Young, R.W. Storts, A.J. Steelman, M.W. Meagher, and C.J. Welsh. 2006b. Restraint stress facilitates systemic dissemination of Theiler's virus and alters its pathogenecity. *Microbial pathogenesis* 41:133-143.

Miller, D.J., K.S. Sanborn, J.A. Katzmann, and M. Rodriguez. 1994. Monoclonal autoantibodies promote central nervous system repair in an animal model of multiple sclerosis. *The Journal of neuroscience : the official journal of the Society for Neuroscience* 14:6230-6238.

Miller, S.D., and T.N. Eagar. 2001. Functional role of epitope spreading in the chronic pathogenesis of autoimmune and virus-induced demyelinating diseases. *Advances in experimental medicine and biology* 490:99-107.

Miller, S.D., Y. Katz-Levy, K.L. Neville, and C.L. Vanderlugt. 2001. Virus-induced autoimmunity: epitope spreading to myelin autoepitopes in Theiler's virus infection of the central nervous system. *Advances in virus research* 56:199-217.

Miller, S.D., C.L. Vanderlugt, W.S. Begolka, W. Pao, K.L. Neville, R.L. Yauch, and B.S. Kim. 1997. Epitope spreading leads to myelin-specific autoimmune responses in SJL mice chronically infected with Theiler's virus. *Journal of neurovirology* 3 Suppl 1:S62-65.

Milo, R., and E. Kahana. 2010. Multiple sclerosis: geoepidemiology, genetics and the environment. *Autoimmunity reviews* 9:A387-394.

Mkhikian, H., A. Grigorian, C.F. Li, H.L. Chen, B. Newton, R.W. Zhou, C. Beeton, S. Torossian, G.G. Tatarian, S.U. Lee, K. Lau, E. Walker, K.A. Siminovitch, K.G. Chandy, Z. Yu, J.W. Dennis, and M. Demetriou. 2011. Genetics and the environment converge to dysregulate N-glycosylation in multiple sclerosis. *Nature communications* 2:334.

Moisan, S., M. Demers, J. Mercier, T. Magnaldo, E.F. Potworowski, and Y. St-Pierre. 2003. Upregulation of galectin-7 in murine lymphoma cells is associated with progression toward an aggressive phenotype. *Leukemia : official journal of the Leukemia Society of America, Leukemia Research Fund, U.K* 17:751-759.

Mok, S.W., C. Riemer, K. Madela, D.K. Hsu, F.T. Liu, S. Gultner, I. Heise, and M. Baier. 2007. Role of galectin-3 in prion infections of the CNS. *Biochemical and biophysical research communications* 359:672-678.

Molina-Holgado, E., A. Arevalo-Martin, A. Castrillo, L. Bosca, J.M. Vela, and C. Guaza. 2002a. Interleukin-4 and interleukin-10 modulate nuclear factor kappaB activity and nitric oxide synthase-2 expression in Theiler's virus-infected brain astrocytes. *Journal of neurochemistry* 81:1242-1252.

Molina-Holgado, E., A. Arevalo-Martin, S. Ortiz, J.M. Vela, and C. Guaza. 2002b. Theiler's virus infection induces the expression of cyclooxygenase-2 in murine astrocytes: inhibition by the anti-inflammatory cytokines interleukin-4 and interleukin-10. *Neuroscience letters* 324:237-241.

Monteyne, P., J.F. Bureau, and M. Brahic. 1997. The infection of mouse by Theiler's virus: from genetics to immunology. *Immunological reviews* 159:163-176.

Morga, E., C. Faber, and P. Heuschling. 1998. Cultured astrocytes express regional heterogeneity of the immunoreactive phenotype under basal conditions and after gamma-IFN induction. *Journal of neuroimmunology* 87:179-184.

Moutsatsos, I.K., M. Wade, M. Schindler, and J.L. Wang. 1987. Endogenous lectins from cultured cells: nuclear localization of carbohydrate-binding protein 35 in proliferating 3T3 fibroblasts. *Proceedings of the National Academy of Sciences of the United States of America* 84:6452-6456.

Murray, P.D., K. Krivacic, A. Chernosky, T. Wei, R.M. Ransohoff, and M. Rodriguez. 2000. Biphasic and regionally-restricted chemokine expression in the central nervous system in the Theiler's virus model of multiple sclerosis. *Journal of neurovirology* 6 Suppl 1:S44-52.

Murray, P.D., K.D. Pavelko, J. Leibowitz, X. Lin, and M. Rodriguez. 1998. CD4(+) and CD8(+) T cells make discrete contributions to demyelination and neurologic disease in a viral model of multiple sclerosis. *Journal of virology* 72:7320-7329.

Muzio, L., F. Cavasinni, C. Marinaro, A. Bergamaschi, A. Bergami, C. Porcheri, F. Cerri, G. Dina, A. Quattrini, G. Comi, R. Furlan, and G. Martino. 2010. Cxcl10 enhances blood cells migration in the sub-ventricular zone of mice affected by experimental autoimmune encephalomyelitis. *Molecular and cellular neurosciences* 43:268-280.

Nait-Oumesmar, B., L. Decker, F. Lachapelle, V. Avellana-Adalid, C. Bachelin, and A. Baron-Van Evercooren. 1999. Progenitor cells of the adult mouse subventricular zone proliferate, migrate and differentiate into oligodendrocytes after demyelination. *The European journal of neuroscience* 11:4357-4366.

Nait-Oumesmar, B., N. Picard-Riera, C. Kerninon, L. Decker, D. Seilhean, G.U. Hoglinger, E.C. Hirsch, R. Reynolds, and A. Baron-Van Evercooren. 2007. Activation of the subventricular zone in multiple sclerosis: evidence for early glial progenitors. *Proceedings of the National Academy of Sciences of the United States of America* 104:4694-4699.

Najar, M., G. Raicevic, H. Id Boufker, B. Stamatopoulos, C. De Bruyn, N. Meuleman, D. Bron, M. Toungouz, and L. Lagneaux. 2010. Modulated expression of adhesion molecules and galectin-1: role during mesenchymal stromal cell immunoregulatory functions. *Experimental hematology* 38:922-932.

Nakashima, I., K. Fujihara, H. Miyazawa, T. Misu, J. Fujimori, S. Sato, and Y. Itoyama. 2006. Relevance of callosal and periventricular MRI lesions to oligoclonal bands in multiple sclerosis. *Acta neurologica Scandinavica* 113:125-131.

Nam, S.C., Y. Kim, D. Dryanovski, A. Walker, G. Goings, K. Woolfrey, S.S. Kang, C. Chu, A. Chenn, F. Erdelyi, G. Szabo, P. Hockberger, and F.G. Szele. 2007. Dynamic features of postnatal subventricular zone cell motility: a two-photon time-lapse study. *The Journal of comparative neurology* 505:190-208.

Nangia-Makker, P., Y. Honjo, R. Sarvis, S. Akahani, V. Hogan, K.J. Pienta, and A. Raz. 2000. Galectin-3 induces endothelial cell morphogenesis and angiogenesis. *The American journal of pathology* 156:899-909.

Nansen, A., O. Marker, C. Bartholdy, and A.R. Thomsen. 2000. CCR2+ and CCR5+ CD8+ T cells increase during viral infection and migrate to sites of infection. *European journal of immunology* 30:1797-1806.

Nelson, A.L., A.J. Bieber, and M. Rodriguez. 2004. Contrasting murine models of MS. *International MS journal / MS Forum* 11:95-99.

Nguyen-Ba-Charvet, K.T., N. Picard-Riera, M. Tessier-Lavigne, A. Baron-Van Evercooren, C. Sotelo, and A. Chedotal. 2004. Multiple roles for slits in the control of cell migration in the rostral migratory stream. *The Journal of neuroscience : the official journal of the Society for Neuroscience* 24:1497-1506.

Nieminen, J., A. Kuno, J. Hirabayashi, and S. Sato. 2007. Visualization of galectin-3 oligomerization on the surface of neutrophils and endothelial cells using

fluorescence resonance energy transfer. *The Journal of biological chemistry* 282:1374-1383.

Njenga, M.K., P.D. Murray, D. McGavern, X. Lin, K.M. Drescher, and M. Rodriguez. 1999. Absence of spontaneous central nervous system remyelination in class II-deficient mice infected with Theiler's virus. *Journal of neuropathology and experimental neurology* 58:78-91.

O'Shea, H., J. Crang, P. Tonks, A.A. Nash, and J.K. Fazakerley. 1997. The PI capsid region of Theiler's virus controls replication in mouse glial cell cultures. *Archives of virology* 142:1521-1535.

O'Toole, S.A., B.L. Sheppard, E.P. McGuinness, N.C. Gleeson, M. Yoneda, and J. Bonnar. 2003. The MTS assay as an indicator of chemosensitivity/resistance in malignant gynaecological tumours. *Cancer detection and prevention* 27:47-54.

Obuchi, M., and Y. Ohara. 1999. Theiler's murine encephalomyelitis virus (TMEV): the role of a small out-of-frame protein in viral persistence and demyelination. *Japanese journal of infectious diseases* 52:228-233.

Ochieng, J., R. Fridman, P. Nangia-Makker, D.E. Kleiner, L.A. Liotta, W.G. Stetler-Stevenson, and A. Raz. 1994. Galectin-3 is a novel substrate for human matrix metalloproteinases-2 and -9. *Biochemistry* 33:14109-14114.

Ochieng, J., B. Green, S. Evans, O. James, and P. Warfield. 1998. Modulation of the biological functions of galectin-3 by matrix metalloproteinases. *Biochimica et biophysica acta* 1379:97-106.

Ocklenburg, F., D. Moharregh-Khiabani, R. Geffers, V. Janke, S. Pfoertner, H. Garritsen, L. Groebe, J. Klempnauer, K.E. Dittmar, S. Weiss, J. Buer, and M. Probst-Kepper. 2006. UBD, a downstream element of FOXP3, allows the identification of LGALS3, a new marker of human regulatory T cells. *Laboratory investigation; a journal of technical methods and pathology* 86:724-737.

Odinak, M.M., G.N. Bisaga, A.V. Novitskii, V.V. Tyrenko, M.S. Fominykh, A.A. Bilibina, P.V. Krugliakov, and D.G. Polyntsev. 2011. [Transplantation of mesenchymal stem cells in multiple sclerosis]. *Zhurnal nevrologii i psikhiatrii imeni S.S. Korsakova / Ministerstvo zdravookhraneniia i meditsinskoi promyshlennosti Rossiiskoi Federatsii, Vserossiiskoe obshchestvo nevrologov [i] Vserossiiskoe obshchestvo psikhiat* 111:72-76.

Offner, H., B. Celnik, T.S. Bringman, D. Casentini-Borocz, G.E. Nedwin, and A.A. Vandenbark. 1990. Recombinant human beta-galactoside binding lectin suppresses clinical and histological signs of experimental autoimmune encephalomyelitis. *Journal of neuroimmunology* 28:177-184.

Oleszak, E.L., J.R. Chang, H. Friedman, C.D. Katsetos, and C.D. Platsoucas. 2004. Theiler's virus infection: a model for multiple sclerosis. *Clinical microbiology reviews* 17:174-207.

Oleszak, E.L., B.E. Hoffman, J.R. Chang, E. Zaczynska, J. Gaughan, C.D. Katsetos, C.D. Platsoucas, and N. Harvey. 2003. Apoptosis of infiltrating T cells in the central nervous system of mice infected with Theiler's murine encephalomyelitis virus. *Virology* 315:110-123.

Oliveira, F.L., C. Brand, A.A. Paula, K.D. Arcanjo, D.K. Hsu, F.T. Liu, C.M. Takiya, R. Borojevic, R. Chammas, and M.C. El-Cheikh. 2011. Lack of galectin-3 disturbs mesenteric lymph node homeostasis and B cell niches in the course of Schistosoma mansoni infection. *PloS one* 6:e19216.

Olson, J.K., J.L. Croxford, M.A. Calenoff, M.C. Dal Canto, and S.D. Miller. 2001. A virus-induced molecular mimicry model of multiple sclerosis. *The Journal of clinical investigation* 108:311-318.

Olson, J.K., A.M. Ercolini, and S.D. Miller. 2005. A virus-induced molecular mimicry model of multiple sclerosis. *Current topics in microbiology and immunology* 296:39-53.

Ono, K., H. Tomasiewicz, T. Magnuson, and U. Rutishauser. 1994. N-CAM mutation inhibits tangential neuronal migration and is phenocopied by enzymatic removal of polysialic acid. *Neuron* 13:595-609.

Orlacchio, A., P. Sarchielli, V. Gallai, A. Datti, C. Saccardi, and C.A. Palmerini. 1997. Activity levels of a beta1,6 N-acetylglucosaminyltransferase in lymphomonocytes from multiple sclerosis patients. *Journal of the neurological sciences* 151:177-183.

Palma, J.P., and B.S. Kim. 2004. The scope and activation mechanisms of chemokine gene expression in primary astrocytes following infection with Theiler's virus. *Journal of neuroimmunology* 149:121-129.

Palma, J.P., D. Kwon, N.A. Clipstone, and B.S. Kim. 2003. Infection with Theiler's murine encephalomyelitis virus directly induces proinflammatory cytokines in primary astrocytes via NF-kappaB activation: potential role for the initiation of demyelinating disease. *Journal of virology* 77:6322-6331.

Pasquini, L.A., V. Millet, H.C. Hoyos, J.P. Giannoni, D.O. Croci, M. Marder, F.T. Liu, G.A. Rabinovich, and J.M. Pasquini. 2011. Galectin-3 drives oligodendrocyte differentiation to control myelin integrity and function. *Cell death and differentiation* 18:1746-1756.

Patani, R., M. Balaratnam, A. Vora, and R. Reynolds. 2007. Remyelination can be extensive in multiple sclerosis despite a long disease course. *Neuropathology and applied neurobiology* 33:277-287.

Patrikios, P., C. Stadelmann, A. Kutzelnigg, H. Rauschka, M. Schmidbauer, H. Laursen, P.S. Sorensen, W. Bruck, C. Lucchinetti, and H. Lassmann. 2006. Remyelination is extensive in a subset of multiple sclerosis patients. *Brain : a journal of neurology* 129:3165-3172.

Paty, D., D. Studney, K. Redekop, and F. Lublin. 1994. MS COSTAR: a computerized patient record adapted for clinical research purposes. *Annals of neurology* 36 Suppl:S134-135.

Pavelko, K.D., K.M. Drescher, D.B. McGavern, C.S. David, and M. Rodriguez. 2000. HLA-DQ polymorphism influences progression of demyelination and neurologic deficits in a viral model of multiple sclerosis. *Molecular and cellular neurosciences* 15:495-509.

Payne, N.L., G. Sun, D. Herszfeld, P.A. Tat-Goh, P.J. Verma, H.C. Parkington, H.A. Coleman, M.A. Tonta, C. Siatskas, and C.C. Bernard. 2012. Comparative study on the therapeutic potential of neurally differentiated stem cells in a mouse model of multiple sclerosis. *PloS one* 7:e35093.

Peng, H., Y. Huang, J. Rose, D. Erichsen, S. Herek, N. Fujii, H. Tamamura, and J. Zheng. 2004. Stromal cell-derived factor 1-mediated CXCR4 signaling in rat and human cortical neural progenitor cells. *Journal of neuroscience research* 76:35-50.

Perez, L., J.C. Alvarez-Cermeno, C. Rodriguez, E. Roldan, and J.A. Brieva. 1995. B cells capable of spontaneous IgG secretion in cerebrospinal fluid from patients with multiple sclerosis: dependency on local IL-6 production. *Clinical and experimental immunology* 101:449-452.

Pesheva, P., S. Kuklinski, H.J. Biersack, and R. Probstmeier. 2000. Nerve growth factor-mediated expression of galectin-3 in mouse dorsal root ganglion neurons. *Neuroscience letters* 293:37-40.

Pesheva, P., S. Kuklinski, B. Schmitz, and R. Probstmeier. 1998. Galectin-3 promotes neural cell adhesion and neurite growth. *Journal of neuroscience research* 54:639-654.

Petridis, A.K., A. El-Maarouf, and U. Rutishauser. 2004. Polysialic acid regulates cell contact-dependent neuronal differentiation of progenitor cells from the subventricular zone. *Developmental dynamics : an official publication of the American Association of Anatomists* 230:675-684.

Picard-Riera, N., L. Decker, C. Delarasse, K. Goude, B. Nait-Oumesmar, R. Liblau, D. Pham-Dinh, and A.B. Evercooren. 2002. Experimental autoimmune encephalomyelitis mobilizes neural progenitors from the subventricular zone to undergo oligodendrogenesis in adult mice. *Proceedings of the National Academy of Sciences of the United States of America* 99:13211-13216.

Pichiecchio, A., E. Tavazzi, G. Maccabelli, M. Ponzio, A. Romani, R. Schiappacassa, G.U. Poloni, D. Franciotta, L. Roccatagliata, R. Bergamaschi, and S. Bastianello. 2009. MR peri-CSF lesions and CSF oligoclonal bands in Italian multiple sclerosis patients. *Acta neurologica Scandinavica* 120:242-245.

Pirko, I., T.K. Nolan, S.K. Holland, and A.J. Johnson. 2008. Multiple sclerosis: pathogenesis and MR imaging features of T1 hypointensities in a [corrected] murine model. *Radiology* 246:790-795.

Pluchino, S., L. Muzio, J. Imitola, M. Deleidi, C. Alfaro-Cervello, G. Salani, C. Porcheri, E. Brambilla, F. Cavasinni, A. Bergamaschi, J.M. Garcia-Verdugo, G. Comi, S.J. Khoury, and G. Martino. 2008. Persistent inflammation alters the function of the endogenous brain stem cell compartment. *Brain : a journal of neurology* 131:2564-2578.

Pluchino, S., A. Quattrini, E. Brambilla, A. Gritti, G. Salani, G. Dina, R. Galli, U. Del Carro, S. Amadio, A. Bergami, R. Furlan, G. Comi, A.L. Vescovi, and G. Martino. 2003. Injection of adult neurospheres induces recovery in a chronic model of multiple sclerosis. *Nature* 422:688-694.

Plumb, J.A., R. Milroy, and S.B. Kaye. 1989. Effects of the pH dependence of 3-(4,5-dimethylthiazol-2-yl)-2,5-diphenyl-tetrazolium bromide-formazan absorption on chemosensitivity determined by a novel tetrazolium-based assay. *Cancer research* 49:4435-4440.

Poisa-Beiro, L., S. Dios, H. Ahmed, G.R. Vasta, A. Martinez-Lopez, A. Estepa, J. Alonso-Gutierrez, A. Figueras, and B. Novoa. 2009. Nodavirus infection of sea bass (Dicentrarchus labrax) induces up-regulation of galectin-1 expression with potential anti-inflammatory activity. *Journal of immunology* 183:6600-6611.

Polman, C.H., S.C. Reingold, B. Banwell, M. Clanet, J.A. Cohen, M. Filippi, K. Fujihara, E. Havrdova, M. Hutchinson, L. Kappos, F.D. Lublin, X. Montalban, P. O'Connor, M. Sandberg-Wollheim, A.J. Thompson, E. Waubant, B. Weinshenker, and J.S. Wolinsky. 2011. Diagnostic criteria for multiple sclerosis: 2010 revisions to the McDonald criteria. *Annals of neurology* 69:292-302.

Povlsen, G.K., V. Berezin, and E. Bock. 2008. Neural cell adhesion molecule-180-mediated homophilic binding induces epidermal growth factor receptor (EGFR) down-regulation and uncouples the inhibitory function of EGFR in neurite outgrowth. *Journal of neurochemistry* 104:624-639.

Prineas, J.W., R.O. Barnard, E.E. Kwon, L.R. Sharer, and E.S. Cho. 1993. Multiple sclerosis: remyelination of nascent lesions. *Annals of neurology* 33:137-151.

Prineas, J.W., E.E. Kwon, E.S. Cho, and L.R. Sharer. 1984. Continual breakdown and regeneration of myelin in progressive multiple sclerosis plaques. *Annals of the New York Academy of Sciences* 436:11-32.

Pringproa, K., K. Rohn, M. Kummerfeld, K. Wewetzer, and W. Baumgartner. 2010. Theiler's murine encephalomyelitis virus preferentially infects immature stages of the murine oligodendrocyte precursor cell line BO-1 and blocks oligodendrocytic differentiation in vitro. *Brain research* 1327:24-37.

Probstmeier, R., D. Montag, and M. Schachner. 1995. Galectin-3, a beta-galactoside-binding animal lectin, binds to neural recognition molecules. *Journal of neurochemistry* 64:2465-2472.

Puryear, W.B., X. Yu, N.P. Ramirez, B.M. Reinhard, and S. Gummuluru. 2012. HIV-1 incorporation of host-cell-derived glycosphingolipid GM3 allows for capture by mature dendritic cells. *Proceedings of the National Academy of Sciences of the United States of America* 109:7475-7480.

Qu, W.S., Y.H. Wang, J.P. Wang, Y.X. Tang, Q. Zhang, D.S. Tian, Z.Y. Yu, M.J. Xie, and W. Wang. 2010. Galectin-1 enhances astrocytic BDNF production and improves functional outcome in rats following ischemia. *Neurochemical research* 35:1716-1724.

Rabinovich, G.A., A. Ariel, R. Hershkoviz, J. Hirabayashi, K.I. Kasai, and O. Lider. 1999. Specific inhibition of T-cell adhesion to extracellular matrix and proinflammatory cytokine secretion by human recombinant galectin-1. *Immunology* 97:100-106.

Rabinovich, G.A., L.G. Baum, N. Tinari, R. Paganelli, C. Natoli, F.T. Liu, and S. Iacobelli. 2002. Galectins and their ligands: amplifiers, silencers or tuners of the inflammatory response? *Trends in immunology* 23:313-320.

Rabinovich, G.A., F.T. Liu, M. Hirashima, and A. Anderson. 2007. An emerging role for galectins in tuning the immune response: lessons from experimental models of inflammatory disease, autoimmunity and cancer. *Scandinavian journal of immunology* 66:143-158.

Raine, C.S., and E. Wu. 1993. Multiple sclerosis: remyelination in acute lesions. *Journal of neuropathology and experimental neurology* 52:199-204.

Rajasagi, N.K., A. Suryawanshi, S. Sehrawat, P.B. Reddy, S. Mulik, M. Hirashima, and B.T. Rouse. 2012. Galectin-1 reduces the severity of herpes simplex virus-induced ocular immunopathological lesions. *Journal of immunology* 188:4631-4643.

Ramaswamy, S., G.E. Goings, K.E. Soderstrom, F.G. Szele, and D.A. Kozlowski. 2005. Cellular proliferation and migration following a controlled cortical impact in the mouse. *Brain research* 1053:38-53.

Ransohoff, R.M., T. Wei, K.D. Pavelko, J.C. Lee, P.D. Murray, and M. Rodriguez. 2002. Chemokine expression in the central nervous system of mice with a viral disease resembling multiple sclerosis: roles of CD4+ and CD8+ T cells and viral persistence. *Journal of virology* 76:2217-2224.

Rasmussen, S., J. Imitola, A. Ayuso-Sacido, Y. Wang, S.C. Starossom, P. Kivisakk, B. Zhu, M. Meyer, R.T. Bronson, J.M. Garcia-Verdugo, and S.J. Khoury. 2011. Reversible neural stem cell niche dysfunction in a model of multiple sclerosis. *Annals of neurology* 69:878-891.

Reichert, F., and S. Rotshenker. 1999. Galectin-3/MAC-2 in experimental allergic encephalomyelitis. *Experimental neurology* 160:508-514.

Rossi, S., C. Motta, V. Studer, V. De Chiara, F. Barbieri, F. Monteleone, A. Fornasiero, G. Coarelli, G. Bernardi, G. Cutter, O. Stuve, M. Salvetti, and D. Centonze. 2012. Effect of Glatiramer acetate on disease reactivation in MS patients discontinuing natalizumab. *European journal of neurology : the official journal of the European Federation of Neurological Societies*

Rothenaigner, I., S. Kramer, M. Ziegler, H. Wolff, A. Kleinschmidt, and R. Brack-Werner. 2007. Long-term HIV-1 infection of neural progenitor populations. *Aids* 21:2271-2281.

Rowitch, D.H. 2004. Glial specification in the vertebrate neural tube. *Nature reviews. Neuroscience* 5:409-419.

Ruas, L.P., E.S. Bernardes, M.L. Fermino, L.L. de Oliveira, D.K. Hsu, F.T. Liu, R. Chammas, and M.C. Roque-Barreira. 2009. Lack of galectin-3 drives response to Paracoccidioides brasiliensis toward a Th2-biased immunity. *PloS one* 4:e4519.

Rubio, N., and L. Capa. 1993. Differential IL-1 synthesis by astrocytes from Theiler's murine encephalomyelitis virus-susceptible and -resistant strains of mice. *Cellular immunology* 149:237-247.

Rubio, N., and F. Sanz-Rodriguez. 2007. Induction of the CXCL1 (KC) chemokine in mouse astrocytes by infection with the murine encephalomyelitis virus of Theiler. *Virology* 358:98-108.

Rubio, N., F. Sanz-Rodriguez, and H.L. Lipton. 2006. Theiler's virus induces the MIP-2 chemokine (CXCL2) in astrocytes from genetically susceptible but not from resistant mouse strains. *Cellular immunology* 239:31-40.

Ruebel, K.H., L. Jin, X. Qian, B.W. Scheithauer, K. Kovacs, N. Nakamura, H. Zhang, A. Raz, and R.V. Lloyd. 2005. Effects of DNA methylation on galectin-3 expression in pituitary tumors. *Cancer research* 65:1136-1140.

Rus, H., C. Cudrici, and F. Niculescu. 2005a. C5b-9 complement complex in autoimmune demyelination and multiple sclerosis: dual role in neuroinflammation and neuroprotection. *Annals of medicine* 37:97-104.

Rus, H., C. Cudrici, and F. Niculescu. 2005b. The role of the complement system in innate immunity. *Immunologic research* 33:103-112.

Russo, I., S. Barlati, and F. Bosetti. 2011. Effects of neuroinflammation on the regenerative capacity of brain stem cells. *Journal of neurochemistry* 116:947-956.

Rutishauser, U., and L. Landmesser. 1996. Polysialic acid in the vertebrate nervous system: a promoter of plasticity in cell-cell interactions. *Trends in neurosciences* 19:422-427.

Sadovnick, A.D., H. Armstrong, G.P. Rice, D. Bulman, L. Hashimoto, D.W. Paty, S.A. Hashimoto, S. Warren, W. Hader, T.J. Murray, and et al. 1993. A population-based study of multiple sclerosis in twins: update. *Annals of neurology* 33:281-285.

Saegusa, J., D.K. Hsu, H.Y. Chen, L. Yu, A. Fermin, M.A. Fung, and F.T. Liu. 2009. Galectin-3 is critical for the development of the allergic inflammatory response in a mouse model of atopic dermatitis. *The American journal of pathology* 174:922-931.

Sajad, M., R. Chawla, J. Zargan, S. Umar, M. Sadaqat, and H.A. Khan. 2011a. Cytokinetics of adult rat SVZ after EAE. *Brain research* 1371:140-149.

Sajad, M., J. Zargan, J. Sharma, R. Chawla, R. Arora, S. Umar, and H.A. Khan. 2011b. Increased spontaneous apoptosis of rat primary neurospheres in vitro after experimental autoimmune encephalomyelitis. *Neurochemical research* 36:1017-1026.

Sakaguchi, M., Y. Imaizumi, and H. Okano. 2007. Expression and function of galectin-1 in adult neural stem cells. *Cellular and molecular life sciences : CMLS* 64:1254-1258.

Sakaguchi, M., Y. Imaizumi, T. Shingo, H. Tada, K. Hayama, O. Yamada, T. Morishita, T. Kadoya, N. Uchiyama, T. Shimazaki, A. Kuno, F. Poirier, J. Hirabayashi, K. Sawamoto, and H. Okano. 2010. Regulation of adult neural progenitor cells by Galectin-1/beta1 Integrin interaction. *Journal of neurochemistry* 113:1516-1524.

Sakaguchi, M., T. Shingo, T. Shimazaki, H.J. Okano, M. Shiwa, S. Ishibashi, H. Oguro, M. Ninomiya, T. Kadoya, H. Horie, A. Shibuya, H. Mizusawa, F. Poirier, H. Nakauchi, K. Sawamoto, and H. Okano. 2006. A carbohydrate-binding protein, Galectin-1, promotes proliferation of adult neural stem cells. *Proceedings of the National Academy of Sciences of the United States of America* 103:7112-7117.

Salameh, B.A., I. Cumpstey, A. Sundin, H. Leffler, and U.J. Nilsson. 2010. 1H-1,2,3-triazol-1-yl thiodigalactoside derivatives as high affinity galectin-3 inhibitors. *Bioorganic & medicinal chemistry* 18:5367-5378.

Sanai, N., T. Nguyen, R.A. Ihrie, Z. Mirzadeh, H.H. Tsai, M. Wong, N. Gupta, M.S. Berger, E. Huang, J.M. Garcia-Verdugo, D.H. Rowitch, and A. Alvarez-Buylla. 2011. Corridors of migrating neurons in the human brain and their decline during infancy. *Nature* 478:382-386.

Sanchez-Felipe, L., E. Villar, and I. Munoz-Barroso. 2012. alpha2-3- and alpha2-6- N-linked sialic acids allow efficient interaction of Newcastle Disease Virus with target cells. *Glycoconjugate journal*

Sanchez-Ruderisch, H., C. Fischer, K.M. Detjen, M. Welzel, A. Wimmel, J.C. Manning, S. Andre, and H.J. Gabius. 2010. Tumor suppressor p16 INK4a: Downregulation of galectin-3, an endogenous competitor of the pro-anoikis effector galectin-1, in a pancreatic carcinoma model. *The FEBS journal* 277:3552-3563.

Sano, H., D.K. Hsu, J.R. Apgar, L. Yu, B.B. Sharma, I. Kuwabara, S. Izui, and F.T. Liu. 2003. Critical role of galectin-3 in phagocytosis by macrophages. *The Journal of clinical investigation* 112:389-397.

Sano, H., D.K. Hsu, L. Yu, J.R. Apgar, I. Kuwabara, T. Yamanaka, M. Hirashima, and F.T. Liu. 2000. Human galectin-3 is a novel chemoattractant for monocytes and macrophages. *Journal of immunology* 165:2156-2164.

Sato, S., N. Ouellet, I. Pelletier, M. Simard, A. Rancourt, and M.G. Bergeron. 2002. Role of galectin-3 as an adhesion molecule for neutrophil extravasation during streptococcal pneumonia. *Journal of immunology* 168:1813-1822.

Saura, J. 2007. Microglial cells in astroglial cultures: a cautionary note. *Journal of neuroinflammation* 4:26.

Schachter, H. 1991. The 'yellow brick road' to branched complex N-glycans. *Glycobiology* 1:453-461.

Serafini, B., M. Severa, S. Columba-Cabezas, B. Rosicarelli, C. Veroni, G. Chiappetta, R. Magliozzi, R. Reynolds, E.M. Coccia, and F. Aloisi. 2010. Epstein-Barr virus latent infection and BAFF expression in B cells in the multiple sclerosis brain: implications for viral persistence and intrathecal B-cell activation. *Journal of neuropathology and experimental neurology* 69:677-693.

Shah, A.H., and H.L. Lipton. 2002. Low-neurovirulence Theiler's viruses use sialic acid moieties on N-linked oligosaccharide structures for attachment. *Virology* 304:443-450.

Shipley, M.T., and G.D. Adamek. 1984. The connections of the mouse olfactory bulb: a study using orthograde and retrograde transport of wheat germ agglutinin conjugated to horseradish peroxidase. *Brain research bulletin* 12:669-688.

Sieve, A.N., A.J. Steelman, C.R. Young, R. Storts, T.H. Welsh, C.J. Welsh, and M.W. Meagher. 2004. Chronic restraint stress during early Theiler's virus infection exacerbates the subsequent demyelinating disease in SJL mice. *Journal of neuroimmunology* 155:103-118.

Silva, A.M., E. Santos, I. Moreira, A. Bettencourt, E. Coutinho, A. Goncalves, C. Pinto, X. Montalban, and S. Cavaco. 2012. Olfactory dysfunction in multiple sclerosis: association with secondary progression. *Multiple sclerosis* 18:616-621.

Silverman, A.M., R. Nakata, H. Shimada, R. Sposto, and Y.A. Declerck. 2012. A galectin-3-dependent pathway upregulates interleukin-6 in the microenvironment of human neuroblastoma. *Cancer research* 72:2228-2238.

Sioud, M., A. Mobergslien, A. Boudabous, and Y. Floisand. 2010. Evidence for the involvement of galectin-3 in mesenchymal stem cell suppression of allogeneic T-cell proliferation. *Scandinavian journal of immunology* 71:267-274.

Sioud, M., A. Mobergslien, A. Boudabous, and Y. Floisand. 2011. Mesenchymal stem cell-mediated T cell suppression occurs through secreted galectins. *International journal of oncology* 38:385-390.

So, E.Y., and B.S. Kim. 2009. Theiler's virus infection induces TLR3-dependent upregulation of TLR2 critical for proinflammatory cytokine production. *Glia* 57:1216-1226.

Sommer, L., and M. Rao. 2002. Neural stem cells and regulation of cell number. *Progress in neurobiology* 66:1-18.

Song, S., N. Mazurek, C. Liu, Y. Sun, Q.Q. Ding, K. Liu, M.C. Hung, and R.S. Bresalier. 2009. Galectin-3 mediates nuclear beta-catenin accumulation and Wnt signaling in human colon cancer cells by regulation of glycogen synthase kinase-3beta activity. *Cancer research* 69:1343-1349.

Sorgeloos, F., D. Vertommen, M.H. Rider, and T. Michiels. 2011. Theiler's virus L protein is targeted to the mitochondrial outer membrane. *Journal of virology* 85:3690-3694.

Sotthibundhu, A., Q.X. Li, W. Thangnipon, and E.J. Coulson. 2009. Abeta(1-42) stimulates adult SVZ neurogenesis through the p75 neurotrophin receptor. *Neurobiology of aging* 30:1975-1985.

Stancic, M., D. Slijepcevic, A. Nomden, M.J. Vos, J.C. de Jonge, A.H. Sikkema, H.J. Gabius, D. Hoekstra, and W. Baron. 2012. Galectin-4, a novel neuronal regulator of myelination. *Glia* 60:919-935.

Stancic, M., J. van Horssen, V.L. Thijssen, H.J. Gabius, P. van der Valk, D. Hoekstra, and W. Baron. 2011. Increased expression of distinct galectins in multiple sclerosis lesions. *Neuropathology and applied neurobiology* 37:654-671.

Starossom, S.C., I.D. Mascanfroni, J. Imitola, L. Cao, K. Raddassi, S.F. Hernandez, R. Bassil, D.O. Croci, J.P. Cerliani, D. Delacour, Y. Wang, W. Elyaman, S.J. Khoury, and G.A. Rabinovich. 2012. Galectin-1 Deactivates Classically Activated Microglia and Protects from Inflammation-Induced Neurodegeneration. *Immunity*

Stavrou, S., G. Ghadge, and R.P. Roos. 2011. Apoptotic and antiapoptotic activity of L protein of Theiler's murine encephalomyelitis virus. *Journal of virology* 85:7177-7185.

Storch, M.K., S. Piddlesden, M. Haltia, M. Iivanainen, P. Morgan, and H. Lassmann. 1998. Multiple sclerosis: in situ evidence for antibody- and complement-mediated demyelination. *Annals of neurology* 43:465-471.

Stowell, S.R., C.M. Arthur, P. Mehta, K.A. Slanina, O. Blixt, H. Leffler, D.F. Smith, and R.D. Cummings. 2008. Galectin-1, -2, and -3 exhibit differential recognition of sialylated glycans and blood group antigens. *The Journal of biological chemistry* 283:10109-10123.

Sundholm-Peters, N.L., H.K. Yang, G.E. Goings, A.S. Walker, and F.G. Szele. 2005. Subventricular zone neuroblasts emigrate toward cortical lesions. *Journal of neuropathology and experimental neurology* 64:1089-1100.

Suzuki, S., L.M. Gerhold, M. Bottner, S.W. Rau, C. Dela Cruz, E. Yang, H. Zhu, J. Yu, A.B. Cashion, M.S. Kindy, I. Merchenthaler, F.H. Gage, and P.M. Wise. 2007.

Estradiol enhances neurogenesis following ischemic stroke through estrogen receptors alpha and beta. *The Journal of comparative neurology* 500:1064-1075.

Tan, C.S., L.C. Ellis, C. Wuthrich, L. Ngo, T.A. Broge, Jr., J. Saint-Aubyn, J.S. Miller, and I.J. Koralnik. 2010. JC virus latency in the brain and extraneural organs of patients with and without progressive multifocal leukoencephalopathy. *Journal of virology* 84:9200-9209.

Tan, I.L., J.C. McArthur, D.B. Clifford, E.O. Major, and A. Nath. 2011. Immune reconstitution inflammatory syndrome in natalizumab-associated PML. *Neurology* 77:1061-1067.

Tepavcevic, V., F. Lazarini, C. Alfaro-Cervello, C. Kerninon, K. Yoshikawa, J.M. Garcia-Verdugo, P.M. Lledo, B. Nait-Oumesmar, and A. Baron-Van Evercooren. 2011. Inflammation-induced subventricular zone dysfunction leads to olfactory deficits in a targeted mouse model of multiple sclerosis. *The Journal of clinical investigation* 121:4722-4734.

Thacker, E.L., F. Mirzaei, and A. Ascherio. 2006. Infectious mononucleosis and risk for multiple sclerosis: a meta-analysis. *Annals of neurology* 59:499-503.

Thored, P., U. Heldmann, W. Gomes-Leal, R. Gisler, V. Darsalia, J. Taneera, J.M. Nygren, S.E. Jacobsen, C.T. Ekdahl, Z. Kokaia, and O. Lindvall. 2009. Long-term accumulation of microglia with proneurogenic phenotype concomitant with persistent neurogenesis in adult subventricular zone after stroke. *Glia* 57:835-849.

Thored, P., J. Wood, A. Arvidsson, J. Cammenga, Z. Kokaia, and O. Lindvall. 2007. Long-term neuroblast migration along blood vessels in an area with transient angiogenesis and increased vascularization after stroke. *Stroke; a journal of cerebral circulation* 38:3032-3039.

Tonra, J.R., B.S. Reiseter, R. Kolbeck, K. Nagashima, R. Robertson, B. Keyt, and R.M. Lindsay. 2001. Comparison of the timing of acute blood-brain barrier breakdown to rabbit immunoglobulin G in the cerebellum and spinal cord of mice with experimental autoimmune encephalomyelitis. *The Journal of comparative neurology* 430:131-144.

Toscano, M.A., G.A. Bianco, J.M. Ilarregui, D.O. Croci, J. Correale, J.D. Hernandez, N.W. Zwirner, F. Poirier, E.M. Riley, L.G. Baum, and G.A. Rabinovich. 2007. Differential glycosylation of TH1, TH2 and TH-17 effector cells selectively regulates susceptibility to cell death. *Nature immunology* 8:825-834.

Toscano, M.A., L. Campagna, L.L. Molinero, J.P. Cerliani, D.O. Croci, J.M. Ilarregui, M.B. Fuertes, I.M. Nojek, J.P. Fededa, N.W. Zwirner, M.A. Costas, and G.A. Rabinovich. 2011. Nuclear factor (NF)-kappaB controls expression of the immunoregulatory glycan-binding protein galectin-1. *Molecular immunology* 48:1940-1949.

Toscano, M.A., A.G. Commodaro, J.M. Ilarregui, G.A. Bianco, A. Liberman, H.M. Serra, J. Hirabayashi, L.V. Rizzo, and G.A. Rabinovich. 2006. Galectin-1 suppresses autoimmune retinal disease by promoting concomitant Th2- and T regulatory-mediated anti-inflammatory responses. *Journal of immunology* 176:6323-6332.

Toscano, M.A., J.E. Tongren, J. Brian de Souza, F.T. Liu, E.M. Riley, and G.A. Rabinovich. 2012. Endogenous galectin-3 controls experimental malaria in a species-specific manner. *Parasite immunology*

Tran, P.B., G. Banisadr, D. Ren, A. Chenn, and R.J. Miller. 2007. Chemokine receptor expression by neural progenitor cells in neurogenic regions of mouse brain. *The Journal of comparative neurology* 500:1007-1033.

Tran, P.B., D. Ren, T.J. Veldhouse, and R.J. Miller. 2004. Chemokine receptors are expressed widely by embryonic and adult neural progenitor cells. *Journal of neuroscience research* 76:20-34.

Trottier, M., P. Kallio, W. Wang, and H.L. Lipton. 2001. High numbers of viral RNA copies in the central nervous system of mice during persistent infection with Theiler's virus. *Journal of virology* 75:7420-7428.

Trottier, M., B.P. Schlitt, A.Y. Kung, and H.L. Lipton. 2004. Transition from acute to persistent Theiler's virus infection requires active viral replication that drives proinflammatory cytokine expression and chronic demyelinating disease. *Journal of virology* 78:12480-12488.

Trottier, M., B.P. Schlitt, and H.L. Lipton. 2002. Enhanced detection of Theiler's virus RNA copy equivalents in the mouse central nervous system by real-time RT-PCR. *Journal of virological methods* 103:89-99.

Tsai, C.M., C.H. Guan, H.W. Hsieh, T.L. Hsu, Z. Tu, K.J. Wu, C.H. Lin, and K.I. Lin. 2011. Galectin-1 and galectin-8 have redundant roles in promoting plasma cell formation. *Journal of immunology* 187:1643-1652.

Tsunoda, I. 2008. Axonal degeneration as a self-destructive defense mechanism against neurotropic virus infection. *Future virology* 3:579-593.

Tsunoda, I., L.Q. Kuang, and R.S. Fujinami. 2002. Induction of autoreactive CD8+ cytotoxic T cells during Theiler's murine encephalomyelitis virus infection: implications for autoimmunity. *Journal of virology* 76:12834-12844.

Tsunoda, I., L.Q. Kuang, J.E. Libbey, and R.S. Fujinami. 2003. Axonal injury heralds virus-induced demyelination. *The American journal of pathology* 162:1259-1269.

Tsunoda, I., C.I. Kurtz, and R.S. Fujinami. 1997. Apoptosis in acute and chronic central nervous system disease induced by Theiler's murine encephalomyelitis virus. *Virology* 228:388-393.

Tsunoda, I., T.E. Lane, J. Blackett, and R.S. Fujinami. 2004. Distinct roles for IP-10/CXCL10 in three animal models, Theiler's virus infection, EAE, and MHV infection, for multiple sclerosis: implication of differing roles for IP-10. *Multiple sclerosis* 10:26-34.

Tsunoda, I., J.E. Libbey, and R.S. Fujinami. 2009. Theiler's murine encephalomyelitis virus attachment to the gastrointestinal tract is associated with sialic acid binding. *Journal of neurovirology* 15:81-89.

Tsunoda, I., T. Tanaka, Y. Saijoh, and R.S. Fujinami. 2007. Targeting inflammatory demyelinating lesions to sites of Wallerian degeneration. *The American journal of pathology* 171:1563-1575.

Turbic, A., S.Y. Leong, and A.M. Turnley. 2011. Chemokines and inflammatory mediators interact to regulate adult murine neural precursor cell proliferation, survival and differentiation. *PloS one* 6:e25406.

Uliasz, T.F., M.E. Hamby, N.A. Jackman, J.A. Hewett, and S.J. Hewett. 2012. Generation of primary astrocyte cultures devoid of contaminating microglia. *Methods in molecular biology* 814:61-79.

Ulrich, R., W. Baumgartner, I. Gerhauser, F. Seeliger, V. Haist, U. Deschl, and S. Alldinger. 2006. MMP-12, MMP-3, and TIMP-1 are markedly upregulated in chronic demyelinating theiler murine encephalomyelitis. *Journal of neuropathology and experimental neurology* 65:783-793.

Ulrich, R., F. Seeliger, M. Kreutzer, P.G. Germann, and W. Baumgartner. 2008. Limited remyelination in Theiler's murine encephalomyelitis due to insufficient oligodendroglial differentiation of nerve/glial antigen 2 (NG2)-positive putative

oligodendroglial progenitor cells. *Neuropathology and applied neurobiology* 34:603-620.

Ure, D.R., and M. Rodriguez. 2002. Polyreactive antibodies to glatiramer acetate promote myelin repair in murine model of demyelinating disease. *FASEB journal : official publication of the Federation of American Societies for Experimental Biology* 16:1260-1262.

van Neerven, S., T. Regen, D. Wolf, A. Nemes, S. Johann, C. Beyer, U.K. Hanisch, and J. Mey. 2010. Inflammatory chemokine release of astrocytes in vitro is reduced by all-trans retinoic acid. *Journal of neurochemistry* 114:1511-1526.

Veyrac, A., and J. Bakker. 2011. Postnatal and adult exposure to estradiol differentially influences adult neurogenesis in the main and accessory olfactory bulb of female mice. *FASEB journal : official publication of the Federation of American Societies for Experimental Biology* 25:1048-1057.

Vyakarnam, A., S.F. Dagher, J.L. Wang, and R.J. Patterson. 1997. Evidence for a role for galectin-1 in pre-mRNA splicing. *Molecular and cellular biology* 17:4730-4737.

Vyakarnam, A., A.J. Lenneman, K.M. Lakkides, R.J. Patterson, and J.L. Wang. 1998. A comparative nuclear localization study of galectin-1 with other splicing components. *Experimental cell research* 242:419-428.

Wada, K., H. Arai, M. Takanashi, J. Fukae, H. Oizumi, T. Yasuda, Y. Mizuno, and H. Mochizuki. 2006. Expression levels of vascular endothelial growth factor and its receptors in Parkinson's disease. *Neuroreport* 17:705-709.

Wada, Y., and R.S. Fujinami. 1993. Viral infection and dissemination through the olfactory pathway and the limbic system by Theiler's virus. *The American journal of pathology* 143:221-229.

Walther, M., S. Kuklinski, P. Pesheva, O. Guntinas-Lichius, D.N. Angelov, W.F. Neiss, H. Asou, and R. Probstmeier. 2000. Galectin-3 is upregulated in microglial cells in response to ischemic brain lesions, but not to facial nerve axotomy. *Journal of neuroscience research* 61:430-435.

Walzel, H., A.A. Fahmi, M.A. Eldesouky, E.F. Abou-Eladab, G. Waitz, J. Brock, and M. Tiedge. 2006. Effects of N-glycan processing inhibitors on signaling events and induction of apoptosis in galectin-1-stimulated Jurkat T lymphocytes. *Glycobiology* 16:1262-1271.

Wang, C.R., A.L. Shiau, S.Y. Chen, Z.S. Cheng, Y.T. Li, C.H. Lee, Y.T. Yo, C.W. Lo, Y.S. Lin, H.Y. Juan, Y.L. Chen, and C.L. Wu. 2010a. Intra-articular lentivirus-mediated delivery of galectin-3 shRNA and galectin-1 gene ameliorates collagen-induced arthritis. *Gene therapy* 17:1225-1233.

Wang, J., Z.H. Lu, H.J. Gabius, C. Rohowsky-Kochan, R.W. Ledeen, and G. Wu. 2009. Cross-linking of GM1 ganglioside by galectin-1 mediates regulatory T cell activity involving TRPC5 channel activation: possible role in suppressing experimental autoimmune encephalomyelitis. *Journal of immunology* 182:4036-4045.

Wang, J.L., R.M. Gray, K.C. Haudek, and R.J. Patterson. 2004. Nucleocytoplasmic lectins. *Biochimica et biophysica acta* 1673:75-93.

Wang, T., M.H. Lee, T. Johnson, R. Allie, L. Hu, P.A. Calabresi, and A. Nath. 2010b. Activated T-cells inhibit neurogenesis by releasing granzyme B: rescue by Kv1.3 blockers. *The Journal of neuroscience : the official journal of the Society for Neuroscience* 30:5020-5027.

Weinstock-Guttman, B., M. Ramanathan, and R. Zivadinov. 2008. Interferon-beta treatment for relapsing multiple sclerosis. *Expert opinion on biological therapy* 8:1435-1447.

Welser, J.V., and R. Milner. 2012. Derivation of microglia-free astrocyte cultures from neural stem cells. *Methods in molecular biology* 814:81-91.

Widera, D., I. Mikenberg, M. Elvers, C. Kaltschmidt, and B. Kaltschmidt. 2006a. Tumor necrosis factor alpha triggers proliferation of adult neural stem cells via IKK/NF-kappaB signaling. *BMC neuroscience* 7:64.

Widera, D., I. Mikenberg, A. Kaus, C. Kaltschmidt, and B. Kaltschmidt. 2006b. Nuclear Factor-kappaB controls the reaggregation of 3D neurosphere cultures in vitro. *European cells & materials* 11:76-84; discussion 85.

Wildbaum, G., N. Netzer, and N. Karin. 2002. Plasmid DNA encoding IFN-gamma-inducible protein 10 redirects antigen-specific T cell polarization and suppresses experimental autoimmune encephalomyelitis. *Journal of immunology* 168:5885-5892.

Wilson, H.C., N.J. Scolding, and C.S. Raine. 2006. Co-expression of PDGF alpha receptor and NG2 by oligodendrocyte precursors in human CNS and multiple sclerosis lesions. *Journal of neuroimmunology* 176:162-173.

Wolswijk, G. 1998. Chronic stage multiple sclerosis lesions contain a relatively quiescent population of oligodendrocyte precursor cells. *The Journal of neuroscience : the official journal of the Society for Neuroscience* 18:601-609.

Wu, C., A. Chang, M.C. Smith, R. Won, X. Yin, S.M. Staugaitis, D. Agamanolis, G.J. Kidd, R.H. Miller, and B.D. Trapp. 2009. Beta4 tubulin identifies a primitive cell source for oligodendrocytes in the mammalian brain. *The Journal of neuroscience : the official journal of the Society for Neuroscience* 29:7649-7657.

Wuest, T.R., and D.J. Carr. 2008. Dysregulation of CXCR3 signaling due to CXCL10 deficiency impairs the antiviral response to herpes simplex virus 1 infection. *Journal of immunology* 181:7985-7993.

Xu, J., B.X. Ji, L. Su, H.Q. Dong, W.L. Sun, S.G. Wan, Y.O. Liu, P. Zhang, and C.Y. Liu. 2011. Clinical outcome of autologous peripheral blood stem cell transplantation in opticospinal and conventional forms of secondary progressive multiple sclerosis in a Chinese population. *Annals of hematology* 90:343-348.

Yamane, J., S. Ishibashi, M. Sakaguchi, T. Kuroiwa, Y. Kanemura, M. Nakamura, H. Miyoshi, K. Sawamoto, Y. Toyama, H. Mizusawa, and H. Okano. 2011. Transplantation of human neural stem/progenitor cells overexpressing galectin-1 improves functional recovery from focal brain ischemia in the Mongolian gerbil. *Molecular brain* 4:35.

Yamout, B., R. Hourani, H. Salti, W. Barada, T. El-Hajj, A. Al-Kutoubi, A. Herlopian, E.K. Baz, R. Mahfouz, R. Khalil-Hamdan, N.M. Kreidieh, M. El-Sabban, and A. Bazarbachi. 2010. Bone marrow mesenchymal stem cell transplantation in patients with multiple sclerosis: a pilot study. *Journal of neuroimmunology* 227:185-189.

Yan, Y.P., B.T. Lang, R. Vemuganti, and R.J. Dempsey. 2009. Galectin-3 mediates post-ischemic tissue remodeling. *Brain research* 1288:116-124.

Yang, H., H.S. Taylor, C. Lei, C. Cheng, and W. Zhang. 2011. Hormonal regulation of galectin 3 in trophoblasts and its effects on endometrium. *Reproductive sciences* 18:1118-1127.

Yang, H.K., N.L. Sundholm-Peters, G.E. Goings, A.S. Walker, K. Hyland, and F.G. Szele. 2004. Distribution of doublecortin expressing cells near the lateral ventricles in the adult mouse brain. *Journal of neuroscience research* 76:282-295.

Yang, R.Y., D.K. Hsu, and F.T. Liu. 1996. Expression of galectin-3 modulates T-cell growth and apoptosis. *Proceedings of the National Academy of Sciences of the United States of America* 93:6737-6742.

Yauch, R.L., and B.S. Kim. 1994. A predominant viral epitope recognized by T cells from the periphery and demyelinating lesions of SJL/J mice infected with Theiler's virus is located within VP1(233-244). *Journal of immunology* 153:4508-4519.

Ye, Z., and J.D. Marth. 2004. N-glycan branching requirement in neuronal and postnatal viability. *Glycobiology* 14:547-558.

Yin, P., A.M. Knolhoff, H.J. Rosenberg, L.J. Millet, M.U. Gillette, and J.V. Sweedler. 2012a. Peptidomic analyses of mouse astrocytic cell lines and rat primary cultured astrocytes. *Journal of proteome research* 11:3965-3973.

Yin, P., A.M. Knolhoff, H.J. Rosenberg, L.J. Millet, M.U. Gillette, and J.V. Sweedler. 2012b. Peptidomic Analyses of Mouse Astrocytic Cell Lines and Rat Primary Cultured Astrocytes. *Journal of proteome research*

Young, C.C., K.J. Brooks, A.M. Buchan, and F.G. Szele. 2011. Cellular and molecular determinants of stroke-induced changes in subventricular zone cell migration. *Antioxidants & redox signaling* 14:1877-1888.

Zambrano, A., L. Solis, N. Salvadores, M. Cortes, R. Lerchundi, and C. Otth. 2008. Neuronal cytoskeletal dynamic modification and neurodegeneration induced by infection with herpes simplex virus type 1. *Journal of Alzheimer's disease : JAD* 14:259-269.

Zettl, U.K., T. Kuhlmann, and W. Bruck. 1998. Bcl-2 expressing T lymphocytes in multiple sclerosis lesions. *Neuropathology and applied neurobiology* 24:202-208.

Zhang, J., J. Liu, B. Katafiasz, H. Fox, and H. Xiong. 2011. HIV-1 gp120-induced axonal injury detected by accumulation of beta-amyloid precursor protein in adult rat corpus callosum. *Journal of neuroimmune pharmacology : the official journal of the Society on NeuroImmune Pharmacology* 6:650-657.

Zhang, R.L., Y. LeTourneau, S.R. Gregg, Y. Wang, Y. Toh, A.M. Robin, Z.G. Zhang, and M. Chopp. 2007. Neuroblast division during migration toward the ischemic striatum: a study of dynamic migratory and proliferative characteristics of neuroblasts from the subventricular zone. *The Journal of neuroscience : the official journal of the Society for Neuroscience* 27:3157-3162.

Zhang, Y., Q. Zhang, Y. Gao, X. He, H. Kong, Y. Jiang, Y. Guan, X. Xia, Y. Shu, Y. Kawaoka, Z. Bu, and H. Chen. 2012. Key molecular factors in HA and PB2 contribute to the efficient transmission of the 2009 H1N1 pandemic influenza virus. *Journal of virology*

Zhang, Z., R. Yang, W. Cai, Y. Bai, M. Sokabe, and L. Chen. 2010. Treatment with progesterone after focal cerebral ischemia suppresses proliferation of progenitor cells but enhances survival of newborn neurons in adult male mice. *Neuropharmacology* 58:930-939.

Zhao, L.R., and S.C. Nam. 2007. Multiphoton microscope imaging: the behavior of neural progenitor cells in the rostral migratory stream. *Neuroscience letters* 425:83-88.

Zhou, L., X. Lin, T.J. Green, H.L. Lipton, and M. Luo. 1997. Role of sialyloligosaccharide binding in Theiler's virus persistence. *Journal of virology* 71:9701-9712.

Zhou, L., Y. Luo, Y. Wu, J. Tsao, and M. Luo. 2000. Sialylation of the host receptor may modulate entry of demyelinating persistent Theiler's virus. *Journal of virology* 74:1477-1485.

Zhu, C., A.C. Anderson, A. Schubart, H. Xiong, J. Imitola, S.J. Khoury, X.X. Zheng, T.B. Strom, and V.K. Kuchroo. 2005. The Tim-3 ligand galectin-9 negatively regulates T helper type 1 immunity. *Nature immunology* 6:1245-1252.

Zoll, J., S. Erkens Hulshof, K. Lanke, F. Verduyn Lunel, W.J. Melchers, E. Schoondermark-van de Ven, M. Roivainen, J.M. Galama, and F.J. van Kuppeveld.

2009. Saffold virus, a human Theiler's-like cardiovirus, is ubiquitous and causes infection early in life. *PLoS pathogens* 5:e1000416.

Zuberi, R.I., D.K. Hsu, O. Kalayci, H.Y. Chen, H.K. Sheldon, L. Yu, J.R. Apgar, T. Kawakami, C.M. Lilly, and F.T. Liu. 2004. Critical role for galectin-3 in airway inflammation and bronchial hyperresponsiveness in a murine model of asthma. *The American journal of pathology* 165:2045-2053.

Zubieta, M.R., D. Furman, M. Barrio, A.I. Bravo, E. Domenichini, and J. Mordoh. 2006. Galectin-3 expression correlates with apoptosis of tumor-associated lymphocytes in human melanoma biopsies. *The American journal of pathology* 168:1666-1675.

APPENDIX

7.1 Solutions and Reagents

1. Cryoprotectant
2. DNAse buffer
3. Homogenisation buffer
4. PFA 4%
5. PB 0.1M
6. PBS 0.1M
7. TAE buffer

Cryoprotectant

Sucrose	300g
Ethylene glycol	300 mL
PB 0.1M	
Final volume	1000mL

DNAase buffer

Tris-hydrochloride	Tris-HCL	10mM (0.32g)
Sodium Chloride	NaCl	50mM (0.58g)
Magnesium chloride	MgCl	10mM (2g)
Dithiothreitol	DTT	1mM
Sodium phosphate dibasic Anhydrous	Na2HPO4	14.4g
Glycerol		100mL
Distilled water		
Final volume		200 mL

Homogenisation buffer

Tris base	50mM	1.21 g
NaCl	150mM	1.75g
EDTA	1mM	0.06g
SDS	0.1%	0.2g
Triton-X 100	1%	2mL
dH20		
Final volume		200mL

PFA (4%w/v)

Paraformaldehyde	20g
PBS 0.1M	400mL
Heat to 70C in fume cupboard on magnetic stirrer.	
Add 2 drops of 10mM NaOH to clear. pH to 7.4	
Final volume	500mL

PB 0.1 M pH 7.4

Monobasic solution A (0.2M)		
Sodium phosphate monobasic	NaH2PO4	27.8g
Distilled water		Fill to 1000mL
Dibasic solution B (0.2M)		
Sodium phosphate dibasic anhydrous	Na2HPO4	28.4g
Distilled water		
Final volume		1000mL

PB (0.1M)

Monobasic solution A (0.2M)	140mL
Dibasic solution B (0.2M)	360mL
Distilled water	500mL
Final volume	1000mL

PBS 10X 1M pH 7.4 – use at 1X

Sodium chloride	NaCl	80g
Potassium chloride	KCL	2g
Potassium dihydrogen phosphate	KH2PO4	2.4g
Sodium phosphate dibasic anhydrous	Na2HPO4	14.4g
Distilled water (dH20)		
Final volume		1000mL

TAE buffer 50X – use at 1X

Tris-base	242g
Glacial acetic acid	57.1mL
EDTA 0.5M	100mL
For 250mL 0.5M EDTA ph8	
46.5g EDTA and 5.5g NaOH pellet in fill to 250mL	
Distilled water	
Final volume	1000mL

Table 2. Fold changes in gene expression in SVZ tissue and astrocytes cultures after TMEV infection by RT-PCR array

Gene Name	Gene symbol	Differential expression (fold) : TMEV/Control			
		B6 $^{+/+}$	B6 $^{-/-}$	SJL $^{+/+}$	SVZ astrocytes
B-cell leukaemina/Lymphoma 6	Bcl6	1.1	1.2	1.1	1.8
Complement component 3	C3	**66.8**	**82.3**	**4.2**	0.7
Complement component 3a receptor 1	C3ar1	**13.1**	**7.2**	**5.7**	**43.1**
Complement component 4B	C4b	**11.3**	**12.3**	**4.9**	0.7
Chemokine (C-C) motif ligand 1	Ccl1	**11.8**	3.1	2.9	0.6
Chemokine (C-C) motif ligand 11	Ccl11	**20.4**	2.9	1.1	0.6
Chemokine (C-C) motif ligand 12	Ccl12	**63.9**	**45.1**	**45.5**	**349**
Chemokine (C-C) motif ligand 17	Ccl17	2.4	2.1	0.9	2.8
Chemokine (C-C) motif ligand 19	Ccl19	**8.6**	**12.8**	3.4	1.6
Chemokine (C-C) motif ligand 2	Ccl2	**277.6**	**187.9**	**43.5**	**4.6**
Chemokine (C-C) motif ligand 20	Ccl20	1.6	1.3	1.1	1.6
Chemokine (C-C) motif ligand 22	Ccl22	**14.1**	**13.7**	**2.2**	0.6
Chemokine (C-C) motif ligand 24	Ccl24	1.1	1.3	1.5	0.6
Chemokine (C-C) motif ligand 25	Ccl25	0.8	0.7	1.0	0.9
Chemokine (C-C) motif ligand 3	Ccl3	**6.9**	**5.7**	3.6	**32.9**
Chemokine (C-C) motif ligand 4	Ccl4	**5.8**	**5.9**	2.3	**81**
Chemokine (C-C) motif ligand 5	Ccl5	**257.8**	**376.8**	**639.4**	**37.3**
Chemokine (C-C) motif ligand 7	Ccl7	**354.3**	**142.8**	**99.5**	**13.4**
Chemokine (C-C) motif ligand 8	Ccl8	**29.2**	**65.2**	**148.8**	**26.8**
Chemokine (C-C)motif receptor 1	Ccr1	**6.9**	**8.4**	2.3	**31.1**
Chemokine (C-C)motif receptor 2	Ccr2	**17.3**	**34.3**	**6.3**	1.2
Chemokine (C-C)motif receptor 3	Ccr3	**6.4**	**10.4**	3.0	2.9
Chemokine (C-C)motif receptor 4	Ccr4	**4.0**	3.2	2.0	0.6
Chemokine (C-C)motif receptor 7	Ccr7	**4.2**	1.5	1.6	0.6
CD14 antigen	Cd40	**16.7**	**7.4**	**5.2**	**12.4**
CD40 antigen	Cd40lg	**10.8**	3.8	**12.1**	0.6
CD40 ligand	Cebpb	**4.9**	2.4	2.0	1.3
CCAAAT/enchancer binding protein, beta	Crp	1.6	1.3	1.1	0.6
C-reactive protein	Csf1	2.8	**4.1**	1.4	3.8
Colony stimulating factor 1 (macrophage)	Cxcl1	**6.0**	2.0	1.1	**5.6**
Chemokine (C-X-C motif) ligand 1	Cxcl10	**798.0**	**389.9**	**70.9**	**139.1**
Chemokine (C-X-C motif) ligand 11	Cxcl11	**46.8**	**26.8**	**61.3**	**17.7**
Chemokine (C-X-C motif) ligand 2	Cxcl2	3.3	2.2	1.2	**22.3**
Chemokine (C-X-C motif) ligand 3	Cxcl3	1.6	1.3	1.1	**12.6**
Chemokine (C-X-C motif) ligand 5	Cxcl5	1.5	0.4	1.6	**118.6**
Chemokine (C-X-C motif) ligand 6	Cxcl9	**626.0**	**470.3**	**254.8**	**11**
Chemokine (C-X-C motif) ligand receptor 4	Cxcr4	1.7	1.6	1.8	0.3
Fas ligand (TNF superfamily, member 6)	Fasl	**39.8**	**13.9**	**7.1**	0.5
Fms-related tyrosine kinase 3 ligand	Flt3l	3.6	3.1	3.1	2.6
FBJ osteosarcoma oncogene	Fos	1.6	0.9	1.3	2.3
Histone deactylase 4	Hdac4	0.7	1.8	0.7	0.9
Interferon gamma	Ifng	**25.8**	**19.4**	**6.4**	0.6

Gene Name	Gene symbol	Differential expression (fold) : TMEV/Control			
		B6 $^{+/+}$	B6 $^{-/-}$	SJL $^{+/+}$	SVZ astrocytes
Interleukin 10	Il10	**5.8**	**5.2**	**13.9**	3.4
Interleukin 10 receptor beta	Il10rb	2.2	3.4	1.4	1.8
Interleukin 8	Il18	0.8	1.7	1.0	0.6
Interleukin 8 receptor accessory protein	Il18rap	**12.3**	**13.8**	2.5	**5.2**
Interleukin 1 alpha	Il1a	**4.4**	**8.6**	**4.7**	**12.9**
Interleukin 1 beta	Il1b	**30.7**	**31.7**	**8.3**	**4.6**
Interleukin	Il1f10	1.6	1.3	1.1	0.6
Interleukin 1 receptor, type I	Il1r1	1.7	1.2	1.0	1.7
Interleukin 1 receptor accessory protein	Il1rap	0.9	1.0	0.7	0.3
Interleukin 1 receptor antagonist	Il1rn	3.7	3.0	2.0	**8.3**
Interleukin 22	Il22	1.6	1.3	1.1	0.6
Interleukin 22 receptor accessory protein	Il22ra2	1.6	1.3	1.1	0.6
Interleukin 23, alpha subuni p19	Il23a	1.6	1.3	1.1	0.6
Interleukin 23 receptor	Il23r	1.6	1.3	1.1	0.8
Interleukin 6	Il6	3.9	2.2	2.3	**73**
Interleukin 6 receptor, alpha	Il6ra	1.9	2.3	1.0	0.2
Interleukin 7	Il7	1.7	1.3	1.1	2.3
Interleukin 8 receptor alpha	Il8ra	1.6	1.3	1.1	0.6
Interleukin 8 receptor beta	Il8rb	1.6	1.3	1.1	0.6
Interleukin 9	Il9	1.4	1.4	1.1	0.6
Integrin beta 2	Itgb2	**8.0**	**6.4**	**6.3**	**29.6**
Kininogen 1	Kng1	1.6	1.3	1.1	0.9
Lymphotaxin A	Lta	1.7	2.1	2.1	0.6
Lymphotaxin B	Ltb	**15.1**	**13.9**	**8.0**	1.6
Lymphocyte antigen 96	Ly96	3.7	4.1	1.7	1.6
Myeloid differentiation primary response gene 88	Myd88	3.9	2.6	2.0	1.7
Nuclear factor of activated T-cells	Nfatc3	0.9	2.7	1.4	1.5
Nuclear factor of k polypeptide gene enhancer in B-cells, p105	Nfkb1	1.6	2.5	2.1	2.1
Nitric oxide synthase 2, inducible	Nos2	2.5	0.9	0.5	0.4
Nuclear receptor subfamily 3, group C, member 1	Nr3c1	0.7	1.6	0.9	0.7
Receptor (TNFRSF)-interacting serine-threonine kinase 2	Ripk2	1.0	2.0	1.5	**6.3**
Toll-interleukin 1 receptor domain-containing adaptor protein	Tirap	1.7	1.2	1.5	1.3
Toll-like receptor 1	Tlr1	**5.1**	**9.3**	2.6	0.7
Toll-like receptor 2	Tlr2	**13.6**	**19.6**	**8.6**	**7.6**
Toll-like receptor 3	Tlr3	2.2	3.7	1.2	1.5
Toll-like receptor 4	Tlr4	3.1	3.9	1.5	1.5
Toll-like receptor 5	Tlr5	1.0	1.5	1.0	**5.1**
Toll-like receptor 6	Tlr6	2.4	5.2	2.0	1.9
Toll-like receptor 7	Tlr7	3.3	5.1	3.2	**24.4**

Gene Name	Gene symbol	Differential expression (fold) : TMEV/Control			
		B6 $^{+/+}$	B6 $^{-/-}$	SJL $^{+/+}$	SVZ astrocytes
Tnf	**21.1**	**17.5**	**6.1**	**6.13**	**11.8**
Tnfsf14	**11.3**	**10.7**	**4.4**	**4.4**	0.5
Tollip	0.7	1.7	0.9	0.87	1.9

*Values are averages for triplicate samples. Table shows that genes present on the Sabiosciences RT-PCR array PAMM-077. Gene changes shown here TMEV over control. Values for genes which were induced more than 4-fold are shown in bold.